

INFORMATION TO USERS

This manuscript has been reproduced from the microfilm master. UMI films the text directly from the original or copy submitted. Thus, some thesis and dissertation copies are in typewriter face, while others may be from any type of computer printer.

The quality of this reproduction is dependent upon the quality of the copy submitted. Broken or indistinct print, colored or poor quality illustrations and photographs, print bleedthrough, substandard margins, and improper alignment can adversely affect reproduction.

In the unlikely event that the author did not send UMI a complete manuscript and there are missing pages, these will be noted. Also, if unauthorized copyright material had to be removed, a note will indicate the deletion.

Oversize materials (e.g., maps, drawings, charts) are reproduced by sectioning the original, beginning at the upper left-hand corner and continuing from left to right in equal sections with small overlaps.

ProQuest Information and Learning
300 North Zeeb Road, Ann Arbor, MI 48106-1346 USA
800-521-0600

UMI[®]

University of Alberta

**The Role of 5-HT in the Development of Motoneuron Persistent Sodium
Currents after Chronic Spinal Injury**

by

Philip J. Harvey



A thesis submitted to the Faculty of Graduate Studies and Research in partial fulfillment of
the requirements for the degree of **Doctor of Philosophy**.

Centre for Neuroscience

Edmonton, Alberta

Fall, 2005



Library and
Archives Canada

Bibliothèque et
Archives Canada

0-494-08653-X

Published Heritage
Branch

Direction du
Patrimoine de l'édition

395 Wellington Street
Ottawa ON K1A 0N4
Canada

395, rue Wellington
Ottawa ON K1A 0N4
Canada

Your file *Votre référence*

ISBN:

Our file *Notre référence*

ISBN:

NOTICE:

The author has granted a non-exclusive license allowing Library and Archives Canada to reproduce, publish, archive, preserve, conserve, communicate to the public by telecommunication or on the Internet, loan, distribute and sell theses worldwide, for commercial or non-commercial purposes, in microform, paper, electronic and/or any other formats.

The author retains copyright ownership and moral rights in this thesis. Neither the thesis nor substantial extracts from it may be printed or otherwise reproduced without the author's permission.

AVIS:

L'auteur a accordé une licence non exclusive permettant à la Bibliothèque et Archives Canada de reproduire, publier, archiver, sauvegarder, conserver, transmettre au public par télécommunication ou par l'Internet, prêter, distribuer et vendre des thèses partout dans le monde, à des fins commerciales ou autres, sur support microforme, papier, électronique et/ou autres formats.

L'auteur conserve la propriété du droit d'auteur et des droits moraux qui protègent cette thèse. Ni la thèse ni des extraits substantiels de celle-ci ne doivent être imprimés ou autrement reproduits sans son autorisation.

In compliance with the Canadian Privacy Act some supporting forms may have been removed from this thesis.

Conformément à la loi canadienne sur la protection de la vie privée, quelques formulaires secondaires ont été enlevés de cette thèse.

While these forms may be included in the document page count, their removal does not represent any loss of content from the thesis.

Bien que ces formulaires aient inclus dans la pagination, il n'y aura aucun contenu manquant.


Canada

“The first effect of injury done to the nervous system is a diminution of its functions; whilst the second or ulterior effect is the augmentation of those functions.”

- Marshall Hall, 1841

For Gab; who put up with me throughout.

ABSTRACT

Months after sacral spinal transection in rats (chronic spinal rats), motoneurons below the injury exhibit large, low-threshold persistent inward currents (PICs), composed of persistent sodium currents (Na PICs) and persistent calcium currents (Ca PICs), which are responsible for the development of muscle spasms after injury (spasticity). Using an *in vitro* model of spasticity in the adult rat sacrocaudal cord, it was determined that motoneurons of normal adult rats also exhibited Na and Ca PICs when the spinal cord was acutely transected at the sacral level (acute spinal rats), but they were less than half the amplitude of PICs in chronic spinal rats. The Na PIC was identified as being critical for initiating and maintaining repetitive firing, and was modulated by drugs acting at 5-HT₂ and α 1-noradrenergic (α 1-NE) receptors. Specifically, 5-HT₂ receptor agonists facilitated the Na PIC and improved the spike and repetitive firing in motoneurons of acute spinal rats. Motoneurons of chronic spinal rats responded to 5-HT receptor agonists the same as with acute spinalization, but at much lower doses, indicating that motoneurons develop a 30-fold supersensitivity to 5-HT with chronic transection. In motoneurons of both acute and chronic spinal rats, antagonists acting at 5-HT_{2A} (ketanserin), 5-HT_{2C} (RS 102221) and α 1-NE (WB 4101) receptors combined to eliminate the Na PIC and block repetitive firing, even without application of exogenous agonists. Therefore, endogenous intraspinal sources of 5-HT and NE maintain the Na PICs observed *in vitro*. In acute spinal rats, these monoamines are likely to be leaking from cut descending monoaminergic terminals. In chronic spinal rats, the supersensitivity of motoneurons to residual low levels of monoamines (likely of intraspinal neural origin) maintains the large Na PICs. Because this intraspinal source of monoamines is not appropriately regulated, PICs are tonically large, leading to long-lasting muscle

spasms characteristic of spasticity. Therefore, spasticity may potentially be treated using monoaminergic antagonists to block motoneuron PICs, or else by preventing denervation supersensitivity from developing.

ACKNOWLEDGEMENTS

I must express my appreciation and gratitude to my supervisor and mentor Dr. David Bennett, and to those on my advisory committee Drs. Tessa Gordon and Arthur Prochazka.

A thank-you also to Yunru Li for laying the groundwork of my thesis, and to her brother Xiaole, to whom I pass the torch. Special thanks to Leo Sanelli for his friendship, and expert technical assistance, to Al Denington and Neil Tyreman for technical help, to Joey Grochmal for work on the rubrospinal electrophysiology, and to Jan Kowalczewski and George Braybrook for assisting with electron micrographs of electrodes.

Scholarship funding was provided by the Natural Sciences and Engineering Research Council (NSERC), the Alberta Heritage Foundation for Medical Research (AHFMR), the Neuroscience Canada Foundation and the Walter H. Johns Memorial Foundation. Funding for the Bennett lab was provided by NIH grant #RO1 NS47567-01, NSERC, AHFMR, the Canadian Foundation for Innovation and the Canadian Institutes of Health Research.

TABLE OF CONTENTS

CHAPTER 1:	INTRODUCTION	1
1.1	Clinical spasticity with chronic spinal cord injury	1
1.2	Mechanisms of spasticity	2
1.3	Characteristics of motoneuron persistent inward currents	3
1.3.1	Persistent calcium currents	4
1.3.2	Persistent sodium currents	5
1.3.3	Outward potassium currents	5
1.4	Modulation of motoneuron PICs by monoamines	6
1.5	Hypothesis	9
1.6	Animal model of spasticity	10
1.7	Thesis outline	11
1.8	Bibliography for Chapter 1	13
CHAPTER 2:	PERSISTENT SODIUM CURRENTS AND REPETITIVE FIRING	23
2.1	BACKGROUND	23
2.2	METHODS	24
2.2.1	<i>In vitro</i> preparation	24
2.2.2	Intracellular recording	25
2.2.3	Drugs and solutions	25
2.2.4	Persistent inward currents in current and voltage clamp recording	26
2.2.5	Data analysis	29
2.3	RESULTS	29
2.3.1	The resting membrane potential of motoneurons in acute spinal rats was more hyperpolarized relative to firing threshold than in chronic spinal rats.	29
2.3.2	Normal motoneurons have small, but variable, PICs after acute spinal transection.	30

2.3.3	Persistent sodium and calcium currents make up the total PIC in acute spinal rats.	33
2.3.4	Na PIC and Ca PIC are both much larger after chronic injury.	39
2.3.5	PICs do not require fast synaptic transmission or spike-mediated transmission.	39
2.3.6	Motoneurons that lack Na PICs show poor repetitive firing.	42
2.3.7	Recruitment and firing occurs in acute spinal motoneurons with small Na PICs.	45
2.3.8	Motoneurons with a negative-slope region had enhanced firing.	46
2.3.9	Large Na PICs allow very slow steady firing.	46
2.3.10	Frequency-current slope is not related to Na PIC amplitude.	52
2.3.11	Na PICs are essential in firing.	52
2.4	DISCUSSION	55
2.4.1	Variation in Na PIC amplitude with state of animal preparation.	58
2.4.2	Role of endogenous monoamines in regulating Na PIC and motoneuron properties.	59
2.4.3	Role of Na PIC in repetitive firing.	60
2.4.4	Spinal shock after injury, and impact on acute slice preparations.	62
2.5	Bibliography for Chapter 2	63
 CHAPTER 3: 5-HT₂ RECEPTOR ACTIVATION FACILITATES PERSISTENT SODIUM CURRENTS		67
3.1	BACKGROUND	67
3.2	METHODS	68
3.2.1	<i>In vitro</i> preparation	68
3.2.2	Drugs and solutions	69
3.2.3	Persistent inward currents in voltage and current clamp recording	69
3.2.4	Data analysis	70
3.3	RESULTS	70
3.3.1	5-HT enhances PICs in motoneurons of acute spinal rats.	73

3.3.2	5-HT also induces changes in input resistance, resting potential and spike properties.	73
3.3.3	5-HT ₂ receptors facilitate the total PIC.	76
3.3.4	5-HT ₂ receptors facilitate the Na PIC.	76
3.3.5	5-HT ₂ receptor activation does not affect input resistance or resting membrane potential but does hyperpolarize the spike threshold and facilitate the spike.	79
3.3.6	Na PICs are supersensitive to 5-HT ₂ receptor activation with DOI in chronic spinal rats.	79
3.3.7	Effects of DOI in chronic spinal rat motoneurons are specific to Na channel facilitation.	80
3.3.8	PICs are also supersensitive to 5-HT itself in chronic spinal rats.	80
3.3.8	All effects of 5-HT on motoneurons become supersensitive to 5-HT after chronic injury.	81
3.3.10	5-HT ₂ receptor agonists act slowly on the Na PIC.	82
3.3.11	Paradoxical effects of 5-HT on self-sustained firing.	82
3.3.12	5-HT ₂ receptor activation produces very slow firing mediated by Na PICs.	85
3.3.13	Motoneurons with poor repetitive firing are rescued by 5-HT ₂ receptor action.	88
3.4	DISCUSSION	93
3.4.1	5-HT ₂ receptor activation modulates Na channels.	93
3.4.2	5-HT ₂ receptors selectively modulate Na currents, whereas other 5-HT receptors modulate input resistance and membrane potential.	95
3.4.3	Supersensitivity of motoneurons to residual 5-HT contributes to recovery of PICs after chronic injury.	96
3.4.4	Effects of supersensitivity of R _m and V _m to 5-HT in motoneurons with long-term injury.	97
3.4.5	Possible mechanisms of supersensitivity.	97
3.4.6	Supersensitivity to norepinephrine.	98
3.4.7	Functional implications of 5-HT activity on normal motoneurons.	98

3.4.8	Supersensitivity causes spasticity.	99
3.5	Bibliography for Chapter 3	100
CHAPTER 4: MONOAMINE ANTAGONISTS AND PERSISTENT SODIUM CURRENTS		107
4.1	BACKGROUND	107
4.2	METHODS	109
4.2.1	<i>In vitro</i> preparation	109
4.2.2	Drugs and solutions	110
4.2.3	Persistent inward currents in voltage and current clamp recording	110
4.2.4	Data analysis	111
4.3	RESULTS	111
4.3.1	Endogenous monoamines sustain Na PICs after chronic spinal transection.	114
4.3.2	Endogenous monoamines sustain Na PICs in motoneurons of acute spinal rats.	117
4.3.3	5-HT _{2A} , 5-HT _{2C} and α 1-NE receptors are all involved in facilitating the Na PIC.	117
4.3.4	Endogenous monoamines are critical for repetitive firing in motoneurons.	120
4.3.5	Monoamine receptor blockade increases depolarization-induced sodium spike inactivation	123
4.3.6	Tonic activity at any single monoaminergic receptor is sufficient to maintain repetitive firing.	126
4.3.7	Minimum firing rate is increased by monoamine receptor antagonists.	126
4.3.8	Firing rate increased, but F-I slope unchanged, by monoamine receptor antagonists.	129
4.3.9	Monoamine receptor antagonists do not directly block Na channels.	132

^

4.3.10	Without nimodipine, monoamine receptor blockade does not block Ca PIC, but still disrupts firing.	132
4.3.11	Prolonged treatment with cadmium also eliminates the Na PIC.	137
4.4	DISCUSSION	140
4.4.1	Endogenous monoamines are essential for Na PICs.	141
4.4.2	Critical role of Na PICs in firing.	142
4.4.3	Possible mechanisms by which monoamines modulate the Na PIC.	142
4.4.4	The general action of 5-HT ₂ receptors is very slow to reverse.	143
4.4.5	Other endogenous transmitters could regulate Na PICs.	144
4.4.6	Monoamines in the acute spinal state likely arise from cut descending terminals.	145
4.4.7	Intraspinal monoamines act on supersensitive receptors to induce spasticity with chronic spinal cord injury.	146
4.4.8	Summary and implications for management of spasticity.	148
4.5	Bibliography for Chapter 4	149
 CHAPTER 5: CONCLUSION		155
5.1	The etiology of spasticity following SCI	155
5.2	Future directions	156
 APPENDIX: RUBROSPINAL TRACT STIMULATION AND REGENERATION		157
A.1	BACKGROUND	157
A.2	METHODS	158
A.2.1	Stimulating microwires.	158
A.2.2	Recording from the red nucleus during rubrospinal tract stimulation.	159
A.2.3	Rubrospinal tract stimulation and regeneration into a peripheral nerve graft.	160
A.2.4	Influence of RST stimulation on BDNF and GAP-43 mRNA	163

	expression.	
A.2.5	RT-PCR.	164
A.2.6	<i>In situ</i> hybridisation of red nuclei.	164
A.2.7	Electrical stimulation and regeneration in the peripheral nervous system using the femoral nerve-nerve suture model.	165
A.2.8	Experimental design and statistical analysis.	165
A.3	RESULTS	166
A.3.1	Microwires used to stimulate the rubrospinal tract.	166
A.3.2	Red nucleus recordings to quantify rubrospinal tract activation with microwires.	166
A.3.3	Current spread from the microwires.	170
A.3.4	Lack of rubrospinal tract damage after one hour of supramaximal stimulation.	170
A.3.5	Rubrospinal tract regeneration into a peripheral nerve graft.	171
A.3.6	Failure to improve regeneration after one hour of rubrospinal tract stimulation.	171
A.3.7	Counts of regenerating cervical neurons.	174
A.3.8	Cell body response to antidromic stimulation as measured by ISH and RT-PCR.	174
A.3.9	Failure of longer duration stimulation to affect BDNF.	177
A.3.10	Failure of one hour of electrical stimulation to improve femoral motoneuron regeneration.	182
A.4	DISCUSSION	182
A.4.1	Influence of antidromic stimulation on CNS regeneration.	182
A.4.2	Mechanisms of activity-dependent regeneration.	185
A.4.3	Relevance of the mode of input in neural response to injury.	186
A.4.4	Possible explanations for failure of stimulation to promote regeneration of femoral motoneurons.	187
A.4.5	Summary	188
A.5	List of Abbreviations	190
A.6	Bibliography for Appendix	191

LIST OF FIGURES

CHAPTER 2: Persistent Sodium Currents and Repetitive Firing

Figure 2-1:	Intracellular motoneuron recording methods for rat <i>in vitro</i> sacrocaudal cord.	28
Figure 2-2:	Motoneurons from acute spinal rats have small persistent inward currents (PICs).	32
Figure 2-3:	TTX-sensitive Na PICs and TTX-resistant Ca PICs in motoneurons of acute spinal rats.	35
Figure 2-4:	Ca PIC is blocked by nimodipine, leaving only a TTX-sensitive Na PIC in motoneurons from acute spinal rats.	38
Figure 2-5:	Variability in repetitive firing ability is related to Na PIC amplitude.	41
Figure 2-6:	Na PIC amplitude controls firing ability near threshold.	44
Figure 2-7:	Motoneurons of acute spinal rats, with large enough Na PICs to produce a negative-slope region, exhibited steady very slow firing similar to that commonly seen in chronic spinal rats.	48
Figure 2-8:	Na PIC amplitude correlates with minimum firing rate.	51
Figure 2-9:	F-I slope is not related to the Na PIC amplitude.	54
Figure 2-10:	Selectively blocking the Na PIC eliminates repetitive firing, but not the fast sodium spike.	57

CHAPTER 3: 5-HT₂ Receptor Activation Facilitates Persistent Sodium Currents

Figure 3-1:	Persistent inward currents (PICs) in motoneurons are facilitated by 5-HT and are supersensitive to 5-HT after chronic spinal transection.	72
Figure 3-2:	Motoneurons from chronic spinal rats are supersensitive to multiple effects of 5-HT.	75
Figure 3-3:	Na PICs in motoneurons are facilitated by the 5-HT ₂ receptor agonist DOI, and motoneurons of chronic spinal rats are supersensitive to DOI.	78
Figure 3-4:	Self-sustained firing is influenced by 5-HT-induced change in PIC	84

	activation voltage relative to firing level.	
Figure 3-5:	With Ca PIC blocked, DOI increases self-sustained firing and enables very slow firing.	87
Figure 3-6:	DOI rescues healthy motoneurons with no Na PIC and enables them to generate repetitive firing with slow current ramps.	90
Figure 3-7:	DOI restores firing ability in motoneuron with Ca PIC but no Na PIC.	92
CHAPTER 4: Monoamine Antagonists and Persistent Sodium Currents		
Figure 4-1:	In motoneurons of chronic spinal rats, Na PIC is blocked by antagonists acting on 5-HT _{2A} , 5-HT _{2C} , and α 1-NE receptors.	113
Figure 4-2:	In motoneurons of acute spinal rats, the Na PIC is also eliminated by monoamine receptor blockade.	116
Figure 4-3:	Both α 1-NE and 5-HT _{2A/2C} receptors are involved in tonic activation of the persistent sodium current.	119
Figure 4-4:	Repetitive firing during slow current ramps eliminated by blocking 5-HT _{2A} , 5-HT _{2C} , and α 1-NE receptors.	122
Figure 4-5:	Loss of action potential generation occurs simultaneously to loss of Na PIC as monoamine receptor blockade takes effect.	125
Figure 4-6:	The monoamine receptor antagonists that act to reduce the Na PIC, increase the overall firing rate, but do not affect the F-I slope.	128
Figure 4-7:	Small Na PIC in α 1-NE receptor antagonist WB 4101 can still be facilitated by 5-HT ₂ receptor agonist DOI.	131
Figure 4-8:	High doses of monoamine receptor agonists can compete with antagonists to restore the Na PIC.	134
Figure 4-9:	In absence of nimodipine, monoamine receptor blockade does not eliminate the Ca PIC, but does inhibit firing.	136
Figure 4-10:	Na PICs can be eliminated with long-term cadmium (Cd ²⁺), and restored by exogenous 5-HT.	139

APPENDIX: Rubrospinal Tract Stimulation and Regeneration

Figure A-1:	Protocol for investigating activity-dependent CNS regeneration.	162
Figure A-2:	Assessing supramaximal stimulation of the rubrospinal tract can be achieved with a single microwire implanted in the dorsolateral cervical spinal cord.	168
Figure A-3:	Regeneration into a cervical peripheral nerve graft, as determined by the number of microruby-positive neurons.	173
Figure A-4:	Number of labelled neurons in red nuclei were normalised to the average number of labelled cervical neurons near the graft junction.	176
Figure A-5:	BDNF mRNA not upregulated in the red nuclei at 48 hours after axotomy and antidromic stimulation.	179
Figure A-6:	BDNF was not detected in the red nuclei using RT-PCR, and GAP-43 levels were not elevated with stimulation.	181
Figure A-7:	One hour of electrical stimulation did not increase the number of femoral motoneurons regenerating at 3 weeks.	184

LIST OF ABBREVIATIONS USED

5-HT	5-hydroxytryptamine (serotonin)
5-HTP	5-HT precursor protein
5,7-DHT	5,7-dihydroxytryptamine
8-OH-DPAT	(±)-8-Hydroxy-2-dipropylaminotetralin
α 1-NE	α 1-norepinephrine (noradrenergic) receptor
ΔI	self-sustained firing ($\Delta I = I_{start} - I_{end}$)
Δ PIC	drug-induced PIC
ACh	acetylcholine
ACPD	1-Aminocyclopentane-1,3-dicarboxylic acid
ACSF	artificial cerebrospinal fluid
AHP	afterhyperpolarization
AMPA	a-Amino-3-hydroxy-5-methyl-4-isoxazolepropionic acid
AP5	D(-)-2-Amino-5-phosphonopentanoic acid
Ca PIC	persistent calcium current
C_{av}	voltage-gated calcium channel
CNQX	6-cyano-7-nitroquinoxaline-2,3-dione
CNS	central nervous system
DCC	discontinuous current clamp
DHPG	(RS)-3,5-Dihydroxyphenylglycine
DOI	(±)-1-(2,5-dimethoxy-4-iodophenyl)-2-aminopropane
DSP-4	N(2-chloroethyl)-N-ethyl-2-bromobenzylamine
dV/dt	depolarization rate
dV/dt _{max}	maximum rate of rise of action potential
EPSP	excitatory post-synaptic potential
F	firing frequency
GABA	γ -aminobutyric acid
G_{min}	minimum I-V slope during ascending voltage ramp
I	current
I_{cnd}	cessation of firing on descending current ramp
I_h	hyperpolarization-activated non-selective cation current

I_{start}	initiation of firing on ascending current ramp
IP3	inositol-1,4,5-triphosphate
K_{Ca}	calcium-activated potassium current
K_{Na}	sodium-activated potassium current
L-Ca	calcium current carried by L-type channels
mACSF	modified ACSF
mGluR	metabotropic glutamate receptors
Na PIC	persistent sodium current
nACSF	normal ACSF
NE	norepinephrine
NMDA	N-methyl-D-aspartate
NSR	negative-slope region
pEPSP	polysynaptic excitatory post-synaptic potential
PIC	persistent inward current
pCPA	p-chlorophenylalanine
PKC	protein kinase C
REM	rapid eye movement
R_m	membrane input resistance
RS 102221	8-[5-(2,4-Dimethoxy-5-(4-trifluoromethylphenylsulphonamido)phenyl-5-oxopentyl]-1,3,8-triazaspiro[4.5]decane-2,4-dione
SCI	spinal cord injury
SEVC	single-electrode voltage clamp
SK	slow potassium (K_{Ca}) current
TRH	thyrotropin-releasing hormone
TTX	tetrodotoxin
V	voltage
$V_{\frac{1}{2}}$	PIC half-activation voltage
V_m	resting membrane potential
V_{START}	PIC voltage onset
V_{th}	spike voltage threshold
WB 4101	2-(2,6-Dimethoxyphenoxyethyl)aminomethyl-1,4-benzodioxane

CHAPTER 1: Introduction

1.1 CLINICAL SPASTICITY WITH CHRONIC SPINAL CORD INJURY

The definition of spasticity is often quoted from Lance (1980) simply as a velocity-dependent increase in tonic stretch reflexes. However, the term 'spasticity' is often broadly used to describe different manifestations of muscle hyperactivity that arise from a variety of neurological conditions, including spinal cord injury (SCI), stroke/hemiplegia, multiple sclerosis, cerebral palsy and others (NINDS 2005). Symptoms include hypertonus, hyperreflexia, clonus and spasms, but the more prominent manifestations vary depending on the site of central nervous system (CNS) injury (Young 1994). Lance's definition, emphasizing changes in stretch reflexes, is far more reflective of stroke than of spinal cord injury. Stroke spasticity is characterized by low-threshold (Ia afferent stretch receptors) hyperreflexia, and hypertonus in flexors of the upper limbs and extensors of the lower limbs (so-called 'anti-gravity' muscles, Young 1994). In contrast, spinal cord injury produces long-lasting muscle spasms, involving both flexors and extensors of affected limbs, that are often best triggered by high-threshold (cutaneous) afferent inputs (Kuhn and Macht 1948; Little et al. 1989). While Lance (1980) and his symposium colleagues have acknowledged other manifestations of spasticity, such as spasms, many subsequent investigators have taken his limited definition as a complete characterization of the spastic syndrome. Thus, they have tried to find physiological changes with injury that explain these velocity-dependent increases in the tonic stretch reflex, with complete disregard for other features of spasticity. Lumping motor symptoms of different etiologies (stroke, SCI, cerebral palsy, etc.) under the same general term, without distinguishing their origin, has also hampered proper research into the nature of spasticity and the effectiveness of pharmacological interventions. Thus, for the purposes of this thesis, I have focused on the cellular origin and development of spasticity, specifically in its manifestation following spinal cord injury, with the understanding that spastic syndromes arising from other CNS disorders likely have different molecular pathologies.

Following spinal cord injury in humans, exaggerated reflexes and increased muscle tone often emerge that contribute to a general spastic syndrome (Ashby and McCrea 1987; Kuhn and Macht 1948; Noth 1991; Young 1994). The central complaint of patients with SCI spasticity is intense muscle contractions (spasms) lasting several seconds, which are triggered by numerous stimuli, including muscle stretch, light touch, heat and/or cold, bladder distension and even emotional tension (Little et al. 1989). Spasms can become very severe, lasting for several minutes and involving both extensor and flexor muscles (Kuhn and Macht 1948). These uncontrolled spasms develop in the weeks to months following both complete and incomplete SCI and can be quite debilitating and painful, interfering with sleep, normal activities and residual locomotor functions (Kita and Goodkin 2000; Kuhn and Macht 1948; Norman et al. 1998). Because of this, muscle spasms may be considered the main disruptive characteristic of the SCI spastic syndrome.

Muscle spasms also interfere with efforts to improve function following SCI. A large portion (37 - 62%) of spinal cord injuries are incomplete (Ackery et al. 2004) and, in such cases, there is considerable potential for recovery of function. For example, treadmill training often improves the stepping ability of such patients, facilitating greater independence in mobility over the course of several weeks to months (reviewed in Harkema 2001). However, the presence of spasticity can severely compromise such efforts at rehabilitation (Delwaide and Pennisi 1994; Little et al. 1989). Thus, before any attempt at recovery of locomotion can be made, clinicians must first treat the spasticity.

In the tradition of Lance (1980), and the widespread conviction that spasticity arises from enhanced stretch reflexes, conventional therapies such as baclofen, gabapentin and the benzodiazepines block spinal reflexes and suppress neural circuitry (Abbruzzese 2002). However, side effects of these treatments typically include sedation and muscle weakness, which themselves can interfere with rehabilitation (Rice 1987). Indeed, while baclofen reduces spasms, it generally does not improve functional locomotor recovery (Duncan et al. 1976), whereas the unconventional antispastic medication cyproheptadine, which is a serotonergic antagonist, increases walking speed and coordination, in addition to reducing muscle spasms and clonus, in severely disabled spinal cord-injured subjects (Norman et al. 1998). Thus, to find better pharmacological strategies that target the debilitating muscle spasms without compromising residual function, a better understanding of the cellular basis of spasticity is required.

1.2 MECHANISMS OF SPASTICITY

As described above, a major component of the spastic syndrome resulting from SCI is the involuntary muscle spasms evoked by brief noxious or innocuous stimuli, which last for 8-10 seconds on average (Kawamura et al. 1989). In subjects exhibiting a spastic syndrome, changes in excitability of several neuronal pathways have been noted, but the degree of these changes has not correlated well with the degree of spasticity assessed clinically (Faist et al. 1994; Hiersemenzel et al. 2000). The spasms consist of persistent muscle contractions that far outlast the duration of the triggering excitatory input, suggesting that they are due to intrinsic voltage-dependent persistent inward currents (PICs) of the motoneurons themselves. Simply put, the PIC producing the spasm is a depolarizing current carried by voltage-sensitive channels that are activated at membrane potentials near spike threshold. Once activated, the current tends to remain activated until the membrane potential is reduced below threshold again. PICs in motoneurons generate sustained depolarizations or 'plateaus' (reviewed in Eken et al. 1989; Powers and Binder 2001), providing a sustained excitatory drive that allows motoneurons to fire repetitively following brief synaptic excitations, or at lower injected currents than required to initiate firing (self-sustained firing, see Hounsgaard et al. 1988). Using an animal model of spasticity that develops in the tail muscles of rats following a low spinal transection (described below), Bennett and colleagues have demonstrated that PICs, and the resulting self-sustained firing behaviour, arise in motoneurons after chronic spinal cord injury (Li and Bennett 2003; Li et al. 2004a) and produce long-lasting spastic reflexes both *in vitro* (Bennett et al. 2001b) and in the awake animal (Bennett et al.

2001a) that are similar to muscle spasms that occur in humans with spinal spasticity (Bennett et al. 1999a; Bennett et al. 2004). Evidence for motoneuron PICs has been found in humans using paired motor unit recordings in both normal individuals (Gorassini et al. 1998; Kiehn and Eken 1997) and in affected muscles of humans with spasticity (Gorassini et al. 2004). These PICs are activated during spontaneous muscle spasms and are triggered by the same muscle vibrations and cutaneous stimuli that trigger spasms (Gorassini et al. 2004). Thus, the prolonged involuntary muscle spasms in subjects with long-term SCI are mediated by the activation of PICs in the motoneurons.

This is not to say that changes in spinal reflex pathways with injury are unimportant in the development of spasticity. Due to their slow kinetics, motoneuron PICs take >200 ms to activate (Li and Bennett 2003). Normally, brief afferent stimulation, especially cutaneous stimulation, produces excitatory post-synaptic potentials (EPSPs) that are not long enough, or of sufficient amplitude, to activate PICs. However, following a complete spinal transection in the rat, such stimulation evokes unusually long (200 - 500 ms) polysynaptic EPSPs (pEPSPs) in motoneurons, likely due to a loss of descending inhibition (Baker and Chandler 1987; Bennett et al. 2004; Li et al. 2004a), which are sufficient to activate PICs. On the other hand, these pEPSPs, being less than half a second long, are not of sufficient duration to sustain the long-lasting (8-10 second) muscle spasms by themselves. Furthermore, enhanced polysynaptic reflexes emerge immediately after spinal cord transection (Baker and Chandler 1987; Li et al. 2004b), whereas symptoms of spasticity take weeks or months to develop in rats (Bennett et al. 1999a) and humans (Ashby and McCrea 1987; Kuhn and Macht 1948). Therefore, while enhanced polysynaptic reflexes are important as a trigger for the spasms, they are not the underlying source.

1.3 CHARACTERISTICS OF MOTONEURON PERSISTENT INWARD CURRENTS

PICs are considered to be a latent property of spinal motoneurons in normal, uninjured conditions (Heckman et al. 2004), and much of what we know about the role of PICs in normal physiological function comes from studies of whole animal preparations (e.g., decerebrate cat, see below). However, investigations into the ionic make-up and modulation of motoneuron PICs are mostly done in reduced preparations (acutely spinalized or slice) in which, most often, PICs must first be induced by exogenous application of agonists acting on serotonin (5-HT), norepinephrine (NE), acetylcholine or glutamate receptors (Alaburda and Hounsgaard 2003; Delmas et al. 1996; Foehring et al. 1989; Hsiao et al. 1998; Hultborn and Kiehn 1992; Lee and Heckman 1999). From these investigations, we know that the net PIC consists of TTX-sensitive persistent sodium currents (Na PICs) and nimodipine-sensitive persistent calcium currents (Ca PICs) (Carlin et al. 2000b; Hounsgaard and Kiehn 1985; Hsiao et al. 1998; Li and Bennett 2003). The Ca PIC is a measure of the net nimodipine-sensitive current, which comprises the inward current through L-type calcium channels (L-Ca current) and any additional currents activated by the increase in intracellular calcium ion concentration, such as calcium-

activated outward potassium currents (Hounsgaard and Mintz 1988; Llinas and Sugimori 1980a, b; Schwindt and Crill 1980).

1.3.1 Persistent calcium currents: A voltage-dependent persistent calcium (L-Ca) current has been identified in motoneurons of acutely isolated spinal cord slice preparations (mouse: Carlin et al. 2000b; turtle: Hounsgaard and Kiehn 1989; guinea pig: Hsiao et al. 1998; rat: Powers and Binder 2003) and in motoneurons from chronic spinal rats (Li and Bennett 2003). This current is carried by a nimodipine-sensitive voltage-gated calcium channel (Hounsgaard and Kiehn 1989; Hsiao et al. 1998; Mills and Pitman 1997; Morisset and Nagy 1999), with an activation threshold of -45 to -55 mV (Hounsgaard and Kiehn 1989; Mills and Pitman 1997; Morisset and Nagy 1999; Voisin and Nagy 2001; Zhang and Harris-Warrick 1995) and slow activation/inactivation kinetics (Perrier et al. 2002). The characteristics of this channel match that reported for the $Ca_v1.3$ L-type calcium channel (Koschak et al. 2001; Xu and Lipscombe 2001), which is less sensitive to dihydropyridines (Hounsgaard and Kiehn 1989; Mills and Pitman 1997; Voisin and Nagy 2001), and is activated at lower thresholds, than conventional high-voltage activated L-type ($Ca_v1.2$) channels (Fanelli et al. 1994; McCarthy and TanPiengco 1992). Generally, the L-Ca current is not studied in isolation from the opposing calcium-activated outward potassium currents (see below), so most studies of the role of the L-Ca current on motoneuron behaviour actually measure the Ca PIC (combined L-Ca and calcium-activated currents). Due to the slow kinetics and lack of inactivation of these L-type Ca channels, the Ca PIC is a key contributor to motoneuron bistable behaviour. Once activated, the Ca PIC produces a steady depolarizing drive of sufficient amplitude to maintain plateau potentials that outlast the stimulus for several seconds, and which may even require a strong hyperpolarizing input to deactivate (reviewed in Kiehn and Eken 1998). This means that motoneurons can be in two stable, but functionally different, states (hence “bistable”). Therefore, so long as the sodium spike does not inactivate, the motoneuron can continue to fire for long periods following a stimulation due to the steady depolarization provided by the Ca PIC (Hounsgaard et al. 1988). In addition to bistable behaviour, the Ca PIC has also been shown to have a role in amplifying synaptic inputs to the motoneurons by shortening the electrotonic distance and providing an additional intrinsic depolarization triggered by post-synaptic potentials (Bennett et al. 1998; Lee and Heckman 2000; Prather et al. 2001). The poor ability to clamp the Ca PIC and the marked activation/inactivation voltage hysteresis indicate that the Ca PIC is localized to the distal dendrites (Bayliss et al. 1997; Bennett et al. 1998; Booth et al. 1997; Carlin et al. 2000b; Lee and Heckman 1996), where it is ideally situated to boost synaptic signals. Facilitation of the Ca PIC by metabotropic agonists has been well-studied in turtle spinal motoneurons by Hounsgaard and colleagues (see Perrier et al. 2002 for review), as has been described previously for PICs in general. These receptors (serotonergic, noradrenergic, muscarinic and metabotropic glutamate receptors) likely converge onto a single pathway leading to increased intracellular calcium concentrations and activation of calmodulin, both of which facilitate the L-type Ca channels (Perrier et al. 2000; Zuhlke et al. 1999). Thus the input-output gain of the motoneurons, which is heavily influenced by the Ca PIC amplitude, can be adjusted by activity at metabotropic receptors.

1.3.2 Persistent sodium currents: The role of the Na PIC in cell behaviour has been studied in muscle fibres, invertebrate neurons and mammalian neocortical neurons (reviewed in Crill 1996); it has also been characterized more recently in facial and spinal motoneurons (Hsiao et al. 1998; Li and Bennett 2003; Li et al. 2004a; Nishimura et al. 1989). Generally, the Na PIC is a fast-onset TTX-sensitive sodium current, activating a few millivolts below spike threshold and deactivating rapidly relative to the Ca PIC (Angstadt and Choo 1996; Elson and Selverston 1997; Hsiao et al. 1998; Li and Bennett 2003; Rekling and Laursen 1989; Schwindt and Crill 1995; Stafstrom et al. 1982). By activating below spike threshold, the Na PIC amplifies synaptic input (Deisz et al. 1991) and accelerates the membrane potential towards spike threshold (Stafstrom et al. 1982), thus facilitating generation of action potentials. During steady firing, the membrane potential traverses the activation range of the Na PIC between spikes, which led Stafstrom et al. (1982) to suggest that the Na PIC must have a role in sustaining steady repetitive firing. However, study of the function of the Na PIC in normal firing behaviour was tricky because TTX blocks both the persistent Na channels mediating the Na PIC, and the transient Na channels mediating the action potential (Taddese and Bean 2002). In fact, it has been argued that the persistent Na current arises from the same channel mediating the transient Na current, albeit in a different modal state (Alzheimer et al. 1993; Crill 1996), or due to allosteric gating kinetics (Taddese and Bean 2002). However, the two currents can be separated for study using riluzole or very low doses of channel blockers to selectively inhibit the Na PIC, based on the higher sensitivity of the Na PIC to these drugs than the action potential (Stafstrom et al. 1985; Urbani and Belluzzi 2000). Riluzole effectively blocks the Na PIC while still preserving the spike and, in riluzole, neurons are not able to sustain repetitive firing (Miles et al. 2005; Urbani and Belluzzi 2000), supporting the contention that the Na PIC is critical for steady repetitive firing. In spinal motoneurons recorded *in vivo*, Lee and Heckman (2001) showed that a fast persistent current, with properties resembling the Na PIC, is absolutely essential for initiating and sustaining repetitive firing during slow depolarizations. In addition to sustaining steady repetitive firing, Na PICs also enable very slow firing, with interspike intervals much longer than the AHP duration ($\ll 6$ Hz, Li et al. 2004a), and thus Na PICs also determine the minimum firing rate of motoneurons. While neuromodulators (e.g., 5-HT, NE, etc.) are known to facilitate PICs, and the Ca PIC in particular (see above), it is not clear how Na PIC amplitude is normally regulated in spinal motoneurons, nor why the Na PICs are so large after chronic spinal cord injury (Li and Bennett 2003; Li et al. 2004a).

1.3.3 Outward potassium currents: Calcium ion influx through L-type channels is opposed by calcium-activated outward potassium currents (K_{Ca}). These are generally considered to be the same as the SK currents mediating the post-spike afterhyperpolarization (AHP); however, with Ca PICs, the Ca^{2+} influx is through low-threshold L-type calcium channels, not the high-threshold N- and P/Q-type Ca channels activated during the action potential (Hounsgaard and Mintz 1988; Schwindt and Crill 1980). With continued membrane depolarization (as with depolarizing ramps in voltage clamp), continual K_{Ca} channel activation due to increasing $[Ca^{2+}]_i$, combined with the increased driving force of potassium ions, overwhelms the L-Ca current, and the net inward current becomes a large net outward current at potentials above -40 mV. Often, in acutely spinalized preparations, the K_{Ca} currents are so large that the net Ca PIC

measured in motoneurons is very small or non-existent. As such, potassium channel blockers are sometimes added to eliminate the K_{Ca} currents and reveal the underlying persistent inward currents (Carlin et al. 2000a; Llinas and Sugimori 1980b; Powers and Binder 2003; Schwindt and Crill 1980). Current flux through L-type $Ca_v1.3$ channels can be studied in isolation from the K_{Ca} current by addition of apamin, which blocks this potassium channel (Hounsgaard and Mintz 1988); however, pharmacological block of the L-type Ca channels with nimodipine indirectly eliminates the K_{Ca} current, making it difficult to study on its own. As such, some reported effects of neuromodulators, such as 5-HT, on the K_{Ca} current may actually be indirect effects secondary to changes in the L-type Ca current (Bayliss et al. 1997). Some evidence suggests that, in motoneurons, 5-HT reduces the K_{Ca} conductance (i.e., the AHP) directly (Hounsgaard and Kiehn 1989; Wallen et al. 1989). However, with the Hounsgaard & Kiehn study, the observed decrease in AHP amplitude with 5-HT can easily be explained by the increased cell conductance due to PIC activation. Even the indirect effect of 5-HT on the K_{Ca} current identified by Bayliss et al. (1997) was only observed in neonatal rat hypoglossal motoneurons, and not in adults. To date, no study has clearly shown that the K_{Ca} current in adult mammalian spinal motoneurons is affected by 5-HT. In addition to the calcium-activated potassium current, persistent sodium currents may induce a sodium-activated potassium current (K_{Na}) with sufficient accumulation of intracellular Na^+ (Safronov and Vogel 1996). Thus the Na^+ influx through persistent sodium channels may also be opposed by outward K^+ currents, even in nimodipine. No attention has been paid to possible K_{Na} currents in studies of motoneuron PICs to date, perhaps because there is no known pharmacological agent that selectively blocks this current, beyond the general potassium channel blockers. Similar to the convention with the Ca PIC, the term 'Na PIC' refers to the net current resulting from inward sodium currents and any Na^+ -activated currents, if present.

Evidence of plateaus and the underlying PICs has been observed under normal non-pathological conditions, in normal awake rats (Eken and Kiehn 1989; Gorassini et al. 1999) and intact humans (Gorassini et al. 1998; Kiehn and Eken 1997). Indeed, PICs have a fundamental role in normal behaviour, amplifying the gain of excitatory and inhibitory synaptic inputs (Heckman et al. 2003; Hultborn et al. 2003; Lee and Heckman 2000). Further, PICs provide sufficient intrinsic depolarization to generate the motoneuron discharge rates required to drive high force production of muscles, whereas synaptic input alone cannot generate these large depolarizations (Binder 2002, 2003; Lee et al. 2003; Rose and Cushing 1999). The degree of synaptic gain, and bistable behaviour, is proportional to PIC amplitude, which is a major determinant of motoneuron excitability.

1.4 MODULATION OF MOTONEURON PICs BY MONOAMINES

What has become clear from studies to date on motoneuron PICs is that they are facilitated by the monoamines 5-HT and NE, normally supplied by descending brainstem innervation from the caudal raphe and locus coeruleus, respectively (described below, and reviewed in Heckman et al. 2004). Notably, during exercise of intact rats, 5-HT

concentrations in the spinal cord increase by 5-fold compared to at rest (Gerin et al. 1995). This is because, in the normal intact spinal cord, the level of activity in the animal, and in the motoneurons themselves, is linked to the amount of brainstem activity in the serotonergic nuclei that project to the spinal cord. Chronic recordings from medullary serotonergic neurons of the caudal raphe in freely moving cats (reviewed in Jacobs et al. 2002) have shown that these neurons have a slow, steady baseline level of activity during the quiet waking state, but increase their activity with the initiation of locomotor patterns such as stretching or walking (Veasey et al. 1995). Indeed, raphespinal neuron activity increases proportional to the speed of walking on a treadmill, and is tightly coupled to the onset and offset of motor activities. However, during so-called paradoxical sleep, characterized by rapid-eye movements (REM) and muscle paralysis, these neurons become virtually silent (Fornal et al. 1985). Pharmacological block of neural activity in the caudal raphe leads to profound muscle inhibition in these cats similar to the REM sleep state, despite the fact that they are still awake. Conversely, peripheral neuromuscular block has no effect on activity of serotonergic neurons (Steinfels et al. 1983). This indicates that the serotonergic neuron activity is driving motor activity, and not the other way around.

Unlike the raphespinal system, activity in the locus coeruleus (the major source of spinal NE) is not directly coupled to the level of locomotor activity, but is linked to physiological state (Rasmussen et al. 1986). That is, activity in the locus coeruleus is at a minimum during REM sleep (Wu et al. 1999), increases with waking and active states and becomes highly active when stressors are presented (i.e., stressful or arousing situations, Abercrombie and Jacobs 1987). This is in keeping with the known key role of the noradrenergic system in the so-called fight-or-flight response. Thus, NE from brainstem sources provides additional drive to the spinal cord, assisting the serotonergic system in facilitating locomotor activities, especially under stressful circumstances. In fact, norepinephrine receptor agonists are the most effective of the monoamines at initiating hindlimb stepping in cats after complete spinal cord transection (Rossignol et al. 1998).

Targeted destruction of descending serotonergic neurons using 5,7-dihydroxytryptamine (5,7-DHT) leads to reduced locomotor activity in awake mice (Chia et al. 1996) and greatly reduced extensor rigidity in decerebrate cats (Sakai et al. 2000), suggesting a loss of motoneuron excitability. For the noradrenergic system, blocking the supply of NE to the spinal cord does not have the straightforward effects on locomotor behaviour as observed with the serotonergic system. The neurotoxin N(2-chloroethyl)-N-ethyl-2-bromobenzylamine (DSP-4) is often used to selectively destroy noradrenergic neurons, but with mixed results on behaviour. While some investigators have reported DSP-4 to reduce motor activity (Archer and Fredriksson 2000), many have found DSP-4 to have no effect on its own, possibly due to compensation via receptor denervation supersensitivity (Harro et al. 1999) or compensatory activity in other motor systems (Steeves et al. 1980).

The simplest and most effective way to cut off the brainstem supply of monoamines to the spinal cord is by complete spinal cord transection, which initially leads to muscle flaccidity below the lesion and lack of reflex responses, a temporary state often described

as 'spinal shock'. However, after spinalization, artificially increasing monoamine levels in the spinal cord, by injection of 5-HT or NE precursors (Barbeau and Rossignol 1991; Jankowska et al. 1967a, b; Viala and Buser 1971), or transplantation of embryonic serotonergic or noradrenergic neurons near the lumbar cord (Privat et al. 1989; Ribotta et al. 2000; Yakovlev et al. 1989), increases muscle tone and reflexes, and can restore locomotor-like patterns of activity in the hindlimbs. Clearly then, the state of spinal shock is not simply due to the loss of descending motor commands, as these are not restored with such treatments to induce locomotion. Rather, spinal shock most likely arises from the sharp decrease in monoamine tone and resulting loss of motoneuron excitability. Thus, the amount of monoamines available in the spinal cord, whatever the source, determines the ability of motoneurons to function. Low levels of monoamines lead to a loss of motoneuron activity, while high levels of spinal cord monoamines, such as during a fight-or-flight response, result in a high level of motoneuron excitability.

PIC amplitude is a major determinant of motoneuron excitability and, as with locomotor activity, PIC amplitude is controlled by the level of monoaminergic tone in the spinal cord (Lee and Heckman 2000, 1996). Many early studies of motoneuron behaviour were done in anaesthetized cats in which brainstem activity was suppressed by barbiturates, and motoneurons exhibited very little evidence of active persistent inward currents (Granit et al. 1966; Lee and Heckman 2000; Schwindt and Crill 1980). In the unanaesthetized decerebrate cat preparation, the brainstem-spinal cord monoaminergic connections are intact and highly active. In these preparations, motoneurons exhibit large PICs and bistable behaviour (Bennett et al. 1998; Hounsgaard et al. 1988; Lee and Heckman 2000). These PICs can be further augmented when the monoaminergic tone is increased by exogenous application of 5-HT and NE agonists (Bennett et al. 1998; Hounsgaard et al. 1988; Lee and Heckman 2000, 1998). Conversely, PIC-induced bistable behaviour is abolished following acute transection of the spinal cord (which severs the descending monoaminergic connections to the motoneurons) but can be restored by exogenous administration of 5-HT or NE precursors (Conway et al. 1988; Hounsgaard et al. 1988). Therefore, descending monoaminergic brainstem innervation is required for motoneurons to exhibit PICs, and the amount of monoamines present in the spinal cord (the level of monoamine 'tone') determines PIC amplitude and thus motoneuron excitability. This presents a paradox then, because with long-term spinal cord injury, motoneurons again express very large PICs (Li and Bennett 2003), despite the continued absence of descending monoaminergic innervation, which is the major source of monoamines in the spinal cord. Three possible explanations present themselves. Either the level of monoamine tone caudal to the transection increases back to normal levels, or motoneurons develop supersensitivity to residual 5-HT and NE to compensate for the drastically reduced level of monoamines. Alternatively, other endogenous metabotropic agonists such as acetylcholine, glutamate or Substance P, which have been shown to facilitate PICs (Russo et al. 1997; Svirskis and Hounsgaard 1998) and are intrinsic to the spinal cord, could be maintaining the large PICs after chronic SCI in the absence of adequate monoamine tone.

The first possibility can be immediately discounted. By two-months post-injury, the amount of 5-HT and NE in the spinal cord below the lesion is reduced to 2 - 15% of

normal (Schmidt and Jordan 2000), as measured by immunohistochemistry (Cassam et al. 1997; Newton and Hamill 1988), fluorometric analysis (Clineschmidt et al. 1971) or high-pressure liquid chromatography-electrochemical detection (Hadjiconstantinou et al. 1984). What is most interesting about this is not that monoamine levels are greatly reduced, but that there is still a basal level of 5-HT and NE remaining below a complete transection, indicating that there are sources of monoamines intrinsic to the spinal cord and independent of the brainstem. Indeed, careful histology of chronic spinal cords below a complete lesion has identified intraspinal serotonergic and noradrenergic neurons, likely associated with the autonomic system (Cassam et al. 1997; Newton and Hamill 1988). In fact, the number of intraspinal noradrenergic neurons actually appears to increase following SCI (Cassam et al. 1997). Therefore, even in the chronic spinal state, there is still a basal level of monoamine tone innervating the motoneurons. However, with acute injury, this basal level is clearly insufficient to drive motoneuron excitability. The development, over time, of denervation supersensitivity of spinal motoneurons to this residual supply of monoamines would explain the large PICs and high excitability. Indeed, hindlimb reflexes undergo denervation supersensitivity to 5-HT and NE in awake animals in the weeks following SCI (Barbeau and Bedard 1981; Nagano et al. 1988; Nozaki et al. 1977; Tremblay et al. 1985), and dorsal root reflexes, recorded *in vitro*, are supersensitive to 5-HT and NE in the chronic spinal rat (Li et al. 2004b). However, it remains to be tested whether the motoneurons themselves, and PICs in particular, become supersensitive to 5-HT and NE after long-term injury. The alternative hypothesis, that PICs of motoneurons are instead facilitated by other metabotropic agonists (glutamate, acetylcholine, etc.) in the absence of monoamines, remains a possibility, but may be discounted if blockade of monoamine receptor activation of motoneurons in chronic spinal rats completely eliminates the PICs (as we indeed report in later chapters).

1.5 HYPOTHESIS

My central hypothesis is that, in chronic spinal rats, the PICs in spinal motoneurons have increased their sensitivity to monoamine facilitation to compensate for the sharply reduced monoamine tone following spinal cord injury. Thus, in the chronic spinal state, denervation supersensitivity enables the residual intraspinal sources of monoamines to maintain adequate, or even exaggerated, motoneuron excitability. However, because the monoamine tone is not controlled by supraspinal centres, the PICs are tonically large, resulting in long-lasting motor activity (i.e., muscle spasms) with any kind of excitatory input. To validate this hypothesis, several facts must be demonstrated experimentally:

1. There is a lower endogenous level of motoneuron excitability immediately following spinal injury than months after a chronic injury. That is, motoneurons of acute spinal rats have smaller PICs, and are more difficult to activate, than motoneurons of chronic spinal rats.
2. Motoneurons of chronic spinal rats are supersensitive to exogenously applied monoamines. This includes determining whether PICs themselves are facilitated at lower

doses after chronic injury than acute injury, and whether motoneurons also become supersensitive to all known actions of 5-HT.

3. Endogenous intraspinal sources of monoamines maintain the PICs after chronic spinal injury, and the PICs can be blocked by adding antagonists to the specific monoamine receptors involved.

To test my hypothesis, I studied the actions of 5-HT on motoneurons, and on the Na PIC in particular. Over the course of these investigations, I characterized the role of the Na PIC in firing behaviour of spinal motoneurons, largely based on our ability to specifically modulate (increase or decrease) the amplitude of the Na PIC using agonists and antagonists to monoamine receptors, without directly blocking the transient Na spike. These experiments were all performed in the *in vitro* adult sacrocaudal spinal cord preparation, described below, that was developed by Bennett and colleagues to investigate spasticity.

1.6 ANIMAL MODEL OF SPASTICITY

Spasticity following spinal cord injury, while common in humans, has been difficult to study experimentally, because in most animal models the spasticity resulting from SCI is comparatively mild (Ashby and McCreia 1987; Hultborn and Malmsten 1983; Noth 1991; Powers and Rymer 1988; Taylor et al. 1997). Generally, incomplete injuries only lead to mild hyperreflexia in animals (Hultborn and Malmsten 1983), whereas complete transection affecting the hindlimbs is complicated by inconvenient and traumatic functional impairments in hindlimb locomotion and bladder function. This led Ritz and coworkers (1992) to develop a cat model of spasticity that developed in the axial musculature of the tail following low sacrocaudal transection. Although the study of axial musculature has been relatively neglected in general, it is involved in spasticity in humans (cf. back muscles, Stauffer 1974) and should therefore be considered relevant to the spastic syndrome.

Bennett and colleagues (Bennett et al. 1999b; 2001a) investigated complete sacral spinal cord transection in rats and found that a spastic syndrome develops in the tail muscles, complete with classic clinical features of spasticity such as flexor and extensor spasms, hyperreflexia and clonus. One advantage of this low spinal transection is the minimal functional impairment and ease of care due to preservation of bladder function, and unimpaired hindlimb locomotion. A further advantage to investigating the sacrocaudal cord of adult rats is that it is small enough to remove and maintain whole *in vitro* (Bennett et al. 2001b), allowing study of physiological changes in reflexes and motoneuron properties that occur with chronic spinal cord injury. Using this model, Bennett and colleagues have demonstrated that the plateaus and PICs in motoneurons below a complete transection recover spontaneously in the weeks following injury (Bennett et al. 2001b; Li and Bennett 2003). These PICs are mediated by a low-threshold L-type calcium current (Ca PIC) and a TTX-sensitive persistent sodium current (Na PIC), as described earlier (Li and Bennett 2003). The recovered excitability due to re-

emergence of large PICs, combined with the loss of descending inhibition of spinal reflexes, results in large long-lasting exaggerated reflexes or spasms in response to brief afferent input (Bennett et al. 2004; Li et al. 2004a; 2004b). Thus, using this model, Bennett and colleagues have clearly shown that the long-lasting muscle spasms characteristic of spinal cord spasticity are due to the re-emergence of large PICs in the motoneurons themselves, and are not merely due to changes in reflex pathways.

1.7 THESIS OUTLINE

My thesis project involved using the Bennett animal model to test the influence of metabotropic receptor activation on spinal motoneuron PICs. The working hypothesis was that motoneurons of chronic spinal rats become supersensitive to residual intraspinal monoamine sources to compensate for the loss of supraspinal monoamine sources, and this leads to large tonically active PICs and the resulting symptoms of spasticity following long-term SCI. I specifically studied the effects of 5-HT receptor activity on motoneuron PICs and other membrane properties, and on the Na PIC in particular. My thesis has been organised into three chapters. The first chapter, entitled “Persistent sodium currents and repetitive firing in motoneurons of the sacrocaudal spinal cord of adult rats”, compares the cell properties of motoneurons immediately following spinal transection (acute spinal condition) to motoneurons in rats after long-term injury (chronic spinal condition), and quantifies the ionic components of the PICs in both. In particular, the role of the Na PIC in motoneuron firing behaviour is characterized. The second chapter, entitled “Serotonin facilitates persistent sodium currents in motoneurons, and chronic spinal cord transection leads to a supersensitivity to serotonin”, quantifies the effect of 5-HT receptor activation on membrane properties and PICs, and investigates the changes in motoneuron sensitivity to 5-HT receptor agonists following chronic spinal transection. Specifically, it reports that motoneurons of chronic spinal rats are supersensitive to 5-HT receptor activation, and that 5-HT₂ receptor activation selectively enhances the Na PIC. Furthermore, facilitation of the Na PIC by 5-HT receptor agonists correlates with improved repetitive firing ability. The third chapter, entitled “Endogenous monoamines are essential for persistent sodium currents and repetitive firing in rat spinal motoneurons”, examines the effect of blocking activity at the 5-HT₂ receptors on Na PICs and motoneuron firing. Antagonists to the 5-HT₂ receptors reduce Na PIC amplitude, despite the absence of previously applied exogenous agonists, indicating that endogenous intraspinal serotonin facilitates the Na PIC. Notably, activity at both 5-HT₂ receptors and α 1-norepinephrine (α 1-NE) receptors has to be blocked simultaneously to completely eliminate the Na PIC, indicating endogenous norepinephrine also facilitates the Na PIC. All repetitive firing during slow depolarizations was also eliminated with blockade of 5-HT₂ and α 1-NE receptor activity, thus demonstrating the critical role of monoamines in facilitating the Na PIC and repetitive firing ability. The combined evidence presented in this thesis supports the hypothesis that motoneurons become supersensitive to 5-HT with chronic spinal cord injury, and intraspinal sources of 5-HT and NE maintain the large Na PICs seen in motoneurons of chronic spinal rats that contribute to spasticity. It remains to be determined whether the Ca PIC is also supersensitive to 5-HT and can be blocked by

monoamine antagonists. Nevertheless, my thesis supports the argument that motoneuron denervation supersensitivity to intraspinal 5-HT and NE is responsible for the muscle spasms characteristic of spasticity due to spinal cord injury.

1.8 BIBLIOGRAPHY FOR CHAPTER 1

Abbruzzese G. The medical management of spasticity. *Eur J Neurol* 9 Suppl 1: 30-34; discussion 53-61, 2002.

Abercrombie ED and Jacobs BL. Single-unit response of noradrenergic neurons in the locus coeruleus of freely moving cats. I. Acutely presented stressful and nonstressful stimuli. *J Neurosci* 7: 2837-2843, 1987.

Ackery A, Tator C, and Krassioukov A. A global perspective on spinal cord injury epidemiology. *J Neurotrauma* 21: 1355-1370, 2004.

Alaburda A and Hounsgaard J. Metabotropic modulation of motoneurons by scratch-like spinal network activity. *J Neurosci* 23: 8625-8629, 2003.

Alzheimer C, Schwandt PC, and Crill WE. Modal gating of Na⁺ channels as a mechanism of persistent Na⁺ current in pyramidal neurons from rat and cat sensorimotor cortex. *J Neurosci* 13: 660-673, 1993.

Angstadt JD and Choo JJ. Sodium-dependent plateau potentials in cultured Retzius cells of the medicinal leech. *J Neurophysiol* 76: 1491-1502, 1996.

Archer T and Fredriksson A. Effects of clonidine and alpha-adrenoceptor antagonists on motor activity in DSP4-treated mice I: dose-, time- and parameter-dependency. *Neurotox Res* 1: 235-247, 2000.

Ashby P and McCrea DA. Neurophysiology of spinal spasticity. In: *Handbook of the Spinal Cord*, edited by Davidoff RA. New York: Marcel Dekker Inc., 1987, p. 120-143.

Baker LL and Chandler SH. Characterization of postsynaptic potentials evoked by sural nerve stimulation in hindlimb motoneurons from acute and chronic spinal cats. *Brain Res* 420: 340-350, 1987.

Barbeau H and Bedard P. Denervation supersensitivity to 5-hydroxytryptophan in rats following spinal transection and 5,7-dihydroxytryptamine injection. *Neuropharmacology* 20: 611-616, 1981.

Barbeau H and Rossignol S. Initiation and modulation of the locomotor pattern in the adult chronic spinal cat by noradrenergic, serotonergic and dopaminergic drugs. *Brain Res* 546: 250-260, 1991.

Bayliss DA, Viana F, Talley EM, and Berger AJ. Neuromodulation of hypoglossal motoneurons: cellular and developmental mechanisms. *Respir Physiol* 110: 139-150, 1997.

Bennett DJ, Gorassini M, Fouad K, Sanelli L, Han Y, and Cheng J. Spasticity in rats with sacral spinal cord injury. *J Neurotrauma* 16: 69-84, 1999a.

- Bennett DJ, Gorassini MA, and Siu M. In vitro preparation to study spasticity in chronic spinal rats. *Soc Neuroscience Abst* 25: 1394, 1999b.
- Bennett DJ, Hultborn H, Fedirchuk B, and Gorassini M. Synaptic activation of plateaus in hindlimb motoneurons of decerebrate cats. *J Neurophysiol* 80: 2023-2037, 1998.
- Bennett DJ, Li Y, Harvey PJ, and Gorassini M. Evidence for plateau potentials in tail motoneurons of awake chronic spinal rats with spasticity. *J Neurophysiol* 86: 1972-1982, 2001a.
- Bennett DJ, Li Y, and Siu M. Plateau potentials in sacrocaudal motoneurons of chronic spinal rats, recorded in vitro. *J Neurophysiol* 86: 1955-1971, 2001b.
- Bennett DJ, Sanelli L, Cooke CL, Harvey PJ, and Gorassini MA. Spastic long-lasting reflexes in the awake rat after sacral spinal cord injury. *J Neurophysiol* 91: 2247-2258, 2004.
- Binder MD. Integration of synaptic and intrinsic dendritic currents in cat spinal motoneurons. *Brain Res Brain Res Rev* 40: 1-8, 2002.
- Binder MD. Intrinsic dendritic currents make a major contribution to the control of motoneurone discharge. *J Physiol* 552: 665, 2003.
- Booth V, Rinzel J, and Kiehn O. Compartmental model of vertebrate motoneurons for Ca²⁺-dependent spiking and plateau potentials under pharmacological treatment. *J Neurophysiol* 78: 3371-3385, 1997.
- Carlin KP, Jiang Z, and Brownstone RM. Characterization of calcium currents in functionally mature mouse spinal motoneurons. *Eur J Neurosci* 12: 1624-1634, 2000a.
- Carlin KP, Jones KE, Jiang Z, Jordan LM, and Brownstone RM. Dendritic L-type calcium currents in mouse spinal motoneurons: implications for bistability. *Eur J Neurosci* 12: 1635-1646, 2000b.
- Cassam AK, Llewellyn-Smith IJ, and Weaver LC. Catecholamine enzymes and neuropeptides are expressed in fibres and somata in the intermediate gray matter in chronic spinal rats. *Neuroscience* 78: 829-841, 1997.
- Chia LG, Ni DR, Cheng LJ, Kuo JS, Cheng FC, and Dryhurst G. Effects of 1-methyl-4-phenyl-1,2,3,6-tetrahydropyridine and 5,7-dihydroxytryptamine on the locomotor activity and striatal amines in C57BL/6 mice. *Neurosci Lett* 218: 67-71, 1996.
- Clineschmidt BV, Pierce JE, and Lovenberg L. Tryptophan hydroxylase and serotonin in spinal cord and brain stem before and after chronic transection. *J Neurochem* 18: 1593-1596, 1971.

Conway BA, Hultborn H, Kiehn O, and Mintz I. Plateau potentials in alpha-motoneurons induced by intravenous injection of L-dopa and clonidine in the spinal cat. *J Physiol* 405: 369-384, 1988.

Crill WE. Persistent sodium current in mammalian central neurons. *Annu Rev Physiol* 58: 349-362, 1996.

Deisz RA, Fortin G, and Zieglansberger W. Voltage dependence of excitatory postsynaptic potentials of rat neocortical neurons. *J Neurophysiol* 65: 371-382, 1991.

Delmas P, Niel JP, and Gola M. Muscarinic activation of a novel voltage-sensitive inward current in rabbit prevertebral sympathetic neurons. *Eur J Neurosci* 8: 598-610, 1996.

Delwaide PJ and Pennisi G. Tizanidine and electrophysiologic analysis of spinal control mechanisms in humans with spasticity. *Neurology* 44: S21-27; discussion S27-28, 1994.

Duncan GW, Shahani BT, and Young RR. An evaluation of baclofen treatment for certain symptoms in patients with spinal cord lesions. A double-blind, cross-over study. *Neurology* 26: 441-446, 1976.

Eken T, Hultborn H, and Kiehn O. Possible functions of transmitter-controlled plateau potentials in alpha motoneurons. *Prog Brain Res* 80: 257-267; discussion 239-242, 1989.

Eken T and Kiehn O. Bistable firing properties of soleus motor units in unrestrained rats. *Acta Physiol Scand* 136: 383-394, 1989.

Elson RC and Selverston AI. Evidence for a persistent Na⁺ conductance in neurons of the gastric mill rhythm generator of spiny lobsters. *J Exp Biol* 200 (Pt 12): 1795-1807, 1997.

Faist M, Mazevet D, Dietz V, and Pierrot-Deseilligny E. A quantitative assessment of presynaptic inhibition of Ia afferents in spastics. Differences in hemiplegics and paraplegics. *Brain* 117 (Pt 6): 1449-1455, 1994.

Fanelli RJ, McCarthy RT, and Chisholm J. Neuropharmacology of nimodipine: from single channels to behavior. *Ann N Y Acad Sci* 747: 336-350, 1994.

Foehring RC, Schwindt PC, and Crill WE. Norepinephrine selectively reduces slow Ca²⁺- and Na⁺-mediated K⁺ currents in cat neocortical neurons. *J Neurophysiol* 61: 245-256, 1989.

Fornal C, Auerbach S, and Jacobs BL. Activity of serotonin-containing neurons in nucleus raphe magnus in freely moving cats. *Exp Neurol* 88: 590-608, 1985.

Gerin C, Becquet D, and Privat A. Direct evidence for the link between monoaminergic descending pathways and motor activity. I. A study with microdialysis probes implanted in the ventral funiculus of the spinal cord. *Brain Res* 704: 191-201, 1995.

- Gorassini M, Bennett DJ, Kiehn O, Eken T, and Hultborn H. Activation patterns of hindlimb motor units in the awake rat and their relation to motoneuron intrinsic properties. *J Neurophysiol* 82: 709-717, 1999.
- Gorassini MA, Bennett DJ, and Yang JF. Self-sustained firing of human motor units. *Neurosci Lett* 247: 13-16, 1998.
- Gorassini MA, Knash ME, Harvey PJ, Bennett DJ, and Yang JF. Role of motoneurons in the generation of muscle spasms after spinal cord injury. *Brain* 127: 2247-2258, 2004.
- Granit R, Kernell D, and Lamarre Y. Algebraical summation in synaptic activation of motoneurons firing within the 'primary range' to injected currents. *J Physiol* 187: 379-399, 1966.
- Hadjiconstantinou M, Panula P, Lackovic Z, and Neff NF. Spinal cord serotonin: A biochemical and immunohistochemical study following transection. *Brain Res* 322: 245-254, 1984.
- Harkema SJ. Neural plasticity after human spinal cord injury: application of locomotor training to the rehabilitation of walking. *Neuroscientist* 7: 455-468, 2001.
- Harro J, Pahkla R, Modiri AR, Harro M, Kask A, and Oreland L. Dose-dependent effects of noradrenergic denervation by DSP-4 treatment on forced swimming and beta-adrenoceptor binding in the rat. *J Neural Transm* 106: 619-629, 1999.
- Heckman CJ, Gorassini MA, and Bennett DJ. Persistent inward currents in motoneuron dendrites: Implications for motor output. *Muscle Nerve* 31: 135-156, 2004.
- Heckman CJ, Lee RH, and Brownstone RM. Hyperexcitable dendrites in motoneurons and their neuromodulatory control during motor behavior. *Trends Neurosci* 26: 688-695, 2003.
- Hiersemenzel LP, Curt A, and Dietz V. From spinal shock to spasticity: neuronal adaptations to a spinal cord injury. *Neurology* 54: 1574-1582, 2000.
- Hounsgaard J, Hultborn H, Jespersen B, and Kiehn O. Bistability of alpha-motoneurons in the decerebrate cat and in the acute spinal cat after intravenous 5-hydroxytryptophan. *J Physiol* 405: 345-367, 1988.
- Hounsgaard J and Kiehn O. Ca⁺⁺ dependent bistability induced by serotonin in spinal motoneurons. *Exp Brain Res* 57: 422-425, 1985.
- Hounsgaard J and Kiehn O. Serotonin-induced bistability of turtle motoneurons caused by a nifedipine-sensitive calcium plateau potential. *J Physiol* 414: 265-282, 1989.
- Hounsgaard J and Mintz I. Calcium conductance and firing properties of spinal motoneurons in the turtle. *J Physiol* 398: 591-603, 1988.

- Hsiao CF, Del Negro CA, Trueblood PR, and Chandler SH. Ionic basis for serotonin-induced bistable membrane properties in guinea pig trigeminal motoneurons. *J Neurophysiol* 79: 2847-2856, 1998.
- Hultborn H, Denton ME, Wienecke J, and Nielsen JB. Variable amplification of synaptic input to cat spinal motoneurons by dendritic persistent inward current. *J Physiol* 552: 945-952, 2003.
- Hultborn H and Kiehn O. Neuromodulation of vertebrate motor neuron membrane properties. *Curr Opin Neurobiol* 2: 770-775, 1992.
- Hultborn H and Malmsten J. Changes in segmental reflexes following chronic spinal cord hemisection in the cat. I. Increased monosynaptic and polysynaptic ventral root discharges. *Acta Physiol Scand* 119: 405-422, 1983.
- Jacobs BL, Martin-Cora FJ, and Fomal CA. Activity of medullary serotonergic neurons in freely moving animals. *Brain Res Brain Res Rev* 40: 45-52, 2002.
- Jankowska E, Jukes MG, Lund S, and Lundberg A. The effect of DOPA on the spinal cord. 5. Reciprocal organization of pathways transmitting excitatory action to alpha motoneurons of flexors and extensors. *Acta Physiol Scand* 70: 369-388, 1967a.
- Jankowska E, Jukes MG, Lund S, and Lundberg A. The effect of DOPA on the spinal cord. 6. Half-centre organization of interneurons transmitting effects from the flexor reflex afferents. *Acta Physiol Scand* 70: 389-402, 1967b.
- Kawamura J, Ise M, and Tagami M. The clinical features of spasms in patients with a cervical cord injury. *Paraplegia* 27: 222-226, 1989.
- Kiehn O and Eken T. Functional role of plateau potentials in vertebrate motor neurons. *Curr Opin Neurobiol* 8: 746-752, 1998.
- Kiehn O and Eken T. Prolonged firing in motor units: evidence of plateau potentials in human motoneurons? *J Neurophysiol* 78: 3061-3068, 1997.
- Kita M and Goodkin DE. Drugs used to treat spasticity. *Drugs* 59: 487-495, 2000.
- Koschak A, Reimer D, Huber I, Grabner M, Glossmann H, Engel J, and Striessnig J. alpha 1D (Cav1.3) subunits can form l-type Ca²⁺ channels activating at negative voltages. *J Biol Chem* 276: 22100-22106, 2001.
- Kuhn RA and Macht MB. Some manifestations of reflex activity in spinal man with particular reference to the occurrence of extensor spasm. *Bull Johns Hopkins Hosp* 84: 43-75, 1948.
- Lance JW. Symposium Synopsis. *Spasticity Disordered Motor Control*, edited by Feldman RG, Young RR and Koella WP. Yearbook Medical, Chicago, 1980, p. 485-494.

- Lee RH and Heckman CJ. Adjustable amplification of synaptic input in the dendrites of spinal motoneurons in vivo. *J Neurosci* 20: 6734-6740, 2000.
- Lee RH and Heckman CJ. Bistability in spinal motoneurons in vivo: systematic variations in persistent inward currents. *J Neurophysiol* 80: 583-593, 1998.
- Lee RH and Heckman CJ. Enhancement of bistability in spinal motoneurons in vivo by the noradrenergic alpha1 agonist methoxamine. *J Neurophysiol* 81: 2164-2174, 1999.
- Lee RH and Heckman CJ. Influence of voltage-sensitive dendritic conductances on bistable firing and effective synaptic current in cat spinal motoneurons in vivo. *J Neurophysiol* 76: 2107-2110, 1996.
- Lee RH, Kuo JJ, Jiang MC, and Heckman CJ. Influence of active dendritic currents on input-output processing in spinal motoneurons in vivo. *J Neurophysiol* 89: 27-39, 2003.
- Li Y and Bennett DJ. Persistent sodium and calcium currents cause plateau potentials in motoneurons of chronic spinal rats. *J Neurophysiol* 90: 857-869, 2003.
- Li Y, Gorassini MA, and Bennett DJ. Role of persistent sodium and calcium currents in motoneuron firing and spasticity in chronic spinal rats. *J Neurophysiol* 91: 767-783, 2004a.
- Li Y, Harvey PJ, Li X, and Bennett DJ. Spastic long-lasting reflexes of the chronic spinal rat studied in vitro. *J Neurophysiol* 91: 2236-2246, 2004b.
- Little JW, Micklesen P, Umlauf R, and Britell C. Lower extremity manifestations of spasticity in chronic spinal cord injury. *Am J Phys Med Rehabil* 68: 32-36, 1989.
- Llinas R and Sugimori M. Electrophysiological properties of in vitro Purkinje cell dendrites in mammalian cerebellar slices. *J Physiol* 305: 197-213, 1980a.
- Llinas R and Sugimori M. Electrophysiological properties of in vitro Purkinje cell somata in mammalian cerebellar slices. *J Physiol* 305: 171-195, 1980b.
- McCarthy RT and TanPiengco PE. Multiple types of high-threshold calcium channels in rabbit sensory neurons: high-affinity block of neuronal L-type by nimodipine. *J Neurosci* 12: 2225-2234, 1992.
- Miles GB, Dai Y, and Brownstone RM. Mechanisms underlying the early phase of spike frequency adaptation in mouse spinal motoneurons. *J Physiol*, 2005.
- Mills JD and Pitman RM. Electrical properties of a cockroach motor neuron soma depend on different characteristics of individual Ca components. *J Neurophysiol* 78: 2455-2466, 1997.
- Morisset V and Nagy F. Ionic basis for plateau potentials in deep dorsal horn neurons of the rat spinal cord. *J Neurosci* 19: 7309-7316, 1999.

- Nagano N, Ono H, Ozawa M, and Fukuda H. The spinal reflex of chronic spinal rats is supersensitive to 5-HTP but not to TRH or 5-HT agonists. *Eur J Pharmacol* 149: 337-344, 1988.
- Newton BW and Hamill RW. The morphology and distribution of rat serotonergic intraspinal neurons: an immunohistochemical study. *Brain Res Bull* 20: 349-360, 1988.
- NINDS. Spasticity Information Page: National Institutes of Health: National Institute of Neurological Disorders and Stroke, 2005.
- Nishimura Y, Schwindt PC, and Crill WE. Electrical properties of facial motoneurons in brainstem slices from guinea pig. *Brain Res* 502: 127-142, 1989.
- Norman KE, Pepin A, and Barbeau H. Effects of drugs on walking after spinal cord injury. *Spinal Cord* 36: 699-715, 1998.
- Noth J. Trends in the pathophysiology and pharmacotherapy of spasticity. *J Neurol* 238: 131-139, 1991.
- Nozaki M, Bell JA, Vaupel DB, and Martin WR. Responses of the flexor reflex to LSD, tryptamine, 5-hydroxytryptophan, methoxamine, and d-amphetamine in acute and chronic spinal rats. *Psychopharmacology (Berl)* 55: 13-18, 1977.
- Perrier JF, Alaburda A, and Hounsgaard J. Spinal plasticity mediated by postsynaptic L-type Ca²⁺ channels. *Brain Res Brain Res Rev* 40: 223-229, 2002.
- Perrier JF, Mejia-Gervacio S, and Hounsgaard J. Facilitation of plateau potentials in turtle motoneurons by a pathway dependent on calcium and calmodulin. *J Physiol* 528 Pt 1: 107-113, 2000.
- Powers RK and Binder MD. Input-output functions of mammalian motoneurons. *Rev Physiol Biochem Pharmacol* 143: 137-263, 2001.
- Powers RK and Binder MD. Persistent sodium and calcium currents in rat hypoglossal motoneurons. *J Neurophysiol* 89: 615-624, 2003.
- Powers RK and Rymer WZ. Effects of acute dorsal spinal hemisection on motoneuron discharge in the medial gastrocnemius of the decerebrate cat. *J Neurophysiol* 59: 1540-1556, 1988.
- Prather JF, Powers RK, and Cope TC. Amplification and linear summation of synaptic effects on motoneuron firing rate. *J Neurophysiol* 85: 43-53, 2001.
- Privat A, Mansour H, Rajaofetra N, and Geffard M. Intraspinous transplants of serotonergic neurons in the adult rat. *Brain Res Bull* 22: 123-129, 1989.

- Rasmussen K, Morilak DA, and Jacobs BL. Single unit activity of locus coeruleus neurons in the freely moving cat. I. During naturalistic behaviors and in response to simple and complex stimuli. *Brain Res* 371: 324-334, 1986.
- Rekling JC and Laursen AM. Evidence for a persistent sodium conductance in neurons from the nucleus prepositus hypoglossi. *Brain Res* 500: 276-286, 1989.
- Ribotta MG, Provencher J, Feraboli-Lohnherr D, Rossignol S, Privat A, and Orsal D. Activation of locomotion in adult chronic spinal rats is achieved by transplantation of embryonic raphe cells reinnervating a precise lumbar level. *J Neurosci* 20: 5144-5152, 2000.
- Rice GP. Pharmacotherapy of spasticity: some theoretical and practical considerations. *Can J Neurol Sci* 14: 510-512, 1987.
- Ritz LA, Friedman RM, Rhoton EL, Sparkes ML, and Vierck CJJ. Lesions of cat sacrocaudal spinal cord: a minimally disruptive model of injury. *J Neurotrauma* 9: 219-230, 1992.
- Rose PK and Cushing S. Non-linear summation of synaptic currents on spinal motoneurons: lessons from simulations of the behaviour of anatomically realistic models. *Prog Brain Res* 123: 99-107, 1999.
- Rossignol S, Chau C, Brustein E, Giroux N, Bouyer L, Barbeau H, and Reader TA. Pharmacological activation and modulation of the central pattern generator for locomotion in the cat. *Ann N Y Acad Sci* 860: 346-359, 1998.
- Russo RE, Nagy F, and Hounsgaard J. Modulation of plateau properties in dorsal horn neurones in a slice preparation of the turtle spinal cord. *J Physiol* 499 (Pt 2): 459-474, 1997.
- Safronov BV and Vogel W. Properties and functions of Na(+)-activated K⁺ channels in the soma of rat motoneurons. *J Physiol* 497 (Pt 3): 727-734, 1996.
- Sakai M, Matsunaga M, Kubota A, Yamanishi Y, and Nishizawa Y. Reduction in excessive muscle tone by selective depletion of serotonin in intercollicularly decerebrated rats. *Brain Res* 860: 104-111, 2000.
- Schmidt BJ and Jordan LM. The role of serotonin in reflex modulation and locomotor rhythm production in the mammalian spinal cord. *Brain Res Bull* 53: 689-710, 2000.
- Schwindt PC and Crill WE. Amplification of synaptic current by persistent sodium conductance in apical dendrite of neocortical neurons. *J Neurophysiol* 74: 2220-2224, 1995.
- Schwindt PC and Crill WE. Properties of a persistent inward current in normal and TEA-injected motoneurons. *J Neurophysiol* 43: 1700-1724, 1980.

- Stafstrom CE, Schwindt PC, Chubb MC, and Crill WE. Properties of persistent sodium conductance and calcium conductance of layer V neurons from cat sensorimotor cortex in vitro. *J Neurophysiol* 53: 153-170, 1985.
- Stafstrom CE, Schwindt PC, and Crill WE. Negative slope conductance due to a persistent subthreshold sodium current in cat neocortical neurons in vitro. *Brain Res* 236: 221-226, 1982.
- Stauffer ES. Trauma. In: *Spinal Deformity in Neurological and Muscular Disorders*, edited by Hardy JH. St, Louis: C.V. Mosby, 1974, p. 219 - 239.
- Steeves JD, Schmidt BJ, Skovgaard BJ, and Jordan LM. Effect of noradrenaline and 5-hydroxytryptamine depletion on locomotion in the cat. *Brain Res* 185: 349-362, 1980.
- Steinfelds GF, Heym J, Strecker RE, and Jacobs BL. Raphe unit activity in freely moving cats is altered by manipulations of central but not peripheral motor systems. *Brain Res* 279: 77-84, 1983.
- Svirskis G and Hounsgaard J. Transmitter regulation of plateau properties in turtle motoneurons. *J Neurophysiol* 79: 45-50, 1998.
- Taddese A and Bean BP. Subthreshold sodium current from rapidly inactivating sodium channels drives spontaneous firing of tuberomammillary neurons. *Neuron* 33: 587-600, 2002.
- Taylor JS, Friedman RF, Munson JB, and Vierck CJJ. Stretch hyperreflexia of triceps surae muscles in the conscious cat after dorsolateral spinal lesions. *J Neurosci* 17: 5004-5015, 1997.
- Tremblay LE, Bedard PJ, Maheux R, and Di Paolo T. Denervation supersensitivity to 5-hydroxytryptamine in the rat spinal cord is not due to the absence of 5-hydroxytryptamine. *Brain Res* 330: 174-177, 1985.
- Urbani A and Belluzzi O. Riluzole inhibits the persistent sodium current in mammalian CNS neurons. *Eur J Neurosci* 12: 3567-3574, 2000.
- Veasey SC, Fornal CA, Metzler CW, and Jacobs BL. Response of serotonergic caudal raphe neurons in relation to specific motor activities in freely moving cats. *J Neurosci* 15: 5346-5359, 1995.
- Viala D and Buser P. [Methods of obtaining locomotor rhythms in the spinal rabbit by pharmacological treatments (DOPA, 5-HTP, D-amphetamine)]. *Brain Res* 35: 151-165, 1971.
- Voisin DL and Nagy F. Sustained L-type calcium currents in dissociated deep dorsal horn neurons of the rat: characteristics and modulation. *Neuroscience* 102: 461-472, 2001.

Wallen P, Buchanan JT, Grillner S, Hill RH, Christenson J, and Hokfelt T. Effects of 5-hydroxytryptamine on the afterhyperpolarization, spike frequency regulation, and oscillatory membrane properties in lamprey spinal cord neurons. *J Neurophysiol* 61: 759-768, 1989.

Wu MF, Gulyani SA, Yau E, Mignot E, Phan B, and Siegel JM. Locus coeruleus neurons: cessation of activity during cataplexy. *Neuroscience* 91: 1389-1399, 1999.

Xu W and Lipscombe D. Neuronal Ca(V)1.3alpha(1) L-type channels activate at relatively hyperpolarized membrane potentials and are incompletely inhibited by dihydropyridines. *J Neurosci* 21: 5944-5951, 2001.

Yakovleff A, Roby-Brami A, Guezard B, Mansour H, Bussel B, and Privat A. Locomotion in rats transplanted with noradrenergic neurons. *Brain Res Bull* 22: 115-121, 1989.

Young RR. Spasticity: a review. *Neurol* 44: S12-S20, 1994.

Zhang B and Harris-Warrick RM. Calcium-dependent plateau potentials in a crab stomatogastric ganglion motor neuron. I. Calcium current and its modulation by serotonin. *J Neurophysiol* 74: 1929-1937, 1995.

Zuhlke RD, Pitt GS, Deisseroth K, Tsien RW, and Reuter H. Calmodulin supports both inactivation and facilitation of L-type calcium channels. *Nature* 399: 159-162, 1999.

CHAPTER 2: Persistent sodium currents and repetitive firing in motoneurons of the sacrocaudal spinal cord of adult rats.

2.1 BACKGROUND

Spinal motoneurons possess voltage-gated persistent sodium and calcium currents (persistent inward currents, PICs) that are activated at low thresholds just above the resting membrane potential. These PICs play a major role in amplifying synaptic inputs (Deisz et al. 1991; Prather et al. 2001) and sustaining repetitive firing (Lee and Heckman 1998a, b; Schwandt and Crill 1982). PICs in motoneurons are strongly facilitated by the monoamines serotonin (5-HT: Hounsgaard and Kiehn 1989; Perrier and Hounsgaard 2003) and norepinephrine (NE: Lee and Heckman 1999), consistent with the dense monoamine innervation of motoneurons (Alvarez et al. 1998; Schroder and Skagerberg 1985). Most, but not all, 5-HT and NE in the spinal cord derives from descending brainstem tracts, and accordingly motoneurons in brainstem-intact animals (Hounsgaard et al. 1988a) and humans (Gorassini et al. 1998; Kiehn and Eken 1997) exhibit bistable behaviours consistent with large PICs. That is, PICs are large enough to produce sustained depolarizations (plateaus) and firing (self-sustained firing) that, because PICs are voltage-gated, can be turned on or off by brief excitatory or inhibitory inputs (bistable behaviour). Spinal transection immediately eliminates such bistable behaviour, likely due to the loss of brainstem-induced release of monoamines onto motoneurons because bistable behaviour can be recovered by exogenous application of monoamines (Conway et al. 1988; Hounsgaard et al. 1988a). However, PICs are not completely eliminated by an acute spinal transection; they are usually just reduced enough to stop bistable behaviour (Bennett et al. 2001).

In motoneurons of acute spinal rats the contributions of persistent sodium currents (Na PICs) and persistent calcium currents (Ca PICs) to the total PIC have thus far not been quantified, and thus we do not know whether the loss of PICs with spinal transection mainly results from a loss of Ca PICs, or Na PICs, or both. We do know that with long-term spinal injury (chronic spinal rat) large PICs return (Bennett et al. 2001; Li and Bennett 2003), and these include both large Na and Ca PICs of about equal size. It remains to be determined if the Na and Ca PIC are also present in equal proportions in acute spinal rats. Thus, one of our objectives was to quantify the Na and Ca PICs in motoneurons of acute spinal rats, and compare these to the PICs found in chronic spinal rats (Li and Bennett 2003) and other motoneurons of acutely isolated spinal cord slice preparations (motoneurons from different muscles. Turtle: Hounsgaard and Kiehn 1989; guinea pig: Hsiao et al. 1998; rat: Powers and Binder 2003). For this we recorded PICs in motoneurons in an *in vitro* preparation (Bennett et al. 2001), where the sacrocaudal spinal cord was acutely removed from normal adult rats (acute spinal).

Previously, the persistent sodium current (Na PIC) has been argued to play a critical role in repetitive firing in motoneurons (Lee and Heckman 2001; Li et al. 2004a). Without a fast persistent inward current, like the Na PIC, repetitive firing is disrupted in motoneurons (Lee and Heckman 2001), as has been shown in other neurons (French et al. 1990; Urbani and Belluzzi 2000). In the course of quantifying the Na PICs in acute spinal rats, we found that,

although on average the Na PIC was small, a considerable variability existed in the Na PIC amplitude: some rats had little or no Na PIC and others had moderately large Na PICs. Thus, a second objective of our study was to examine how variations in the size of Na PICs affected the repetitive firing ability of motoneurons. We found that the Na PIC was absolutely essential for repetitive firing, in that the few motoneurons that lacked Na PICs also had no ability to produce steady repetitive firing even though they otherwise appeared to be healthy motoneurons with normal fast sodium spikes.

This chapter forms the basis for the two subsequent chapters (Harvey et al. 2005a, b) in which we examined how monoamine receptors modulate the Na PICs in the motoneurons of the present study. There, we found that 5-HT application facilitated the Na PIC in acute spinal rats and, importantly, could rescue a cell that was initially without firing ability, by producing a Na PIC and thereby enabling repetitive firing (Harvey et al. 2005a). Furthermore, we showed that 5-HT and NE receptor antagonists could completely eliminate the Na PIC in both acute and chronic spinal rats (Harvey et al. 2005b). Thus, despite the loss of brainstem-derived monoamines, spinal sources of monoamines (reviewed in Schmidt and Jordan 2000) must play a primary role in facilitating the Na PIC, and ultimately enable motoneurons to fire repetitively.

2.2 METHODS

Intracellular recordings were made from motoneurons in the *in vitro* sacrocaudal spinal cord of both normal adult rats (female Sprague-Dawley; 1 – 6 months old, average age = 3.4 ± 1.2 months, $n = 41$) and spastic adult rats with chronic spinal cord injury (3 – 5 months old, average age = 4.0 ± 0.6 months, $n = 34$). When the sacrocaudal cord was removed from normal rats for this *in vitro* recording, the cord was transected at the S2 level at the time of removal; thus these 41 rats were termed acute spinal rats. For the spastic chronic spinal rat, a complete spinal cord transection was made at the S2 sacral level when the adult rat was 40 to 55 days old (Bennett et al. 1999; Bennett et al. 2001b,c). Usually, within 1 month, dramatic spasticity developed in the tail muscles, which are innervated by sacrocaudal motoneurons below the level of the injury. Only rats more than 1.5 months and less than 4 months post-injury, and with clear spasticity, were used for *in vitro* recording of the motoneurons (the 34 chronic spinal rats). Bennett et al. (1999) describe the details of the chronic spinal transection and spasticity assessment. All experimental procedures were conducted in accordance with guidelines for the ethical treatment of animals issued by the Canadian Council on Animal Care, and approved by the University of Alberta Health Sciences Animal Policy and Welfare Committee.

2.2.1 *In vitro* preparation

Details of the *in vitro* procedures have been described in previous publications (Bennett et al. 2001; Li and Bennett 2003). Briefly, normal and chronic spinal rats were anaesthetized with urethane (0.18 g/100 g; maximum of 0.45 g per rat for rats over 250 g), and the whole caudal cord between the T13 and L6 vertebrae (corresponding to spinal L6 to cauda equina)

was exposed and continuously wetted with modified artificial cerebrospinal fluid (mACSF). The rat was administered pure oxygen with a mask for 5 minutes before quickly removing the cord and immersing it in a dissection chamber containing mACSF. All spinal roots were removed except for the S4 and Ca1 ventral roots, and the dorsal surface of the cord was glued (super glue, RP 1500; Adhesive Systems) onto a small piece of nappy paper to improve stability. After a total time of 1.5 hours in the dissection chamber at room temperature (20° C), the cord was transferred to a recording chamber containing normal artificial CSF (nACSF) maintained at 24° C and continuously flowing at > 5 ml/min. The cord was secured at the bottom of the recording chamber with the ventral side up by pinning the nappy paper to which it was glued onto the Sylgard base. After allowing an hour in the recording chamber to wash out any residual anaesthetic or kynurenic acid, the bathing solution was switched to nACSF containing a cocktail of fast synaptic transmission blockers (AP5, CNQX, strychnine and picrotoxin; see below). The nACSF was oxygenated in an elevated 200-mL source bottle, and then ran through the recording chamber. This nACSF running out of the recording chamber was continuously collected, filtered and returned to the source bottle using a peristaltic pump. Because of the large volume (200 ml) being recycled in this way and the small volume of the cord (< 0.05 ml), a significant accumulation of metabolic by-products was not likely.

2.2.2 *Intracellular recording*

Intracellular recording methods were as described in Li and Bennett (2003). Briefly, sharp intracellular electrodes were made from thick-walled glass capillary tubes (1.5mm O.D.; Warner GC 150F-10) using a Sutter P-87 micropipette puller and filled with a mixture of 1M K-acetate and 1M KCl. Electrodes (Fig. 2-1A) were bevelled down from an initial resistance of 40-60 M Ω to 25-30 M Ω using a rotary beveller (Sutter BV-10). The bevel and wide electrode shaft gave good current-passing capabilities, and the sharp tip of the bevel was critical for breaking through the tough pia and connective tissue in these adult rats, prior to penetrating the motoneurons. A stepper-motor micromanipulator (660, Kopf) was used to advance the electrodes through the tissue and into cells. Motoneurons were identified via antidromic stimulation of the S4 and Ca1 ventral roots, which were wrapped around Ag-AgCl electrodes above the recording chamber and sealed with high-vacuum grease. Only motoneurons with a stable penetration, resting potential below -60 mV and antidromic spike height over 60 mV from rest were included in this study. Data were collected with an Axoclamp 2b intracellular amplifier (Axon Instruments, Burlingame, CA) running in discontinuous current clamp (DCC, switching rate 5-8 kHz, output bandwidth 3.0 kHz) or discontinuous single-electrode voltage clamp (SEVC; gain 0.8 to 2.5 nA/mV) modes.

2.2.3 *Drugs and solutions*

Two kinds of artificial cerebrospinal fluid (ACSF) were used in these experiments; a modified ACSF (mACSF) designed to minimize potential excitotoxicity was used in the dissection chamber prior to recording, and a normal ACSF (nACSF) was used in the recording chamber. Composition of the mACSF was (in mM) 118 NaCl, 24 NaHCO₃, 1.5

CaCl₂, 3 KCl, 5 MgCl₂, 1.4 NaH₂PO₄, 1.3 MgSO₄, 25 D-glucose and 1 kynurenic acid. Normal ACSF was composed of (in mM) 122 NaCl, 24 NaHCO₃, 2.5 CaCl₂, 3 KCl, 1 MgCl₂ and 12 D-glucose. Both types of ACSF were saturated with 95% O₂-5% CO₂ and maintained at pH 7.4. A synaptic transmission blocking cocktail was usually added to the nACSF; it consisted of 50 μM D(-)-2-Amino-5-phosphonopentanoic acid (AP5; Tocris, U.S.A.), 10 μM 6-cyano-7-nitroquinoxaline-2,3-dione (CNQX; Tocris), 1 μM strychnine (Sigma, U.S.A.) and 100 μM picrotoxin (Tocris) to block NMDA, AMPA, glycine and GABA_A receptors, respectively. Additional drugs were added as required, including 0.5 - 2 μM tetrodotoxin (TTX; Alamone Labs, Israel) to block voltage-dependent Na channels, 15 μM nimodipine (Tocris) or 400 μM Cd²⁺ (Sigma) to block voltage-dependent L-type Ca channels, and 20 μM riluzole (Tocris) to block persistent sodium currents.

2.2.4 Persistent inward currents in current and voltage clamp recording

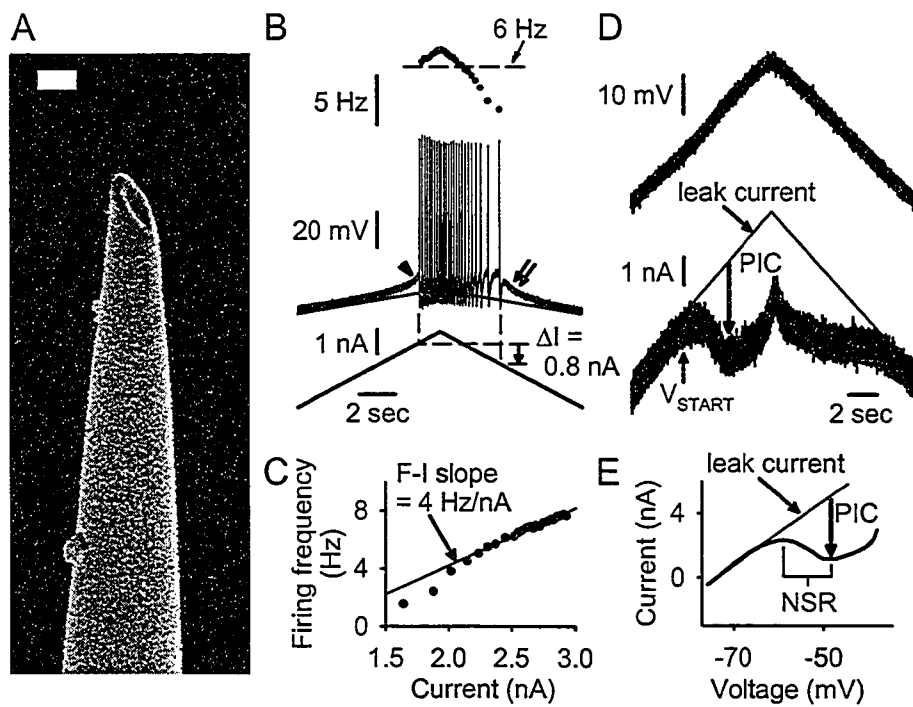
Slow triangular current ramps (0.4 nA/s) were applied to the motoneurons to measure firing and basic cell properties (Fig. 2-1B). The input resistance was measured during the ramp over a 5-mV range near rest and subthreshold to PIC onset. The firing level, or spike voltage threshold (V_{th}), was averaged from five consecutive spikes starting with the 2nd spike on the up ramp, and was taken as the potential at which the rate of change of membrane potential (dV/dt) first exceeded 10 V/s (Li et al. 2004). The spike overshoot (above 0 mV) was calculated as the average peak depolarization during the action potential from these same five spikes. Bistable behaviour was quantified by measuring self-sustained firing (ΔI): that is, when the motoneuron continued to fire at less current than was initially required to recruit firing. This was quantified during current ramps by subtracting the current at de-recruitment (I_{end}) from the current at recruitment (I_{start}), so that $\Delta I = I_{start} - I_{end}$. A subthreshold activation of the PIC (e.g. subthreshold plateau) was identified by extrapolating to higher potentials the linear sub-threshold current-voltage relation (*thin line* in Fig. 2-1B) from a region at least 5 mV below spike voltage threshold, and comparing this to the actual depolarization. In motoneurons with large PICs, the plateau potential was seen as a subthreshold acceleration (arrowhead in Fig. 2-1B) in membrane potential prior to the first spike, and a long after-depolarization following cessation of firing (double arrow in Fig. 2-1B). Instantaneous firing frequency (F) as a function of current (F - I relation) was computed using a custom Linux-based program (G.R. Detillieux, Winnipeg) from the current ramp recordings (Fig. 2-1C). The F - I slope was calculated for linear regions of the F - I relation using a regression. Minimum firing rate was determined by taking the average of the last interspike interval from 2-3 consecutive current ramps, or from threshold current steps in the case of motoneurons that did not fire during normal slow current ramps. Antidromic spike height was measured following stimulation of the ventral roots, while the cell was at rest.

Slow triangular voltage ramps (3.5 mV/s), from approximately -80 mV to -40 mV and back to -80 mV, were used to quantify the PICs (Fig. 2-1D). During the increasing portion of the ramp, the current initially increased linearly with voltage due to the passive leak conductance. A linear relation was fit in this region (10 mV below the PIC onset) and extrapolated into more depolarized potentials (*thin line* labelled 'leak current' in Fig. 2-1D).

Figure 2-1

Intracellular motoneuron recording methods for rat *in vitro* sacrocaudal cord. *A*: Electron microscope image of a bevelled intracellular electrode tip. The electrode was bevelled by holding the tip against a rotating stone (at 22°), while continuously monitoring its resistance with saline on the stone, until the resistance dropped to 25 – 30 M Ω . Scale bar equals 200 nm. *B*: Intracellular recording in DCC mode of motoneuron from a chronic spinal rat. *Bottom trace*: slow triangular current ramp (0.4 nA/s). *Middle trace*: membrane potential with repetitive firing, showing extrapolated leak potential (thin line). Note subthreshold acceleration (arrowhead), self-sustained firing (positive $\Delta I = 0.8$ nA; dashed lines indicate onset and offset of firing), and afterpotential (double arrow). *Top trace*: firing frequency (horizontal line indicates 6 Hz). Note hysteresis in firing frequency. *C*: Instantaneous firing frequency (*F*) from triangular current ramp in *B*, plotted against current (*I*). F-I slope measured by regression analysis of linear region of F-I plot was 4 Hz/nA in this cell. *D*: Same motoneuron as *B*, during slow triangular voltage ramp from -80 mV to -40 mV and back to -80 mV (3.5 nA/s; *top trace*) in SEVC mode. At PIC onset (V_{START}), the current (*bottom trace*) deviated from the extrapolated leak current (thin line). PIC amplitude estimated from maximum difference between leak current and actual current, shown with downward arrow. *E*: Same data as *D*, with current filtered and plotted against voltage (I-V plot). Note negative-slope region (NSR) in I-V relation.

Figure 2 - 1



With further depolarization, there was a downward deviation from this extrapolated leak current, as the PIC was activated (at V_{START}). The PIC was quantified as the peak amplitude of this downward deviation (initial peak on up ramp; downward arrow in Fig. 2-1D). Large PICs caused an outright negative slope in the current response (Fig. 2-1E; negative-slope region (NSR) in the I-V relation). Smaller PICs produced a downward deflection in the current response (flattening of I-V slope) without producing a negative-slope region (as in Fig. 2-2B). A linear current response, not deviating downward from the leak current line (linear I-V relation), was taken to indicate the absence of any PIC (as in Fig. 2-5B). The onset voltage of the PIC, V_{START} , was defined as the voltage at which the slope of the I-V relation was reduced to halfway from the leak current slope (maximum slope) to the minimum positive slopes (halfway to zero in the case of cells with a negative-slope region). This is different from the onset voltage that we previously defined for the PIC, V_{on} , which was simply the voltage at which the I-V slope first reached zero (Li and Bennett 2003). However, V_{on} is not possible to pick in cells without a negative-slope region. Thus we do not use V_{on} .

2.2.5 Data analysis

Data were analyzed in Clampfit 8.0 (Axon Instruments, USA), and figures were made in Sigmaplot (Jandel Scientific, USA). Data are shown as mean \pm standard deviation. A Student's *t*-test was used to test for statistical differences, and a paired *t*-test was used when analyzing cells before and after drug application, with a significance level of $P < 0.05$.

2.3 RESULTS

2.3.1 The resting membrane potential of motoneurons in acute spinal rats was more hyperpolarized relative to the firing threshold than in chronic spinal rats.

The whole sacrocaudal spinal cord was removed from 41 normal adult rats (1 - 6 months old) and maintained *in vitro*. Because the cord was transected at the time of removal, this was termed the acute spinal condition. Sharp intracellular recordings were made from a total of 58 motoneurons in these acute spinal rats. These motoneurons were compared to a further 42 motoneurons that were likewise recorded *in vitro*, but their cords were taken from 34 rats that had undergone a sacral spinal cord transection over 1.5 months previously (chronic spinal condition). In control motoneurons recorded prior to application of TTX or nimodipine, the average resting membrane potential (V_m) was about 2 mV more hyperpolarized in acute spinal rats (-72.7 ± 5.8 mV; $n = 28$) than in chronic spinal rats (-70.6 ± 7.2 mV; $n = 20$), though this was not significant due to the large variability between cells. Likewise, the average spike voltage threshold (V_{th}) was about 2 mV more depolarized in acute spinal rats ($V_{th} = -50.9 \pm 6.2$ mV) than in chronic spinal rats ($V_{th} = -52.9 \pm 7.4$ mV, measured during current ramp as in Fig. 2-1B), though again this was not significant. However, the difference $V_{th} - V_m$ was significantly larger in acute spinal rats (21.6 ± 5.9 mV) than in chronic spinal rats (17.4 ± 6.2 mV). Thus, motoneurons in acute spinal rats rested further from threshold (hyperpolarized by about 4 mV) than in chronic spinal rats.

The membrane input resistance (R_m), measured near rest, was also significantly lower in acute spinal ($5.2 \pm 2.3 \text{ M}\Omega$) compared to chronic spinal ($6.7 \pm 2.9 \text{ M}\Omega$) rat motoneurons. During current ramps, acute spinal rat motoneurons required significantly more current to fire ($3.7 \pm 2.5 \text{ nA}$) compared to chronic spinal rat motoneurons ($1.8 \pm 1.2 \text{ nA}$), consistent with the lower input resistance and higher spike threshold relative to rest ($V_{th} - V_m$) in acute spinal rats. Thus, motoneurons in acute spinal rats were more difficult to activate than in chronic spinal rats.

The spike height and overshoot (absolute value over 0 mV), as measured during current ramps, were not significantly different in acute and chronic spinal rats ($92.0 \pm 8.7 \text{ mV}$ and $+19.3 \pm 7.3 \text{ mV}$ respectively in acute spinal rats, versus $88.3 \pm 10.5 \text{ mV}$ and $+17.7 \pm 7.3 \text{ mV}$ in chronic spinal rats).

2.3.2 Normal motoneurons have small, but variable, persistent inward currents (PICs) after acute spinal transection.

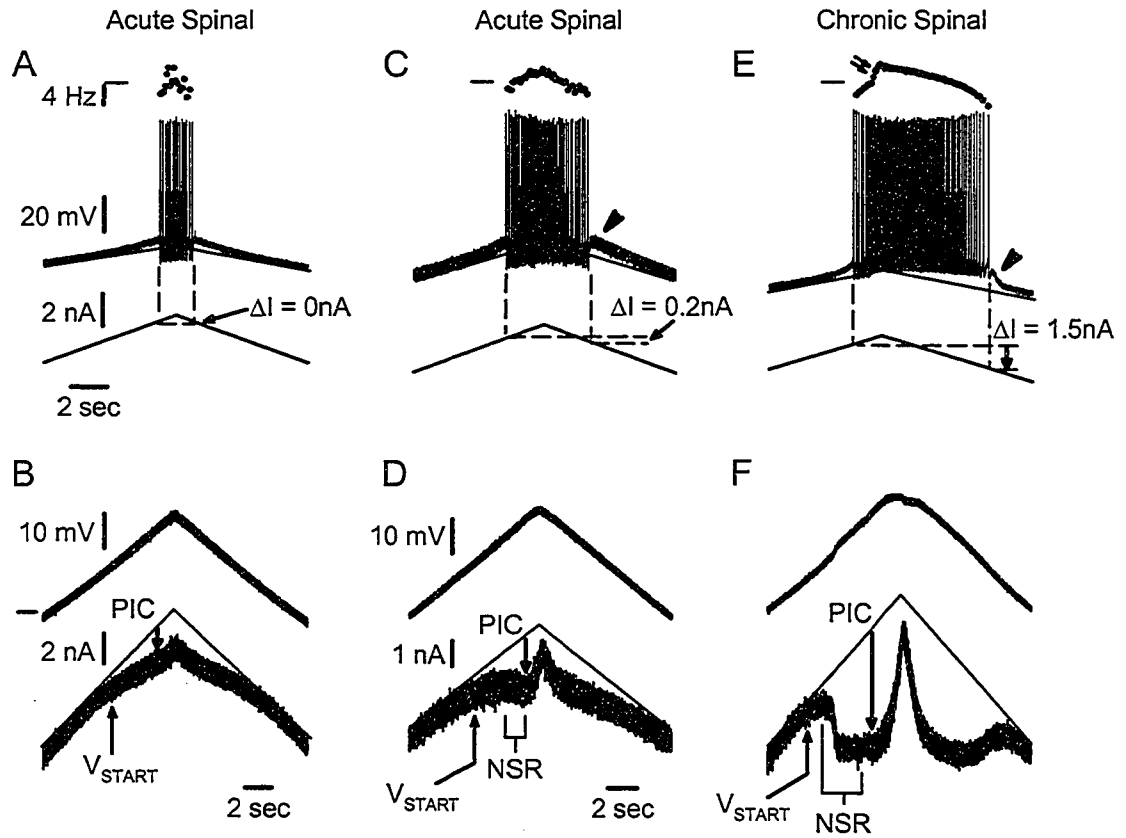
When a slow voltage ramp was applied to a motoneuron in the acute spinal rat, the recorded current increased relatively linearly in the subthreshold region near rest, due to the passive leak current (*thin line* in Fig. 2-2B), but, at more depolarized levels between -60 and -45 mV, the current usually deviated downward from the linearly extrapolated leak current (downward arrow from thin line in Fig. 2-2B). This downward deviation from the leak current was used as an estimate of the net persistent inward current (PIC). For acute spinal rats this PIC was, on average, $1.11 \pm 1.21 \text{ nA}$ ($n = 28$; Fig. 2-3C), which was significantly smaller than the net PIC for chronic spinal rats ($2.79 \pm 0.94 \text{ nA}$, $n = 7$; Fig. 2-3C, described below; PIC measured in all cases at its peak on the upward current ramp, at downward arrow in Figs. 2-2B, D, and F). The average onset voltage, V_{START} , for the acute spinal rats was $-57.2 \pm 5.0 \text{ mV}$ (Fig. 2-3B).

Among acute spinal rat motoneurons, the amplitude of the PIC was highly variable. Some motoneurons (25.0%, $n = 7/28$) had small PICs that only produced an inflection in the current response, lowering the slope, but not producing a negative-slope region (Fig. 2-2B). A further 28.6% ($n = 8/28$) of motoneurons did not exhibit detectable PICs at all, in that the current response was linear (not shown, but see Fig. 2-5B described later). Finally, the remaining motoneurons (46.4%, $n = 13/28$), had PICs large enough to produce a negative-slope region in the current response (Fig. 2-2D), although the depth of this negative-slope region of these 13 cells was usually small ($0.84 \pm 0.63 \text{ nA}$) and significantly smaller than in a comparable population of motoneurons from chronic spinal rats ($1.70 \pm 0.55 \text{ nA}$; see Fig. 2-2F, described below). Usually, the PIC amplitudes from all motoneurons of a given rat were similar, and the above variability was due to large between-rat variations (see Discussion for possible reasons).

Figure 2-2

Motoneurons from acute spinal rats have small persistent inward currents (PICs). *A*: Recording of a motoneuron in acute spinal rat that did not exhibit any self-sustained firing during a triangular current ramp ($\Delta I = 0$ nA). *B*: Voltage clamp recording from same cell with slow voltage ramp starting at -80 mV (horizontal mark). Note small PIC that induces an inflection (flattening) in current response. *C*: Different motoneuron from acute spinal rat with small subthreshold acceleration in membrane potential prior to the first spike, and small afterdepolarization following cessation of firing (arrowhead). Firing frequency increased linearly with current, and there was a small amount of self-sustained firing ($\Delta I > 0$ nA; see Methods). *D*: Voltage ramps for cell in *C* showing PIC inducing a small negative-slope region (NSR) associated with self-sustained firing ability. *E*: Motoneuron from chronic spinal rat showing much greater self-sustained firing (greater ΔI), and non-linearity (acceleration) in firing frequency induced by Ca PIC onset (double arrow). *F*: Large PICs and negative-slope region (NSR) associated with self-sustained firing in *E*. Scale bars in *A* apply to *C* and *E*. Scale bars in *D* also apply to *F*.

Figure 2 - 2



Consistent with the small PICs in motoneurons of acute spinal rats, they also had little or no self-sustained firing (ΔI small; see Methods for definition). That is, the ΔI in acute spinal rats was on average 0.16 ± 0.44 nA, which was significantly smaller than in chronic spinal rats ($\Delta I = 0.57 \pm 0.42$ nA; see Fig. 2-2E) and not significantly different from zero, consistent with previous reports of bistable behaviour being minimal in acute spinal rats (Bennett et al. 2001; Li et al. 2004a). Furthermore, in acute spinal rats, the firing frequency varied relatively linearly with current (Fig. 2-2C), in contrast to chronic spinal rats where there was at times an abrupt acceleration in firing (non-linearity, double arrow in Fig. 2-2E) that has previously been shown to be due to the onset of a large Ca PIC (Li et al. 2004a).

Although ΔI was generally low in acute spinal rats, a negative-slope region in the total PIC was closely linked to self-sustained firing. Of the motoneurons that had a negative-slope region, 11/13 exhibited some small degree of self-sustained firing, with an average $\Delta I = 0.34 \pm 0.40$ nA. For the 7 cells with a PIC but no negative-slope region, however, there was, on average, no significant self-sustained firing (average $\Delta I = 0.00 \pm 0.27$ nA). Finally, the cells that did not exhibit appreciable PICs never had self-sustained firing ($n = 8/8$); indeed, repetitive firing did not usually occur at all in these cells (see Fig. 2-5A, described below).

2.3.3 *Persistent sodium and calcium currents make up the total PIC in acute spinal rats.*

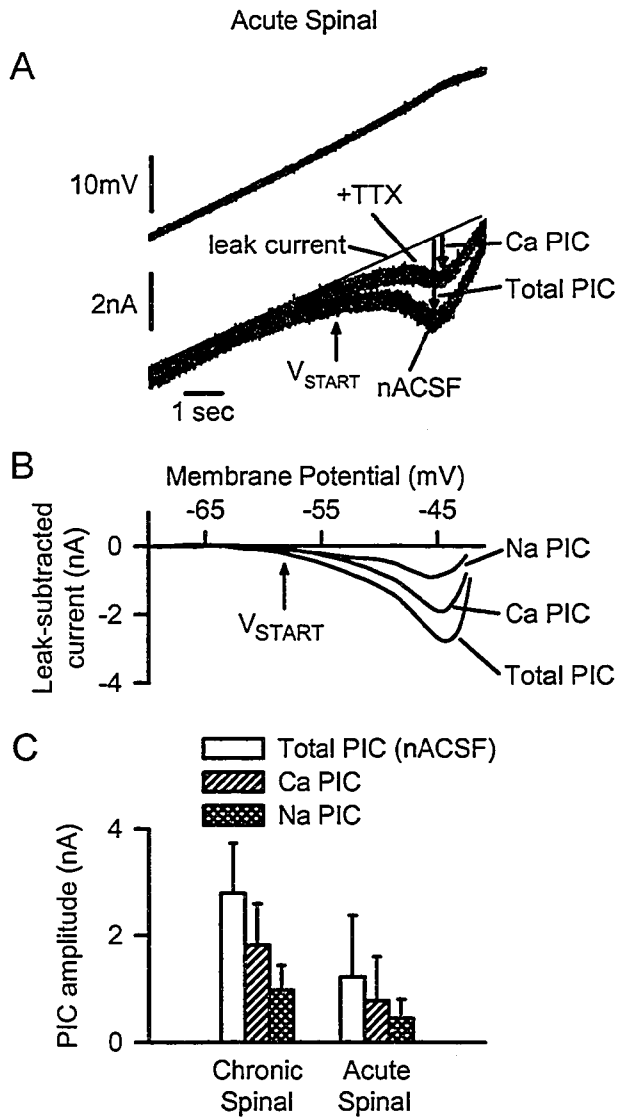
The PICs in motoneurons of acute spinal rats resulted from two major currents: a TTX-sensitive persistent sodium current (Na PIC) and a nimodipine-sensitive persistent calcium current (Ca PIC; mediated by nimodipine-sensitive L-type calcium channels). That is, TTX ($2 \mu\text{M}$) reduced the PIC significantly by $40.8 \pm 10.1\%$ ($n = 7$, see Fig. 2-3A), suggesting that nearly half the PIC was due to persistent sodium currents (Na PIC). This TTX-sensitive current was directly measured by subtracting the current response before and after TTX as shown in Fig. 2-3B (trace labelled Na PIC); it was, on average, 0.44 ± 0.36 nA and had an onset voltage of -61.3 ± 3.6 mV (V_{START} in Fig. 2-3A and B). The remaining PIC in TTX was quantified by subtracting the leak current (see Methods, middle trace in Fig. 2-3B, labelled Ca PIC). This remaining TTX-resistant PIC was on average 0.78 ± 0.82 nA (or 59.2% of the total PIC), had an onset voltage of -54.5 ± 3.6 mV and was mediated by calcium currents (Ca PIC) because it was blocked by the non-specific calcium channel blocker cadmium ($400 \mu\text{M}$, $n = 4$), as in chronic spinal rat motoneurons (Li and Bennett 2003). Nimodipine ($15 \mu\text{M}$) and TTX ($2 \mu\text{M}$) also completely blocked the PIC ($n = 7$), so the Ca PIC was mediated by the nimodipine-sensitive L-type calcium channel (likely by the low-threshold $\text{CaV}(1.3)$ L-type Ca channel, Xu and Lipscombe 2001). Thus, as in motoneurons of chronic spinal rats (Li and Bennett 2003), the PIC in acute spinal rat motoneurons consists of only two major currents: a Na PIC and Ca PIC, both of which were initiated subthreshold to spike threshold (-50.9 mV, described above).

The reduction of the PIC by $2 \mu\text{M}$ TTX (as in Fig. 2-3) was rapid and occurred just before the block of all fast sodium-spiking ability in the motoneuron (at about 2 min after application), supporting the idea that the main action of TTX on the PIC was to directly block the sodium channels underlying the Na PIC in the motoneuron. TTX also blocks any

Figure 2-3

TTX-sensitive Na PICs and TTX-resistant Ca PICs in motoneurons of acute spinal rats. *A*: Current response to voltage ramp before and after TTX application, with leak current shown with thin line (as in upward ramp of Fig. 2-2D). PICs indicated by downward arrows. Notice reduction in PIC with TTX, leaving only a TTX-resistant PIC (Ca PIC). *B*: Filtered data from *A* with the leak current (thin line in *A*) subtracted (leak-subtracted current), and plotted against voltage. The trace labelled total PIC is the leak-subtracted current in nACSF, and the trace labelled Ca PIC is the leak-subtracted TTX-resistant current in *A*, which is Cd^{2+} -sensitive (not shown). The trace labelled Na PIC is the difference between the total PIC and Ca PIC (TTX-sensitive PIC). *C*: Averages of total PIC, Na PIC and Ca PIC peak amplitudes from all acute and chronic spinal rats tested with TTX, each significantly larger in chronic spinal rats.

Figure 2 - 3



spike-mediated transmitter release onto motoneurons, and thus may have possibly had indirect effects on the Ca PIC, if the Ca PIC depends on this transmitter release (e.g., 5-HT release). However, this indirect effect should be slow, due to the slow actions of such neuromodulators on the Na PIC (>10 mins; Harvey et al. 2005a,b) and is thus unlikely to have affected the above results, considering the rapid action of TTX. Furthermore, as detailed below, the Ca and Na PICs do not depend on neuronal activity in the spinal cord in general, because they persist for many hours with all fast synaptic transmission blocked with CNQX, AP5, strychnine and picrotoxin (without TTX; see Methods). Thus, we interpret the TTX-sensitive PIC as a Na PIC on the motoneuron, as demonstrated previously in chronic spinal rats (Li and Bennett 2003).

The Na PIC was also measured by first applying nimodipine (15 μ M) to block the Ca PIC (Fig. 2-4A). The remaining PIC in nimodipine was purely a Na PIC (seen after leak current subtraction in Fig. 2-4B), because it was quickly and completely blocked by 2 μ M TTX (nimodipine + TTX traces in Figs. 2-4A and B). The motoneuron in Figures 2-4A and B had a particularly large PIC, and is shown to clearly demonstrate the PIC components. Figures 2-4C and D show a motoneuron with a PIC more typical of acute spinal rats. On average, the Na PIC measured in nimodipine was 0.55 ± 0.74 nA ($n = 31$ motoneurons), and its onset voltage ($V_{\text{START}} = -62.3 \pm 6.2$ mV) was significantly lower than the spike threshold ($V_{\text{th}} = -50.9 \pm 6.2$ mV). This Na PIC was 49.5% of the total PIC measured without nimodipine (1.11 ± 1.21 nA, $n = 28$, see above). Thus, the Ca PIC blocked by nimodipine was, on average, 50.5% of the total PIC. This is close to the proportion of the PIC eliminated by a complete calcium channel block with cadmium (400 μ M; $69.7 \pm 12.8\%$; significant reduction; $n = 3$) and the proportion remaining after addition of TTX (59.2%, see above), suggesting again that the Ca PIC is mediated by nimodipine-sensitive L-type calcium channels. Comparing across all cells in acute spinal rats, the Na PIC (peak Na PIC measured on upward ramp, as usual) was not significantly correlated with the input conductance measured at rest (correlation coefficient $r = 0.06$, $n = 31$, $P = 0.7$).

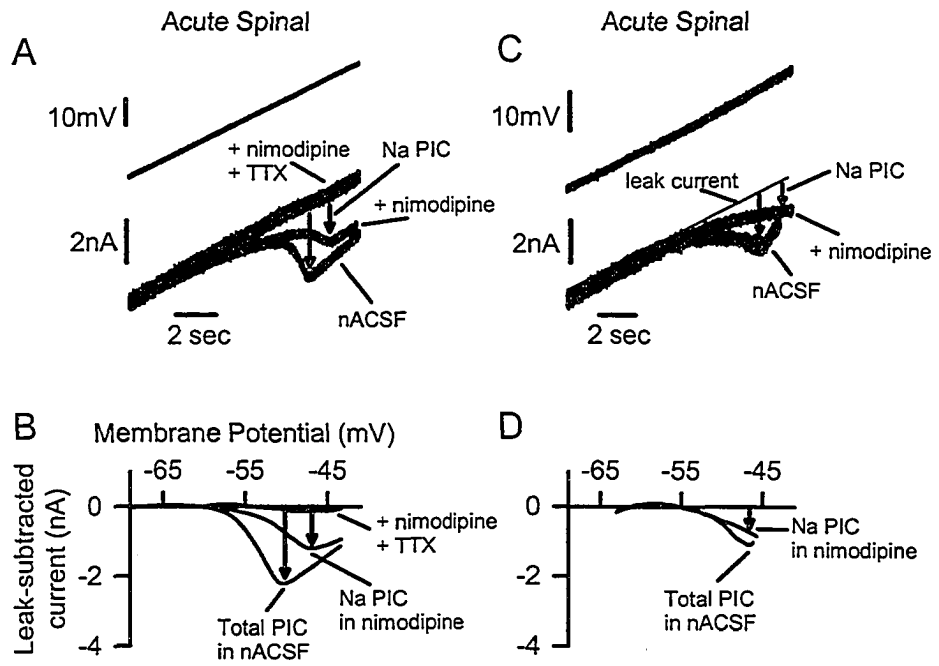
Using nimodipine to isolate and quantify the Na PIC is particularly convenient for several reasons: 1) The PIC measured in nimodipine was clearly blocked by TTX and very similar to the TTX-sensitive current measured prior to nimodipine application in other cells (0.55 ± 0.74 nA compared to 0.44 ± 0.36 nA; Fig. 2-4B versus 2-3B); 2) Fast sodium spikes were not affected by nimodipine (see Li et al. 2004a) and thus the relation between the Na PIC and firing could be studied; and 3) Multiple motoneuron recordings and Na PIC estimates could be obtained in the same preparation, unlike with estimating the Na PIC by direct TTX application, where no further motoneurons could be located and identified in TTX, because the antidromic ventral root activation of the motoneurons was irreversibly blocked. Thus, the nimodipine-resistant PIC was used as the standard method of quantifying the Na PIC, in this and subsequent chapters (Harvey et al. 2005a, b).

In nimodipine, the majority of motoneurons (58.8%; $n = 20/34$) had a small Na PIC that was not large enough to produce a negative-slope region in the current trace, but instead only produced a flattening or inflection, as in Figure 2-5D. A few motoneurons had a large enough Na PIC to produce a negative-slope region (11.8%; $n = 4/34$), as in Figure 2-5F. The

Figure 2-4

Ca PIC is blocked by nimodipine, leaving only a TTX-sensitive Na PIC in motoneurons from acute spinal rats. *A*: Same format as Fig. 2-3A, but with 15 μ M nimodipine added first to block L-type calcium channels mediating the Ca PIC. Downward arrows indicate the amplitude of the total PIC prior to nimodipine (left) and the Na PIC in nimodipine (right). Addition of TTX blocked the Na PIC, leaving linear current response. *B*: Filtered and leak-subtracted currents from *A*, plotted against voltage (I-V plots, as in Fig. 2-3B), showing total PIC in nACSF, Na PIC in nimodipine and block of all PICs in nimodipine and TTX. *C* and *D*: Same format as *A* and *B*, but from different acute spinal rat motoneuron with smaller, more typical Na PIC remaining in nimodipine. TTX was not added in this motoneuron.

Figure 2 - 4



remaining cells (29.4%, 10/34) exhibited no detectable Na PIC, with a relatively linear I-V relation, as in Figure 2-5B.

2.3.4 *Na PIC and Ca PIC are both much larger after chronic injury.*

The sodium and calcium components of the PIC in motoneurons of chronic spinal rats were much larger than those measured in acute spinal rats. Consistent with our earlier observations (Li and Bennett 2003), the total PIC in chronic spinal rat motoneurons was 2.79 ± 0.94 nA ($n = 7$ cells prior to TTX application; see Fig. 2-3C and large PIC in Fig. 2-2F), and this was reduced in TTX by, on average, 0.97 ± 0.46 nA (34.8%; TTX-sensitive Na PIC), leaving a 1.82 ± 0.78 nA Ca PIC (65.2% of total) that was nimodipine-sensitive. Likewise, when nimodipine was added alone to motoneurons of chronic spinal rats, the remaining PIC (Na PIC estimate in nimodipine) was, on average, 1.31 ± 0.93 nA ($n = 19$), which was similar to the Na PIC measured by direct application of TTX (0.97 ± 0.46 nA). Either method of estimating the Na and Ca PICs gave currents in chronic spinal rats that were more than double those in acute spinal rat motoneurons (Na PIC 220 - 238%, and Ca PIC 233 - 264% of the values in acute spinal rat motoneurons, both differences significant; Fig. 2-3C). These large PICs almost always produced negative-slope regions in the I-V relation ($n = 17/20$), as in Figure 2-2F, and as previously reported (Li and Bennett 2003). In chronic spinal rats, the onset voltage (V_{START}) of the Na and Ca PICs were, respectively, -65.3 ± 6.3 mV and -57.1 ± 7.1 mV, which were a few millivolts lower, though not significantly different, than the corresponding V_{START} values in acute spinal rats. The Na PIC onset (V_{START}) was significantly lower than the spike voltage threshold (V_{th}), as in acute spinal rats. In summary, after chronic spinal injury, the PICs were twice as large as those seen in acute spinal injury, but were still made up of Na and Ca PICs in similar proportions (about 40% Na PIC and 60% Ca PIC) and with similar onset voltages. Across all motoneurons of chronic spinal rats, the Na PIC was weakly, but significantly, correlated with the input conductance (correlation coefficient $r = 0.47$, $n = 19$, $P = 0.04$).

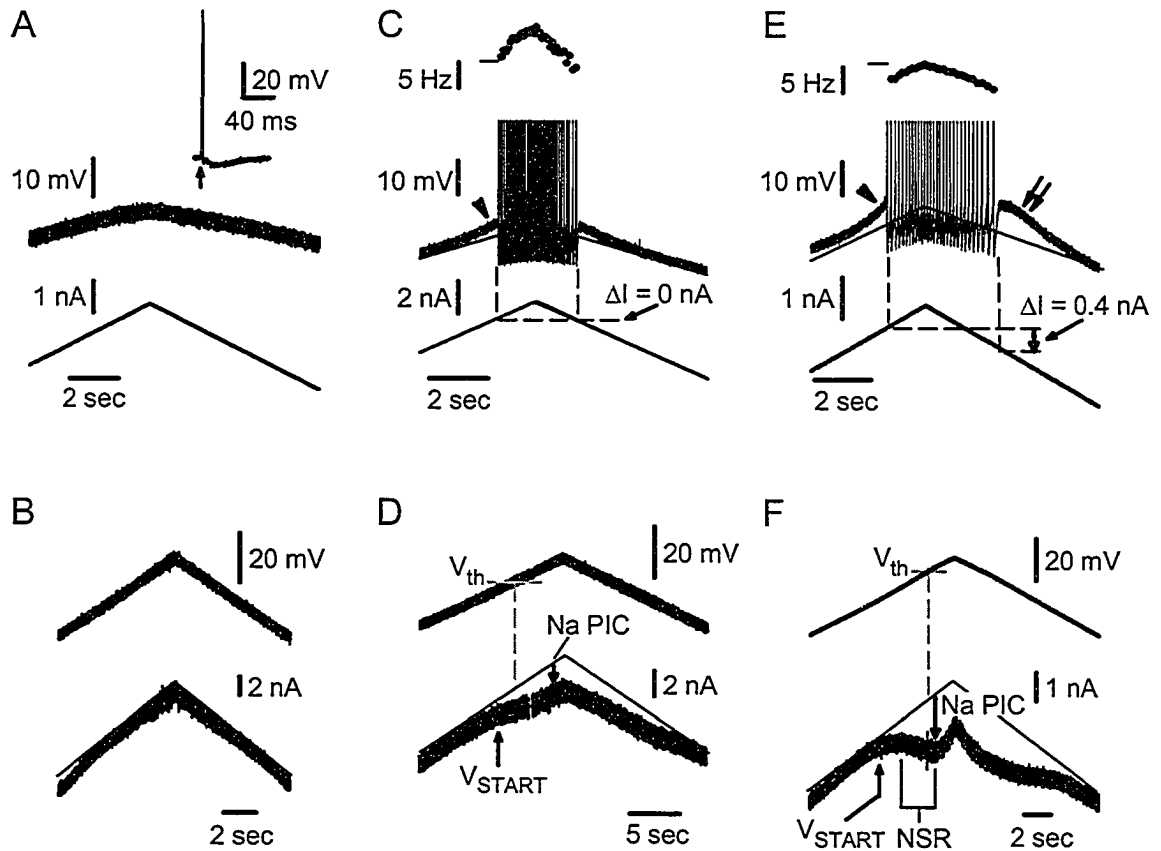
2.3.5 *PICs do not require fast synaptic transmission or spike-mediated transmission.*

With the exception of some motoneurons to which we initially added TTX or Cd^{2+} (e.g. Fig. 2-3), all the results described in this paper were recorded during a complete blockade of fast synaptic transmission using CNQX, AP5, strychnine and picrotoxin to block the AMPA/kainate, NMDA, glycine and GABA_A receptors, respectively (see Methods). Under this condition the total PIC was not significantly different to the total PIC previously reported without this synaptic blockade (Li and Bennett 2003). Thus, the total PIC did not depend on fast synaptic transmission (such as NMDA receptor activation) or associated spinal circuit behaviour. Also, in fast synaptic blockade, large Ca and Na PICs existed in motoneurons of chronic spinal rats (see Fig. 2-2F), as seen without this blockade (Li and Bennett, 2003). However, there was a tendency (though not quite significant, $P = 0.09$) for there to be relatively smaller Na PICs in the fast synaptic blockade, compared to without (Na PIC was 29.6 ± 5.2 % of total PIC in synaptic blockade, compared to 39.5 ± 12.0 % without). Thus, blockade of fast synaptic transmission may have indirectly eliminated a

Figure 2-5

Variability in repetitive firing ability is related to Na PIC amplitude. All recordings (*A-F*) are from motoneurons of acute spinal rats with 15 μM nimodipine present to block Ca PICs (same format as Fig. 2-2). *A*: Motoneuron that was unable to initiate repetitive firing with standard slow current ramps, although it had a full-height spike (inset) in response to antidromic stimulation (up arrow). *B*: Motoneurons with poor firing ability, as in *A*, lacked Na PICs (linear current response to voltage ramp; same cell as in *A*). *C*: Typical motoneuron for acute spinal rats, with small subthreshold acceleration (arrowhead) and repetitive firing (top of spikes clipped), but no self-sustained firing ($\Delta I = 0$ nA). *D*: These typical motoneurons had small Na PICs that only caused a flattening in the current response to a voltage ramp and no negative-slope region (NSR). Note that V_{START} occurs below firing level (V_{th}). *E*: Extreme motoneuron that had self-sustained firing ($\Delta I > 0$ nA) and relatively low minimum firing rate (< 6 Hz). Note large subthreshold acceleration (arrowhead) and after-potential (double arrow) indicating underlying Na plateau. *F*: The same motoneuron as in *E* had a Na PIC large enough to induce a negative-slope region. Horizontal marks at left of frequency plots indicate 10 Hz.

Figure 2 - 5



neuromodulator that somewhat facilitated the Na PIC, and at the same time inhibited the Ca PIC, so that there was no net effect on the total PIC. Interestingly, GABA_B receptor activation has this effect on motoneurons (Li et al. 2004b), and thus, there may have been tonic GABAergic neuron activity that was blocked by the fast synaptic blockade.

In general, we found that the fast synaptic transmission blockade rendered the cord electrically completely silent, with no spontaneous synaptic potentials or synaptic noise recorded on the motoneurons (not shown). Thus, if transmitters endogenous to the spinal cord (e.g., 5-HT in cut descending terminals or intrinsic 5-HT neurons) were in part responsible for enabling the large PICs that we recorded with fast synaptic blockade (see Discussion and Harvey et al. 2005b), then these neuromodulatory transmitters must have been released from last-order neurons (not depending on excitation) directly onto the motoneurons. This transmitter (e.g. 5-HT) may have been released from these last-order neurons in a manner that does not depend on spiking (leak via spontaneous vesicle release) because the Ca PIC persisted for hours (up to 5 hours tested) when recorded in the presence of TTX (which blocks spike transmission and Na PIC, n = 6).

2.3.6 *Motoneurons that lack Na PICs show poor repetitive firing.*

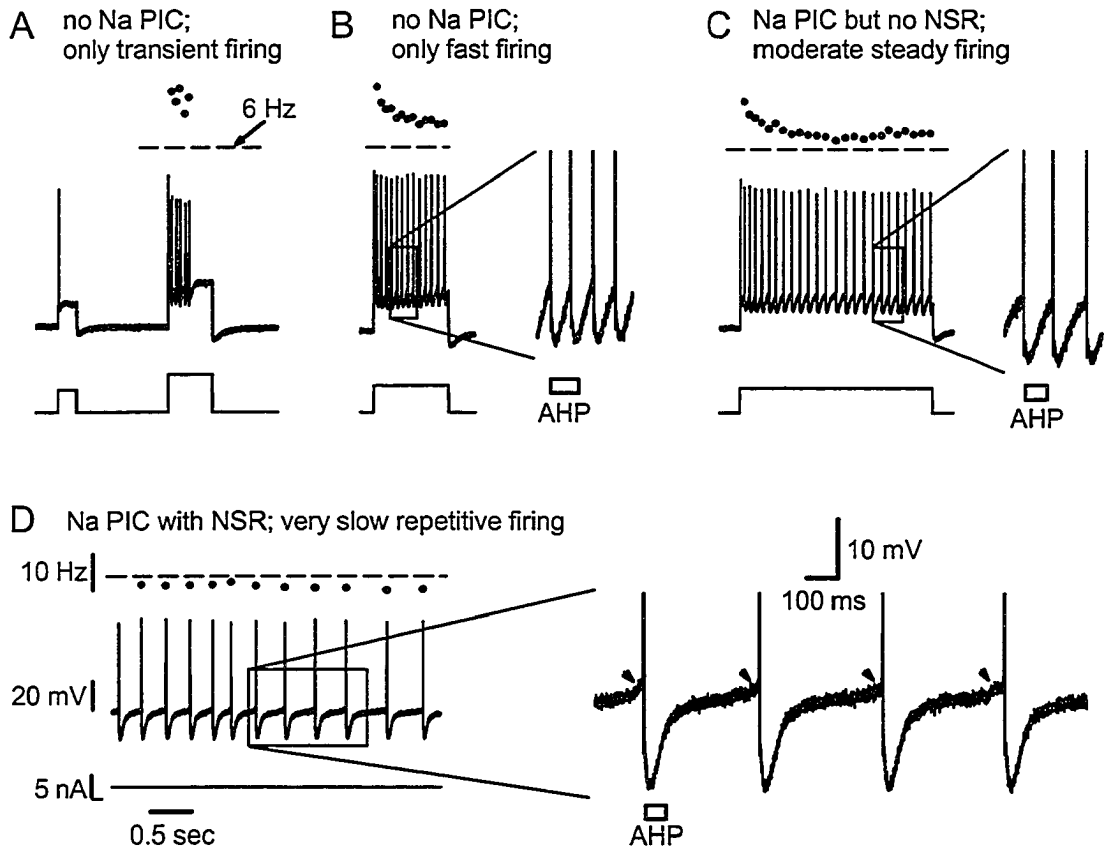
The large variation in Na PICs in acute spinal rats provided an opportunity to examine the role of the Na PIC in recruitment and firing of motoneurons. In the few motoneurons that entirely lacked Na PICs (Fig. 2-5B; n = 10/34), repetitive firing was difficult to initiate, as would be predicted given the importance of Na PICs in firing (see riluzole experiments described below, and Li et al. 2004, Lee and Heckman 2001). That is, during our standard slow current ramp, firing was not usually initiated in these neurons (80% of these neurons had no firing, n = 8/10 neurons); instead, the response was simply a linear depolarization of the membrane potential, even when the potential increased well past the average spike threshold (-50.9 ± 6.2 mV), up to -40 mV (Fig. 2-5A). In half of these neurons, faster ramps could sometimes initiate high frequency firing (50%; n = 4/8 neurons; not shown), but the remaining neurons (n = 4/8) could not fire repetitively at all during ramps (Fig. 2-5A), even during fast current ramps up to 4 nA/s (10× normal slow ramp speed). The latter motoneurons, with no steady repetitive firing ability during fast ramps, were able to fire transiently but only during antidromic activation (inset in Fig. 2-5A) or fast current steps (Figs. 2-6A and B). Usually, prolonged step depolarizations would only generate a few spikes at the leading edge of the step (Fig. 2-6A). Occasionally, during very large current steps, these neurons could fire repetitively throughout the step, but only at high rates well above the usual minimum rate in acute motoneurons ($\gg 6$ Hz; Fig. 2-6B).

The neurons that lacked Na PICs (n = 10/34) were not damaged cells in that they exhibited a healthy resting potential (average $V_m = -72.6 \pm 4.7$ mV) and input resistance (average $R_m = 3.5 \pm 1.2$ M Ω). More importantly, they also had large healthy fast sodium spikes (average spike height was 84.3 ± 12.7 mV) that could be evoked by antidromic stimulation (inset in Fig. 2-5A) or current steps (Fig. 2-6A). Thus, the poor spike initiation and repetitive firing in these cells was not due to a direct failure of the fast sodium spike. Also, based on their input resistance, antidromic stimulation response latency, spike shape (not shown) and long AHP

Figure 2-6

Na PIC amplitude controls firing ability near threshold. All traces recorded in current clamp, with depolarizing steps from rest in acute spinal rat motoneurons in nimodipine (Ca PIC blocked). *A*: Example motoneuron with no Na PIC (as in Fig. 2-5B), where only transient firing occurred with depolarizing steps at threshold (*left*), or above threshold (*right*). *B*: Different motoneuron with no Na PIC; repetitive firing occurred with large step pulses in this cell, but only at high rates ($\gg 6$ Hz), whereas firing was only transient with smaller current steps, like in *A* (not shown). Inset in *B* is close-up on a few spikes. Note that interspike interval is shorter than AHP duration (indicated by box). *C*: Motoneuron with a small Na PIC but no negative-slope region (as in Fig. 2-5D); in this cell repetitive firing occurred near threshold, and the maximum interspike interval was roughly equal to the AHP duration (inset). *D*: Motoneuron with large Na PIC and negative-slope region (as in Fig. 2-5F); in this cell, slow steady firing below 6 Hz (horizontal dashed line) was produced when the cell was held near threshold. Note interspike interval much longer than AHP duration (inset), and fast acceleration in membrane potential just prior to each spike (arrowheads). Horizontal mark in current scale bar in *D* indicates 0 nA. All figures and insets to same scale shown in *D*.

Figure 2 - 6



(inset in Fig. 2-5A), these recordings were definitely from motoneurons proper, and not from motor axons. When some firing was evoked in these motoneurons without a Na PIC (e.g. with a fast ramp), the maximum rate of rise of potential during the first spike of repetitive firing (dV/dt_{\max}) was significantly less in these neurons (126.8 ± 41.4 V/s) than in motoneurons that had a Na PIC (163.6 ± 28.1 V/s). This might, in part, simply be the lack of a Na PIC that accelerates the membrane potential prior to the spike (described in detail below), but also may reflect greater fast transient sodium channel inactivation, as has previously been suggested in other motoneurons with spike accommodation (Schlue et al. 1974: accommodation is defined to occur when current threshold during slow ramps is much higher than rheobase). Perhaps the amount of transient sodium channel inactivation and the size of the Na PIC are linked, if a common sodium channel underlies both transient and persistent sodium currents (Crill 1996).

2.3.7 *Recruitment and firing occurs in acute spinal motoneurons with small Na PICs.*

In contrast to motoneurons without Na PICs, motoneurons that had even small Na PICs were readily recruited and fired repetitively during slow current ramps (Fig. 2-5C, in nimodipine). Typically, motoneurons in acute spinal rats had small Na PICs that were not large enough to produce a negative-slope region in the I-V relation, as described above (Fig. 2-5D; $n = 20/34$), and thus could not exhibit bistable behaviour (e.g., plateaus, self-sustained firing or after-potentials). However, the Na PIC produced a downward (inward) inflection in the I-V relation, and this always occurred subthreshold to the firing level ($V_{\text{START}} < V_{\text{th}}$); thus, the Na PIC was able to assist in recruiting the neuron. That is, during slowly increasing current ramps, the Na PIC activation caused an acceleration in the depolarization just subthreshold to firing. This subthreshold acceleration was caused by the Na PIC, because it was blocked by TTX (see Fig. 2-10D described below) and it did not occur in cells that did not have a Na PIC, even when a fast ramp was used to induce firing (not shown). Further, motoneurons without a Na PIC did not fire during slow ramps, as described above, and thus it is this Na PIC-mediated subthreshold acceleration that is critical for initiating spiking with normal speed current ramps (see Discussion). In some neurons with clear Na PICs, this subthreshold acceleration was accompanied by a small oscillation in the membrane potential (noise) just prior to recruitment (about 2 mV oscillations at about 10 Hz; e.g. left of inset in Fig. 2-7B, and also see Fig. 2-6A in Li et al. 2004), and this oscillation was also mediated by sodium currents (e.g. Na PIC, as in Geijo-Barrientos and Pastore 1995) because it was not seen in TTX. In these cells, the first spike at recruitment was triggered by one of these noisy oscillation cycles.

In most motoneurons of acute spinal rats with typical small Na PICs (not large enough to produce a negative-slope region) following recruitment, the firing continued at currents above the recruitment threshold, but, as soon as the injected current dropped below recruitment threshold (during the downward current ramp), firing stopped and then the potential decreased symmetrically to the response on the upward ramp (no after-potential; Fig. 2-5C, in nimodipine). These cells showed no self-sustained firing during slow current ramps (ΔI never > 0 ; Fig. 2-5C) and at times exhibited some late spike frequency adaptation,

with $\Delta I < 0$ (not shown), unlike in chronic spinal rats (Li et al. 2004a) or in acute spinal rats with negative-slope regions induced by a large Na PIC (Fig. 2-5E, described below).

In these neurons without a large enough Na PIC to produce a negative-slope region, the average minimum firing rate was 8.3 ± 3.1 Hz, and the corresponding interspike interval was 120 ± 45 ms, which was similar to the AHP duration (50 - 150 ms; Figs. 2-6B and C; see also Li et al. 2004). Importantly, these neurons never produced steady very slow firing (< 6 Hz) as described below for neurons with a negative-slope region. Thus, a Na PIC-induced negative-slope region is critical for steady slow firing at < 6 Hz.

2.3.8 Motoneurons with a negative-slope region had enhanced firing.

A few motoneurons of acute spinal rats ($n = 4/34$) exhibited such large spontaneous Na PICs (measured in nimodipine; Fig. 2-5F) that they had a large negative-slope region in the current-voltage relation, which theoretically indicated that these cells should exhibit all-or-nothing bistable behaviour (sodium plateau potentials and self-sustained firing), as is common in motoneurons of chronic spinal rats (Li et al. 2004). Indeed, these large Na PICs were associated with self-sustained firing during triangular current ramps ($\Delta I > 0$; Fig. 2-5E) or following pulses (Fig. 2-7B). Also, these motoneurons with large Na PICs had subthreshold sodium plateau potentials that led to a large acceleration in potential prior to recruitment (arrowhead in Fig. 2-5E), and an after-potential after de-recruitment (double arrow). Ultimately, the response to the triangular current ramp was asymmetrical, with more firing on the downward ramp and a prolonged depolarization (after potential), unlike in other acute spinal rat motoneurons. The subthreshold acceleration prior to recruitment was caused by the Na PIC, because it was blocked by TTX (not shown), as described above for cells with smaller Na PICs, and clearly led to the initiation of the first spike during a current ramp.

2.3.9 Large Na PICs allow very slow steady firing.

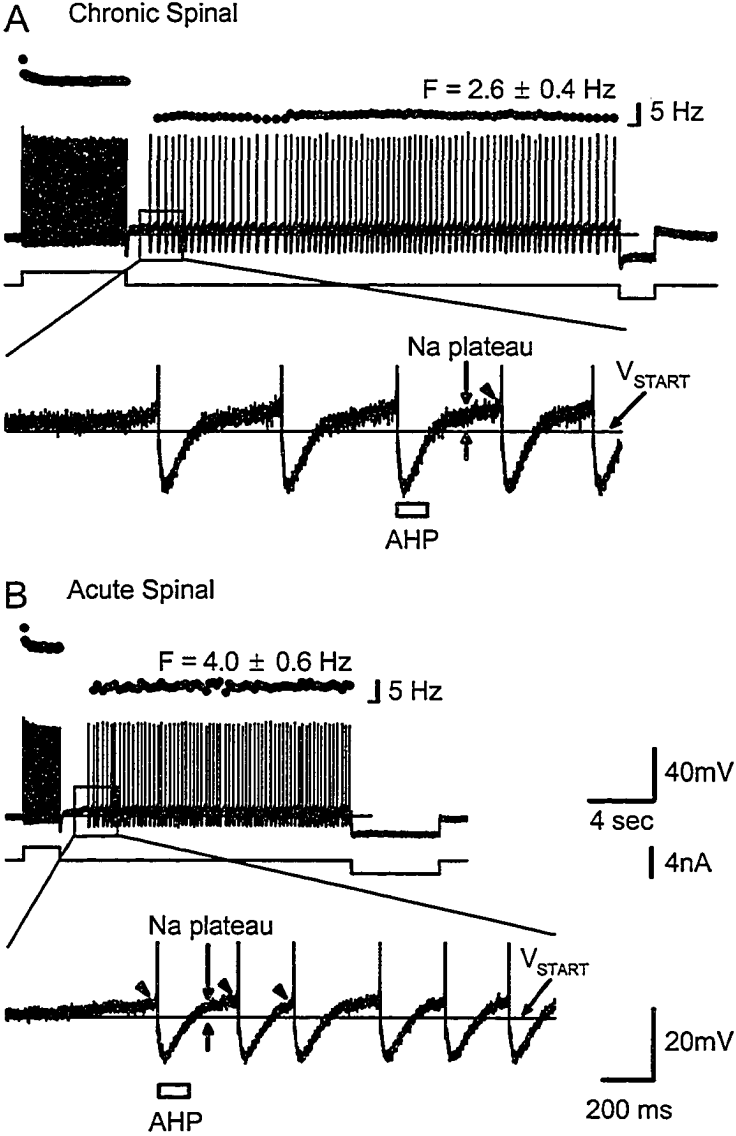
These few extreme motoneurons in acute spinal rats with large enough Na PICs to produce a negative-slope region all produced very slow firing (< 6 Hz, corresponding to interspike intervals much longer than the AHP duration) when the membrane potential was near threshold (Fig. 2-6D and Fig. 2-7B); this, too, relied on the bistable (plateau) behaviour of the Na PIC, as detailed below. On average, the minimum firing rate in these 4 cells (5.0 ± 0.8 Hz) was significantly lower than the average minimum rate in motoneurons of acute spinal rats without negative-slope regions (8.3 ± 3.1 Hz), and closer to that in chronic spinal rats (4.6 ± 1.9 Hz, in nimodipine).

Previously, Li et al. (2004) demonstrated that chronic spinal rat motoneurons with large Na PICs exhibit similar very low frequency steady firing (very slow firing, much < 6 Hz) with interspike intervals up to 1 sec and much longer than the AHP duration (50 - 150 ms). This very slow firing depends on the Na PIC (eliminated by a Na PIC block) but not the Ca PIC (nimodipine-resistant, Li et al. 2004a). We also found that motoneurons of chronic spinal

Figure 2-7

Motoneurons of acute spinal rats, with large enough Na PICs to produce a negative-slope region, exhibited steady very slow firing similar to that commonly seen in chronic spinal rats. *A, top*: Current clamp recording of chronic spinal rat motoneuron held near threshold (in nimodipine). Brief depolarizing current pulse initiated a Na plateau and self-sustained firing at very low average frequency (2.6 ± 0.4 Hz), terminated by a hyperpolarizing current pulse (at right). *Bottom*: amplification of *top* trace showing long interspike intervals (longer than AHP). Note that the Na PIC was activated prior to each spike (Na plateau above V_{START} , then fast acceleration at arrowhead), but the AHP dropped the membrane potential below V_{START} , which deactivated the Na PIC/plateau. *B, top*: Motoneuron from acute spinal rat (in nimodipine) that had Na PIC large enough to produce a negative-slope region, also had steady slow firing mediated by Na plateaus as in *A*. *Bottom*: Steady repetitive firing at frequencies below 6 Hz, with interspike intervals again greatly exceeding the AHP duration (determined from antidromic stimulation at rest). Again, note activation of Na plateau (vertical arrows) and fast acceleration (arrowhead) prior to the spike. Scale bars in *B* also apply to *A*. Horizontal mark at bottom of frequency scale bars indicates 0 Hz.

Figure 2 - 7



rats exhibited very slow firing (in nimodipine); furthermore, we found that this very slow firing persisted in the presence of fast synaptic transmission blocking agents (including AP5) and thus does not depend on persistent calcium currents or NMDA receptors (Fig. 2-7A).

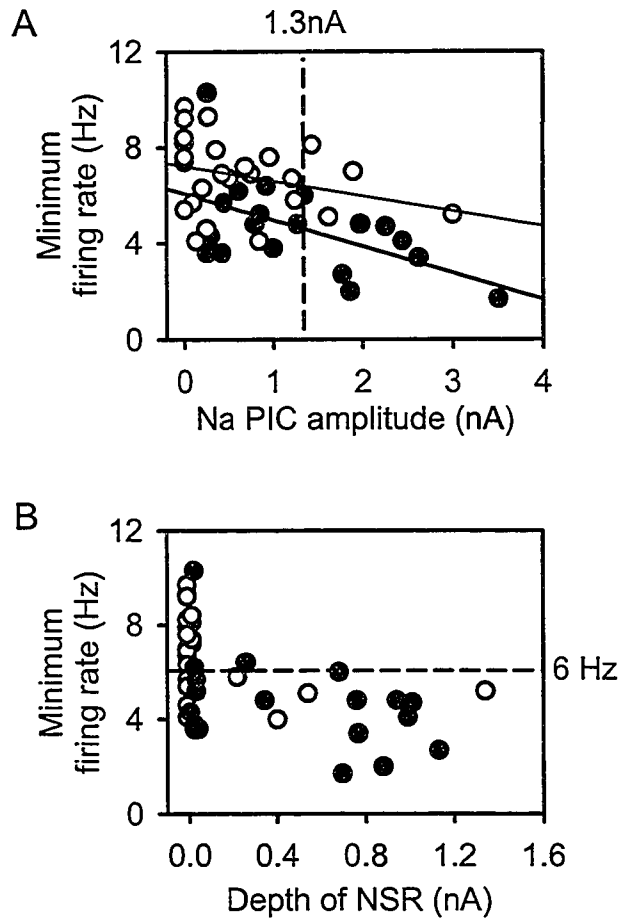
The detailed mechanism of how the Na PIC causes very slow firing is demonstrated in Figure 2-7 for both chronic and acute spinal rats (see also Li et al. 2004). When the membrane potential was just subthreshold for the spike, the Na PIC came on slowly, causing an initially slowly increasing subthreshold sodium plateau (see slow ramp-up in potential at vertical arrow in Fig. 2-7A). Further, as the potential depolarized during this plateau, the Na PIC came on much more quickly (Na PIC is a fast current at more depolarized levels; Li and Bennett 2003), and thus helped accelerate the potential just prior to the spike (at arrowheads), and ultimately helped initiate a spike (left side of inset in Figs. 2-7A or B). However, because the Na PIC deactivates quickly with hyperpolarization (Li and Bennett 2003), the spike's AHP deactivated the Na PICs/plateau (potential well below V_{START} of Na PIC, thin line) and left the membrane potential again just subthreshold for the spike at the end of the 100-ms AHP (AHP estimated from antidromic pulse at rest, indicated with bar). The sodium plateau then re-activated (bracketed by thick arrows) and produced a second spike, but again this plateau was terminated by the AHP. This repeated sodium plateau (Na PIC) activation and deactivation behaviour caused slow firing, because this slow firing was eliminated with a low dose of TTX (0.5 μ M) or riluzole (20 μ M) that reduced the Na PIC and eliminated the negative-slope region prior to blocking spiking (not shown, but see Li et al. 2004a).

Considering the dependence of slow firing on the Na PIC, the larger Na PICs in chronic spinal rat motoneurons should explain the higher incidence of slow firing, compared to that of acute spinal rats; furthermore, cells with larger Na PICs ought to, in general, have lower minimum rates. To examine this, we determined the relationship between the minimum firing rate and the Na PIC amplitude (Fig. 2-8A). For chronic spinal rat motoneurons, there was indeed a significant correlation between Na PIC amplitude and the minimum firing rate (solid circles, thick regression line; $r = 0.538$, $n = 19$, $P = 0.02$), and most of these motoneurons had a negative-slope region (Fig. 2-8B, solid circles). Furthermore, cells with Na PICs larger than 1.3 nA (mean Na PIC amplitude) had a much lower minimum firing rate (3.3 ± 1.2 Hz, $n = 7$) compared to the minimum rate in cells with Na PICs smaller than 1.3 nA (5.4 ± 1.8 Hz; $n = 12$; significant difference). Acute spinal rat motoneurons exhibited a trend towards this relationship, but the correlation was not quite significant (open circles, thin regression line; $r = 0.302$, $n = 25$, $P = 0.1$) because there were only a few neurons with a large Na PIC. However, the 4 cells that did have a large enough Na PIC to produce a clear negative-slope region (open circles at right of Fig. 2-8B) exhibited some of the slowest firing amongst this group of cells (< 6 Hz, significantly lower rate than cells without a negative-slope region). Thus, larger persistent sodium currents, especially those that induced negative-slope regions, are associated with lower minimum firing rates.

Figure 2-8

Na PIC amplitude correlates with minimum firing rate. *A*: In chronic spinal rat motoneurons (solid circles, thick regression line), large Na PICs correlated significantly with low minimum firing rates ($r = 0.538$). Acute spinal rat motoneurons (open circles, thin regression line) also had a trend toward Na PICs correlating with minimum firing rates, but this was not significant. *B*: Motoneurons with a negative-slope region (NSR) in the current trace were more likely to exhibit steady slow firing (< 6 Hz, below horizontal dashed line). The 4 acute spinal rat motoneurons with an NSR (open circles at right) had minimum firing rates at low end of the range for normal motoneurons. With chronic spinal injury, many more motoneurons had a negative-slope region in current trace, and all these had an average minimum firing rate below 6 Hz.

Figure 2 - 8



2.3.10 Frequency-current slope is not related to Na PIC amplitude

When only a Na PIC was present (with Ca PIC blocked with nimodipine), during increasing current ramps, the firing rate response increased relatively linearly (linear F-I relation; Fig. 2-5E). As previously reported (Li et al. 2004), this is because the Ca PIC causes the main non-linearity in the F-I relation (acceleration in firing; double arrow in Fig. 2-2E, top), and this non-linearity is blocked by nimodipine. On average, the slope of the frequency-current (F-I) relation in nimodipine was significantly smaller in chronic spinal rats (5.5 ± 1.6 Hz/nA; $n = 16$) compared to in acute spinal rats (7.4 ± 2.3 Hz/nA; $n = 16$; right of Fig. 2-9). Because the chronic spinal rats have larger Na PICs, this might suggest that a shallower F-I slope is associated with larger Na PICs. However, the F-I slope was not significantly correlated to Na PIC amplitude in either acute or chronic spinal rat motoneurons (Fig. 2-9; Acute: thin line, $r = 0.157$; Chronic: thick line, $r = 0.138$). We also found that the F-I slope was not significantly correlated with the minimum slope-conductance of the I-V relation, G_{\min} (where G_{\min} is the slope the I-V relation at the NSR in cells with a NSR, or just the minimum slope in other cells; $r = 0.221$, $N=18$, $P = 0.4$). Thus, the F-I slope is not related to the Na PIC, unlike with the Ca PIC (Li et al. 2004a). Considering that changes in the Na PIC are not associated with changes in the F-I slope, whereas increases in the Na PIC lower the minimum firing rate (see above), the major action of the Na PIC on the F-I relation is to vertically shift the F-I relation to lower rates (compare frequency plots in Figs. 2-5C and 2-5E), allowing an overall broader range of firing (maximum rate in acute and chronic spinal rats is similar, not shown).

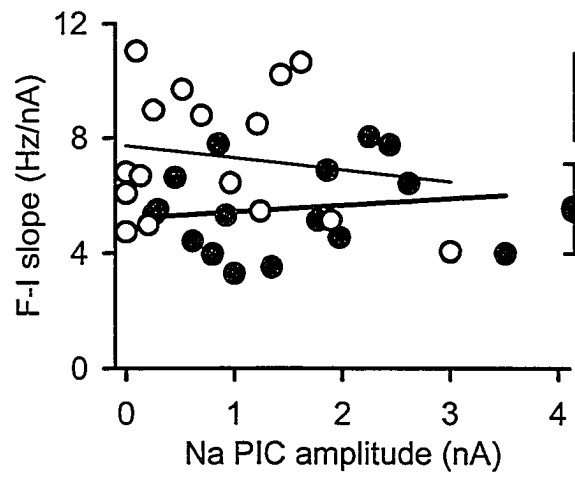
2.3.11 Na PICs are essential in firing.

To definitively prove that the Na PIC was essential for steady repetitive firing, we blocked the Na PIC without blocking the spike, using either a low dose of TTX ($< 1 \mu\text{M}$, $n = 6$) or riluzole ($20 \mu\text{M}$, $n = 9$, combined data from acute and chronic spinal rats). When low-dose TTX was applied to a motoneuron, the Na PIC was blocked (Fig. 2-10B and E) prior to affecting the fast sodium spike (Fig. 2-10C), because the Na PIC is more sensitive to sodium channel blockers (Stafstrom et al. 1985). This low dose of TTX ($0.5 \mu\text{M}$, as in Figs. 2-10D to 2-10F) gave a longer period of time where the fast sodium spike was unaffected while the Na PIC was blocked (minutes; Na PIC measured in nimodipine), compared to the normal $2\text{-}\mu\text{M}$ dose, which blocked both almost simultaneously. Riluzole ($20 \mu\text{M}$) had the same effect as low-dose TTX, but worked very slowly, taking one hour to completely block the Na PIC (not shown), and another hour to affect the fast sodium spike. With either TTX or riluzole, during the period when the Na PIC was blocked and the spike was unaffected, the repetitive firing during a current ramp was always eliminated (compare firing in Fig. 2-10A to lack of firing in Fig. 2-10D). Thus, the Na PIC was absolutely essential for spike initiation during a ramp. During this period, a fast current step still initiated a few spikes (Figs. 2-10C and G), and this was how we demonstrated that the fast sodium spike was unaffected after the Na PIC block (overlapping spikes in Fig. 2-10C, before and after low-dose TTX). However, this step-evoked firing was never sustained (Fig. 2-10F in TTX, and Fig. 2-10G in riluzole),

Figure 2-9

F-I slope is not related to the Na PIC amplitude. F-I slope measured from response to slow current ramps in the presence of nimodipine (Ca PIC blocked) in motoneurons from acute spinal (open circles, thin regression line) and chronic spinal (solid circles, thick regression line) rats, and plotted against Na PIC amplitude. No significant correlation was observed between F-I slope and Na PIC amplitude in either group. Average F-I slopes plotted at right show that motoneurons of acute spinal rats had significantly higher F-I slopes than motoneurons of chronic spinal rats.

Figure 2 - 9



and thus sustained repetitive firing also required a Na PIC. Antidromic activation of the motoneurons also initiated normal full-height sodium spikes in riluzole (Fig. 2-10H).

Repeated short intracellular current pulses (not shown) or antidromic stimulation at moderately low frequencies (10 Hz, Fig. 2-10H) usually gave repeated full unattenuated spikes, demonstrating that failure to fire repetitively during a ramp or step input was not simply due to a failure of spikes with repetition. However, higher frequency stimulation (20 Hz) at times led to spike inactivation, with a broadening of the spike over the course of many stimulations, and then ultimately complete failure of spiking (at *; Fig. 2-10I). Such spike inactivation did not occur prior to riluzole or low-dose TTX (see repetitive firing in Fig. 2-10A), and thus subtle changes in the fast transient sodium channel inactivation occurred in addition to the block of the Na PIC with these drugs. Thus, spike initiation and repetitive firing depends primarily on the Na PIC, but also on a relative lack of spike inactivation.

The cells just described in Fig. 2-10, were recorded in the presence of nimodipine to block the Ca PIC; in these cells, there was robust repetitive firing during a current ramp (Fig. 2-10A) and clear Na PICs (Fig. 2-10B) prior to the application of TTX or riluzole. In the absence of nimodipine, application of TTX or riluzole to block the Na PIC also eliminated repetitive firing during a current ramp (not shown), prior to blocking the fast sodium spike. Thus, the Ca PIC itself is not sufficient for steady repetitive firing. In low-dose TTX without nimodipine, there was still a Ca PIC that produced a calcium plateau in chronic spinal rats (Li et al. 2004a), and this sometimes triggered a few spikes at its onset (not shown). In this way, the Ca PIC onset acted like a current step (as in Figs. 2-10E and 2-10G) producing a rapid depolarization that initiated a spike.

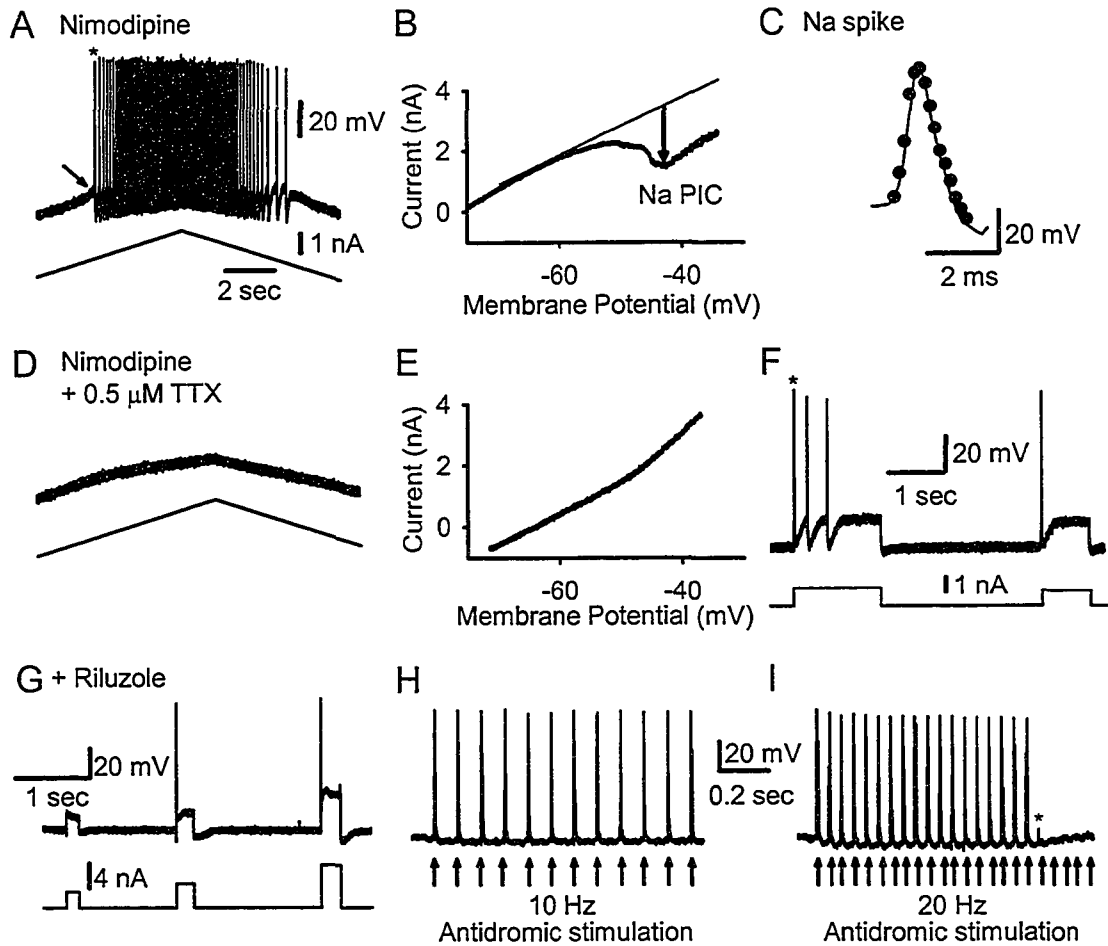
2.4 DISCUSSION

The results demonstrate that normal motoneurons have Na and Ca PICs immediately after spinal transection (acute spinal condition), but these are small and only increase substantially with long-term injury (chronic spinal). Interestingly, the PICs occur immediately after spinal transection despite the massive loss of brainstem-derived monoamines (5-HT and NE) that normally regulate PICs (Hounsgaard et al. 1988a; Hultborn and Kiehn 1992; Lee and Heckman 1998a). The small PICs in acute spinal rats generally do not lead to pronounced bistable behaviour (plateau potentials and self-sustained firing), consistent with previous studies of acute spinal animals (cat: Conway et al. 1988; turtle: Hounsgaard et al. 1988b; guinea pig: Nishimura et al. 1989; rat: Powers and Binder 2003). However, these PICs are usually sufficient to at least produce an inflection (flattening) in the I-V relation, which has previously been argued to underlie graded amplification of motoneuron responses near threshold (as in Figure 2-5, see also Li and Bennett 2003; Prather et al. 2001; Schwindt and Crill 1982) and participate in recruitment and repetitive firing.

Figure 2-10

Selectively blocking the Na PIC eliminates repetitive firing, but not the fast sodium spike. *A*: Motoneuron from chronic spinal rat recorded in nimodipine showing typical repetitive firing during slow current ramps. *B*: Current-voltage plot response to slow voltage ramp in nimodipine, for same cell as in *A*. Note the clear negative-slope region and large Na PIC (downward arrow). *C*: Overlay of the first spike from current ramp in nimodipine (thin line, from *A*) with the first spike from current step in nimodipine plus low-dose TTX (dots; from spike in *F*). *D*: Application of low-dose TTX ($0.5 \mu\text{M}$) to the cell in *A* and *B* (with nimodipine present) eliminated all repetitive firing ability during slow current ramps, even though the fast sodium spike was not blocked (*C* and *F*). *E*: Na PIC was blocked by low-dose TTX, when lack of firing in *D* was recorded. *F*: In low-dose TTX, current steps still elicited 1-3 spikes, indicating transient sodium currents were not blocked. *G*: Another motoneuron with riluzole ($20 \mu\text{M}$), rather than TTX, used to block the Na PIC (PIC not shown). Again, only transient firing was possible during current steps (*G*) and not ramps (not shown). *H*: With the Na PIC blocked in riluzole, the motoneurons could still fire in response to repeated antidromic stimulation (one spike for each stimulation at arrow; 10 Hz repetition); thus the spike was still capable of being activated repeatedly. *I*: Same as *H*, but at 20 Hz antidromic stimulation. Spike activation eventually failed (at *) with repeated high frequency stimulation.

Figure 2 - 10



The results also demonstrate that all motoneurons that lack the ability to produce steady repetitive firing during slow current ramps also lack a Na PIC, suggesting that Na PICs are necessary for steady repetitive firing. Conversely, most neurons that did not have any detectable Na PIC could not fire repetitively during a slow current ramp. A few of these neurons could fire repetitively during slow ramps (2/10), but this may have been due to small Na PICs that were not detectable. That is, even when an I-V relation is relatively linear, suggesting no detectable Na PIC (see Methods), then TTX application can at times still reveal a small TTX-sensitive Na PIC (unpublished findings). Taken together, these results suggest that repetitive firing is highly correlated with the presence of a Na PIC.

To directly prove that the Na PIC is essential for repetitive firing, the Na PIC must be blocked without blocking the sodium spike, and this has been done by blocking the Na PIC with riluzole or low-dose TTX (see Results), or else using a depolarization block (Lee and Heckman 2001). In riluzole or low-dose TTX, repetitive firing is eliminated as expected when the Na PIC is blocked, even though transient firing is possible with a fast current step. Thus, riluzole creates a situation like in neurons that naturally lack Na PICs (compare Figs. 2-10D and 2-5A). This verifies the essential role of the Na PIC in repetitive firing, supporting the conclusions of Lee and Heckman (2001) in cat motoneurons and Stafstrom et al. (1985) in cat neocortical cells. Further evidence for the role of the Na PIC in firing comes from our companion paper, where we show that motoneurons that lack repetitive firing and Na PICs can be rescued by application of 5-HT₂ receptor agonists, which increase the Na PIC and thus enable repetitive firing (Harvey et al. 2005a). Conversely, 5-HT and NE antagonists eliminate the Na PIC and repetitive firing, like riluzole, though these antagonists do so by indirectly modulating the Na PIC through receptors linked to Gq-protein coupled intracellular pathways (Harvey et al. 2005b).

2.4.1 Variation in Na PIC amplitude with state of animal preparation.

In acute spinal rats, the Na PIC is usually large enough to assist in spike initiation and enable repetitive firing, but not so large as to produce bistable plateau behaviour. In a few extreme acute spinal rat motoneurons (11.8%), the Na PIC is so large that it does produce a substantial negative-slope region in the I-V relation that enables Na plateaus, and slow subthreshold oscillations, resulting in the characteristic very slow firing seen with large Na PICs (Li et al. 2004a). On the other extreme, in the motoneurons without clear Na PICs (29.4%), repetitive firing is poor or absent, consistent with the fundamental role of the Na PIC in enabling repetitive firing, as discussed above. From the wide variation in Na PICs in acute spinal rats, it is clear that any motoneuron that can produce steady repetitive firing is likely to have at least a small Na PIC, and larger Na PICs are associated with slower firing (lower minimum rates).

For comparison, it is noteworthy that motoneurons from deeply pentobarbital-anaesthetized animals have no evidence of bistable behaviour (no plateaus or self-sustained firing, Lee and Heckman 2000; Powers and Binder 1995; Prather et al. 2001), consistent with a direct inhibition of the Ca PIC by pentobarbital (Guertin and Hounsgaard 1999), and reduced

brainstem activity in this preparation. However, many motoneurons in these anaesthetized animals still fire repetitively during a slow current ramp or steady current step; thus, given the absolutely critical role of the Na PIC in steady repetitive firing, it is likely that some weak Na PIC exists in these motoneurons. Indeed, Lee and Heckman (2001) have shown that a persistent inward current with characteristics of the Na PIC does exist in motoneurons of pentobarbitol-anaesthetized cats. However, it is not uncommon to encounter healthy motoneurons in anaesthetized cats that will *not* exhibit steady repetitive firing (CJ Heckman personal communication, Granit et al. 1956). These are typically not reported on in detail and considered abnormal (termed phasic or accommodating in early reports, Granit et al. 1956), but, in retrospect, they may simply be healthy motoneurons that lack a Na PIC, as we have seen.

In contrast, PICs in brainstem-intact decerebrate cats or intact rats or humans produce pronounced bistable behaviour, including long-lasting self-sustained firing (Eken et al. 1989; Gorassini et al. 1998; Hounsgaard et al. 1988a; Kiehn and Eken 1997), likely because of facilitation from brainstem-derived monoamines. Thus, on a continuum, PICs are smallest in the barbiturate-anaesthetized state, larger in the acute spinal state and largest in the brainstem-intact state. The latter may vary considerably depending on brainstem activity, and the brainstem-intact decerebrate cat likely does not have as large PICs as in the intact awake animal or human (Gorassini et al. 2002), because we know that PICs can be further increased in the decerebrate state by application of 5-HT or NE agonists (Conway et al. 1988; Hounsgaard et al. 1988a; Lee and Heckman 1999). The effect of PICs in chronic spinal rats (e.g., self-sustained firing) are at least as large as in normal intact animals (see Discussion in Li et al. 2004a), and thus serve as a reasonable comparison to those in acute spinal rats.

2.4.2 *Role of endogenous monoamines in regulating Na PIC and motoneuron properties.*

Considering that the PICs can be very small or absent in healthy motoneurons of some acute spinal animals, the question is: what enables the moderately large PICs in other acute spinal animals? We know that many exogenously applied neuromodulators, including 5-HT, NE, acetylcholine and glutamate can facilitate PICs in motoneurons (Alaburda and Hounsgaard 2003; Delgado-Lezama et al. 1997; Hultborn and Kiehn 1992; Kiehn and Harris-Warrick 1992; Lee and Heckman 1999). However, the results presented in Chapter 4 (Harvey et al. 2005b) suggest that *Na PICs in the spinal animal depend primarily on residual monoamines (5-HT and NE) in the spinal cord* (the level of these residual monoamines we refer to as monoamine tone). That is, in spinal rats, the naturally occurring Na PICs and associated repetitive firing are blocked by antagonizing monoamine receptors, and thus there must be some endogenous monoamine tone underlying these Na PICs (Harvey et al. 2005b). Furthermore, application of monoamine receptor agonists facilitates the Na PIC and rescues firing in motoneurons that otherwise cannot fire repetitively (Harvey et al. 2005a), suggesting that they initially lacked monoamine tone. In general, variations in monoamine tone may underlie the variations in PICs from rat to rat, and so rats that have little monoamine tone have little or no PICs, and do not fire slowly. The fact that motoneurons fire repetitively in reduced preparations where the spinal cord is acutely sliced (Perrier et

al. 2000) or where motoneurons are cultured (Kuo et al. 2004), suggests that residual monoamines, or a similar neuromodulator, are also available to facilitate the Na PIC in these more reduced preparations, though this remains to be verified.

The origins of the monoamines in acute and chronic spinal rats are discussed in Chapter 4 (Harvey et al. 2005b). Suffice it to say, that there are residual monoamines in the spinal cord facilitating both Na and Ca PICs, even in the chronic spinal rat (Cassam et al. 1997; Newton and Hamill 1988). Further, our present results indicate that these monoamines must be released from spinal sources (e.g., 5-HT neurons) that do not depend on general neuronal activity, because Ca and Na PICs persist in a blockade of fast synaptic transmission that renders the cord synaptically quiet. Whether the release of 5-HT from these cells is from spontaneous firing or from non-spike mediated transmitter release (leak) is uncertain, though there may be some leak because Ca PICs persist in long-term blockade of spikes with TTX.

PICs in motoneurons of chronic spinal rats become supersensitive to monoamines, as to be expected from the massive denervation from the descending brainstem monoamine tracts (Harvey et al. 2005a). Thus, small amounts of residual monoamines in the cord produce large PICs, and this ultimately explains the large PICs found in the chronic spinal rats (Harvey et al. 2005b). This denervation supersensitivity of PICs essentially replaces the effect of the lost brainstem monoamines, returning the motoneurons to a state closer to that of the normal intact animal. Supersensitivity to residual monoamines after chronic injury likely also explains why motoneurons of chronic spinal rats have a higher input resistance and rest closer to the spike threshold than motoneurons of acute spinal rats (see Results). That is, in addition to its effects on PICs, 5-HT also increases the input resistance in motoneurons (White and Fung 1989), depolarizes the resting membrane potential (White and Fung 1989) and hyperpolarizes the spike threshold (Fedirchuk and Dai 2004; Harvey et al. 2005a). All these membrane properties become supersensitive to 5-HT in chronic spinal rats (Harvey et al. 2005a), and thus supersensitivity to residual spinal 5-HT should increase the input resistance and depolarize cells closer to the spike threshold, as was observed in motoneurons from chronic spinal rats.

2.4.3 Role of Na PIC in repetitive firing.

The Na PIC is always activated subthreshold to the spike, and thus plays a major role in spike initiation (see Results, and Crill 1996; Li et al. 2004a). Without a Na PIC, during slowly increasing excitation to a motoneuron (ramp), the membrane potential slowly depolarizes and spikes are not initiated (as in Fig. 2-5A), likely because inactivation of the transient sodium channel overwhelms its activation (as suggested by Lee and Heckman, 2001). A spike can be initiated during a more rapid depolarizing excitation (such as a step; Fig. 2-6A), because the rapid excitation replaces the action of the Na PIC. Once firing is initiated, it can continue, provided that the depolarizing upswing at the end of each AHP is rapid enough to initiate a spike without the help of large Na PICs, and this may explain why fast repetitive firing is possible in some acute spinal motoneurons that lack Na PICs (as in Fig. 2-6B) or in hypoglossal motoneurons when the Na PIC is reduced with phenetol (Zeng et al. 2005). Basically, any form of depolarization that sufficiently rapidly depolarizes the

membrane (above a minimum slope dV/dt) can initiate a spike (such as a fast-onset Ca PIC). However, except during rapid firing, the upswing at the end of the AHP is slow and insufficient to cause spike initiation by itself, so firing stops after a few spikes. This is the usual situation in the extreme acute spinal motoneurons that have little or no Na PIC (as in Fig. 2-6A). Furthermore, cells without a Na PIC show evidence of somewhat increased spike inactivation (see Results), which makes spike initiation and firing even more difficult. This subtle spike inactivation invariably occurs when the Na PIC is blocked with riluzole (see Results Fig. 2-10I) or monoamine antagonists (Harvey et al. 2005b) or when the Na PIC is just spontaneously absent (see Results), consistent with the idea that different activation states of the same sodium channel may underlie the spike and the Na PIC (Alzheimer et al. 1993; Crill 1996).

Most normal motoneurons in acute spinal rats do, however, have some Na PIC, and this clearly serves to enable repetitive firing, because they fire repetitively during a steady or slowly increasing current injection (see Discussion above and riluzole results). When a Na PIC is present, the spikes are initiated because the Na PIC produces a rapid depolarization (subthreshold acceleration, Fig. 2-5E) that presumably helps the activation of the spike escape its inactivation, during a slow current ramp. Furthermore, the Na PIC is known to be rapidly deactivated upon hyperpolarization (unlike the Ca PIC, Li and Bennett 2003), and thus each AHP must at least partly deactivate the Na PIC (see Results). Therefore, following each AHP, the Na PIC is again available to activate and help initiate a new spike. In this way, the Na PIC enables repetitive firing. Just at threshold the Na PIC initially comes on slowly (ramps up), but eventually it comes on more rapidly, causing a rapid acceleration that triggers a spike (at arrowheads in Fig. 2-6 or 2-7). This slow followed by fast activation could be due to a voltage-dependent time constant of the Na PIC (like with the Ca PIC; Li and Bennett, 2003), or due to two distinct Na currents making up the Na PIC, one slower sodium current (and perhaps additionally an I_h current, Pape 1996) and a second faster higher threshold sodium current.

As the firing rate increases, the firing level rises and the AHPs produce less absolute hyperpolarization; thus, ultimately, the minimum potential reached during AHPs is more depolarized during fast firing (i.e., bottoms of AHPs depolarize; Figs. 2-2E and 2-5E; see also Schwindt & Crill 1982 and Bennett et al. 1998). Thus, the Na PIC should be less affected (less deactivated) by the AHPs during fast firing. Thus, the Na PIC may not play such a critical role in fast firing, which is consistent with the finding that reducing the Na PIC with monoamine antagonists does not lower the F-I slope (Harvey et al. 2005b) and reducing the Na PIC with phenetol does not affect late spike frequency adaptation during fast firing (Zeng et al. 2005). Further, the F-I slope does not increase in cells with larger Na PICs (Fig. 2-8). Oddly enough, Lee and Heckman (2001) found a positive correlation with the F-I slope and Na PIC. However, they only indirectly inferred the Na PIC from the response to high frequency oscillations (120 Hz), and thus likely also included other non-persistent currents that correlated with the F-I slope.

In acute spinal rats the Na PICs are usually too small to produce an outright negative-slope region in the I-V relation, so Na PICs do not activate in an all-or-nothing manner (no Na plateau produced), unlike the usual case in chronic spinal rats (Li et al. 2004a), or in normal

motoneurons treated with 5-HT (Harvey et al. 2005a). Thus, in acute spinal rats, once firing is initiated, it can easily be stopped by decreasing the excitation from current injection. That is, once firing slows sufficiently during decreasing current injection (triangular current injection), the upswing of the AHP and the weak depolarization from the Na PIC are not sufficient to overcome the decreasing excitation, so the minimum rate of change of potential (dV/dt) for spike initiation is not reached. At this point firing stops, and this is sometimes at a current greater than that required to recruit the motoneuron ($\Delta I < 0$; i.e., late spike frequency adaptation occurs, see Bennett et al. 2001b).

2.4.4 *Spinal shock after injury and impact on acute slice preparations.*

In summary, compared to motoneurons of chronic spinal rats or normal motoneurons treated with 5-HT (Harvey et al. 2005a), greater excitation is required to recruit motoneurons after acute spinal transection because they rest further from threshold, they have lower input resistance and they have less Ca and Na PICs to help bring the membrane to threshold. Also, if firing is initiated, it does not always continue, especially at low rates, because of the weak Na PICs. Together, these factors play a major role in determining the reduced motoneuron excitability following acute spinal cord injury, and ultimately this helps explain the spinal shock state seen clinically after injury. The reduced excitability seen in acute injury, can be increased by monoamine antagonists (Harvey et al. 2005b) or overcome with monoamine agonists (Harvey et al. 2005a). Thus, the massive loss of brainstem-derived monoamines may play a central role in spinal shock following acute injury.

Most of what we know about 'normal' motoneurons derives from acute slice preparations (turtle, guinea pig, mouse, etc.), which also suffer from the same massive loss of brainstem monoamines as do acute spinal animals. Thus, the firing behaviour of motoneurons in these slice preparations is compromised. The motoneurons of chronic spinal rats are much closer to normal because they have PICs more comparable to the brainstem-intact animal (Lee and Heckman 1998a) and have had months to compensate for the loss of monoamines by increasing sensitivity of receptor pathways that facilitate the PICs (Harvey et al. 2005a, b). Motoneurons of chronic spinal rats do, however, have a significant reduction in dendritic size, compared to normal (e.g., Kitzman 2005), and it remains to be determined whether this influences the function of the motoneuron.

2.5 BIBLIOGRAPHY FOR CHAPTER 2

Alaburda A and Hounsgaard J. Metabotropic modulation of motoneurons by scratch-like spinal network activity. *J Neurosci* 23: 8625-8629, 2003.

Alvarez FJ, Pearson JC, Harrington D, Dewey D, Torbeck L, and Fyffe RE. Distribution of 5-hydroxytryptamine-immunoreactive boutons on alpha-motoneurons in the lumbar spinal cord of adult cats. *J Comp Neurol* 393: 69-83, 1998.

Alzheimer C, Schwandt PC, and Crill WE. Modal gating of Na⁺ channels as a mechanism of persistent Na⁺ current in pyramidal neurons from rat and cat sensorimotor cortex. *J Neurosci* 13: 660-673, 1993.

Bennett DJ, Gorassini M, Fouad K, Sanelli L, Han Y, and Cheng J. Spasticity in rats with sacral spinal cord injury. *J Neurotrauma* 16: 69-84, 1999.

Bennett DJ, Hultborn H, Fedirchuk B, and Gorassini M. Synaptic activation of plateaus in hindlimb motoneurons of decerebrate cats. *J Neurophysiol* 80: 2023-2037, 1998.

Bennett DJ, Li Y, and Siu M. Plateau potentials in sacrocaudal motoneurons of chronic spinal rats, recorded in vitro. *J Neurophysiol* 86: 1955-1971, 2001.

Cassam AK, Llewellyn-Smith IJ, and Weaver LC. Catecholamine enzymes and neuropeptides are expressed in fibres and somata in the intermediate gray matter in chronic spinal rats. *Neuroscience* 78: 829-841, 1997.

Conway BA, Hultborn H, Kiehn O, and Mintz I. Plateau potentials in alpha-motoneurons induced by intravenous injection of L-dopa and clonidine in the spinal cat. *J Physiol* 405: 369-384, 1988.

Crill WE. Persistent sodium current in mammalian central neurons. *Annu Rev Physiol* 58: 349-362, 1996.

Deisz RA, Fortin G, and Zieglansberger W. Voltage dependence of excitatory postsynaptic potentials of rat neocortical neurons. *J Neurophysiol* 65: 371-382, 1991.

Delgado-Lezama R, Perrier JF, Nedergaard S, Svirskis G, and Hounsgaard J. Metabotropic synaptic regulation of intrinsic response properties of turtle spinal motoneurons. *J Physiol* 504 (Pt 1): 97-102, 1997.

Eken T, Hultborn H, and Kiehn O. Possible functions of transmitter-controlled plateau potentials in alpha motoneurons. *Prog Brain Res* 80: 257-267; discussion 239-242, 1989.

Fedirchuk B and Dai Y. Monoamines increase the excitability of spinal neurons in the neonatal rat by hyperpolarizing the threshold for action potential production. *J Physiol* 557: 355-361, 2004.

French CR, Sah P, Buckett KJ, and Gage PW. A voltage-dependent persistent sodium current in mammalian hippocampal neurons. *J Gen Physiol* 95: 1139-1157, 1990.

Geijo-Barrientos E and Pastore C. The effects of dopamine on the subthreshold electrophysiological responses of rat prefrontal cortex neurons in vitro. *Eur J Neurosci* 7: 358-366, 1995.

Gorassini MA, Bennett DJ, and Yang JF. Self-sustained firing of human motor units. *Neurosci Lett* 247: 13-16, 1998.

Granit R, Henatsch HD, and Steg G. Tonic and phasic ventral horn cells differentiated by post-tetanic potentiation in cat extensors. *Acta Physiol Scand* 37: 114-126, 1956.

Guertin PA and Hounsgaard J. Non-volatile general anaesthetics reduce spinal activity by suppressing plateau potentials. *Neuroscience* 88: 353-358, 1999.

Harvey PJ, Li Y, Li X, and Bennett DJ. Chapter 3: Serotonin facilitates persistent sodium currents in motoneurons, and spinal cord transection leads to a supersensitivity to serotonin. *From: The Role of 5-HT in the Development of Motoneuron Persistent Sodium Currents after Chronic Spinal Injury* Ph.D. Dissertation: pp. 75-120, 2005a.

Harvey PJ, Li Y, Li X, and Bennett DJ. Chapter 4: Endogenous monoamines are essential for persistent sodium currents and repetitive firing in rat spinal motoneurons. *From: The Role of 5-HT in the Development of Motoneuron Persistent Sodium Currents after Chronic Spinal Injury* Ph.D. Dissertation: pp. 121-174, 2005b.

Hounsgaard J, Hultborn H, Jespersen B, and Kiehn O. Bistability of alpha-motoneurons in the decerebrate cat and in the acute spinal cat after intravenous 5-hydroxytryptophan. *J Physiol* 405: 345-367, 1988a.

Hounsgaard J and Kiehn O. Serotonin-induced bistability of turtle motoneurons caused by a nifedipine-sensitive calcium plateau potential. *J Physiol* 414: 265-282, 1989.

Hounsgaard J, Kiehn O, and Mintz I. Response properties of motoneurons in a slice preparation of the turtle spinal cord. *J Physiol* 398: 575-589, 1988b.

Hsiao CF, Del Negro CA, Trueblood PR, and Chandler SH. Ionic basis for serotonin-induced bistable membrane properties in guinea pig trigeminal motoneurons. *J Neurophysiol* 79: 2847-2856, 1998.

Hultborn H and Kiehn O. Neuromodulation of vertebrate motor neuron membrane properties. *Curr Opin Neurobiol* 2: 770-775, 1992.

Kiehn O and Eken T. Prolonged firing in motor units: evidence of plateau potentials in human motoneurons? *J Neurophysiol* 78: 3061-3068, 1997.

- Kiehn O and Harris-Warrick RM. Serotonergic stretch receptors induce plateau properties in a crustacean motor neuron by a dual-conductance mechanism. *J Neurophysiol* 68: 485-495, 1992.
- Kitzman P. Alteration in axial motoneuronal morphology in the spinal cord injured spastic rat. *Exp Neurol* 192: 100-108, 2005.
- Kuo JJ, Schonewille M, Siddique T, Schults AN, Fu R, Bar PR, Anelli R, Heckman CJ, and Kroese AB. Hyperexcitability of cultured spinal motoneurons from presymptomatic ALS mice. *J Neurophysiol* 91: 571-575, 2004.
- Lee RH and Heckman CJ. Adjustable amplification of synaptic input in the dendrites of spinal motoneurons in vivo. *J Neurosci* 20: 6734-6740, 2000.
- Lee RH and Heckman CJ. Bistability in spinal motoneurons in vivo: systematic variations in persistent inward currents. *J Neurophysiol* 80: 583-593, 1998a.
- Lee RH and Heckman CJ. Bistability in spinal motoneurons in vivo: systematic variations in rhythmic firing patterns. *J Neurophysiol* 80: 572-582, 1998b.
- Lee RH and Heckman CJ. Enhancement of bistability in spinal motoneurons in vivo by the noradrenergic alpha 1 agonist methoxamine. *J Neurophysiol* 81: 2164-2174, 1999.
- Lee RH and Heckman CJ. Essential role of a fast persistent inward current in action potential initiation and control of rhythmic firing. *J Neurophysiol* 85: 472-475, 2001.
- Li Y and Bennett DJ. Persistent sodium and calcium currents cause plateau potentials in motoneurons of chronic spinal rats. *J Neurophysiol* 90: 857-869, 2003.
- Li Y, Gorassini MA, and Bennett DJ. Role of persistent sodium and calcium currents in motoneuron firing and spasticity in chronic spinal rats. *J Neurophysiol* 91: 767-783, 2004a.
- Li Y, Li X, Harvey PJ, and Bennett DJ. Effects of baclofen on spinal reflexes and persistent inward currents in motoneurons of chronic spinal rats with spasticity. *J Neurophysiol* 92: 2694-2703, 2004b.
- Newton BW and Hamill RW. The morphology and distribution of rat serotonergic intraspinal neurons: an immunohistochemical study. *Brain Res Bull* 20: 349-360, 1988.
- Nishimura Y, Schwindt PC, and Crill WE. Electrical properties of facial motoneurons in brainstem slices from guinea pig. *Brain Res* 502: 127-142, 1989.
- Pape HC. Queer current and pacemaker: the hyperpolarization-activated cation current in neurons. *Annu Rev Physiol* 58: 299-327, 1996.

- Perrier JF and Hounsgaard J. 5-HT₂ receptors promote plateau potentials in turtle spinal motoneurons by facilitating an L-type calcium current. *J Neurophysiol* 89: 954-959, 2003.
- Perrier JF, Mejia-Gervacio S, and Hounsgaard J. Facilitation of plateau potentials in turtle motoneurons by a pathway dependent on calcium and calmodulin. *J Physiol* 528 Pt 1: 107-113, 2000.
- Powers RK and Binder MD. Effective synaptic current and motoneuron firing rate modulation. *J Neurophysiol* 74: 793-801, 1995.
- Powers RK and Binder MD. Persistent sodium and calcium currents in rat hypoglossal motoneurons. *J Neurophysiol* 89: 615-624, 2003.
- Prather JF, Powers RK, and Cope TC. Amplification and linear summation of synaptic effects on motoneuron firing rate. *J Neurophysiol* 85: 43-53, 2001.
- Schlue WR, Richter DW, Mauritz KH, and Nacimiento AC. Responses of cat spinal motoneuron somata and axons to linearly rising currents. *J Neurophysiol* 37: 303-309, 1974.
- Schmidt BJ and Jordan LM. The role of serotonin in reflex modulation and locomotor rhythm production in the mammalian spinal cord. *Brain Res Bull* 53: 689-710, 2000.
- Schroder HD and Skagerberg G. Catecholamine innervation of the caudal spinal cord in the rat. *J Comp Neurol* 242: 358-368, 1985.
- Schwindt PC and Crill WE. Factors influencing motoneuron rhythmic firing: results from a voltage-clamp study. *J Neurophysiol* 48: 875-890, 1982.
- Stafstrom CE, Schwindt PC, Chubb MC, and Crill WE. Properties of persistent sodium conductance and calcium conductance of layer V neurons from cat sensorimotor cortex in vitro. *J Neurophysiol* 53: 153-170, 1985.
- Urbani A and Belluzzi O. Riluzole inhibits the persistent sodium current in mammalian CNS neurons. *Eur J Neurosci* 12: 3567-3574, 2000.
- White SR and Fung SJ. Serotonin depolarizes cat spinal motoneurons in situ and decreases motoneuron afterhyperpolarizing potentials. *Brain Res* 502: 205-213, 1989.
- Xu W and Lipscombe D. Neuronal Ca_v1.3 α (1) L-type channels activate at relatively hyperpolarized membrane potentials and are incompletely inhibited by dihydropyridines. *J Neurosci* 21: 5944-5951, 2001.
- Zeng J, Powers RK, Newkirk G, Yonkers M, and Binder MD. Contribution of persistent sodium currents to spike-frequency adaptation in rat hypoglossal motoneurons. *J Neurophysiol* 93: 1035-1041, 2005.

CHAPTER 3: Serotonin facilitates persistent sodium currents in motoneurons, and chronic spinal cord transection leads to a supersensitivity to serotonin.

3.1 BACKGROUND

Spinal motoneurons exhibit large persistent inward currents (PICs) that greatly augment synaptic input, enable sustained depolarizations (plateaus) and produce firing that outlasts a stimulation (self-sustained firing: Bennett et al. 1998; Hounsgaard et al. 1988) in unanesthetized animals (Lee and Heckman 1998; Li and Bennett 2003; Schwindt and Crill 1984), and even in awake humans (Gorassini et al. 2002; Kiehn and Eken 1997). PICs are composed of two currents: a TTX-sensitive persistent sodium current (Na PIC) and a nimodipine-sensitive persistent calcium current (Ca PIC) (Carlin et al. 2000; Hsiao et al. 1998; Li and Bennett 2003). Nimodipine blocks not only the inward current from the L-type Ca channel but also outward currents triggered by Ca^{2+} influx, which combined form the net Ca PIC (Hounsgaard and Mintz 1988; Schwindt and Crill 1984). In this paper, we focus on the Na PIC, which was studied in isolation by adding nimodipine to block the Ca PIC (Li et al. 2004a).

PICs are considered to be a latent property of normal motoneurons (see Heckman et al. 2004) that are regulated by the synaptic input of endogenous neuromodulators such as norepinephrine (NE), serotonin (5-HT), acetylcholine and glutamate (Alaburda and Hounsgaard 2003; Delgado-Lezama et al. 1997; Hultborn and Kiehn 1992; Lee and Heckman 1999). The brainstem-derived monoamines (5-HT and NE) play a major role in facilitating PICs, because acute spinal cord transection largely eliminates plateaus and self-sustained firing associated with PICs (Harvey et al. 2005a; Hounsgaard et al. 1988) and subsequent application of monoamine agonists recovers plateau properties (Conway et al. 1988; Hounsgaard et al. 1988). We know that 5-HT can induce Na PICs and Ca PICs in acute spinal animals or acutely sliced spinal cords (guinea pig: Hsiao et al. 1998; rat: Li et al. 2004c; turtle: Perrier and Hounsgaard 2003). The details of how Ca PICs are facilitated by neuromodulators have been well-described in turtle motoneurons; they involve 5-HT₂ receptors and intracellular calcium and calmodulin (Perrier and Hounsgaard 2003; Perrier et al. 2000). However, the regulation of Na PICs in motoneurons by 5-HT is less well understood (see Discussion). Thus, the first goal of the present paper was to quantify how 5-HT, and in particular 5-HT₂ receptor agonists, modulate the Na PIC in acute spinal rats. We studied motoneurons of the whole sacrocaudal spinal cord of adult rats that had been acutely transected at the upper sacral level, removed from the animal and maintained *in vitro* (Bennett et al. 2001b; Li and Bennett 2003). We found that the natural ligand 5-HT had complex effects on the motoneurons, including increasing the Na PIC, increasing the input resistance and depolarizing the resting membrane potential. In contrast, the 5-HT₂ receptor agonist (\pm)-1-(2,5-dimethoxy-4-iodophenyl)-2-aminopropane (DOI) selectively increased the Na PIC, without changing other membrane properties.

Curiously, motoneurons below a complete spinal transection spontaneously redevelop plateaus and large PICs in the months following injury (Li and Bennett 2003); this leads to

the spastic syndrome seen *in vivo*, characterized by intense prolonged and uncontrolled muscle spasms (Bennett et al. 2001a; Li et al. 2004a). These large PICs are present despite the complete degeneration of brainstem axons in the chronic spinal state (Haggendal and Dahlstrom 1973), resulting in loss of the major source of monoamines. With this dramatic reduction in 5-HT availability, motoneuron responses below the transection become much more sensitive to 5-HT in terms of increasing reflex excitability and spontaneous motoneuron firing (Barbeau and Bedard 1981; Li et al. 2004b). It may be that the motoneurons and the PICs themselves become supersensitive to 5-HT; thus, the second goal of this paper was to examine that possibility. We found that the Na PIC was a remarkable 30-fold more sensitive to 5-HT compared to acute spinal rats, such that the Na PIC was increased with very small doses of 5-HT (via the 5-HT₂ receptors, as with motoneurons of acute spinal rats). Because PICs do indeed become supersensitive to 5-HT, residual basal levels of 5-HT caudal to the injury (Hadjiconstantinou et al. 1984; Newton and Hamill 1988) should in principle play a major role in producing the large PICs seen in the chronic spinal state; this idea is verified in Chapter 4 (Harvey et al. 2005b).

3.2 METHODS

Intracellular recordings were made from motoneurons in the *in vitro* sacrocaudal spinal cord of adult female Sprague-Dawley rats (200 - 600g). Both normal animals (n = 37, age 1 - 6 months, average age = 3.3 ± 1.1 months) and rats with spasticity due to chronic spinal injury (n = 29, age 3 - 5 months, average age = 3.9 ± 0.6 months) were included in the present study. For normal rats, the cord was transected at the S2 level at the time of removal of the sacrocaudal cord (acute spinal rats). For spastic chronic spinal rats, a complete transection at the S2 level was made at 40 to 55 days of age. Usually, within 1 month, dramatic spasticity developed in the tail muscles, which are innervated by sacrocaudal motoneurons below the level of the injury (see Bennett et al. 1999; Bennett et al. 2001a for details of the animal model and spasticity assessment). Only rats more than 1.5 months, and less than 4 months, post-injury with clear spasticity were used for *in vitro* recording of the motoneurons. All experimental procedures were conducted in accordance with guidelines for the ethical treatment of animals issued by the Canadian Council on Animal Care and approved by the University of Alberta Health Sciences Animal Policy and Welfare Committee.

3.2.1 *In vitro* preparation

Details of the *in vitro* procedures have been described at length in Chapter 2 and previous publications (Bennett et al. 2001b; Harvey et al. 2005a; Li and Bennett 2003). Briefly, under urethane anaesthesia (0.18 g/100 g), the sacrocaudal spinal cords of both normal and chronic spinal rats were removed to a dissection chamber containing modified artificial cerebrospinal fluid (mACSF) for preparation, and then transferred to a recording chamber containing normal artificial cerebrospinal fluid (nACSF). Residual anaesthetic, and kynurenic acid from the mACSF, were allowed to wash-out for 1 hour in the recording chamber before the bathing solution was switched to nACSF containing a cocktail of fast

synaptic transmission blockers (AP5, CNQX, strychnine and picrotoxin; see below). A total volume of 200 ml nACSF was oxygenated in a source bottle and superfused over the spinal cord. This nACSF was then collected, filtered and recycled continuously back into the source bottle using a peristaltic pump. Drugs were added to this continuously recycling volume of fluid as required. Drug wash-out was done by switching to a separate bottle with 200 ml fresh nACSF containing only the cocktail of fast synaptic transmission blockers. Often 15 μM nimodipine was added at the beginning of the experiment to isolate the Na PIC by blocking the L-type calcium channels mediating the Ca PIC (Harvey et al. 2005a; Li and Bennett 2003).

3.2.2 *Drugs and solutions*

Two kinds of artificial cerebrospinal fluid (ACSF) were used in these experiments: a modified ACSF (mACSF) designed to minimize potential excitotoxicity was used in the dissection chamber prior to recording, and a normal ACSF (nACSF) was used in the recording chamber. Composition of the mACSF was (in mM) 118 NaCl, 24 NaHCO₃, 1.5 CaCl₂, 3 KCl, 5 MgCl₂, 1.4 NaH₂PO₄, 1.3 MgSO₄, 25 D-glucose and 1 kynurenic acid. The nACSF was composed of (in mM) 122 NaCl, 24 NaHCO₃, 2.5 CaCl₂, 3 KCl, 1 MgCl₂ and 12 D-glucose. Both types of ACSF were saturated with 95% O₂-5% CO₂ and maintained at pH 7.4. The synaptic transmission blocking cocktail added to the nACSF contained 50 μM D-(-)-2-Amino-5-phosphopentanoic acid (AP5, Tocris, U.S.A.), 10 μM 6-cyano-7-nitroquinoxaline-2,3-dione (CNQX, Tocris), 1 μM strychnine (Sigma, U.S.A.) and 100 μM picrotoxin (Tocris) to block NMDA, AMPA/kainate, glycine and GABA_A receptors, respectively. Additional drugs were added as required, including 0.3 - 50 μM 5-hydroxytryptamine (5-HT; Sigma), 1 - 50 μM of the 5-HT₂ receptor agonist (\pm)-1-(2,5-dimethoxy-4-iodophenyl)-2-aminopropane (DOI, Sigma), 10 μM of the 5-HT_{2A} receptor antagonist ketanserin (Tocris), 2 μM of the 5-HT_{2C} receptor antagonist RS 102221 (Tocris), 2 μM tetrodotoxin (TTX; Alamone Labs, Israel) to block transient and persistent voltage-dependent Na channels, and 15 μM nimodipine (Tocris) to block voltage-dependent L-type Ca channels mediating the persistent calcium current.

3.2.3 *Persistent inward current in voltage and current clamp recording*

Intracellular recording electrodes and methods were as described in Li and Bennett (2003) and Harvey et al. (2005a). Motoneurons were identified via antidromic stimulation of the ventral roots. Only motoneurons with a stable penetration (resting potential (V_m) below -60 mV and antidromic spike height over 60 mV from rest) were included in this study. Slow triangular current ramps (0.4 nA/s) in discontinuous current clamp (DCC) were used to measure firing, frequency-current (F-I) responses and self-sustained firing (ΔI) (Harvey et al. 2005a; Li and Bennett 2003). Slow voltage ramps (3.5 mV/s) in single-electrode voltage clamp (SEVC) were used to measure the PICs, as described in detail previously (Harvey et al. 2005a; Li and Bennett 2003). In summary, to estimate the PIC, the leak current was first determined from a linear regression to the current response near rest and subthreshold to the PIC. Then this leak current was extrapolated to the potentials where the PIC was activated.

Finally, the PIC was quantified as the initial maximum difference between the recorded current and the extrapolated leak current (initial peak PIC). The onset voltage of the PIC (V_{START}) was computed as described previously (Harvey et al. 2005a).

Basic cell properties, such as input resistance (R_m), and spike threshold (V_{th}), were determined from the current-clamp ramps. Measurements and calculations were performed as described in detail in Chapter 2 (Harvey et al. 2005a), with the following additional measurements: The PIC half-activation voltage ($V_{1/2}$) was measured, in cells with a negative-slope region, as the voltage where the PIC was half activated (halfway between initial zero-slope conductance and peak PIC, see Li et al. 2004a). For motoneurons lacking a negative-slope region, $V_{1/2}$ was considered to be the potential at which the derivative of the current reached a minimum. The influence of agonists on the PIC was measured by taking the difference in maximum leak-subtracted current before and after drug application, and this was called the drug-induced PIC. The spike afterhyperpolarization (AHP) was recorded following antidromic activation across a range of potentials. Ultimately the depth of the medium duration AHP was quantified at -70 mV before and after 5-HT application to control for 5-HT-induced changes in resting membrane potential.

3.2.4 Data analysis

Data were analyzed in Clampfit 8.0 (Axon Instruments, U.S.A.), and figures were made in Sigmaplot (Jandel Scientific, U.S.A.). Data are shown as mean \pm standard deviation. A Student's *t*-test was used to test for statistical differences, and a paired *t*-test was used when analyzing cells before and after drug application, with a significance level of $P < 0.05$.

3.3 RESULTS

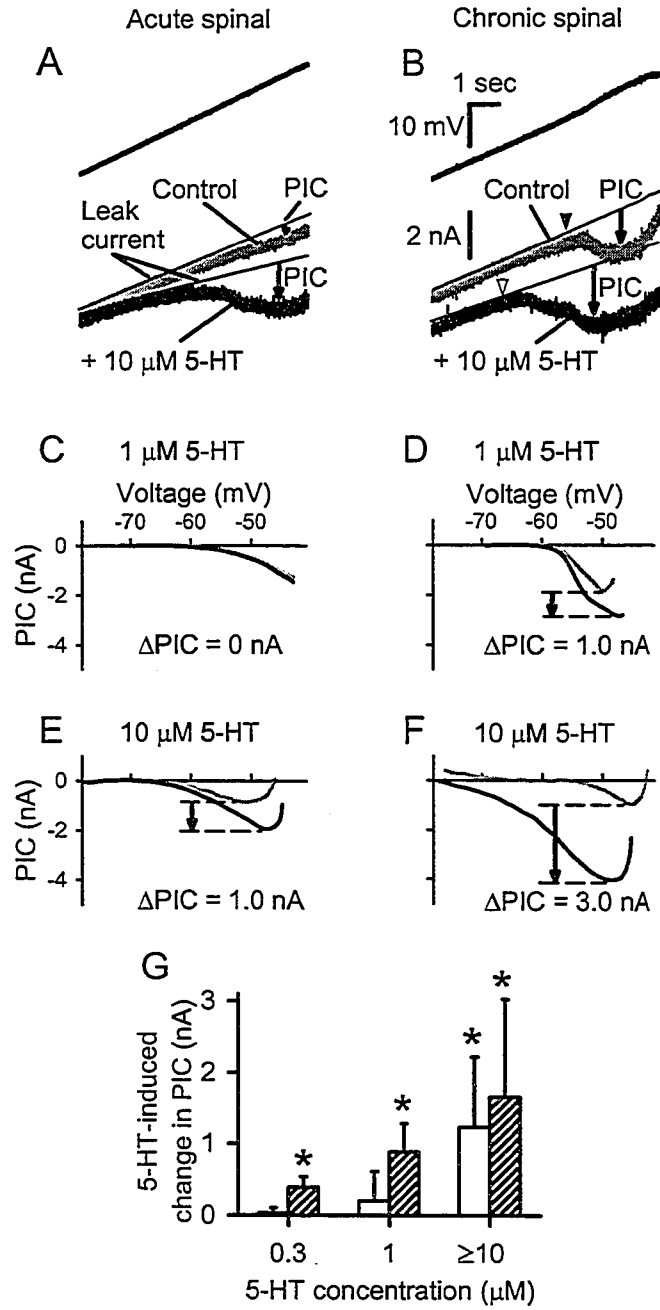
Intracellular recordings were made from motoneurons of the whole sacrocaudal spinal cord of adult rats. For this the sacrocaudal cord of 37 normal adult rats was maintained *in vitro*, by acutely transecting the spinal cord at the upper sacral level and transferring all the spinal cord caudal to the transection to a recording chamber (termed *acute spinal rats*; $n = 61$ motoneurons recorded). In a further 29 adult rats the S2 sacral spinal cord was transected in a prior surgery and, after at least 1.5 months recovery, when all descending 5-HT axons had sufficient time to degenerate, the whole sacrocaudal spinal cord was likewise removed and maintained *in vitro* for recording (*chronic spinal rats*; $n = 37$ motoneurons recorded).

The basic membrane properties and persistent inward currents (PICs) in these motoneurons, prior to the addition of any neuromodulators, are detailed in Chapter 2 (Harvey et al. 2005a). To summarize, motoneurons from normal rats recorded in the acute spinal state were found to rest further from the spike threshold, have a lower input resistance and require more current to recruit than in chronic spinal rats (Harvey et al. 2005a). Furthermore, after chronic spinal injury, motoneurons had much larger PICs than immediately after injury. That is, in chronic spinal rat motoneurons during a slow voltage ramp (voltage-clamp), the recorded current initially increased linearly with voltage, consistent with a simple leak current in this

Figure 3-1

Persistent inward currents (PICs) in motoneurons are facilitated by 5-HT and are supersensitive to 5-HT after chronic spinal transection. *A*: In motoneuron from acute spinal rat, a slow voltage ramp (3.5 mV/s) from -80 to -40 mV (*top*) was used to measure the PIC (*bottom*) before and after 5-HT application. The PIC was quantified as the difference between the leak current (thin line) and the recorded current (downward arrow). Note that PIC was increased by 10 μM 5-HT (black trace) compared to control (grey trace). *B*: Motoneuron from chronic spinal rat. Same format and scale as in *A*. 5-HT again increased the PIC amplitude and lowered onset voltage of the PIC (V_{START} ; black arrowhead – control, white arrowhead – 5-HT). Also, note in *A* and *B* the decrease in input conductance and depolarization of resting potential (at a given current) with 5-HT. *C - F*: Filtered data from voltage ramps, with leak current subtracted, plotted against membrane potential. Typical motoneurons before (grey traces) and after (black traces) 5-HT application of varying dose. Drug-induced PIC (ΔPIC) was calculated as the difference in maximum leak-subtracted currents (downward arrow). Low-dose (1 μM) 5-HT did not change PIC ($\Delta\text{PIC} = 0$ nA) in acute spinal rat (*C*), but did increase it in chronic spinal rat (*D*). High dose 5-HT (≥ 10 μM) increased PIC in both acute (*E*) and chronic (*F*) spinal rats, but the effect was larger in chronic spinal rats. (*G*) Group data showing average change in PIC amplitude with various doses of 5-HT. Open bars – acute spinal, shaded bars – chronic spinal. Asterisk (*) indicates effect significantly greater than zero ($P < 0.05$). PIC amplitude significantly increased at low doses (≤ 1 μM) of 5-HT in motoneurons from chronic spinal rats, while high doses (≥ 10 μM) were required to facilitate PICs in acute spinal rats.

Figure 3 - 1



subthreshold region (thin line in Fig. 3-1B), but at about -60 mV, the current deviated downward sharply from the expected leak current, due to the activation of a PIC (PIC amplitude indicated by length of arrow in Fig. 3-1B). This PIC was usually large enough to produce a pronounced negative-slope region in the current trace (Fig. 3-1B, black trace; PIC on average was 2.79 ± 0.94 nA). In acute spinal rats, a similar PIC was seen during a voltage ramp, but it was much smaller than in chronic spinal rats (on average 1.11 ± 1.21 nA) and it did not usually produce a negative-slope region (Fig. 3-1A). When there was a negative-slope region, it was small (see details in Harvey et al. 2005a). In acute spinal rats, the Ca PICs and Na PICs were on average 0.78 ± 0.82 nA and 0.55 ± 0.74 nA, respectively. In chronic spinal rats, the Ca PICs and Na PICs were on average 1.82 ± 0.78 nA and 1.31 ± 0.93 nA, respectively.

3.3.1 5-HT enhances PICs in motoneurons of acute spinal rats.

When 5-HT was applied to the spinal cord of acute spinal rats at moderate to high doses (10 - 50 μ M, n = 9), the net PIC recorded in motoneurons was significantly increased by 1.23 ± 0.99 nA (mean \pm SD; Figs. 3-1A, E and G; increase measured as the change in maximum leak-subtracted current induced by 5-HT; see Methods). These recordings were made in the presence of a fast synaptic transmission blockade (see Methods); thus, the 5-HT-induced PIC likely resulted from the direct action of 5-HT on motoneurons, rather than on interneurons. The mean onset voltage of the PIC (V_{START}) was also lowered by, on average, 4.3 ± 5.7 mV (n = 6 at ≥ 10 μ M; range = +1.1 to -12.1 mV), although this reduction was not quite significant ($P = 0.1$) due to the wide range of changes in V_{START} . Lower doses of 5-HT (0.3 - 1.0 μ M) had no significant effects on the PICs (n = 8, Figs. 3-1C and G) or other membrane properties (see Fig. 3-2 described below).

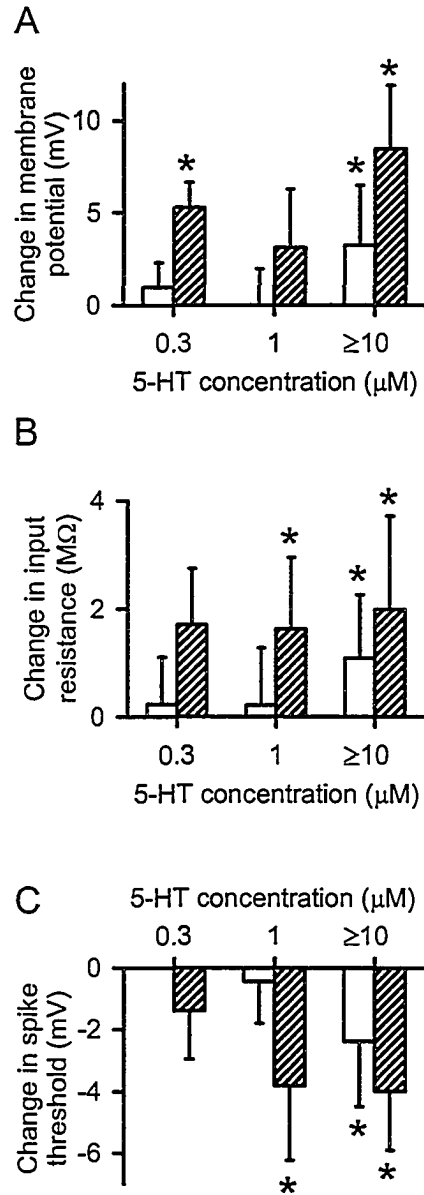
3.3.2 5-HT also induces changes in input resistance, resting potential and spike properties.

5-HT had more complicated effects on motoneurons of acute spinal rats than merely facilitating the PIC. Doses of 10 - 50 μ M 5-HT produced a significant depolarization of the resting membrane potential by 3.2 ± 3.2 mV (Fig. 3-2A) and a significant increase in input resistance of 1.1 ± 1.2 M Ω , (21.3% increase, Fig. 3-2B, n = 10). With 10 - 50 μ M 5-HT, there was also a significant reduction of spike voltage threshold (V_{th}) by 2.4 ± 2.1 mV (Fig. 3-2C, similar to Fedirchuk and Dai 2004), and a significant increase of 2.5 ± 2.3 mV in the spike height, as measured by the spike overshoot (potential above 0 mV; not shown). Together, these effects made motoneurons substantially easier to depolarize and recruit after 5-HT application, and indeed the current required to recruit the motoneurons during slow current ramps was significantly reduced by 2.3 ± 1.8 nA in 5-HT, to an average current threshold of 2.1 ± 1.9 nA (n = 12). Application of 5-HT at any dose did not significantly change the amplitude of the post-spike AHP (measured at -70 mV).

Figure 3-2

Motoneurons from chronic spinal rats are supersensitive to the multiple effects of 5-HT. Group data are shown for average change in cell property with various doses of 5-HT. Open bars – acute spinal, shaded bars – chronic spinal. Asterisk (*) indicates effect significantly greater than zero ($P < 0.05$). Low doses ($0.3 - 1 \mu\text{M}$) of 5-HT significantly depolarized the resting potential (V_m ; *A*), increased the input resistance (R_m ; *B*) and lowered the spike voltage threshold (V_{th} ; *C*) in chronic spinal rats, whereas, high doses of 5-HT ($> 10 \mu\text{M}$) were required to affect these parameters in acute spinal rats.

Figure 3 - 2



3.3.3 *5-HT₂ receptors facilitate the total PIC.*

Application of the 5-HT₂ receptor antagonists ketanserin (10 μ M; 5-HT_{2A}) and RS 102221 (2 μ M; 5-HT_{2C}) inhibited the PIC induced by 5-HT (not shown), and even inhibited the spontaneously occurring PIC without 5-HT (see details in Harvey et al. 2005b), suggesting that 5-HT₂ receptors are involved in regulating the PIC. To directly test this, we applied the 5-HT₂ agonist (\pm)-1-(2,5-dimethoxy-4-iodophenyl)-2-aminopropane (DOI) to motoneurons of acute spinal rats. At a 30 μ M dose, DOI significantly increased the total PIC (measured in the absence of nimodipine) by 0.97 ± 0.85 nA ($n = 7$; see Fig. 3-7 described later), and significantly lowered the onset voltage of the PIC (V_{START} ; from -62.4 ± 3.1 mV to -69.0 ± 5.0 mV), suggesting that indeed 5-HT₂ receptors modulate the total PIC (Ca and Na PIC). Lower (1 - 10 μ M) doses of DOI had no effect on the PIC, so unlike in chronic spinal rats described below, motoneurons in acute spinal rats are not very sensitive to DOI.

3.3.4 *5-HT₂ receptors facilitate the Na PIC.*

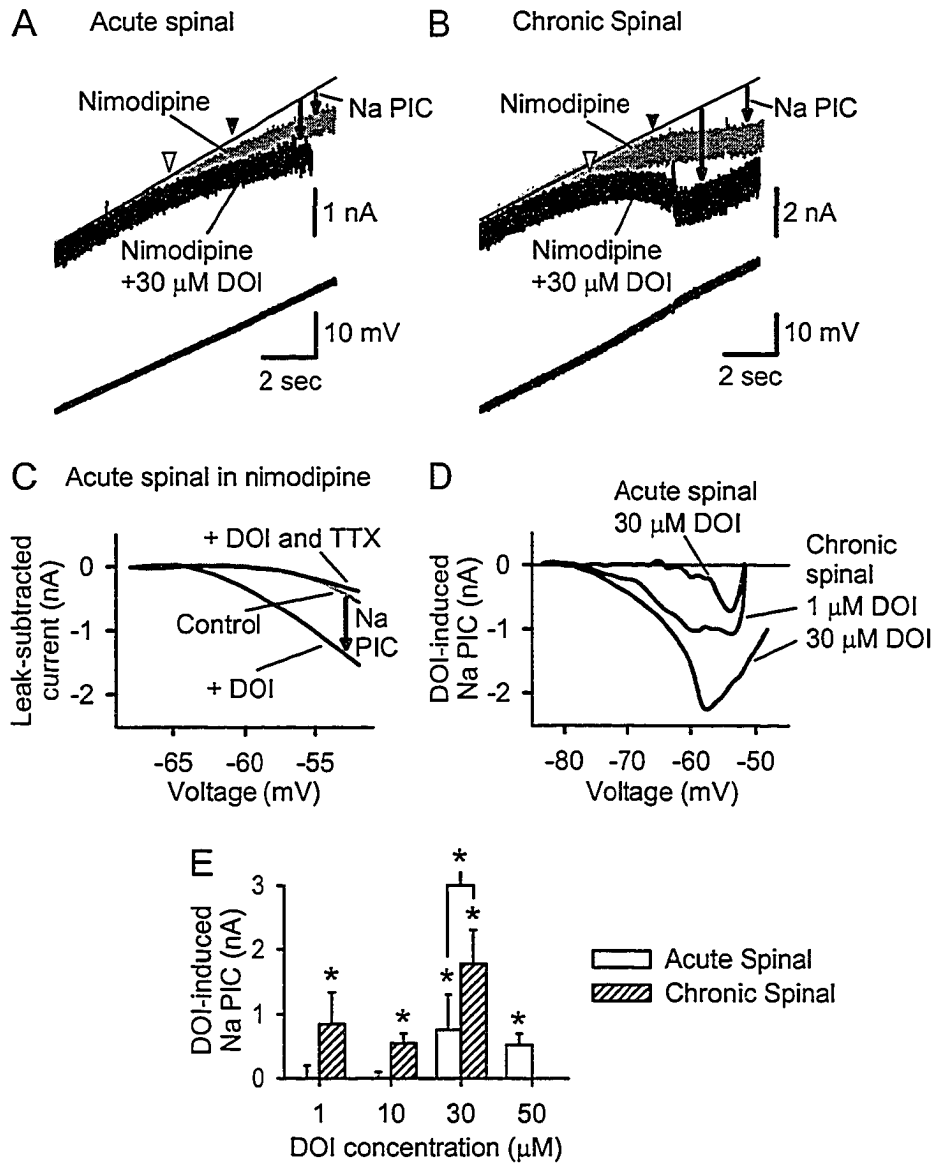
To specifically study the effect of 5-HT receptors on Na PICs, we eliminated the Ca PIC by application of nimodipine, to leave the Na PIC in isolation (Harvey et al. 2005a). In motoneurons of acute spinal rats, the Na PICs were small, or occasionally even absent. When present, they usually did not produce a negative-slope region, and instead only produced an inflection (flattening) in the I-V relation (grey line in Fig. 3-3A), as described in Chapter 2 (Harvey et al. 2005a). In these motoneurons of acute spinal rats, DOI (30 μ M) significantly increased the Na PIC by, on average, 0.75 ± 0.56 nA ($n = 5$; Figs. 3-3A and 3E), and significantly lowered the Na PIC onset voltage V_{START} from -62.3 ± 5.0 mV to -66.1 ± 4.9 mV. This DOI-induced PIC measured in nimodipine was blocked by subsequent application of TTX (Fig. 3-3C), and thus was indeed mediated by a TTX-sensitive Na PIC. While the average DOI-induced increase in the Na PIC measured in nimodipine was less than the DOI-induced increase in total PIC measured without nimodipine (combined Ca and Na PICs), these effects were not significantly different from each other, due to large between-cell variability. Thus, although 5-HT₂ receptor activation (with DOI) clearly facilitated the Na PIC, we do not yet know whether or not 5-HT₂ receptor activation influences the Ca PIC (though our preliminary results suggest that 5-HT and DOI facilitate the Ca PIC; see details in Li and Bennett, in preparation). A higher dose of DOI (50 μ M) had similar effects as 30 μ M DOI, while lower doses of 1 - 10 μ M DOI had no effect on the Na PIC (Fig. 3-3E).

Even cells that had no detectable Na PIC prior to DOI (as in Fig. 3-6B) exhibited a Na PIC after DOI application (30 - 50 μ M, Fig. 3-6D). Most of these cells that initially lacked Na PICs could not fire repetitively with slow current ramps (see Harvey et al. 2005a). As described later, DOI rescued these cells, so that they could fire repetitively on current ramps (Figs. 3-6 and 3-7, described later), consistent with the critical role of the Na PIC in repetitive firing.

Figure 3-3

Na PICs in motoneurons are facilitated by the 5-HT₂ receptor agonist DOI, and motoneurons of chronic spinal rats are supersensitive to DOI. All recordings (*A - D*) done in 15 μ M nimodipine to block Ca PIC (see Methods). *A*: In acute spinal rat motoneuron, high-dose DOI (30 μ M) facilitated the Na PIC and hyperpolarized Na PIC onset (V_{START} ; arrowheads: black – control, white - DOI). Same format as in Fig. 3-1A. *B*: In motoneuron after chronic injury, Na PIC amplitude was increased and PIC onset hyperpolarized by DOI. *C*: Leak-subtracted I-V curves of acute spinal rat motoneurons in nimodipine (control), after DOI application and after TTX application. The Na PIC induced by high-dose DOI was subsequently blocked by TTX. *D*: Current induced by DOI (I-V curve in nimodipine subtracted from I-V curve in nimodipine + DOI). For chronic spinal rat motoneurons, higher doses of DOI induce larger increases in Na PIC amplitude (dose-dependent). Effect of high-dose ($\geq 30 \mu$ M) DOI in acute spinal rats was similar to low-dose ($\leq 10 \mu$ M) in chronic spinal rats. *E*: Group data for DOI effect on Na PIC, measured in nimodipine. Significant effect of DOI for chronic spinal rat motoneurons at all doses tested. Only high doses ($\geq 30 \mu$ M) effective in acute spinal rat motoneurons. 30 μ M DOI had significantly greater effect in chronic versus acute spinal rat motoneurons. Asterisk (*) indicates significant effect of DOI.

Figure 3 - 3



3.3.5 *5-HT₂ receptor activation does not affect input resistance or resting membrane potential but does hyperpolarize the spike threshold and facilitate the spike.*

The 5-HT₂ receptor agonist DOI had a relatively selective effect on the Na PIC in that it did not influence many other motoneuron properties that were affected by 5-HT itself. Unlike 5-HT, DOI did not significantly affect the resting membrane potential (V_m), input resistance (R_m) and spike overshoot, whether tested with nimodipine ($\Delta V_m = -2.1 \pm 6.4$ mV, $\Delta R_m = 0.01 \pm 1.03$ M Ω , Δ overshoot = -2.1 ± 4.3 , $n = 11$; no effects significant), or without nimodipine ($\Delta V_m = -4.4 \pm 4.3$ mV, $\Delta R_m = 0.3 \pm 0.7$ M Ω , Δ overshoot = 1.4 ± 5.8 , $n = 7$; no effects significant). However, 5-HT₂ receptor activation with 30 - 50 μ M DOI significantly hyperpolarized the voltage threshold for fast sodium spikes (V_{th}) by -2.6 ± 3.7 mV ($n = 17$) in motoneurons of acute spinal rats, consistent with the results of Fedirchuk et al. (2004). Further DOI significantly lowered the current threshold for spike activation during slow current ramps, from 3.9 ± 2.2 nA to 2.4 ± 0.9 nA, making these cells easier to activate despite the lack of effect of DOI on the input resistance or resting potential. Also, DOI (30 - 50 μ M) facilitated the fast sodium spike, in that the maximum rate of rise (dV/dt_{max}) of the first spike during our standard slow current ramp was significantly increased by 29.2 ± 9.9 V/s (dV/dt_{max} was 159.0 ± 31.7 V/s prior to DOI). This dV/dt_{max} measure has previously been argued to be linked to sodium channel inactivation during a slow ramp (Schlue et al. 1974), so the DOI-induced increase in dV/dt_{max} can be interpreted as a decreased tendency for sodium spike inactivation. In some cells, DOI was so effective in increasing the rate of rise of the spike that we encountered problems with proper voltage-clamping of the spikes after adding DOI, in that we suffered from more break-away spikes during our slow voltage ramps, compared to before DOI (not shown).

In summary, 5-HT₂ receptor activation facilitates both the transient and persistent sodium currents, and lowers their onset voltages together, consistent with the idea that the parameters of these two currents may be related (see Discussion and Li et al. 2004a). In contrast, 5-HT₂ receptor activation does not alter the resting potential and input resistance, whereas 5-HT does, so these membrane properties must be modulated by other 5-HT receptors (i.e., not 5-HT₂).

3.3.6 *Na PICs are supersensitive to 5-HT₂ receptor activation with DOI in chronic spinal rats.*

Motoneurons of chronic spinal rats responded to 5-HT and DOI in the same way as normal motoneurons in all respects, but with larger responses and much lower doses evoking responses, indicating that a classic denervation supersensitivity had developed from the chronic loss of brainstem-derived 5-HT innervation. That is, high doses of DOI (30 μ M) produced a significantly greater increase in the Na PIC amplitude in chronic spinal (1.78 ± 0.52 nA) compared to acute spinal (0.75 ± 0.56 nA) rat motoneurons (Fig. 3-3D, and compare Fig. 3-3B versus 3-3A; Na PIC measured in nimodipine). Indeed, the DOI-induced Na PIC was significantly larger at all doses of DOI, when compared to equivalent doses in motoneurons of acute spinal rats (Fig. 3-3E). Furthermore, motoneurons of chronic

spinal rats exhibited an approximate 30-fold supersensitivity to DOI, in that as little as 1 μM DOI induced a significant increase in the Na PIC in chronic spinal rats, whereas the minimal effective dose in acute spinal rats was 30 μM (Fig. 3-3E). Further, the low 1 μM DOI dose had a similar effect in motoneurons of chronic spinal rats (0.84 ± 0.50 nA) as the 30 μM dose did in acute spinal rats (Figs. 3-3D and E). Finally, as with acute spinal rat motoneurons, DOI significantly lowered V_{START} of the Na PIC in chronic spinal rats (from, on average, -64.4 ± 5.4 mV ($n = 17$) to -69.9 ± 5.4 mV ($n = 11$); Fig. 3-3B), but again it did so at a much lower dose (as low as 1 μM DOI, compared to ≥ 30 μM DOI required in acute spinal rat motoneurons).

3.3.7 Effects of DOI in chronic spinal rat motoneurons are specific to Na channel facilitation.

There were no significant effects of DOI (at any dose) on resting membrane potential or input resistance in motoneurons of chronic spinal rats, with nimodipine ($\Delta V_m = 0.4 \pm 3.3$ mV, $\Delta R_m = -0.1 \pm 2.4$ M Ω , $n = 12$; no effects significant) or without nimodipine present ($\Delta V_m = -3.1 \pm 3.0$ mV, $\Delta R_m = 1.5 \pm 2.7$ M Ω , $n = 4$; no effects significant), as with acute spinal rats. However, with DOI, the spike voltage threshold was significantly hyperpolarized by 1.9 ± 3.1 mV, and the spike height as measured by the overshoot was significantly increased by 2.3 ± 2.9 mV ($n = 14$, combined data with and without nimodipine), like in acute spinal rats, though with effects at much lower doses than in acute spinal rats (1 - 10 μM ; supersensitivity). Furthermore, the maximum rate of rise of the action potential (dV/dt_{max}) was significantly increased by 22.3 ± 17.0 V/s with 1 - 30 μM DOI (dV/dt_{max} was 158.6 ± 37.2 V/s, $n = 19$ prior to DOI). Thus, 5-HT₂ receptor activation in chronic spinal rat motoneurons is specific to facilitating persistent and transient Na currents, as also found in motoneurons of acute spinal rats, though much lower doses are sufficient for facilitation.

3.3.8 PICs are also supersensitive to 5-HT itself in chronic spinal rats.

The 30-fold supersensitivity to the 5-HT₂ receptor agonist DOI was also seen when 5-HT itself was applied in chronic spinal rats (Fig. 3-1). That is, the PIC was significantly increased by 5-HT doses as low as 0.3 μM (by 0.39 ± 0.15 nA, $n = 3$; Fig. 3-1G), whereas ≥ 10 μM 5-HT was required to significantly increase the PIC in acute spinal rats. Further, the increase in PIC amplitude with 1 μM 5-HT (0.88 ± 0.40 nA, $n = 7$) was significantly greater in chronic spinal than in acute spinal (0.20 ± 0.41 nA, $n = 6$) rat motoneurons (Fig. 3-1G). At doses ≥ 10 μM , 5-HT induced a PIC that was not significantly different between motoneurons of chronic (1.65 ± 1.38 nA, $n = 6$) and acute (1.23 ± 0.99 nA, $n = 9$) spinal rats, suggesting a saturation in the response at these high doses. The onset voltage of the PIC, V_{START} , was also significantly lowered by low doses of 5-HT that had no effect in acute spinal rats (V_{START} lowered from -60.0 ± 5.0 mV to -67.1 ± 6.4 mV, $n = 19$ with doses as low as 0.3 μM 5-HT).

In the presence of nimodipine to block the Ca PIC, the Na PIC alone was also significantly increased by low and high doses of 5-HT (by 0.55 ± 0.38 nA on average for 1 - 30 μ M, n = 6). However, this 5-HT effect was significantly smaller than without the Ca PIC blocked with nimodipine (0.55 nA vs 1.65 nA), and thus 5-HT must also facilitate the Ca PIC (see details in Li and Bennett, in preparation).

3.3.9 *All effects of 5-HT on motoneurons become supersensitive to 5-HT after chronic injury.*

Not only was the PIC supersensitive to 5-HT in chronic spinal rat motoneurons, but the 5-HT-induced changes in resting membrane potential, input resistance and spike voltage threshold were also supersensitive to 5-HT (Figs. 3-2). The lowest dose tested (0.3 μ M) had significant effects on resting membrane potential (Fig. 3-2A) in motoneurons of chronic spinal rats (depolarized by 5.3 ± 1.4 mV), whereas motoneurons of acute spinal rats required at least 10 μ M 5-HT to be depolarized (Fig. 3-2A). Further, at the higher doses (10 - 50 μ M), 5-HT depolarized motoneurons of chronic spinal rats significantly more than acute spinal rat motoneurons (8.5 ± 3.4 mV vs. 3.2 ± 3.2 mV). Similarly, a significant 5-HT-induced increase in input resistance (R_m ; Fig. 3-2B) was observed with low doses (1 μ M) in chronic spinal rats (increase of 1.5 ± 1.3 M Ω , a 22.3% increase), whereas only higher doses of 5-HT (≥ 10 μ M) affected the input resistance in acute spinal rats. At high doses (≥ 10 μ M), 5-HT increased the input resistance by 2.0 ± 1.7 M Ω in motoneurons of chronic spinal rats, compared to 1.1 ± 1.2 M Ω in acute spinal rats..

Facilitation of the fast sodium spike by 5-HT also became supersensitive with chronic spinal transection. The spike voltage threshold (V_{th} ; Fig. 3-2C) in chronic spinal rat motoneurons was significantly hyperpolarized by a low dose of 5-HT (1 μ M; shifted by -4.0 ± 2.3 mV from control), whereas over 10 times more 5-HT was required to significantly hyperpolarize V_{th} in acute spinal rat motoneurons (≥ 10 μ M; see above). The hyperpolarization of V_{th} was maximal at low doses (1 μ M) in motoneurons from chronic spinal rats, because higher doses of 5-HT (≥ 10 μ M) did not further change it (-4.0 ± 1.9 mV). At these higher doses, the effect of 5-HT on V_{th} was not significantly different from that in acute spinal rats (V_{th} lowered by -2.4 ± 2.1 mV with ≥ 10 μ M 5-HT in acute spinal rats; Fig. 3-2C). However, these high doses of 5-HT further facilitated the fast transient sodium current in motoneurons from chronic spinal rats by significantly increasing the spike height (by 3.4 ± 3.7 mV, n = 8, not shown) as measured by the overshoot, whereas there was no significant facilitation for lower doses in chronic or acute spinal rats. The threshold current required to initiate firing was significantly reduced by 2.1 ± 1.0 nA (n = 9) with low doses of 5-HT (1 μ M) in chronic spinal rats, whereas this spike current threshold was only significantly reduced by 5-HT at high doses in acute spinal rats (see above). In fact, the average spike current threshold for chronic spinal rat motoneurons in 5-HT was -0.2 ± 1.2 nA at 1 μ M and -0.7 ± 1.4 nA at ≥ 10 μ M, which meant that many motoneurons in 5-HT were spontaneously firing steadily at rest. Overall, chronic spinal rat motoneurons exhibited a complex supersensitivity to 5-HT. As in acute spinal rats, application of 5-HT at any dose did not significantly change the amplitude of the post-spike AHP in chronic spinal rats (measured at -70 mV).

In summary, the persistent sodium current and the fast transient sodium current (as determined by changes in spike voltage threshold and spike height) appear to be specifically regulated by a supersensitive 5-HT₂ receptor, because they are also influenced by the selective 5-HT₂ receptor agonist DOI. Other properties such as resting membrane potential and input resistance are regulated through supersensitive responses of other 5-HT receptors (non-5-HT₂).

3.4.10 5-HT₂ receptor agonists act slowly on the Na PIC.

The facilitation of the Na PIC by 5-HT or DOI was slow relative to other effects of 5-HT (on V_m and R_m), in both acute and chronic spinal rats. Typically, the Na PIC was increased about 5 - 10 minutes after application of DOI or 5-HT (as measured in nimodipine), and maximum effects took up to 20 minutes. Also, there was no habituation, in that the Na PIC induced by 5-HT or DOI remained unattenuated for long periods (> 1 hour). Following wash-out of 5-HT receptor agonists from the bath, long periods (up to 45 minutes) were required for the Na PIC to return to control levels. The voltage threshold for spike activation V_{th} was modulated slowly with the Na PIC. Thus, the facilitation of the persistent and transient Na channels by the Gq protein-coupled 5-HT₂ receptor appears to have substantially delayed onsets and offsets.

In contrast, the effects of 5-HT that do *not* depend on the 5-HT₂ receptors (DOI-insensitive) occurred with shorter latencies. Changes in resting membrane potential and input resistance occurred within about 2 minutes of application of 5-HT (1 - 30 μ M). This delay is considered very fast because it is similar to the time that it took TTX (2 μ M) to block fast sodium spikes (see Li and Bennett 2003), and much of this delay likely represents the drug diffusion time into the whole sacrocaudal spinal cord preparation. In summary, 5-HT receptor activation much more rapidly affects the resting membrane potential and input resistance compared to the Na PIC. This further supports the notion that 5-HT₂ receptors are involved in modulating the Na PIC, whereas other faster-acting 5-HT receptors modulate the input resistance and resting membrane potential.

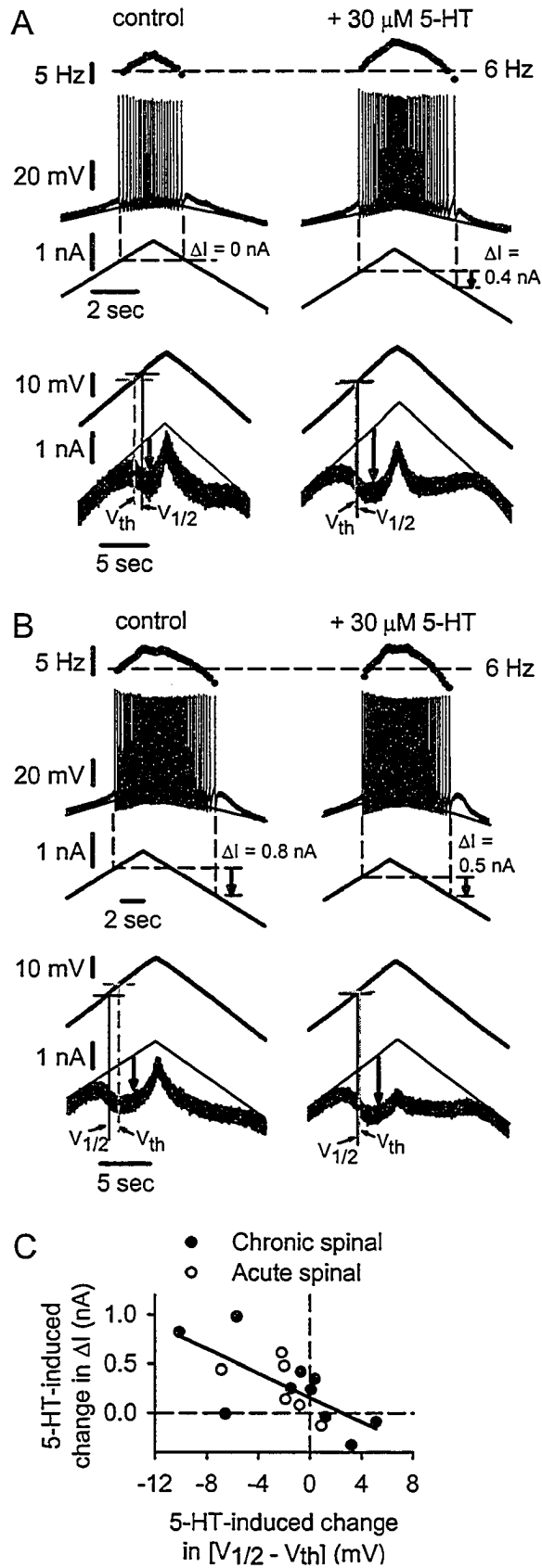
3.4.11 Paradoxical effects of 5-HT on self-sustained firing.

In the majority of cells, 5-HT increased self-sustained firing (without nimodipine; $n = 6/9$ acute, $n = 9/14$ chronic; Fig. 3-4A), whereas, in other cells, self-sustained firing was paradoxically not increased ($n = 2/9$ acute, $n = 3/14$ chronic) or even decreased ($n = 1/9$ acute, $n = 2/14$ chronic; Fig. 3-4B). Previously, we have shown that the size of the PIC (especially Ca PIC) partly determines the degree of self-sustained firing, but the half-activation voltage of the PIC ($V_{1/2}$; see Methods, and Li et al. 2004a) is equally, if not more, important. Specifically, self-sustained firing is most pronounced when the half-activation voltage ($V_{1/2}$) for the PIC is lower than (or near) the spike threshold (V_{th} ; as in Fig. 3-4B control), because the PIC is able to be more fully activated (the membrane potential is kept below V_{th} by the AHPs, Li et al. 2004a). Thus, the activation voltage of the PIC relative to spike threshold ($V_{1/2} - V_{th}$) is a critical factor in determining the degree of self-sustained

Figure 3-4

Self-sustained firing is influenced by 5-HT-induced change in PIC activation voltage relative to firing level. Cells measured in normal ACSF, without Ca PIC blocked. *A*: Motoneuron of a chronic spinal rat. *Top left*: Slow current ramps, with instantaneous firing frequency shown above spikes. Recruitment and de-recruitment thresholds indicated by dashed lines. Note firing stopped at same current on down-ramp as the current at recruitment on up-ramp ($\Delta I = 0$, no self-sustained firing). *Bottom left*: Slow voltage ramp, as in Fig. 3-1A, but here also showing down-ramp. The large PIC is indicated by downward arrow from leak current (thin line). Note PIC half-activation voltage ($V_{1/2}$; solid vertical line) was higher than spike voltage threshold (V_{th} ; dashed line). *Top right*: In 5-HT, current threshold for recruitment greater than threshold at de-recruitment ($\Delta I > 0$ nA, self-sustained firing). *Bottom right*: 5-HT increased PIC amplitude and shifted $V_{1/2}$ more hyperpolarized relative to V_{th} . *B*: A different chronic spinal rat motoneuron, in same format as *A*. *Top*: Self-sustained firing was paradoxically *reduced* in 5-HT (smaller ΔI). *Bottom*: 5-HT increased the total PIC amplitude in this cell, however 5-HT shifted $V_{1/2}$ more depolarized relative to V_{th} . *C*: Each symbol represents an individual motoneuron. Change in self-sustained firing (ΔI) with 5-HT is plotted against change in position of $V_{1/2}$ relative to V_{th} . In all cells shown, 5-HT increased total PIC amplitude. Self-sustained firing increased with 5-HT when $V_{1/2}$ was unchanged, or became more negative, relative to V_{th} (i.e., $\Delta(V_{1/2} - V_{th}) \leq 0$ mV, upper left quadrant). Self-sustained firing decreased when $\Delta(V_{1/2} - V_{th}) > 0$ mV (lower right quadrant).

Figure 3 - 4



firing. 5-HT acts to hyperpolarize both V_{th} and $V_{1/2}$, (and V_{START} , as described above), but often does not affect V_{th} and $V_{1/2}$ equally in the same motoneuron. As such, $V_{1/2}$ can move relative to the spike voltage threshold V_{th} . Accordingly, 5-HT-induced changes in $V_{1/2} - V_{th}$ were significantly correlated with changes in self-sustained firing (ΔI ; $r = 0.69$, $n = 16$, $P = 0.003$), as shown in Figure 3-4C. In cells where half-activation voltage of the PIC shifted positively relative to the spike threshold ($V_{1/2} - V_{th}$ increased), the self-sustained firing decreased (lower right quadrant, see example in Fig. 3-4B), with an average decrease in ΔI of -0.15 ± 0.13 nA ($n = 4$). This decreased self-sustained firing occurred despite an increase in the PIC by 0.96 ± 0.80 mV in these 4 cells, so the changes in $V_{1/2} - V_{th}$ dominated the response, and led to the paradoxical decrease in self-sustained firing. In contrast, in cells where $V_{1/2} - V_{th}$ was unchanged ($n = 3$) or decreased ($n = 8$) with 5-HT, the self-sustained firing increased significantly (upper left quadrant of Fig. 3-4C, see example in Fig. 3-4A), with an average increase in ΔI of 0.44 ± 0.28 nA ($n = 11$). For these cells, the PIC also significantly increased with 5-HT by 1.05 ± 0.63 nA. Thus, the increased PIC amplitude, and hyperpolarization of $V_{1/2}$ relative to V_{th} , together contributed to the increased self-sustained firing (greater ΔI).

The increases in self-sustained firing with 5-HT just described are likely dominated by 5-HT-induced changes in the Ca PIC (threshold and amplitude), as has previously been shown to be the major component of the PIC in determining the self-sustained firing (Li et al. 2004a). However, Na PICs also play a role in self-sustained firing, and in particular cause slow self-sustained firing, as described next.

3.4.12 5-HT₂ receptor activation produces very slow firing mediated by Na PICs.

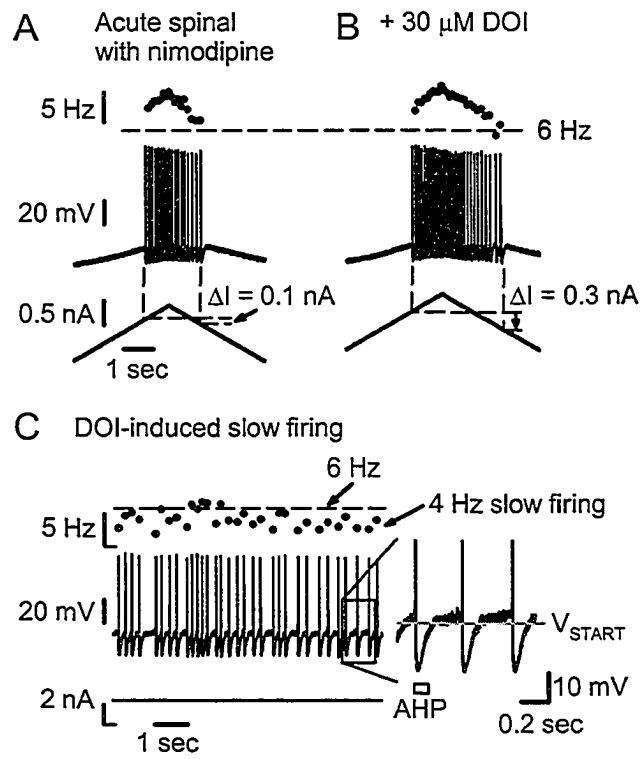
In the presence of nimodipine to block the Ca PIC, 5-HT₂ receptor activation (with DOI or 5-HT) significantly increased the self-sustained firing in acute spinal rats (ΔI increased significantly by 0.21 ± 0.21 nA with ≥ 30 μ M DOI) because the increased Na PIC (see above) enabled sustained slow firing prior to de-recruitment (Figs. 3-5B and C). The Na PIC was always activated subthreshold to the sodium spike, so shifts in $V_{1/2}$ relative to V_{th} were minimal and the effect on self-sustained firing was dominated by changes in Na PIC amplitude. As such, in the absence of a Ca PIC, increases in ΔI with DOI were significantly correlated to increases in Na PIC amplitude (slope = 0.40 nA/nA, $r = 0.86$, $n = 8$, $P = 0.006$). Interestingly, DOI had no significant effect on the F-I slope, despite the large changes in the Na PIC. That is, in acute spinal rats, DOI (≥ 30 μ M) induced a change in F-I slope of only -0.9 ± 2.4 Hz/nA ($n = 6$), and in chronic spinal rats, DOI (≥ 1 μ M) induced a change in F-I slope of -0.5 ± 0.8 Hz/nA ($n = 11$; neither change significantly different than zero). Thus, this input-output gain (F-I slope) does not depend on the Na PIC (though the F-I slope does vary with the Ca PIC, Li et al. 2004a).

The major effect of DOI on firing was to lower the minimum firing rate at de-recruitment (Fig. 3-5B). That is, DOI at high doses (30 μ M or more) significantly lowered the minimum firing rate in motoneurons of acute spinal rats by 1.2 ± 1.2 Hz ($n = 9$). Similarly, 5-HT at high doses (≥ 10 μ M; without nimodipine) also significantly lowered the minimum firing rate by 2.7 ± 3.4 Hz ($n = 11$) in motoneurons of acute spinal rats. The lower minimum rate

Figure 3-5

With Ca PIC blocked, DOI increases self-sustained firing and enables very slow firing. All recordings were done in motoneurons from acute spinal rats, with nimodipine blocking Ca PIC. *A*: Slow triangular current ramp (*bottom*) elicited repetitive firing and very small amount of self-sustained firing (*middle*; $\Delta I = 0.1$ nA). Firing frequency (*top*) not below 6 Hz (horizontal dashed line). *B*: From same motoneuron as in *A*; DOI increased Na PIC amplitude in this cell (not shown). ΔI was increased and firing occurred at less than 6 Hz just prior to de-recruitment. *C*: Different cell in DOI showing continuous firing below 6 Hz with current held at threshold. Close up shown at *right*. Note interspike interval longer than AHP duration (open rectangle).

Figure 3 - 5



that results from an increase in Na PIC amplitude with DOI may seem counterintuitive but occurs because large Na PICs are critical in supporting low-frequency firing. As described by Li et al. (2004a), when the Na PIC is sufficiently large to produce a negative-slope region in the I-V relation, a subthreshold sodium plateau is produced by this Na PIC. Near threshold, this sodium plateau oscillates on and off to produce very slow firing (Fig. 3-5C, acute spinal rat motoneuron in 30 μ M DOI). That is, each sodium plateau onset triggers a spike, which is followed by an AHP that turns off the plateau, but the plateau is again turned on once the AHP ends (Fig. 3-5C, close up on spikes at *right*). This oscillation produces very slow firing, which we define as firing with interspike intervals substantially longer than the AHP duration (< 6 Hz firing, and as slow as 1 Hz, Li et al. 2004a). Thus, the above finding that 5-HT and DOI lowered the minimum firing rate in acute spinal rat motoneurons is consistent with the large increase in the Na PIC and an associated increase in incidence of negative-slope regions with DOI (30.8% of motoneurons in acute spinal rats had negative-slope regions in DOI, compared to 9.1% in control). Furthermore, all cells (100%) that exhibited a Na PIC negative-slope region in DOI (and nimodipine) also exhibited very slow firing (< 6 Hz), with a mean minimum rate of 4.9 ± 0.9 Hz. In contrast, cells that did not exhibit a Na PIC negative-slope region had a significantly higher minimum firing rate (7.0 ± 1.8 Hz), and only 20% of these had firing slower than 6 Hz. Basically, cells of acute spinal rats with an induced Na PIC large enough to produce a negative-slope region exhibit very slow firing similar to that described in chronic spinal rats (Li et al. 2004a).

In chronic spinal rats, dosages of DOI that were effective at increasing the Na PIC (≥ 1 μ M) did not significantly lower the minimum firing rate (changed by -0.6 ± 1.0 Hz, $n = 10$; not significant), or increase self-sustained firing (ΔI only increased by 0.05 ± 0.18 nA, $n = 12$; not significant). Although the Na PIC was increased significantly by DOI (see above), these cells already had large enough Na PICs to exhibit the very slow steady firing phenomenon prior to DOI (minimum firing rate in control plus nimodipine was 4.6 ± 1.9 Hz, see Harvey et al. 2005b), so that DOI did not further slow the firing. Likely the slow firing phenomena is somewhat all-or-nothing, simply requiring a Na PIC with a negative-slope region and associated sodium plateau; it does not matter so much how big the negative-slope region is (Harvey et al. 2005a; Li et al. 2004a).

3.4.13 Motoneurons with poor repetitive firing are rescued by 5HT₂ receptor action.

As described in Chapter 2 (Harvey et al. 2005a), a few motoneurons of acute spinal rats (8/34) were unable to fire repetitively during our standard slow current ramps (Figs. 3-6A and 3-7A), although they could fire transiently with healthy spikes induced by fast current steps (inset of Fig 3-6A) or antidromic activation (inset of Fig. 3-7A). Also, we encountered one unusual motoneuron of a chronic spinal rat that likewise lacked steady repetitive firing (Fig 3-6E), even though all other chronic spinal rats had robust repetitive firing in motoneurons. These cells likely fired poorly because they also lacked a significant Na PIC (Figs. 3-6B and F, linear I-V relation in nimodipine), which has been shown to be critical for spike initiation (Harvey et al. 2005a; Lee and Heckman 2001). Indeed, DOI was found to rescue such poor firing motoneurons by inducing an Na PIC

Figure 3-6

DOI rescues healthy motoneurons with no Na PIC and enables them to generate repetitive firing with slow current ramps. Sections *A - D* are recordings from the same cell. *A*: Motoneuron from acute spinal rat recorded in nimodipine. Same format as in Fig. 3-4A. Slow current ramps well past normal threshold (V_{th} , horizontal dashed line measured in DOI) did not initiate action potentials or repetitive firing. *Inset*: full height action potential triggered by current step. *B*: No Na PIC observed in voltage-clamp ramp prior to DOI. *C*: In this cell, DOI enabled repetitive firing with normal speed current ramps. *D*: Onset of repetitive firing occurred at same time as facilitation of the Na PIC. *E - F*: Same format as *A - D*, but from an unusual chronic spinal rat motoneuron that did not exhibit any Na PIC when recorded in nimodipine. DOI facilitated self-sustained repetitive firing and slow firing (*) during current ramps (*G*), and induced an Na PIC large enough to produce a negative-slope region during voltage ramps (*H*).

Figure 3 - 6

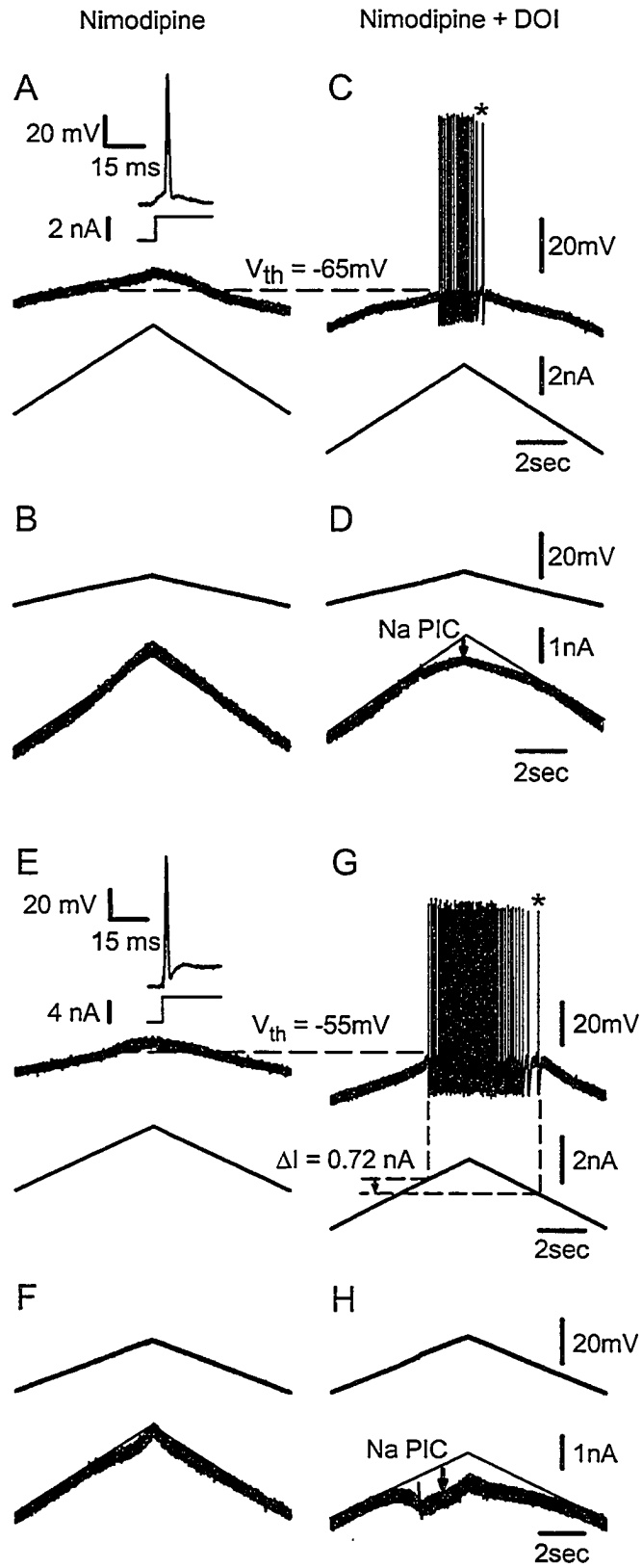
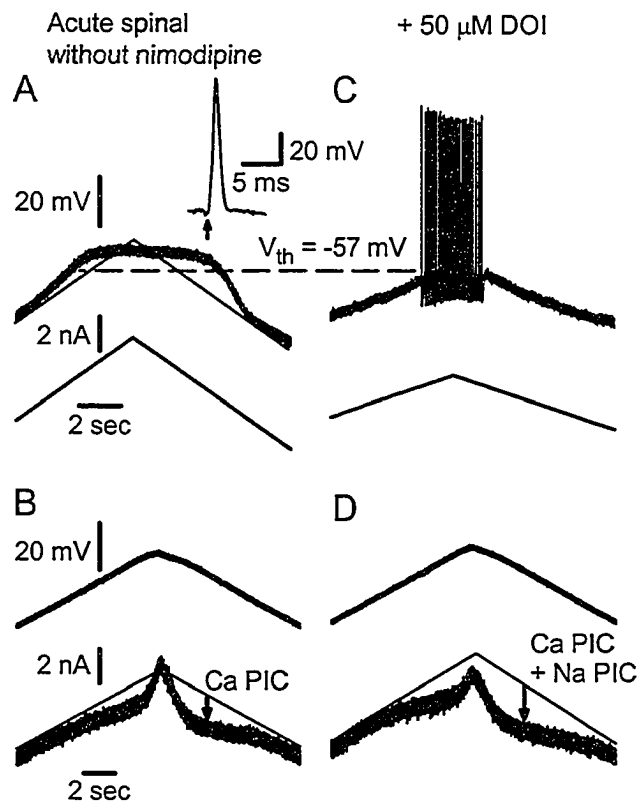


Figure 3-7

DOI restores firing ability in motoneuron with Ca PIC but no Na PIC. Motoneuron from acute spinal rat, recorded without nimodipine present, in same format as Figure 3-6. *A*: Motoneuron was unable to initiate action potentials or repetitive firing with slow current ramp. Note large Ca plateau. Normal size action potential was generated in response to antidromic stimulation (*inset* in *A*). *B*: Without nimodipine, this motoneuron had a Ca PIC. *C*: DOI enabled repetitive firing with slow current ramps. *D*: Amplitude of the total PIC was larger in DOI.

Figure 3 - 7



(Fig. 3-6D), and thus ultimately enabling them to fire repetitively during current ramps (Fig. 3-6C; n = 4 tested with DOI). In two of these four cells, a large enough Na PIC was induced by DOI (esp. Fig. 3-6H) to ultimately enable very slow self-sustained firing (at * in Figs. 3-6C and G), as previously described for cells with large Na PICs (Fig. 3-5 and Harvey et al. 2005a). Thus, 5-HT₂ receptor activation can turn any motoneuron with little or no firing ability into one that behaves very much like a typical excitable motoneuron in a chronic spinal rat.

These kinds of cells that initially had poor repetitive firing ability occurred both with and without the Ca PIC blocked with nimodipine (see Fig. 3-7A, no nimodipine). The cells without nimodipine had moderate PICs (Fig. 3-7B), which we suppose were entirely Ca PICs, because of the lack of repetitive firing and because of their characteristic hysteretic current response on the downward voltage ramp (Li and Bennett 2003). Thus, the Ca PICs were not sufficient to enable steady repetitive firing, unlike the Na PICs. In these cells with a Ca PIC present, DOI enabled repetitive firing (Fig. 3-7C) and increased the amplitude of the PIC (Fig. 3-7D), strongly suggesting a facilitation of the Na PIC (Li et al. 2004a).

3.4 DISCUSSION

The present results demonstrate that 5-HT increases the PICs in motoneurons of both acute and chronic spinal rats, and also modulates a number of other membrane properties that together make the motoneurons more excitable. Specifically, 5-HT augments the Na PICs, lowers the spike threshold and increases the spike height (overshoot), and these sodium channel-related effects are mediated by 5-HT₂ receptors (mimicked by DOI and blocked by 5-HT₂ antagonists). We also found that 5-HT depolarizes the motoneurons and increases their input resistance (consistent with other reports, reviewed in Rekling et al. 2000), but these effects are not mediated by 5-HT₂ receptors (not mimicked by DOI). Interestingly, when 5-HT is applied to acute spinal rats, the combined effects of 5-HT make the motoneurons behave more like excitable motoneurons in chronic spinal rats, which rest closer to threshold, have a higher input resistance and have much larger PICs than in acute spinal rats prior to 5-HT (Harvey et al. 2005a). Thus, it is possible that motoneurons of chronic spinal rats are very excitable precisely because the 5-HT receptor intracellular pathways are strongly activated. Indeed, we have also found that motoneurons of chronic spinal rats are supersensitive to very small amounts of 5-HT, and thus the residual 5-HT below a transection (2 - 15% of normal, Schmidt and Jordan 2000) may be sufficient to endogenously activate the 5-HT receptors. This may ultimately lead to the highly excitable motoneurons in chronic spinal rats. We explore this possibility in Chapter 4 (Harvey et al. 2005b), and in the final section of the Discussion below.

3.4.1 5-HT₂ receptor activation modulates Na channels.

It has been shown that activation of 5-HT₂ receptors on spinal motoneurons leads to facilitation of the Ca PIC (Perrier and Hounsgaard 2003, Li and Bennett, unpublished

observations), and that the intracellular signaling linking the receptors to the Ca channels involves intracellular Ca^{2+} and calmodulin (Perrier et al. 2000). Much less is known regarding modulation of the Na PIC in motoneurons, but what is known is consistent with our findings that 5-HT₂ receptors facilitate the Na PIC (DOI facilitates the Na PIC, and 5-HT₂ receptor antagonists inhibit the Na PIC; see Results and Harvey et al. 2005a). That is, activation of 5-HT_{2A} has been found in neonatal rat phrenic motoneurons to induce a tonic inward current (Lindsay and Feldman 1993) that is sodium-dependent (Lee et al. 1999). Also, 5-HT-treated trigeminal motoneurons in guinea pigs exhibit Na PICs, though the extent to which 5-HT caused these Na PICs is unclear (Hsiao et al. 1998). The Na PICs in cultured neonatal rat spinal motoneurons are also facilitated by 5-HT₂ receptor activation, though this depends on intracellular calcium levels (Jiang et al. 2004, see below). In other neurons, Pena and Ramirez (2002) report that 5-HT_{2A} (though not 5-HT_{2C}) receptors likewise facilitate Na PICs in interneurons involved in respiratory rhythms, and 5-HT enhances the Na PIC in leech locomotor neurons (Angstadt and Friesen 1993). On the other hand, 5-HT_{2A/2C} receptor activation reduces the Na PIC in prefrontal cortex (Carr et al. 2002). In summary, at this stage, it is clear that the 5-HT₂ receptor is involved in modulating persistent sodium currents, and usually facilitates them in motoneurons.

The sodium channels mediating the Na PIC are likely to be similar, if not the same, as those involved in the fast sodium spike, albeit in a different activation state or mode that allows the channels to remain open without inactivating (e.g., modal current of transient Na channel, see Alzheimer et al. 1993; Crill 1996). Regardless of the specific mechanism, the idea that the same sodium channels mediate both the fast sodium spike and the Na PIC is consistent with the findings that 5-HT₂ receptors have a general facilitatory effect on sodium currents in motoneurons; lowering the spike threshold (see Results, and Fedirchuk and Dai 2004), increasing the spike overshoot, decreasing the tendency for sodium channel inactivation during a slow ramp (rate of rise of first spike on ramp increased), lowering the Na PIC threshold and increasing the Na PIC amplitude (see Results).

5-HT₂ receptors are coupled to the G_q-protein that triggers membrane phospholipid turnover (via phospholipase C activation), yielding the intracellular second messengers diacylglycerol and inositol-1,4,5-triphosphate (IP₃), which respectively go on to activate intracellular protein kinase C (PKC) and regulate release of calcium from intracellular calcium stores (reviewed in Hille 2001). Thus, it is not unexpected that 5-HT₂ receptors modulate the persistent and transient sodium currents, given that sodium currents are also modulated by other G_q-coupled receptors, such as the muscarinic (Delmas et al. 1996) and dopaminergic (Gorelova and Yang 2000) receptors. Furthermore, PKC itself has been shown to phosphorylate the sodium channel and thus modulate its conductance (reviewed in Catterall 1999), altering activation and inactivation properties of the channels, and sometimes facilitating the persistent sodium current (Astman et al. 1998; Franceschetti et al. 2000; Numann et al. 1991; Patel et al. 2000). However, in many neuron systems, the net action of PKC is to inhibit the sodium channel (see Catterall 1999), in contrast to our results in motoneurons. Typically, when PKC is shown to inhibit the sodium channel in these neurons, it does so under non-physiological conditions, where intracellular calcium is very low because all Ca currents are blocked (e.g., with Cd^{2+}), or intracellular calcium is buffered. Considering that motoneurons buffer calcium

very poorly (Lips and Keller 1998), they should reach substantial intracellular calcium levels with intracellular Ca^{2+} release, and thus should normally behave very differently than in preparations where Ca^{2+} signaling is blocked. Indeed, intracellular calcium chelation reduces Na PICs in neocortical neurons (Li and Hatton 1996; Schwindt et al. 1992), and recent findings from cultured embryonic spinal motoneurons indicate that 5-HT₂ receptor activation (with DOI) facilitates Na PICs under normal conditions, but reverses to inhibit Na PICs when intracellular calcium is low (i.e., buffered, Jiang et al. 2004).

The Na PIC is also facilitated by the Gi-coupled GABA_B receptor in motoneurons (Li et al. 2004c). Considering that Gi receptors, via the Gβγ subunit, can positively modulate the PKC pathway activated by Gq-coupled receptors (Boyer et al. 1992), it seems likely that sodium currents in motoneurons are ultimately modulated in a PKC-dependent manner. In summary, 5-HT₂ receptor activation, and perhaps more generally any receptor coupled to PKC, modulates sodium currents (transient and persistent) in motoneurons and other neurons.

3.4.2 5-HT₂ receptors selectively modulate Na currents, whereas other 5-HT receptors modulate the input resistance and resting potential.

We have found that 5-HT has several effects on rat motoneurons that are not reproduced by the 5-HT₂ agonist DOI and that occur much faster than the DOI-induced changes in the Na currents. Thus, the 5-HT₂ receptor appears to relatively selectively modulate the Na PIC and the sodium spike. Other 5-HT receptors (non-5-HT₂) must modulate the resting membrane potential and input resistance in motoneurons because 5-HT affected these parameters and DOI did not. 5-HT receptors that have so far been identified on spinal motoneurons include the 1A, 1B, 2A and 2C subtypes (Rekling et al. 2000); however, the specific receptors involved in modulating these non-sodium channel-related parameters are not yet clear for motoneurons. We know in motoneurons that the 5-HT-induced depolarization of the resting potential is in part due to a facilitation of an I_h current (Larkman and Kelly 1997; McLamorn 1995) and this can occur by 5-HT_{1A} receptor activation (Takahashi and Berger 1990). A reduction in resting potassium conductance is also partly responsible for the observed 5-HT-induced depolarization (in addition to I_h facilitation) (Vandermaelen and Aghajanian 1982). A few reports have concluded that the potassium channel closure leading to depolarization and decreased conductance is mediated by 5-HT₂ receptors on brainstem motoneurons (Garratt et al. 1993; Hsiao et al. 1997), in contrast to our observations. However in turtle spinal motoneurons, depolarization and the increase in input resistance are mediated by 5-HT receptors other than 5-HT₂ (Perrier and Hounsgaard 2003), as in our results, so the discrepancy may be related to differences in cell type and/or physiological role (brainstem motoneurons controlling facial and tongue movements versus spinal motoneurons involved in limb movement).

A reduction of the spike afterhyperpolarization (AHP), and associated calcium-activated potassium currents (K_{Ca}), is commonly observed with 5-HT application in many neurons (Ballerini et al. 1994), and is thought to be mediated by 5-HT₄ (Andrade and Chaput 1991)

or 5-HT₇ receptors (Inoue et al. 2002) However, neither of these receptors has been identified on spinal motoneurons (although 5-HT₇ is present on hypoglossal motoneurons, see Rekling et al. 2000), and this is consistent with our finding that the AHP was not affected by 5-HT. Bayliss and colleagues have reported that, while 5-HT reduced AHP amplitude in neonatal hypoglossal motoneurons, it had no effect on adults because the 5-HT_{1A} receptor mediating this effect is dramatically downregulated in adulthood (Bayliss et al. 1997). There remains a possibility, in our motoneurons, that 5-HT induced a reduction in the conductance of the channel carrying the AHP current, but this effect was obscured by the simultaneous reduction in cell conductance, such that the AHP amplitude did not change significantly. That is, a smaller AHP current acted through a greater R_m to produce the same peak hyperpolarization as before 5-HT was added. This remains a subject for future investigations.

3.4.3 Supersensitivity of motoneurons to residual 5-HT contributes to recovery of PICs after chronic injury.

Months after spinal transection, in chronic spinal animals, the descending brainstem-derived axons degenerate (Haggendal and Dahlstrom 1973) and the total level of monoamines available in the spinal cord is reduced substantially (Clineschmidt et al. 1971; Schmidt and Jordan 2000). However, there remains about 2-15% of the normal monoamines, as assessed by immunohistochemistry (Cassam et al. 1997; Newton and Hamill 1988), fluorometric analysis (Clineschmidt et al. 1971) or high-pressure liquid chromatography-electrochemical detection (Hadjiconstantinuo et al. 1984). These residual monoamines, at least in part, occur because there are intrinsic spinal 5-HT neurons, possibly associated with the autonomic system (Hadjiconstantinuo et al. 1984; Newton and Hamill 1988). Further, there are also intrinsic NE neurons normally present in the adult spinal cord, and the number of these NE neurons appears to increase substantially with long-term transection (Cassam et al. 1997).

The small but significant level of residual monoamines (about 10%) becomes particularly relevant when we consider our present finding that, following spinal transection, the Na PICs become supersensitive to 5-HT and, in general, motoneuron responses are found to be supersensitive to both 5-HT and NE agonists (Advokat 2002; Barbeau and Bedard 1981; Li et al. 2004b). In particular, we have found a 30-fold supersensitivity, in that only about 3% (1/30) of the usual 5-HT dose was required to induce PICs in chronic spinal rats, compared to normal. This, taken together with the 10% residual monoamines, suggests that in principle there is about 3 times (10/3) the normal activation of the Na PIC by spinal sources of monoamines. Thus, the residual intrinsic monoaminergic neurons, combined with the motoneuron supersensitivity to monoamines, may explain the exaggerated Na PICs in chronic spinal rats. In Chapter 4 (Harvey et al. 2005b), we verify this idea by demonstrating that monoamine receptor antagonists block the naturally occurring Na PICs in the *absence of exogenously applied monoamine agonists*. Likely, the Ca PICs are also exaggerated in chronic spinal rats by a similar mechanism, because we have recently found a similar supersensitivity of the Ca PIC to monoamines (Li and Bennett, unpublished observation).

An alternative, though unlikely, explanation of our observed differences in 5-HT sensitivity in acute and chronic spinal rats is that motoneurons become relatively insensitive to 5-HT with acute injury compared to normal, and normal sensitivity slowly returns over time with chronic injury. We discount this possibility based on evidence from *in vitro* brainstem-intact spinal cord preparations, for which high doses of 5-HT agonists (5 - 40 μ M) are required to induce spontaneous activity in motoneurons, even with their preserved descending monoaminergic innervation, whereas very low doses (≤ 2 μ M) do not (Ballion et al. 2001; Di Pasquale et al. 1997). Furthermore, the required dose of 5-HT to induce such spontaneous motoneuron activity does not increase with acute injury (Ballion et al. 2001), indicating that injury-induced desensitization does not occur.

3.4.4 *Effects of supersensitivity of R_m and V_m to 5-HT in motoneurons with long-term injury.*

We found that all the effects produced by 5-HT on motoneurons were supersensitive to very low doses of 5-HT in chronic spinal rats. Thus, like the PIC discussed above, the general supersensitivity to 5-HT and residual intrinsic spinal 5-HT in the spinal cord after chronic injury should in principle affect the input resistance, membrane polarization, etc. Indeed, we found that the input resistance was significantly higher in chronic compared to acute spinal rats and the resting membrane potential was closer to the firing threshold, consistent with a greater intrinsic 5-HT activation (Harvey et al. 2005a). The net effect was to make motoneurons from chronic spinal rats easier to activate using intracellular current injection.

3.4.5 *Possible mechanisms of supersensitivity.*

Supersensitivity of spinal reflexes to 5-HT as a result of chronic spinal transection or targeted destruction of serotonergic fibres with 5,7-dihydroxytryptamine is well documented (Barbeau and Bedard 1981; Hains et al. 2003; Li et al. 2004b; Shibuya and Anderson 1968). However, the mechanisms of this supersensitivity are unclear. Monoamine binding sites (receptors) may be initially increased following transection but have returned to normal levels by 2 months post-injury (Frazer and Hensler 1990; Giroux et al. 1999), so upregulation of receptor number is not a likely explanation (at least for the 5-HT_{1A} receptor tested). An alternative explanation is that single receptors can become sensitized by developing higher affinity for ligands through receptor modification. For example, the 5-HT_{2C} receptor pre-mRNA is edited in response to serotonin depletion, resulting in a receptor isoform that has more efficient coupling to G-protein activation, leading to supersensitivity without any change in cytoplasmic mRNA levels (Gurevich et al. 2002).

Interestingly, the 5-HT supersensitization does not depend on the presence of 5-HT in the spinal cord, since destruction of the axons with 5,7-dihydroxytryptamine leads to supersensitivity (Barbeau and Bedard 1981), but p-chlorophenylalanine-induced 5-HT depletion from axon terminals, without destruction, does not lead to supersensitivity (Tremblay and Bedard 1995). Similarly, chronic infusion of the 5-HT precursor 5-HTP following chronic spinal transection does not prevent supersensitivity from developing

(Tremblay et al. 1985). Rather, it appears that the peptides colocalized with 5-HT in raphespinal terminals (substance P or TRH) have a role in regulating sensitization to 5-HT agonists (see Eide and Hole 1993; and Tremblay and Bedard 1995 for reviews). However, it is not clear precisely what signal induces 5-HT supersensitivity in spinal motoneurons.

3.4.6 *Supersensitivity to norepinephrine*

While we only systematically tested for 5-HT receptor supersensitivity in motoneurons following chronic spinal cord injury, it would not be surprising if motoneurons were also supersensitive to the other major descending neuromodulator norepinephrine (NE). Indeed, we have previously found that the spastic reflexes in chronic spinal sacrocaudal cords are supersensitive to NE and the α 1-NE receptor agonist methoxamine, by orders of magnitude (Li et al. 2004b; see also Nozaki et al. 1977). Further, we have found that methoxamine facilitates Na PICs (unpublished observations), and thus Gq-coupled α 1-NE receptor activation also facilitates the Na PICs, just like the Gq-coupled 5-HT₂ receptors.

Interestingly, Nozaki et al. (1977) found that the flexor reflex of chronic spinal rats was supersensitive to D-amphetamine, and we have also found amphetamines to facilitate reflexes and PICs in chronic spinal rats (Bennett, Rank and Li, unpublished results). Amphetamines facilitate presynaptic release and block re-uptake of norepinephrine (and dopamine), and have no direct postsynaptic effect (Carlsson et al. 1965; Hanson 1967; Randrup and Munkvad 1966). Thus, the fact that amphetamines have any effect on spinal reflexes below a chronic transection further supports the notion that there is a residual and endogenous source of monoamines in the chronic spinal cord of rats (see above, and Harvey et al. 2005b), because amphetamines can only work by increasing availability of endogenous transmitters.

3.4.7 *Functional implications of 5-HT activity on normal motoneurons.*

In normal motoneurons of acute spinal rats, much of the facilitation from 5-HT and NE is lost because of the acute loss of brainstem innervation. Accordingly, these neurons have small PICs, rest far from threshold and have a low input resistance (Harvey et al. 2005a). Exogenous application of 5-HT increases the Na PICs and input resistance, depolarizes the membrane potential and lowers the spike threshold. In general, this makes motoneurons more excitable by making them easier to recruit and more prone to sustained firing, and this is likely how the neurons behave in the intact state with brainstem monoamine innervation.

Motoneurons need at least some small Na PIC to initiate repetitive firing (Harvey et al. 2005a; Lee and Heckman 2001); accordingly, we found that 5-HT₂ receptor activation rescues motoneurons that do not have any firing ability or Na PIC, enabling them to fire by inducing an Na PIC. Further, the Na PIC is critical in slow firing (Harvey et al. 2005a; Li et al. 2004a), and thus DOI enables cells to fire at lower rates (see Fig. 3-5). Interestingly, modulating the Na PIC with 5-HT₂ receptor activation does not change the F-I slope (gain),

so Na PICs increase the range over which firing occurs (lower minimum firing frequency), but do not change the gain (in contrast to the conclusions of Lee and Heckman, 2001).

5-HT usually increases the amount of self-sustained firing substantially, and this effect is largely due to an increased Ca PIC, because self-sustained firing is much more prominent when the Ca PIC is not blocked with nimodipine. This 5-HT-induced increase in self-sustained firing also depends critically on how much the spike threshold (V_{th}) changes with 5-HT relative to the PIC half-activation potential ($V_{1/2}$): the largest increases in self-sustained firing with 5-HT occur when V_{th} is initially lower than $V_{1/2}$ (such that, during firing, the Ca PIC is not fully activated and self-sustained firing is minimal), and 5-HT hyperpolarizes $V_{1/2}$ so much relative to V_{th} that the PIC is activated below the spike threshold, resulting in prolonged self-sustained firing. Paradoxically, in a few cells, 5-HT does not increase self-sustained firing, even though the PIC is increased because, in these cells, the spike threshold is lowered more than the PIC activation voltage, so that the PIC is harder to activate compared to the spike (see Results).

3.4.8 Supersensitivity causes spasticity.

Recently, large PICs in motoneurons have been demonstrated to be primarily responsible for the spasticity (including debilitating muscle spasms) that occurs following chronic spinal cord injury in rats (Li et al. 2004a) and humans (Gorassini et al. 2004). The results presented in this chapter, and those of the Chapters 2 and 4 (Harvey et al. 2005a, b) take our understanding of spasticity one-step further. That is, the large PICs that cause spasms result from the development of supersensitivity in motoneurons to residual 5-HT in the spinal cord; thus, ultimately, supersensitivity to 5-HT plays a major role in the development of spasticity following injury. The heightened sensitivity of motoneurons to endogenous 5-HT makes them exhibit large PICs either tonically or at entirely inappropriate times, depending on the activity and/or spontaneous leak of 5-HT from endogenous 5-HT neurons and other sources, perhaps related to the autonomic system (Harvey et al. 2005b; Newton and Hamill 1988). This can lead to intense and prolonged muscle contractions in response to any synaptic input that activates PICs. In Chapter 4 (Harvey et al. 2005b), we demonstrate that Na PICs can be inhibited by drugs that act at the three major Gq-protein coupled monoamine receptors (5-HT_{2A}, 5-HT_{2C} and α 1-NE receptors), and thus these drugs, and other Gq-related drugs, offer a novel approach to treating debilitating muscles spasms.

3.5 BIBLIOGRAPHY FOR CHAPTER 3

Advokat C. Spinal transection increases the potency of clonidine on the tail-flick and hindlimb flexion reflexes. *Eur J Pharmacol* 437: 63-67, 2002.

Alaburda A and Hounsgaard J. Metabotropic modulation of motoneurons by scratch-like spinal network activity. *J Neurosci* 23: 8625-8629, 2003.

Alzheimer C, Schwindt PC, and Crill WE. Modal gating of Na⁺ channels as a mechanism of persistent Na⁺ current in pyramidal neurons from rat and cat sensorimotor cortex. *J Neurosci* 13: 660-673, 1993.

Andrade R and Chaput Y. 5-Hydroxytryptamine₄-like receptors mediate the slow excitatory response to serotonin in the rat hippocampus. *J Pharmacol Exp Ther* 257: 930-937, 1991.

Angstadt JD and Friesen WO. Modulation of swimming behavior in the medicinal leech. II. Ionic conductances underlying serotonergic modulation of swim-gating cell 204. *J Comp Physiol [A]* 172: 235-248, 1993.

Astman N, Gutnick MJ, and Fleidervish IA. Activation of protein kinase C increases neuronal excitability by regulating persistent Na⁺ current in mouse neocortical slices. *J Neurophysiol* 80: 1547-1551, 1998.

Ballerini L, Corradetti R, Nistri A, Pugliese AM, and Stocca G. Electrophysiological interactions between 5-hydroxytryptamine and thyrotropin releasing hormone on rat hippocampal CA1 neurons. *Eur J Neurosci* 6: 953-960, 1994.

Ballion B, Morin D, and Viala D. Forelimb locomotor generators and quadrupedal locomotion in the neonatal rat. *Eur J Neurosci* 14: 1727-1738, 2001.

Barbeau H and Bedard P. Denervation supersensitivity to 5-hydroxytryptophan in rats following spinal transection and 5,7-dihydroxytryptamine injection. *Neuropharmacology* 20: 611-616, 1981.

Bayliss DA, Viana F, Talley EM, and Berger AJ. Neuromodulation of hypoglossal motoneurons: cellular and developmental mechanisms. *Respir Physiol* 110: 139-150, 1997.

Bennett DJ, Gorassini MA, and Siu M. In vitro preparation to study spasticity in chronic spinal rats. *Soc Neuroscience Abst* 25: 1394, 1999.

Bennett DJ, Hultborn H, Fedirchuk B, and Gorassini M. Synaptic activation of plateaus in hindlimb motoneurons of decerebrate cats. *J Neurophysiol* 80: 2023-2037, 1998.

Bennett DJ, Li Y, Harvey PJ, and Gorassini M. Evidence for plateau potentials in tail motoneurons of awake chronic spinal rats with spasticity. *J Neurophysiol* 86: 1972-1982, 2001a.

- Bennett DJ, Li Y, and Siu M. Plateau potentials in sacrocaudal motoneurons of chronic spinal rats, recorded in vitro. *J Neurophysiol* 86: 1955-1971, 2001b.
- Boyer JL, Waldo GL, and Harden TK. Beta gamma-subunit activation of G-protein-regulated phospholipase C. *J Biol Chem* 267: 25451-25456, 1992.
- Carlin KP, Jones KE, Jiang Z, Jordan LM, and Brownstone RM. Dendritic L-type calcium currents in mouse spinal motoneurons: implications for bistability. *Eur J Neurosci* 12: 1635-1646, 2000.
- Carlsson A, Lindqvist M, Dahlstrom A, Fuxe K, and Masuoka D. Effects of the amphetamine group on intraneuronal brain amines in vivo and in vitro. *J Pharm Pharmacol* 17: 521-523, 1965.
- Carr DB, Cooper DC, Ulrich SL, Spruston N, and Surmeier DJ. Serotonin receptor activation inhibits sodium current and dendritic excitability in prefrontal cortex via a protein kinase C-dependent mechanism. *J Neurosci* 22: 6846-6855, 2002.
- Cassam AK, Llewellyn-Smith IJ, and Weaver LC. Catecholamine enzymes and neuropeptides are expressed in fibres and somata in the intermediate gray matter in chronic spinal rats. *Neuroscience* 78: 829-841, 1997.
- Catterall WA. Molecular properties of brain sodium channels: an important target for anticonvulsant drugs. *Adv Neurol* 79: 441-456, 1999.
- Clineschmidt BV, Pierce JE, and Lovenberg L. Tryptophan hydroxylase and serotonin in spinal cord and brain stem before and after chronic transection. *J Neurochem* 18: 1593-1596, 1971.
- Conway BA, Hultborn H, Kiehn O, and Mintz I. Plateau potentials in alpha-motoneurons induced by intravenous injection of L-dopa and clonidine in the spinal cat. *J Physiol* 405: 369-384, 1988.
- Crill WE. Persistent sodium current in mammalian central neurons. *Annu Rev Physiol* 58: 349-362, 1996.
- Delgado-Lezama R, Perrier JF, Nedergaard S, Svirskis G, and Hounsgaard J. Metabotropic synaptic regulation of intrinsic response properties of turtle spinal motoneurons. *J Physiol* 504 (Pt 1): 97-102, 1997.
- Delmas P, Niel JP, and Gola M. Muscarinic activation of a novel voltage-sensitive inward current in rabbit prevertebral sympathetic neurons. *Eur J Neurosci* 8: 598-610, 1996.
- Di Pasquale E, Lindsay A, Feldman J, Monteau R, and Hilaire G. Serotonergic inhibition of phrenic motoneuron activity: an in vitro study in neonatal rat. *Neurosci Lett* 230: 29-32, 1997.

Eide PK and Hole K. The role of 5-hydroxytryptamine (5-HT) receptor subtypes and plasticity in the 5-HT systems in the regulation of nociceptive sensitivity. *Cephalalgia* 13: 75-85, 1993.

Fedirchuk B and Dai Y. Monoamines increase the excitability of spinal neurones in the neonatal rat by hyperpolarizing the threshold for action potential production. *J Physiol* 557: 355-361, 2004.

Franceschetti S, Taverna S, Sancini G, Panzica F, Lombardi R, and Avanzini G. Protein kinase C-dependent modulation of Na⁺ currents increases the excitability of rat neocortical pyramidal neurones. *J Physiol* 528 Pt 2: 291-304, 2000.

Frazer A and Hensler JG. 5-HT_{1A} receptors and 5-HT_{1A}-mediated responses: effect of treatments that modify serotonergic neurotransmission. *Ann N Y Acad Sci* 600: 460-474; discussion 474-465, 1990.

Garratt JC, Alreja M, and Aghajanian GK. LSD has high efficacy relative to serotonin in enhancing the cationic current I_h: intracellular studies in rat facial motoneurons. *Synapse* 13: 123-134, 1993.

Giroux N, Rossignol S, and Reader TA. Autoradiographic study of alpha₁- and alpha₂-noradrenergic and serotonin_{1A} receptors in the spinal cord of normal and chronically transected cats. *J Comp Neurol* 406: 402-414, 1999.

Gorassini M, Yang JF, Siu M, and Bennett DJ. Intrinsic activation of human motoneurons: possible contribution to motor unit excitation. *J Neurophysiol* 87: 1850-1858, 2002.

Gorassini MA, Knash ME, Harvey PJ, Bennett DJ, and Yang JF. Role of motoneurons in the generation of muscle spasms after spinal cord injury. *Brain* 127: 2247-2258, 2004.

Gorelova NA and Yang CR. Dopamine D₁/D₅ receptor activation modulates a persistent sodium current in rat prefrontal cortical neurons in vitro. *J Neurophysiol* 84: 75-87, 2000.

Gurevich I, Englander MT, Adlersberg M, Siegal NB, and Schmauss C. Modulation of serotonin 2C receptor editing by sustained changes in serotonergic neurotransmission. *J Neurosci* 22: 10529-10532, 2002.

Hadjiconstantinou M, Panula P, Lackovic Z, and Neff NF. Spinal cord serotonin: A biochemical and immunohistochemical study following transection. *Brain Res* 322: 245-254, 1984.

Haggendal J and Dahlstrom A. The time course of noradrenaline decrease in rat spinal cord following transection. *Neuropharmacology* 12: 349-354, 1973.

Hains BC, Willis WD, and Hulsebosch CE. Serotonin receptors 5-HT_{1A} and 5-HT₃ reduce hyperexcitability of dorsal horn neurons after chronic spinal cord hemisection injury in rat. *Exp Brain Res* 149: 174-186, 2003.

- Hanson LC. Evidence that the central action of (+)-amphetamine is mediated via catecholamines. *Psychopharmacologia* 10: 289-297, 1967.
- Harvey PJ, Li Y, Li X, and Bennett DJ. Chapter 2: Persistent sodium currents and repetitive firing in motoneurons of the sacrocaudal spinal cord of adult rats. *From: The Role of 5-HT in the Development of Motoneuron Persistent Sodium Currents after Chronic Spinal Injury* Ph.D. Dissertation: pp. 25-74, 2005a.
- Harvey PJ, Li Y, Li X, and Bennett DJ. Chapter 4: Endogenous monoamines are essential for persistent sodium currents and repetitive firing in rat spinal motoneurons. *From: The Role of 5-HT in the Development of Motoneuron Persistent Sodium Currents after Chronic Spinal Injury* Ph.D. Dissertation: pp. 121-174, 2005b.
- Heckman CJ, Gorassini MA, and Bennett DJ. Persistent inward currents in motoneuron dendrites: Implications for motor output. *Muscle Nerve* 31: 135-156, 2004.
- Hille B. *Ion Channels of Excitable Membranes, 3rd edition*. Sunderland, MA: Sinauer Associates, Inc., 2001.
- Hounsgaard J, Hultborn H, Jespersen B, and Kiehn O. Bistability of alpha-motoneurons in the decerebrate cat and in the acute spinal cat after intravenous 5-hydroxytryptophan. *J Physiol* 405: 345-367, 1988.
- Hounsgaard J and Mintz I. Calcium conductance and firing properties of spinal motoneurons in the turtle. *J Physiol* 398: 591-603, 1988.
- Hsiao CF, Del Negro CA, Trueblood PR, and Chandler SH. Ionic basis for serotonin-induced bistable membrane properties in guinea pig trigeminal motoneurons. *J Neurophysiol* 79: 2847-2856, 1998.
- Hsiao CF, Trueblood PR, Levine MS, and Chandler SH. Multiple effects of serotonin on membrane properties of trigeminal motoneurons in vitro. *J Neurophysiol* 77: 2910-2924, 1997.
- Hultborn H and Kiehn O. Neuromodulation of vertebrate motor neuron membrane properties. *Curr Opin Neurobiol* 2: 770-775, 1992.
- Inoue T, Itoh S, Wakisaka S, Ogawa S, Saito M, and Morimoto T. Involvement of 5-HT₇ receptors in serotonergic effects on spike afterpotentials in presumed jaw-closing motoneurons of rats. *Brain Res* 954: 202-211, 2002.
- Jiang MC, Kuo JJ, and Heckman CJ. Regulation of 5-HT₂ receptors on persistent sodium current and its intracellular signaling in cultured mouse spinal cord motoneurons. *2004 Abstract Viewer/Itinerary Planner*, Washington, DC. Society for Neuroscience, 2004.
- Kiehn O and Eken T. Prolonged firing in motor units: evidence of plateau potentials in human motoneurons? *J Neurophysiol* 78: 3061-3068, 1997.

- Larkman PM and Kelly JS. Modulation of IH by 5-HT in neonatal rat motoneurons in vitro: mediation through a phosphorylation independent action of cAMP. *Neuropharmacology* 36: 721-733, 1997.
- Lee K, Dixon AK, and Pinnock RD. Serotonin depolarizes hippocampal interneurons in the rat stratum oriens by interaction with 5HT2 receptors. *Neurosci Lett* 270: 56-58, 1999.
- Lee RH and Heckman CJ. Bistability in spinal motoneurons in vivo: systematic variations in persistent inward currents. *J Neurophysiol* 80: 583-593, 1998.
- Lee RH and Heckman CJ. Enhancement of bistability in spinal motoneurons in vivo by the noradrenergic alpha1 agonist methoxamine. *J Neurophysiol* 81: 2164-2174, 1999.
- Lee RH and Heckman CJ. Essential role of a fast persistent inward current in action potential initiation and control of rhythmic firing. *J Neurophysiol* 85: 472-475, 2001.
- Li Y and Bennett DJ. Persistent sodium and calcium currents cause plateau potentials in motoneurons of chronic spinal rats. *J Neurophysiol* 90: 857-869, 2003.
- Li Y, Gorassini MA, and Bennett DJ. Role of persistent sodium and calcium currents in motoneuron firing and spasticity in chronic spinal rats. *J Neurophysiol* 91: 767-783, 2004a.
- Li Y, Harvey PJ, Li X, and Bennett DJ. Spastic long-lasting reflexes of the chronic spinal rat studied in vitro. *J Neurophysiol* 91: 2236-2246, 2004b.
- Li Y, Li X, Harvey PJ, and Bennett DJ. Effects of baclofen on spinal reflexes and persistent inward currents in motoneurons of chronic spinal rats with spasticity. *J Neurophysiol* 92: 2694-2703, 2004c.
- Li Z and Hatton GI. Oscillatory bursting of phasically firing rat supraoptic neurones in low-Ca²⁺ medium: Na⁺ influx, cytosolic Ca²⁺ and gap junctions. *J Physiol* 496 (Pt 2): 379-394, 1996.
- Lindsay AD and Feldman JL. Modulation of respiratory activity of neonatal rat phrenic motoneurons by serotonin. *J Physiol* 461: 213-233, 1993.
- Lips MB and Keller BU. Endogenous calcium buffering in motoneurons of the nucleus hypoglossus from mouse. *J Physiol* 511 (Pt 1): 105-117, 1998.
- McLarnon JG. Potassium currents in motoneurons. *Prog Neurobiol* 47: 513-531, 1995.
- Newton BW and Hamill RW. The morphology and distribution of rat serotonergic intraspinal neurons: an immunohistochemical study. *Brain Res Bull* 20: 349-360, 1988.

Nozaki M, Bell JA, Vaupel DB, and Martin WR. Responses of the flexor reflex to LSD, tryptamine, 5-hydroxytryptophan, methoxamine, and d-amphetamine in acute and chronic spinal rats. *Psychopharmacology (Berl)* 55: 13-18, 1977.

Numann R, Catterall WA, and Scheuer T. Functional modulation of brain sodium channels by protein kinase C phosphorylation. *Science* 254: 115-118, 1991.

Patel MK, Mistry D, John JE, 3rd, and Mounsey JP. Sodium channel isoform-specific effects of halothane: protein kinase C co-expression and slow inactivation gating. *Br J Pharmacol* 130: 1785-1792, 2000.

Pena F and Ramirez JM. Endogenous activation of serotonin-2A receptors is required for respiratory rhythm generation in vitro. *J Neurosci* 22: 11055-11064, 2002.

Perrier JF and Hounsgaard J. 5-HT₂ receptors promote plateau potentials in turtle spinal motoneurons by facilitating an L-type calcium current. *J Neurophysiol* 89: 954-959, 2003.

Perrier JF, Mejia-Gervacio S, and Hounsgaard J. Facilitation of plateau potentials in turtle motoneurons by a pathway dependent on calcium and calmodulin. *J Physiol* 528 Pt 1: 107-113, 2000.

Randrup A and Munkvad I. Role of catecholamines in the amphetamine excitatory response. *Nature* 211: 540, 1966.

Rekling JC, Funk GD, Bayliss DA, Dong XW, and Feldman JL. Synaptic control of motoneuronal excitability. *Physiol Rev* 80: 767-852, 2000.

Schlue WR, Richter DW, Mauritz KH, and Nacimiento AC. Responses of cat spinal motoneuron somata and axons to linearly rising currents. *J Neurophysiol* 37: 303-309, 1974.

Schmidt BJ and Jordan LM. The role of serotonin in reflex modulation and locomotor rhythm production in the mammalian spinal cord. *Brain Res Bull* 53: 689-710, 2000.

Schwindt PC and Crill WE. Membrane properties of cat spinal motoneurons. In: *Handbook of the Spinal Cord, Vols. 2 and 3*, edited by Davidoff RA. New York: Marcel Dekker, 1984, p. 199-242.

Schwindt PC, Spain WJ, and Crill WE. Effects of intracellular calcium chelation on voltage-dependent and calcium-dependent currents in cat neocortical neurons. *Neuroscience* 47: 571-578, 1992.

Shibuya T and Anderson EG. The influence of chronic cord transection on the effects of 5-hydroxytryptophan, l-tryptophan and pargyline on spinal neuronal activity. *J Pharmacol Exp Ther* 164: 185-190, 1968.

Takahashi T and Berger AJ. Direct excitation of rat spinal motoneurons by serotonin. *J Physiol* 423: 63-76, 1990.

Tremblay LE and Bedard PJ. Action of 5-hydroxytryptamine, substance P, thyrotropin releasing hormone and clonidine on spinal neuron excitability. *J Spinal Cord Med* 18: 42-46, 1995.

Tremblay LE, Bedard PJ, Maheux R, and Di Paolo T. Denervation supersensitivity to 5-hydroxytryptamine in the rat spinal cord is not due to the absence of 5-hydroxytryptamine. *Brain Res* 330: 174-177, 1985.

Vandermaelen CP and Aghajanian GK. Serotonin-induced depolarization of rat facial motoneurons in vivo: comparison with amino acid transmitters. *Brain Res* 239: 139-152, 1982.

CHAPTER 4: Endogenous monoamines are essential for persistent sodium currents and repetitive firing in rat spinal motoneurons.

4.1 BACKGROUND

Motoneurons possess voltage-gated persistent inward currents (PICs), composed of persistent sodium (Na PICs) and persistent calcium (Ca PICs) currents (Carlin et al. 2000; Hounsgaard and Kiehn 1985; Hsiao et al. 1998; Li and Bennett 2003). The Na PIC has been shown to be absolutely essential for normal steady repetitive firing in motoneurons (Harvey et al. 2005a; Lee and Heckman 2001; Miles et al. 2005), and also plays an important role in firing of many other neurons (French et al. 1990; Jahnsen and Llinas 1984; Stafstrom et al. 1982; Taddese and Bean 2002; Urbani and Belluzzi 2000). The Na PIC is not a large current compared to the transient sodium current underlying the spike, but it is rapidly activated just subthreshold to the spike, and thus plays a critical role in assuring a rapid enough depolarization to securely activate spikes (Crill 1996). That is, the transient sodium channel inactivates relatively quickly upon depolarization (Hodgkin and Huxley 1952), and thus spike generation requires the fairly rapid subthreshold depolarization from the Na PIC to assure that transient sodium channel activation keeps pace with the transient sodium channel inactivation (Lee and Heckman 2001). Without a Na PIC present, spikes can only be initiated with rapid-onset stimulations (e.g., current steps) that replace the rapid depolarization of the Na PIC, and steady repetitive firing during a constant depolarizing current is generally absent (except at high rates, Harvey et al. 2005a; Zeng et al. 2005).

Exogenous application of the monoamine serotonin (5-HT) facilitates Na PICs in motoneurons (Harvey et al. 2005b; Hsiao et al. 1998), and accordingly enhances repetitive firing ability (Harvey et al. 2005b). Furthermore, PICs in general (Na and Ca PICs) are enhanced by both 5-HT and norepinephrine (NE) in motoneurons (Conway et al. 1988; Hounsgaard et al. 1988; Lee and Heckman 1999). Thus, endogenous monoamines in the spinal cord should be important in the regulation of Na PICs and normal firing behaviour. The motoneurons in the spinal cord are densely innervated by monoaminergic axons arising from the brainstem (Alvarez et al. 1998), and there are even intrinsic spinal monoaminergic neurons (Cassam et al. 1997; Newton et al. 1986). The purpose of this paper was to examine the importance of the endogenous monoamines 5-HT and NE in regulating the Na PIC and firing.

Immediately after spinal transection (acute spinal), PICs and associated plateau properties are dramatically reduced, consistent with a loss of brainstem-induced release of monoamines (Conway et al. 1988; Hounsgaard et al. 1988). However, the reduction in PICs with spinal injury might just as well be accounted for by a loss of other non-monoamine neuromodulators of the Na PIC derived from supraspinal sources (e.g., glutamate, Delgado-Lezama et al. 1997). So spinal transection experiments do not by themselves give definitive information on the role of monoamines in regulating PICs. Furthermore, while PICs are reduced, they are not completely lost with acute spinal

transection (Harvey et al. 2005a). Also, acute spinal transection does not lead to a complete loss of monoamines, because the terminals of brainstem axons take several weeks to completely degenerate (Haggendal and Dahlstrom 1973; Newton et al. 1986), and non-spike mediated leakage of monoamines from these terminals is likely, especially considering that these axons are injured (see Discussions of Harvey et al. 2005a; 2005b). Thus, the small but significant Na PICs remaining in acute spinal animals might arise from this leak of monoamines. To test this hypothesis that endogenous monoamines in acute spinal rats facilitate Na PICs, a definitive experiment is to block the action of these monoamines with monoamine receptor antagonists. This was the first goal of the present paper and we employed antagonists to the major receptors known to facilitate PICs in motoneurons: the 5-HT_{2A}, 5-HT_{2C} and α 1-NE receptors (Lee and Heckman 1998; Perrier and Hounsgaard 2003).

Another approach to examining the importance of endogenous monoamines in regulating the Na PIC, is to wait for the descending monoaminergic axons to degenerate with long-term transection (chronic spinal state). The obvious advantage of this approach is that the vagaries of monoamine leakage from acutely injured axons are avoided. However, the chronic spinal state is *not* simply characterized by a complete loss of monoamines and Na PICs. That is, while all descending monoaminergic axons degenerate, there still remains about 2 – 15% of the normal levels of monoamines (Schmidt and Jordan 2000), arising from the intrinsic spinal 5-HT and NE neurons (Cassam et al. 1997; Newton et al. 1986) and possibly other sources of 5-HT in the spinal cord (e.g., sympathetic efferents, McNicholas et al. 1980). To further complicate matters, motoneurons of such chronic spinal rats become supersensitive to monoamines (Barbeau and Bedard 1981; Harvey et al. 2005b). Specifically, the Na PIC is enhanced in motoneurons by concentrations of 5-HT that are about only 1/30 (3%) of the normal concentration to enhance Na PIC in normal motoneurons (Harvey et al. 2005b), indicating a 30-fold supersensitivity. Taken together with the 2 - 15% residual monoamines after chronic injury, this 30-fold supersensitivity suggests that the Na PIC may be facilitated at levels near, or even well in excess of, normal ($30 \times (2 - 15\%) = 60 - 450\%$). Indeed, motoneurons in chronic spinal rats have relatively large Na PICs compared to acute spinal rats (Harvey et al. 2005a; Li and Bennett 2003), consistent with this hypothesis that the residual monoamines in the spinal cord act on supersensitive receptors to produce large Na PICs.

A second goal of this paper was thus to directly test this supersensitivity hypothesis, and again we employed a monoamine receptor blockade (with antagonists) to stop the action of these endogenous monoamines on Na PICs in motoneurons. We also examined blocking transmitter release to further confirm the role of endogenous monoamine release in facilitating the Na PIC in chronic spinal rats. Our results demonstrated, as expected, that interrupting the action of endogenous monoamines (e.g., with antagonists) indeed led to a reduction of the Na PICs. However, it was unexpected how complete this effect was: in both chronic and acute spinal rats the monoamine receptor blockade completely eliminated the Na PIC, indicating that the monoamines 5-HT and NE are the major transmitters that regulate the Na PIC. Consistent with this complete loss of the Na PIC, steady repetitive firing during a slow or steady depolarization was also eliminated, even though healthy spikes could be still evoked by rapid depolarizations. Thus, monoamines

appear to be critical for normal steady repetitive firing. Parts of this paper have been published in abstract form (Harvey et al. 2004).

4.2 METHODS

Intracellular recordings were made from motoneurons in the *in vitro* sacrocaudal spinal cord of adult female Sprague-Dawley rats. Both normal adult rats (2 - 4 months old, average age = 3.1 ± 0.5 months, $n = 14$) and spastic adult rats with chronic spinal injury (2.5 - 4.5 months old, average age = 3.8 ± 0.4 months, $n = 23$) were included in the present study. The spinal cord of normal rats was transected at the S2 level at the time of removal of the sacrocaudal cord for recording *in vitro* (acute spinal rats). Chronic spinal rats have a complete transection at the S2 spinal level at age 50 - 55 days, and develop spasticity in the tail muscles within 1 month (Bennett et al. 1999; Bennett et al. 2001b). Only rats more than 1.5 months post-injury with clear spasticity were used for *in vitro* recording (Bennett et al. 2001c; Li and Bennett 2003). All experimental procedures were conducted in accordance with guidelines for the ethical treatment of animals issued by the Canadian Council on Animal Care, and approved by the University of Alberta Health Sciences Animal Policy and Welfare committee.

4.2.1 *In vitro* preparation

Details of the *in vitro* procedures have been described at length in Chapter 2 and previous publications (Bennett et al. 2001c; Harvey et al. 2005a; Li and Bennett 2003). Briefly, normal and chronic spinal rats were anesthetized with urethane (0.18g/100g; maximum of 0.45 mg per rat for animals over 250 g), and the whole sacrocaudal cord was removed to a dissection chamber containing modified artificial cerebrospinal fluid (mACSF). In mACSF, ventral roots rostral to S4, and all dorsal roots, were removed and the dorsal surface was glued (super glue, RP 1500; Adhesive Systems) to nappy paper for stability. After a total time of 1.5 hours in mACSF, the cord was transferred to a recording chamber containing normal artificial cerebrospinal fluid (nACSF) and pinned through the nappy paper to the Sylgard base with the ventral side up. Residual anesthetic, and kynurenic acid from the mACSF, were allowed to wash-out for 1 hour in the recording chamber before the bathing solution was switched to nACSF containing a cocktail of fast synaptic transmission blockers (AP5, CNQX, strychnine and picrotoxin; see below). A total volume of 200 ml nACSF was oxygenated in a source bottle and superfused over the spinal cord. This nACSF was then collected, filtered and recycled continuously back into the source bottle using a peristaltic pump. Drugs were added to this continuously recycling volume of fluid as required. Usually 15 μ M nimodipine was added at the beginning of the experiment to isolate the Na PIC by blocking the L-type calcium channels mediating the Ca PIC (Harvey et al. 2005a; Li and Bennett 2003).

4.2.2 *Drugs and solutions*

Two kinds of artificial cerebrospinal fluid (ACSF) were used in these experiments: a modified ACSF (mACSF), designed to minimize potential excitotoxicity, was used in the dissection chamber prior to recording, and a normal ACSF (nACSF) was used in the recording chamber. Composition of the mACSF was (in mM) 118 NaCl, 24 NaHCO₃, 1.5 CaCl₂, 3 KCl, 5 MgCl₂, 1.4 NaH₂PO₄, 1.3 MgSO₄, 25 D-glucose, and 1 kynurenic acid. The nACSF was composed of (in mM) 122 NaCl, 24 NaHCO₃, 2.5 CaCl₂, 3 KCl, 1 MgCl₂, and 12 D-glucose. Both types of ACSF were saturated with 95% O₂-5% CO₂ and maintained at pH 7.4. The synaptic transmission blocking cocktail added to the nACSF contained 50 μM D-(-)-2-Amino-5-phosphopentanoic acid (AP5, Tocris, U.S.A.), 10 μM 6-cyano-7-nitroquinoxaline-2,3-dione (CNQX, Tocris), 1 μM strychnine (Sigma, U.S.A.) and 100 μM picrotoxin (Tocris) to block NMDA, AMPA/kainate, glycine and GABA_A receptors, respectively. The monoamine receptor blockade consisted of the combination of 4 μM WB 4101 (Tocris), 2 μM RS 102221 (Tocris) and 5 - 10 μM ketanserin (Tocris) to block activity at α1-norepinephrine (α1-NE), 5-HT_{2C} and 5-HT_{2A} receptors respectively. In some cases these drugs were also added individually or in combinations of 2 out of 3 antagonists. RS 102221 is a selective and specific antagonist at the 5-HT_{2C} receptor, with considerably lower affinity for the 5-HT_{2A} receptor (Bonhaus et al. 1997). Although ketanserin is generally considered an antagonist for both 5-HT_{2A} and 5-HT_{2C} receptors, its affinity for the 5-HT_{2A} receptor subtype is slightly higher than for 5-HT_{2C} (Bonhaus 1997). We found that addition of 2 μM RS 102221 subsequent to adding 10 μM ketanserin had additional effects on Na PIC amplitude (see Results), indicating that ketanserin, at the doses used here, did not effectively block the 5-HT_{2C} receptor. Additional drugs were added as required, including 15 μM nimodipine (Tocris) to block L-type Ca channels mediating the persistent calcium current, 50 μM 5-hydroxytryptamine (5-HT; Sigma), 30 μM of the 5-HT₂ receptor agonist (±)-1-(2,5-dimethoxy-4-iodophenyl)-2-aminopropane (DOI; Sigma), and 100 μM of the α1-NE receptor agonist methoxamine (Sigma).

4.2.3 *Persistent inward currents in voltage clamp and current clamp recording*

Intracellular recording electrodes and methods were as described in Li and Bennett (2003) and Harvey et al. (2005a). Motoneurons were identified via antidromic stimulation of the ventral roots. Only motoneurons with a stable penetration (resting potential (V_m) below -60 mV and antidromic spike height over 60 mV from rest) were included in this study. Slow triangular current ramps (0.4 nA/s) in discontinuous current clamp (DCC) were used to measure firing, frequency-current (F-I) relations and self-sustained firing (ΔI) (Harvey et al. 2005a; Li and Bennett 2003). Other cell properties, such as input resistance (R_m), spike threshold (V_{th}), spike overshoot, and spike maximum rate-of-rise (dV/dt_{max}) were determined from the current-clamp ramps as described in detail in Chapter 2 (Harvey et al. 2005a).

Slow voltage ramps (3.5 mV/s) between -80 mV and -40 mV, in discontinuous single-electrode voltage clamp (SEVC) mode, were used to measure the PICs, as described in detail previously (Harvey et al. 2005a; Li and Bennett 2003). In summary, to estimate

the PIC, the leak current was first determined from a linear regression to the current response near rest and subthreshold to the PIC. Then this leak current was extrapolated to the potentials where the PIC was activated. Finally, the PIC was quantified as the initial maximum difference between the recorded current and the extrapolated leak current (initial peak PIC). The onset voltage of the PIC (V_{START}) was computed as described previously (Harvey et al. 2005a). Voltage hysteresis of the PIC was calculated by taking the difference in membrane potential between the first and last points of zero-slope conductance, or the point of minimum slope when there was no negative-slope region (Li and Bennett 2003).

4.2.4 Data analysis

Data were analyzed in Clampfit 9.0 (Axon Instruments, USA) and figures were made in Sigmaplot 8.0 (Jandel Scientific, USA). Data are shown as mean \pm standard deviation. A Student's *t*-test was used to test for statistical differences, with a significance level of $P < 0.05$.

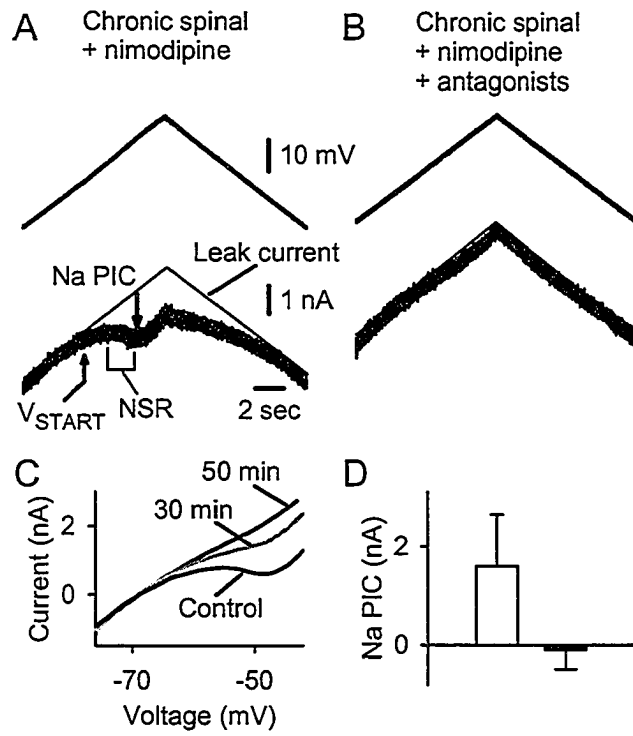
4.3 RESULTS

A total of 55 motoneurons from 23 chronic spinal rats, and 39 motoneurons from 14 acute spinal rats were recorded. Motoneurons were recorded under control conditions in which a fast synaptic transmission blocking cocktail (AP5, CNQX, strychnine and picrotoxin; see Methods) eliminated circuit activity in the spinal cord, and nimodipine was used to block the L-type calcium channel carrying the Ca PIC. Under these control conditions during a slow voltage ramp there was a PIC that was TTX sensitive, and thus resulted from a TTX-sensitive Na PIC, as described in Chapter 2 (Harvey et al. 2005a). In motoneurons of chronic spinal rats ($n = 12$) the Na PIC amplitude was 1.60 ± 1.03 nA, with a voltage onset (V_{START}) of -64.1 ± 5.4 mV. Also, the average resting membrane potential (V_m) was -76.0 ± 8.4 mV, input resistance (R_m) was 7.4 ± 4.3 M Ω , spike voltage threshold (V_{th}) was -56.9 ± 4.2 mV, and spike height (triggered by antidromic stimulation from rest) was 89.6 ± 11.1 mV. In these motoneurons the Na PIC amplitude was on average much larger than in motoneurons of acute spinal rats (more than double, compare Figs. 4-1A and D to Figs. 4-2A and D), as previously reported (Harvey et al. 2005a; Li and Bennett 2003). The average Na PIC amplitude in motoneurons of acute spinal rats ($n = 27$) was 0.62 ± 0.76 nA with a voltage onset of -63.0 ± 5.6 mV. The average resting membrane potential (-75.7 ± 6.2 mV), spike voltage threshold (-56.0 ± 4.9 mV) and spike height (85.7 ± 10.0 mV) were not significantly different than corresponding values in motoneurons of chronic spinal rats, however membrane input resistance was significantly lower (4.8 ± 3.1 M Ω). The current threshold for spike activation during slow current ramps was significantly lower in motoneurons of chronic spinal rats (2.00 ± 1.14 nA) than motoneurons of acute spinal rats (4.02 ± 2.09 nA), and as such motoneurons were easier to activate following long-term spinal transection than immediately after injury, as described previously (Harvey et al. 2005a).

Figure 4-1

In motoneurons of chronic spinal rats, the persistent sodium current (Na PIC) is blocked by antagonists acting on 5-HT_{2A}, 5-HT_{2C}, and α 1-NE receptors (monoamine receptor blockade). *A*: Intracellular recording from motoneuron of chronic spinal rat during slow triangular voltage ramp (3.5 nA/s from -80 mV to -40 mV and back to -80 mV; *top trace*) in SEVC mode, performed during pharmacological block of fast synaptic transmission (using AP5, CNQX, strychnine and picrotoxin) and the Ca PIC (using nimodipine, see Methods) to isolate the Na PIC (control conditions). At Na PIC onset (V_{START}), the current (*bottom trace*) deviated negatively from the extrapolated leak current (thin line), resulting in a negative-slope region (NSR). Na PIC amplitude was estimated from maximum difference between leak current and actual current, shown with downward arrow. *B*: Same cell as in *A*, 50 minutes after addition of ketanserin, RS 102221 and WB 4101 (antagonists). Note absence of negative deviation from leak current, indicating Na PIC was eliminated. *C*: Raw currents from *A* (Control) and *B* (50 min) were filtered and plotted against voltage. Also shown is I-V relation during transition period (30 min, grey line). Note slow reduction in Na PIC amplitude with time. *D*: Average Na PIC amplitude measured in motoneurons of chronic spinal rats under control conditions (white bar), and after addition of monoamine receptor antagonists (black bar). Na PICs were significantly reduced in antagonists, and were not significantly different than zero.

Figure 4-1



Because motoneurons of chronic spinal rats, compared to acute spinal rats, have larger more robust PICs and are easier to depolarize (R_m higher and thus better voltage clamp) we focus on these cells first (Fig. 4-1).

4.3.1 *Endogenous sources of residual monoamines sustain Na PICs after chronic spinal transection.*

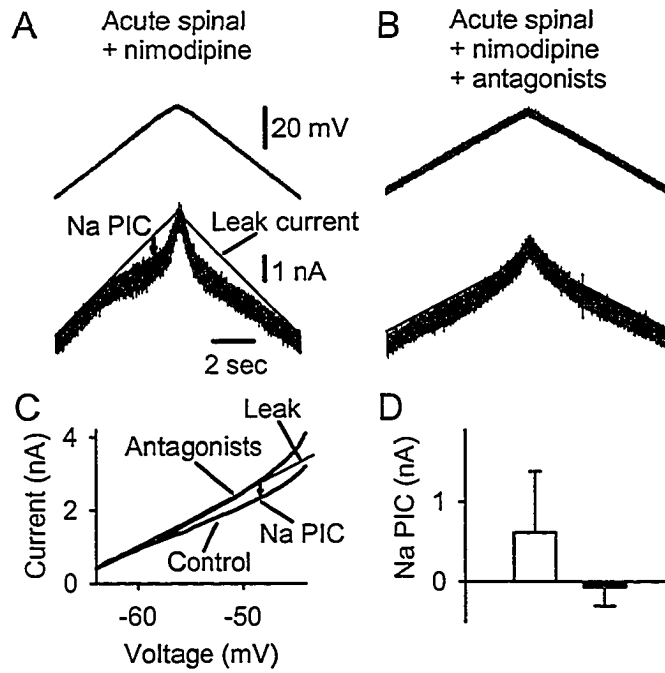
Months after spinal transection (chronic spinal) all descending axons, including the major brainstem monoamine tracts, degenerate (Haggendal and Dahlstrom 1973; Newton et al. 1986), and thus monoamine levels in the spinal cord are reduced dramatically to about 2 - 15% of normal (see Introduction, and Schmidt and Jordan 2000). However, in Chapter 3 (Harvey et al. 2005b), we demonstrated that Na PICs in motoneurons of chronic spinal rats are 30-times more sensitive to monoamines than normal (supersensitive). Thus, we hypothesized that the residual monoamines endogenous to the cord act on supersensitive receptors to produce the large Na PICs seen in chronic spinal rats. To directly test whether endogenous sources of monoamines indeed facilitate the Na PICs in chronic spinal rats we blocked their action by applying antagonists to the major monoamine receptors (5-HT_{2A}, 5-HT_{2C} and α 1-NE; all Gq protein-coupled receptors) known to facilitate PICs *in vivo* (Bennett et al. 1998; Lee and Heckman 1999) and *in vitro* (Harvey et al. 2005b; Perrier and Hounsgaard 2003). That is, we applied a triple-combination of ketanserin (5-HT_{2A} receptor antagonist, 5 - 10 μ M), RS 102221 (5-HT_{2C} receptor antagonist, 2 μ M), and WB 4101 (α 1-NE receptor antagonist, 4 μ M), which we refer to as the *monoamine receptor blockade* for brevity. Remarkably, this monoamine receptor blockade eliminated the Na PIC entirely, so that all motoneurons recorded in this blockade had a relatively linear I-V relation (Fig. 4-1). This elimination of the Na PIC was indirect (via the receptor blockade), but the outcome was similar to when TTX was added to directly block the sodium channels (Harvey et al. 2005a). On average, motoneurons recorded in the monoamine receptor blockade had a Na PIC of -0.09 ± 0.40 nA (Fig. 4-1D, black bar), not significantly different from zero, and significantly less than the large Na PIC in motoneurons of chronic spinal rats under control conditions (1.60 ± 1.03 nA, $n = 12$; Fig. 4-1D, white bar). No exogenous monoamine agonists were in the bath, so the action of the monoamine receptor blockade must have been to block endogenous activation of monoamine receptors. It is surprising how completely the Na PIC was eliminated, not only confirming our hypothesis, but also suggesting that endogenous monoamines acting on supersensitive receptors are the *only* major source of facilitation of the Na PIC.

The monoamine receptor blockade (with ketanserin, RS 102221 and WB 4101) was slow to eliminate the Na PIC in chronic spinal rats (Fig. 4-1C, also in acute spinal rats, not shown), consistent with the known slow reversal of the action of 5-HT (Harvey et al. 2005b; Machacek et al. 2001). That is, the blockade took 10 - 30 minutes to start to have effects (Fig 4-1C, grey line marked '30 min'), and 45 - 90 min to eliminate the Na PIC (Fig. 4-1C, black line marked '50 min'). Because of this slow action, there was a concern that the loss of the Na PIC might be due to deterioration of the motoneurons during prolonged penetration. However, this was not the case, because the Na PIC did not deteriorate in motoneurons held for lengthy periods without antagonist application, and when we

Figure 4-2

In motoneurons of acute spinal rats, the Na PIC is also eliminated by monoamine receptor blockade. *A*: Same format as Fig 4-1A, but from typical motoneuron of acute spinal rat in nimodipine. Note small Na PIC amplitude (downward arrow). *B*: Typical motoneuron from acute spinal rat recorded in monoamine receptor blockade, showing complete absence of Na PIC. *C*: I-V plot for motoneuron held through monoamine receptor blockade. Small Na PIC in control was eliminated 55 minutes after addition of antagonists (linear I-V relation). *D*: Group data for motoneurons of acute spinal rats, as in Fig. 4-1D. Na PIC amplitude significantly reduced in antagonists (black bar) compared to control (white bar), and not significantly different than zero.

Figure 4-2



penetrated and recorded from motoneurons after the monoamine receptor blockade had taken full effect (> 1 hour) all cells had no detectable Na PIC (n = 3 motoneurons of chronic spinal rats, and also n = 5 motoneurons of acute spinal rats, described below).

Motoneurons recorded in the monoamine receptor blockade were considered healthy, with an average resting membrane potential of -73.2 ± 8.0 mV, input resistance of 5.4 ± 1.6 M Ω and antidromic spike height of 87.3 ± 8.4 mV (see inset of Fig. 4-4E), all not significantly different from control. Thus, again the loss of the Na PIC was not a result of cells deteriorating. The lack of change in resting potential and input resistance also supports our conclusions in Chapter 3 (Harvey et al. 2005b) that the 5-HT₂ receptor is not involved in the 5-HT-induced changes in membrane potential and input resistance, whereas it is involved in regulating the Na PIC.

4.3.2 *Endogenous monoamines sustain Na PICs in motoneurons of acute spinal rats.*

In acute spinal rats the pool of endogenous monoamines is larger than in chronic spinal rats, because the terminals of the axotomized brainstem monoamine neurons are not degenerated, and may leak their monoamines (see Discussion). However, the potentially higher concentrations of available monoamines would be acting on receptors that are not supersensitive to monoamines (Harvey et al. 2005b), and thus may only produce the small and variable Na PICs observed (Harvey et al. 2005a). To test whether endogenous monoamines are responsible for the Na PICs in motoneurons of acute spinal rats, we again applied the monoamine receptor blockade of ketanserin, RS 102221 and WB 4101 (Fig. 4-2). Without exception, all motoneurons of acute spinal rats recorded in this monoamine receptor blockade (n = 6) had a relatively linear I-V relation (or net outward current; Figs. 4-2B and C), and thus had little or no detectable Na PIC, with on average a Na PIC amplitude of -0.07 ± 0.24 nA (Fig. 4-2D, black bar) which was not significantly different from zero, and significantly less than the Na PIC in control conditions (0.62 ± 0.76 nA, n = 25; Fig. 4-2D, white bar). In the monoamine receptor blockade motoneurons were again all characterized as viable cells, in that the resting potential was on average $V_m = -70.3 \pm 4.2$ mV and spike height measured by antidromic stimulation from rest was 87.6 ± 14.8 mV (see inset of Fig. 4-4B). So again the monoamine receptor blockade selectively eliminated the Na PIC, consistent with the idea that endogenous monoamines play a central role in facilitating the Na PIC in acute spinal rats, as in chronic spinal rats.

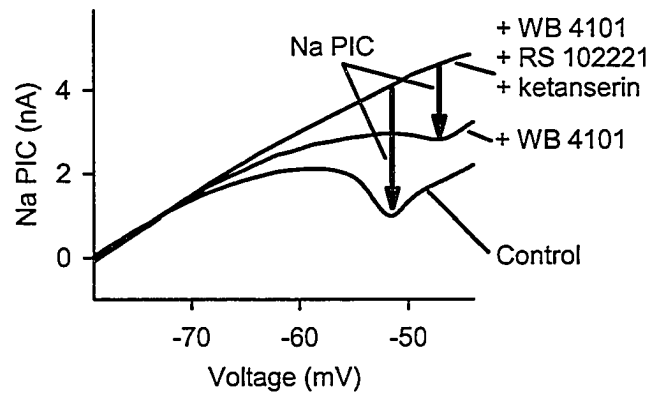
4.3.3 *5-HT_{2A}, 5-HT_{2C} and α 1-NE receptors are all involved in facilitating the Na PIC.*

When just the 5-HT₂ receptor antagonists (combination of RS 102221 for 5-HT_{2C} and ketanserin for 5-HT_{2A}) were applied alone (without the α 1-NE antagonist WB 4101), the Na PIC was significantly reduced to 37.7% of the control values, though there was a significant Na PIC remaining (0.57 ± 0.57 nA, n = 9; compared to 1.60 ± 1.03 nA in control conditions; only chronic spinal animals tested). Thus, endogenous activation of 5-HT₂ receptors partly, but not completely, controls the Na PIC, consistent with the previously established action of 5-HT₂ receptors in facilitating the Na PIC (Harvey et al. 2005b). The remaining portion of

Figure 4-3

Both $\alpha 1$ -NE and 5-HT_{2A/2C} receptors are involved in tonic activation of the persistent sodium current. Overlay of I-V plots from motoneuron of chronic spinal rat held through addition of WB 4101 and then subsequently RS 102221 and ketanserin. Note large Na PIC under control conditions greatly reduced by WB 4101, and eliminated by ketanserin and RS 102221.

Figure 4-3



the Na PIC was due to the action of endogenous NE, because addition of WB 4101 together with the 5-HT₂ receptor antagonists completely eliminated the Na PIC, as discussed above (n = 13, acute and chronic combined). Indeed, application of the NE antagonist WB 4101 alone significantly reduced the Na PIC to 21.9% of the Na PIC amplitude in control conditions (Na PIC was 0.35 ± 0.32 nA in WB 4101; n = 7; see example in Fig. 4-3), but was insufficient to eliminate it completely. The reduction of the Na PIC by either the α 1-NE receptor antagonist (WB 4101) or 5-HT₂ receptor antagonists (ketanserin and RS 102221) clearly did not sum linearly (each caused a much greater than 50% reduction), suggesting that perhaps there is a threshold for readily facilitating the Na PIC (see Discussion) below which the Na PIC is harder to modulate.

Ketanserin is reported to block the 5-HT_{2C} receptors, as well as 5-HT_{2A} receptors (Bonhaus et al. 1997). However, it has a lower affinity for 5-HT_{2C} receptors (Bonhaus et al. 1997), and we did not find it to be an effective 5-HT_{2C} receptor antagonist (even though we used a high dose; 10 μ M). That is, a combination of just ketanserin and WB 4101 did not eliminate the Na PIC (unlike with RS 102221 also present) and left a significant Na PIC of 0.20 ± 0.19 nA (n = 8), suggesting that 5-HT_{2C} receptors were not blocked by ketanserin. Thus, elimination of the Na PIC required the selective 5-HT_{2C} receptor antagonist RS 102221. Likewise, the combined application of WB 4101 and RS 102221 did not reduce the Na PIC to zero (n = 2 cells tested, average Na PIC remaining 0.27 ± 0.03 nA), and thus elimination of the Na PIC also required 5-HT_{2A} receptor antagonism with ketanserin.

In summary, while the combined application of the three antagonists ketanserin, RS 102221 and WB 4101 (monoamine receptor blockade) eliminated the Na PIC, only applying any two of these antagonist left a significant (though small) Na PIC. Thus, the Na PIC is likely supported by endogenous monoamines acting on all three receptors: 5-HT_{2A}, 5-HT_{2C} and α 1-NE. Further, there is a redundancy in action of the three receptors involved, because endogenous activation of any one receptor was enough to sustain some small Na PIC.

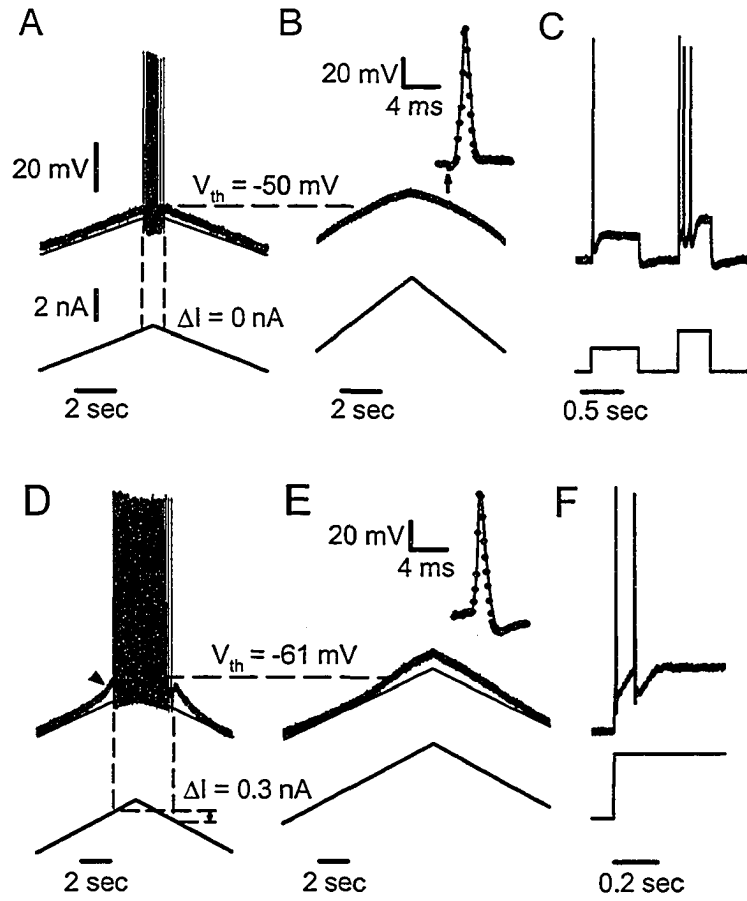
4.3.4 *Endogenous monoamines are critical for repetitive firing in motoneurons.*

Previously it has been reported that the Na PIC is critical for initiation of repetitive firing, because, for example, a *direct* block of the Na PIC with riluzole (or a low dose of TTX) eliminates the ability of motoneurons to fire repetitively during slowly increasing current ramps (Harvey et al. 2005a; Miles et al. 2005). Thus, we evaluated if the *indirect* elimination of the Na PIC seen in the monoamine receptor blockade had a similar detrimental effect on firing. Prior to drug applications, motoneurons in acute (Fig. 4-4A) and chronic (Fig. 4-4D) spinal rats could both readily fire repetitively during slow triangular current injections (see details in Harvey et al. 2005a), whereas in the monoamine receptor blockade, repetitive firing ability during a slow current ramp was lost in all motoneurons of acute spinal rats (Fig. 4-4B; n = 6/6) and all but one motoneuron of chronic spinal rats (Fig. 4-4E, n = 6/7). Even current ramps 2 – 3 times faster than in control conditions did not initiate firing (Fig. 4-4B). This firing ability was lost only when the Na PIC was completely eliminated (> 45 mins after antagonist application; Fig. 4-1), consistent with the link between the Na PIC and firing ability described above. As mentioned above, the antidromic

Figure 4-4

Repetitive firing during slow current ramps eliminated by blocking 5-HT_{2A}, 5-HT_{2C}, and α 1-NE receptors. *A*: Intracellular recording in DCC mode of motoneuron from an acute spinal rat (same cell as in Fig. 4-2C) under control conditions. *Bottom trace*: slow triangular current ramp (0.4 nA/s). *Top trace*: membrane potential with repetitive firing, showing extrapolated leak potential (thin line). Spike voltage threshold (V_{th}) indicated by horizontal dashed line. Note firing ends on down ramp at same current as required to recruit firing (no self-sustained firing, $\Delta I = 0$ nA). *B*: Same motoneuron as in *A*, 55 minutes after addition of ketanserin, RS 102221 and WB 4101. Note inability to initiate repetitive firing, even at potentials more depolarized than V_{th} and despite increased ramp speed (0.8 nA/s). *Inset*: Overlay of spikes triggered by antidromic stimulation (at up-arrow) before (thin line) and after (dotted line) monoamine receptor antagonists blocked firing on current ramps. *C*: Same cell at same time as *B*, showing transient firing triggered by current steps. *D*: Same format as *A*, but from motoneuron of chronic spinal rat (same cell as in Fig. 4-1). Note subthreshold acceleration in membrane potential (arrowhead) and self-sustained firing ($\Delta I > 0$ nA). *E*: Motoneuron in *D*, 50 minutes after addition of monoamine receptor antagonists. Note failure to initiate repetitive firing even above V_{th} . *Inset*: Overlay of first spike triggered by current step before (thin line) and after (dotted line) antagonists blocked firing on slow ramps. *F*: Current step taken at same time as *E*, showing transient firing can be induced by fast depolarizations. Vertical scale bars in *A* apply to all sections.

Figure 4-4



spike evoked from rest was not affected by the monoamine receptor blockade (see insets in Figs. 4-4B and E; solid - control, dotted - antagonists), and thus the loss of repetitive firing was not simply a loss of the sodium spike, but instead a loss of the Na PIC that helped initiate firing during a slow ramp.

It has been previously described that, without a fast persistent current like the Na PIC, spikes are not initiated during a slowly increasing current ramp because inactivation of fast sodium channels immediately follows activation, and readily keeps pace with activation during slow or sustained depolarizations (see Introduction, and Lee and Heckman 2001). The Na PIC normally serves to accelerate the depolarization of the membrane sufficiently to minimize Na channel inactivation and maintain sufficient Na channel availability to produce a spike. Indeed any rapid depolarization (exceeding a critical dV/dt) that replaces this function of the Na PIC can initiate spikes when a Na PIC is not present (see Harvey et al. 2005a). Consistent with this understanding, current steps (Figs. 4-4C and F) or fast ramps (10-times normal speed in Fig. 4-5Dii) were still able to initiate spikes when the Na PIC was eliminated by the monoamine receptor blockade. On average, in this blockade the minimum rate of rise of potential needed to evoke spiking with fast current ramps was $dV/dt = 16.1 \pm 9.5$ mV/s ($n = 11$), which was significantly greater than the rate of rise of potential induced by the standard slow current ramp (prior to Na PIC activation 2.6 ± 0.9 mV/s, $n = 38$), and similar to the rate of rise of potential induced by the Na PIC during the subthreshold acceleration in control conditions (without blockade; $dV/dt = 8.3 \pm 4.6$ mV/s in $n = 28$ motoneurons with a Na PIC).

In the absence of a Na PIC (in monoamine receptor blockade), following initiating of one spike on a step or fast ramp, subsequent spikes arose when there was a fast enough upswing in potential at the end of each AHP (i.e., during fast firing). A dramatic demonstration of this is the fast repetitive firing initiated by a single antidromically evoked spike (at * in Fig. 4-5Diii) during a slow current ramp that could not by itself evoke firing (Fig. 4-5Di). During a current step the firing usually stopped after a few spikes (Figs. 4-4C and F), likely due to the lack of continuing depolarization, insufficient upswing from the AHP and possibly due to spike inactivation (see below, and Harvey et al. 2005a).

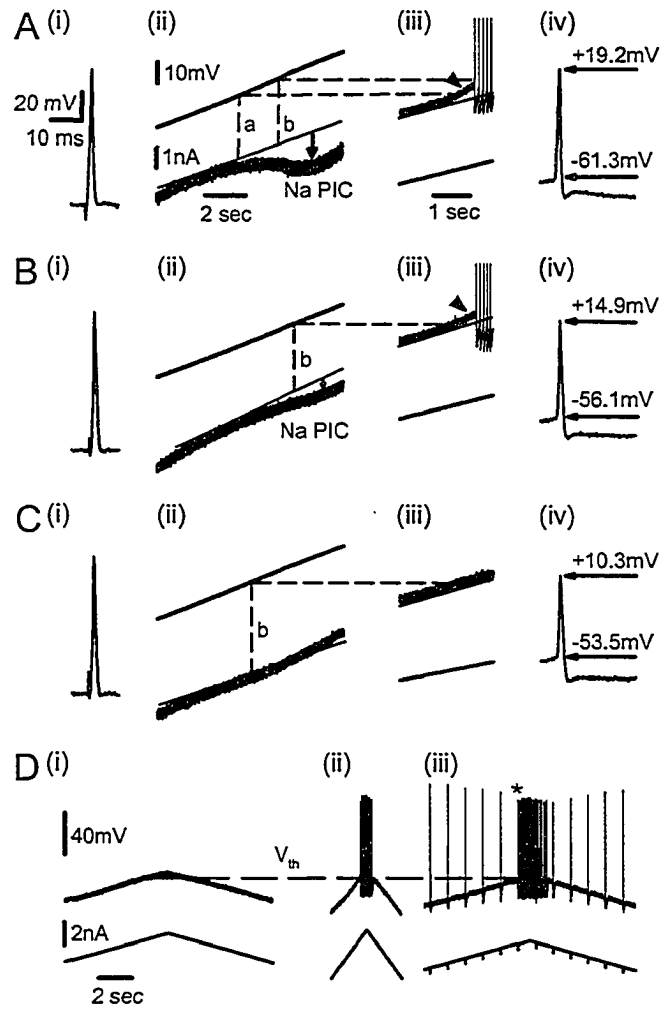
4.3.5 Monoamine receptor blockade increases depolarization-induced sodium spike inactivation.

As stated above, the antidromic spike evoked from rest was not affected by the monoamine receptor blockade. However, the first spike evoked during a slow current ramp was significantly affected by this blockade. Likely this is related to sodium channel inactivation. That is, as just mentioned, during a slow current ramp the fast voltage-gated sodium channel is partly inactivated by the slow depolarization prior to the first spike. Thus, changes in the first spike's threshold (V_{th}), amplitude, and maximum rate of rise (dV/dt_{max}) are all sensitive indicators of the sodium channel availability following partial inactivation, and changes in these parameters have thus been used to infer changes in sodium channel inactivation (Schlue et al. 1974; Schmidt and Stampfli 1966). During the slow onset of the action of the monoamine receptor blockade there was clear evidence for such sodium channel

Figure 4-5

Loss of action potential generation occurs simultaneously to loss of Na PIC as monoamine receptor blockade takes effect. All recordings from the same chronic spinal rat motoneuron; (A) before addition of ketanserin, RS 102221 and WB 4101, (B) during transition phase as antagonists took effect, and (C and D) after antagonists had blocked the Na PIC and repetitive firing. A: (i) Spike triggered by antidromic stimulation from rest (-80 mV). (ii) Slow voltage ramp as in Fig. 4-1A, with only up-ramp shown. Dashed lines indicate V_{START} (a) and V_{th} (b). Note presence of negative-slope region. (iii) Slow current ramp as in Fig. 4-4D, with only the portion of up-ramp near recruitment shown. Note subthreshold acceleration (arrowhead) starting at V_{START} (dashed line a). (iv) Close up of first spike evoked during current ramp in *iii* (same scale as *i*). Horizontal arrows indicate spike threshold (bottom) and spike overshoot (top). B: (i) Antidromic spike during transition period. Note same height as control (in *Ai*). (ii) Voltage ramp. Na PIC reduced in amplitude, with no negative-slope region. (iii) Current ramp. Note spike voltage threshold increased relative to control V_{th} (dashed line b) and subthreshold acceleration was reduced (arrowhead). (iv) First spike from *Biii*. Note higher voltage threshold and less overshoot than control (in *Aiv*). C: (i) Antidromic spike in monoamine receptor antagonists. Note identical height as control antidromic spike. (ii) Voltage ramp. Na PIC completely eliminated by monoamine receptor antagonists. (iii) Current ramp. Note absence of acceleration in membrane potential and no firing even past control V_{th} (b). (iv) Close-up of spike triggered by antidromic activation near V_{th} (indicated by * in *Diii*), with even less overshoot than in *Biv*. D: (i) Slow current ramp (0.4 nA/s) after antagonists eliminated repetitive firing. (ii) Faster current ramp (2.0 nA/s, equivalent to $dV/dt = 16.6$ mV/s) triggered spike and repetitive firing in monoamine receptor blockade. (iii) Slow current ramp with antidromic stimulation applied at 1 sec intervals. Note antidromic spike (marked by *) triggered near V_{th} (measured from *Dii*) initiated repetitive firing whereas slow ramps without antidromic spikes did not (compare to *Di*). All of columns *ii* and *iii* in parts A-C to same vertical scale as *Aii*. Scale bars in *Di* apply to all of D.

Figure 4-5



inactivation, which occurred in parallel to the gradual decrease in the Na PIC. That is, when the Na PIC was only partly eliminated (Fig. 4-5B), during a slow current ramp, there was a characteristic increase in the threshold and decrease in the height of the first spike (Fig. 4-5Biv), as well as a decrease in dV/dt_{\max} ($dV/dt_{\max} = 119.6 \pm 44.6$ V/s for $n = 7$ neurons with partial monoamine receptor block, compared to 161.1 ± 34.1 V/s for $n = 12$ in nimodipine alone; significant difference), all consistent with increased sodium channel inactivation in the subthreshold region. Once the Na PIC was eliminated (at full monoamine receptor block; Figs. 4-5C and D) firing was not evoked by the ramp alone, but could be still triggered by an antidromic stimulation (as described above). The antidromically-evoked spike near the normal spike threshold (V_{th}) had an even lower amplitude (Fig. 4-5Civ) and dV/dt_{\max} , suggesting that even more sodium channel inactivation occurred during the ramp at this point. Across all motoneurons from acute spinal rats, the spike amplitude (overshoot) measured for spikes triggered at or near V_{th} was significantly lower in the full monoamine receptor blockade (5.6 ± 10.7 mV) compared to in control (12.7 ± 5.3 mV). The same was found in motoneurons of chronic spinal rats, where overshoot measured in the three antagonists (11.0 ± 4.8 mV) was significantly lower than control (18.6 ± 5.7 mV). Taken together, the above results suggest that with the monoamine receptor blockade there is greater sodium channel inactivation during a slow current ramp. This occurs in parallel to the decrease in Na PIC, which is likely not a coincidence, since in general the degree of sodium channel inactivation helps determine the size of the Na PIC (see Discussion, and Taddese and Bean 2002).

4.3.6 Tonic activity at any single monoaminergic receptor is sufficient to maintain repetitive firing.

With the exception of a few motoneurons, we did not see the loss of repetitive firing during slow current ramps unless all three antagonists (WB 4101, ketanserin and RS 102221) were added to the bath. In total, 15 of 21 motoneurons (including chronic and acute spinal rats) measured in combinations of any two out of three antagonists still exhibited repetitive firing in response to slow current ramps, and had some Na PIC remaining. This was the case when we omitted either ketanserin ($n = 3$ of 3 still firing), RS 102221 ($n = 5$ of 8), or WB 4101 ($n = 7$ of 10) from the combination of the three antagonists. Thus it appears that in most cases, tonic background activity at any one of the three receptors investigated here is sufficient to allow the motoneuron to trigger a spike during a slow current ramp and maintain repetitive firing. This suggests that all three receptors are involved in enabling repetitive firing, and this is certainly related to the corresponding changes in the Na PIC described above.

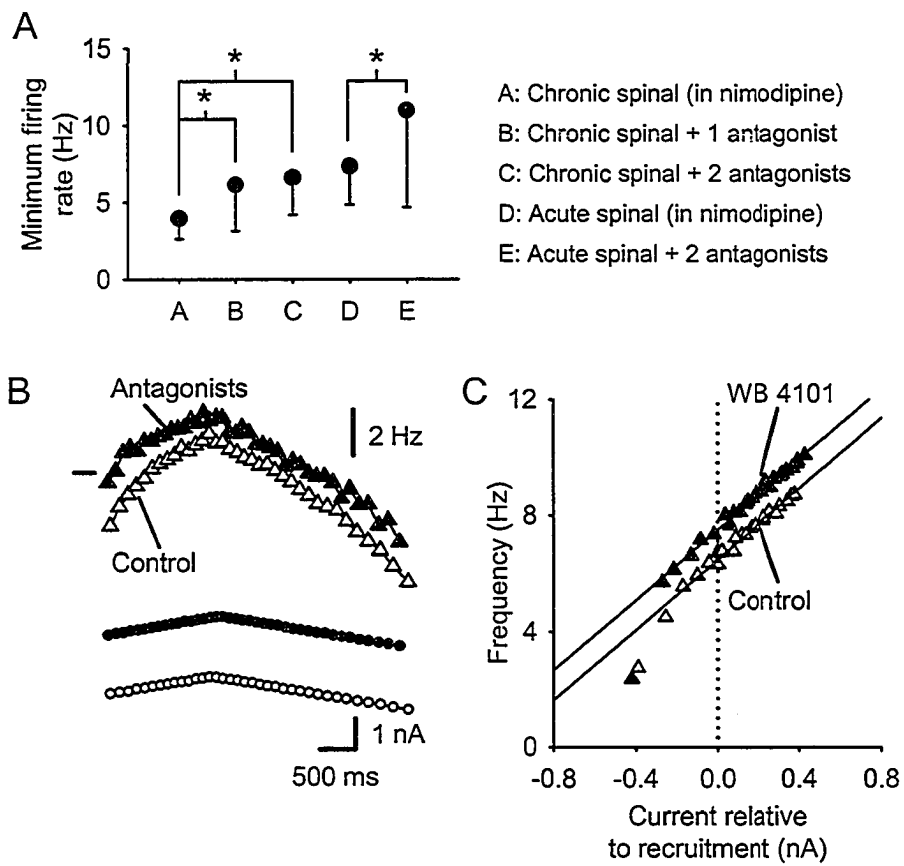
4.3.7 Minimum firing rate is increased by monoamine receptor antagonists.

Although there appears to be redundancy in action of the three receptor subtypes investigated, application of single antagonists had significant effects on firing frequency, especially the minimum firing rate, where the minimum firing rates were calculated from the last interspike interval on the down ramp during current clamp recordings (Fig. 4-6A).

Figure 4-6

The monoamine receptor antagonists that act to reduce the Na PIC, increase the overall firing rate, but do not affect the F-I slope. *A*: Average minimum firing rates (measured as last interspike interval during current ramps) for motoneurons of chronic and acute spinal rats under control conditions, with any 1 antagonist, and with any combination of 2 out of the 3 antagonists. Note significantly higher minimum firing rate in motoneurons of both chronic and acute spinal rats recorded in 1 or 2 antagonists. *B*: Instantaneous firing frequency (triangles) and corresponding current (circles) recorded during slow triangular current ramp in motoneuron of chronic spinal rat held through antagonist action. Open symbols - control; solid symbols - antagonists. Note increase in initial and final firing rate, but no change in modulation of frequency with current input (upward shift in frequency plot but still parallel). Mark at left of frequency plots indicates 10 Hz. *C*: Comparison of F-I plots before and after antagonist application in motoneuron of chronic spinal rat held through drug action (WB 4101). Threshold current was subtracted from actual injected current in both traces. Open triangles - control; solid triangles - WB 4101. Note parallel F-I slopes, with vertical shift compared to control (shift measured at y-intercept, vertical dotted line).

Figure 4-6



Under control conditions (in nimodipine), motoneurons of chronic spinal rats had a significantly lower minimum firing rate than motoneurons of acute spinal rats (4.0 ± 1.3 Hz versus 7.4 ± 2.5 Hz), due to the presence of persistent sodium currents that enable very low frequency firing (see Harvey et al. 2005a; Li and Bennett 2003). With one antagonist, either RS 102221 or WB 4101, in the bath (ketanserin was not tested by itself), the minimum firing rate of chronic spinal rat motoneurons was increased significantly to 6.1 ± 3.0 Hz. This was associated with a significant reduction in depth of the negative-slope region from 0.56 ± 0.46 nA to 0.15 ± 0.20 nA, which supports the role of a negative-slope region in enabling steady slow firing (below 6 Hz, see Harvey et al. 2005a). Having two antagonists in the bath significantly reduced the depth of the negative-slope region to 0.05 ± 0.01 nA and increased the minimum firing rate (6.6 ± 2.4 Hz) compared to control, but the minimum rate was not further increased relative to single antagonists. In motoneurons of acute spinal rats, single antagonists were not tested; however, the minimum firing rate was significantly increased with two antagonists in the bath (to 11.0 ± 6.3 Hz). These results complement the findings with DOI, in which facilitation of the Na PIC significantly reduced the minimum firing rate in neurons which had no slow firing to begin with, thus making acute spinal rat motoneurons appear more like chronic spinal rat motoneurons. Here, the antagonists acted on cells that regularly exhibit slow firing (chronic spinal rat motoneurons), increasing the minimum firing rate such that they appear more like motoneurons of acute spinal rats. Interestingly, the average minimum firing rate for motoneurons of acute spinal rats, which was already relatively high compared to motoneurons of chronic spinal rats, was further increased by combinations of two monoamine receptor antagonists. Thus, even the small persistent sodium currents found normally in motoneurons of acute spinal rats help to lower the minimum firing rate, and eliminating these currents results in faster firing.

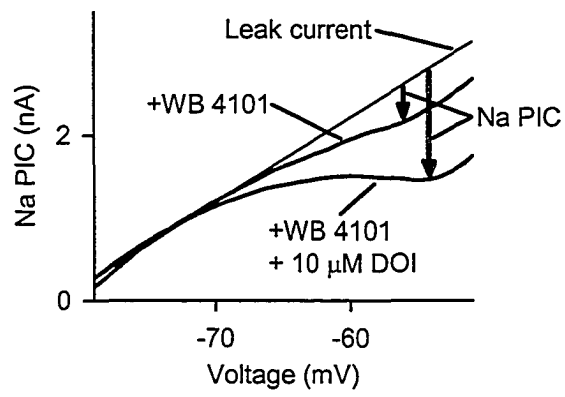
4.3.8 Firing rate increased, but F-I slope unchanged, by monoamine receptor antagonists.

Along with higher average minimum firing rates, motoneurons generally seemed to fire faster in one or more of the monoamine receptor antagonists. An example of this is in Figure 4-6B, showing a motoneuron of a chronic spinal rat before drug application (open symbols), and then just prior to the complete failure of repetitive firing with slow current ramps due to the monoamine receptor blockade (solid symbols). In the monoamine antagonists, firing was initiated at a higher rate than in control conditions, and continued at a higher rate throughout firing. However, the slope of the firing frequency vs. current relation (F-I gain) was not increased, in other words the frequency plots remained parallel. Across cells the F-I slope did not change significantly, with only a $1.0 \pm 11.6\%$ change ($n = 4$ tested in this condition). To quantify the general increase in firing rate in the antagonists, we lined-up the F-I plots at recruitment current as in Figure 4-6C (i.e., recruitment threshold current subtracted from each response; open symbol - control, solid symbol - antagonist) and computed the vertical shift between regression lines fit to each plot, which was significantly shifted by 1.30 ± 0.14 Hz (measured at the y-intercept in Fig. 4-6C). Thus there was a general increase in firing frequency at currents relative to the recruitment current. Furthermore, the lack of effect of antagonists on the F-I slope further indicates that the current-frequency relationship is not influenced by the Na PIC or by drugs that modulate Na PIC amplitude, as shown previously (Harvey et al. 2005a, b).

Figure 4-7

Small Na PIC in α 1-NE receptor antagonist WB 4101 can still be facilitated by 5-HT₂ receptor agonist DOI. Overlay of I-V plots for motoneuron of chronic spinal rat recorded in WB 4101 and after subsequent addition of 10 μ M DOI. Note increase in Na PIC amplitude with DOI.

Figure 4-7



4.3.9 *The monoamine receptor antagonist combination does not directly block Na channels*

To rule out any possible direct block of the Na PIC channels by the monoamine receptor antagonists (Melena et al. 2000; Riccioppo Neto 1979), we demonstrated that the effects of the antagonists on the Na PIC could be overcome by agonists known to facilitate the Na PIC. As described above, WB 4101 blocks $\alpha 1$ -NE receptors and significantly reduces Na PIC amplitude. However, because the 5-HT₂ receptors remain unblocked in WB 4101, normal doses of DOI (10 μ M, Harvey et al. 2005b) were sufficient to restore a large Na PIC (n = 2, Fig. 4-7). Thus the reduction in Na PIC amplitude by the $\alpha 1$ -NE receptor antagonist WB 4101 most likely resulted from a block of the $\alpha 1$ -NE receptor, as intended, and did not result from direct block of the channel carrying the Na PIC

With all the antagonists present (full monoamine receptor blockade) higher doses of agonist must in principle be required to compete with the antagonists to activate the receptors, but at sufficiently high doses should nevertheless rescue the PICs. Indeed, once this monoamine receptor blockade eliminated the Na PIC and repetitive firing in response to slow current ramps (Fig. 4-8A and B), we found that adding high doses of methoxamine ($\alpha 1$ -NE receptor agonist) and 5-HT overcame the antagonist inhibition and restored the Na PIC (n = 3). In the example shown, 100 μ M methoxamine restored the ability to fire repetitively during slow current ramps (Fig. 4-8C), and induced a slight inflection in the voltage ramp current trace (Fig. 4-8D). Subsequent addition of 50 μ M 5-HT to this cell (Fig. 4-8E and F), a particularly high dose for motoneurons of chronic spinal rats (see Harvey et al. 2005b), further increased the Na PIC amplitude and almost induced a negative-slope region. Thus it appears that agonists to the 5-HT and NE receptors can compete with the antagonists to restore the Na PIC in motoneurons, even in the continued presence of antagonists, supporting the conclusion that the antagonist actions are mediated by the intended receptor targets.

4.3.10 *Without nimodipine, monoamine receptor blockade does not block Ca PIC, but still disrupts firing.*

All the cells described above were recorded in presence of nimodipine to block the Ca PIC, which is a current of similar size to the Na PIC (Harvey et al. 2005a; Li and Bennett 2003). However, in some additional motoneurons from chronic spinal rats (n = 6) we also examined the action of the monoamine receptor blockade without nimodipine (Fig. 4-9). In these cells there was a PIC present in the monoamine receptor blockade, and this was likely a Ca PIC, because with nimodipine present this monoamine receptor blockade eliminated the Na PIC (see above; total PIC is made up of only Na and Ca PIC). Further, this PIC was rapidly eliminated by blocking calcium channels with Cd²⁺ (n = 2, not shown). Also, the mean PIC amplitude and onset threshold (V_{START}) recorded in the monoamine receptor blockade were 1.39 ± 0.97 nA and -61.5 ± 9.4 mV, not significantly different from the amplitude (1.82 ± 0.78 nA) and V_{START} (-57.1 ± 7.1 mV) previously reported for the Ca PIC (Harvey et al. 2005a). Finally, the PIC activation threshold was considerably more depolarized than its deactivation (Fig. 4-9A), resulting in an average voltage hysteresis of

Figure 4-8

High doses of monoamine receptor agonists can compete with antagonists to restore the Na PIC. *A*: Slow triangular current ramp in typical motoneuron of a chronic spinal rat in monoamine receptor blockade. Note inability to generate action potentials with slow current ramps. *Inset*: Antidromic action potential triggered at rest. *B*: Slow voltage ramp from same cell as in *A*, showing absence of any Na PIC. *C*: Different cell but same preparation as *A* and *B*. 100 μ M methoxamine restored repetitive firing when added in addition to monoamine receptor antagonists. *D*: Methoxamine also induced a small Na PIC, concurrent with recovery of repetitive firing ability (in *C*). *E*: Same cell as *C* and *D*. 50 μ M 5-HT further facilitated firing (note increased overshoot and hyperpolarized V_{th}) and produced a small after-potential (arrow). *F*: 5-HT further increased Na PIC amplitude. Scale bars in *A* also apply to *C* and *E*. Scale bars in *B* also apply to *D* and *F*.

Figure 4-8

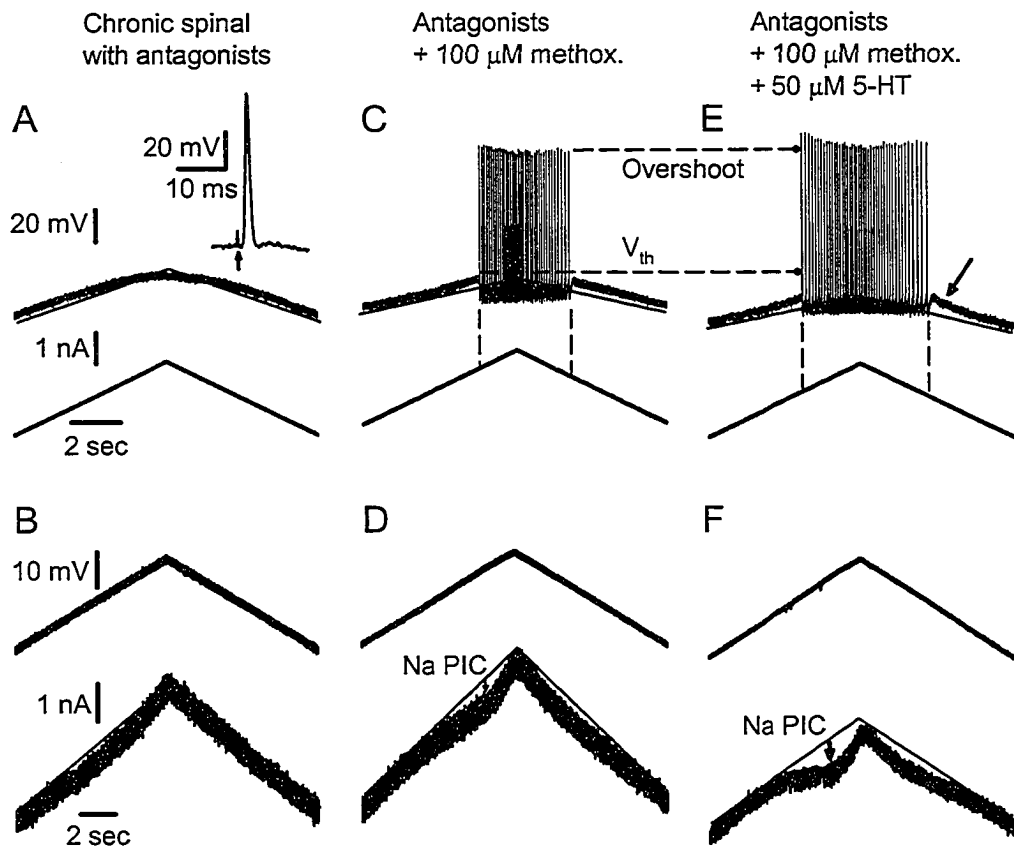
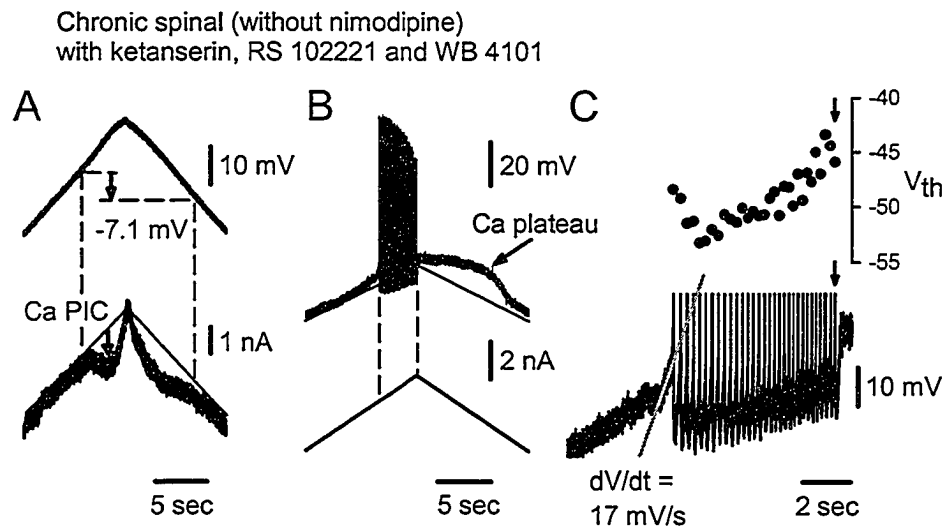


Figure 4-9

In absence of nimodipine, monoamine receptor blockade does not eliminate the Ca PIC, but does inhibit firing. *A*: Voltage ramp, as in Fig. 4-1, in motoneuron of chronic spinal rat recorded in monoamine receptor blockade, but without nimodipine. Remaining PIC is likely a Ca PIC based on high threshold and voltage hysteresis (dashed lines indicating onset and offset of PIC). *B*: Same motoneuron as in *A* during slow current ramp protocol. Note rapid reduction in spike height before spike inactivation uncovered underlying Ca plateau. Dashed lines indicate initiation and cessation of firing. *C*: Close-up of current ramp in *B* during firing. Voltage threshold is shown aligned above each spike. Note acceleration in membrane potential (dV/dt , grey line) leading up to initial spike. Voltage threshold starts off high, is reduced during the first few spikes, but then steadily increases as spike height decreases until firing fails completely (at down arrows).

Figure 4-9



-7.4 ± 3.6 mV, which is a distinctive characteristic of the Ca PIC, not generally seen with the Na PIC (Li and Bennett 2003). The finding that a Ca PIC persists in the monoamine receptor blockade (5-HT₂ and α1-NE receptor antagonists), and yet the Na PIC does not, is odd because the Ca PIC is known to be modulated by 5-HT₂ and α1-NE agonists (Lee and Heckman 1998, 1999; Perrier and Hounsgaard 2003), like the Na PIC. We are currently investigating this issue, and perhaps the answer to this puzzle comes from the finding that the action of 5-HT and 5-HT₂ receptor agonists on increasing the Ca PIC is ultra long-lasting, persisting for > 90 minutes after washing these agonists (Li and Bennett, unpublished results), unlike their action on the Na PIC, which is slow, but washes out in 20 – 40 minutes (Harvey et al. 2005b). In any case, in these cells recorded without nimodipine (n = 6), firing was severely impaired, like in the cells recorded in nimodipine, consistent with a lack of a Na PIC. Two cells could not fire at all during a slow current ramp, and two cells only fired transiently during the onset of the Ca PIC (Fig. 4-9B). In the latter two cells, the Ca PIC onset acted like a current step (as in Fig. 4-4C and F, or fast ramp as in Fig. 4-5Dii) and triggered the onset of rapid firing in the absence of a Na PIC (see expanded onset in Fig. 4-9C, with rapid Ca PIC-induced depolarization indicated). Following the transient firing there emerged a classic calcium plateau (Fig. 4-9B). Under control conditions all motoneurons in chronic spinal rats produced sustained firing during the period where the Ca PIC was activated, and never showed the transient firing pattern seen in Fig. 4-9B (not shown, but see Li et al. 2004).

4.3.11 Prolonged treatment with cadmium also eliminates the Na PIC.

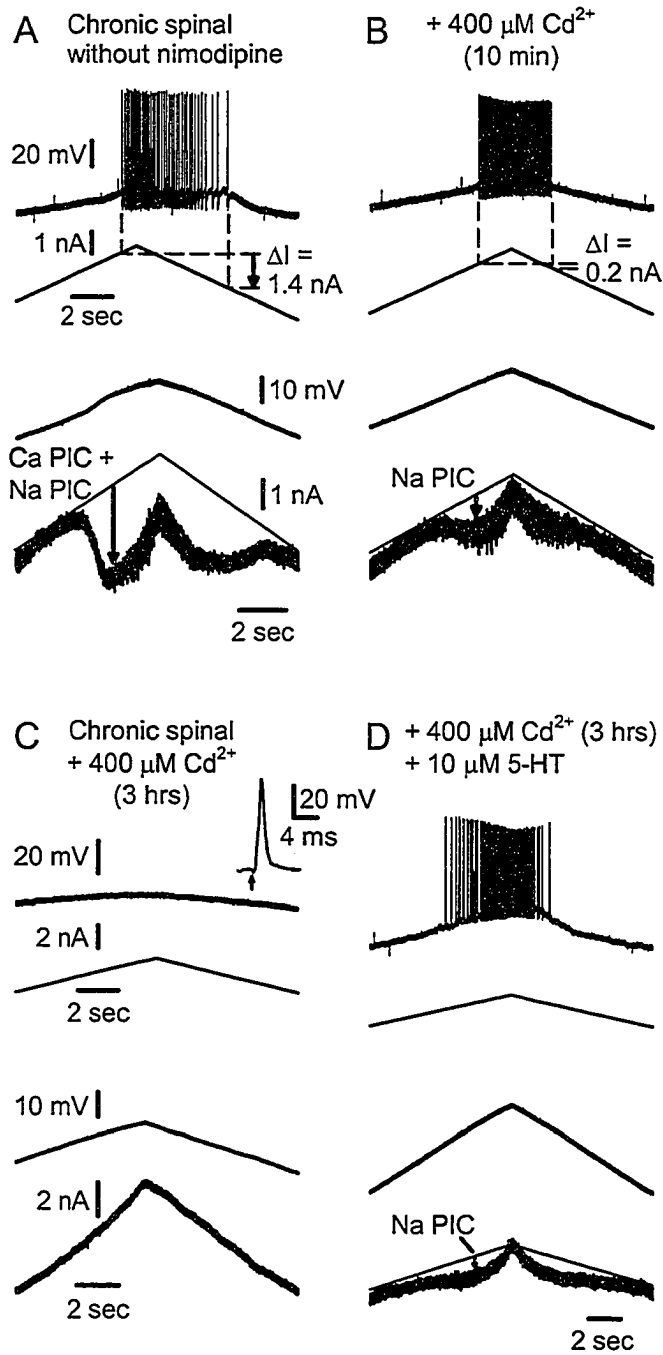
The source of monoamines below a chronic spinal transection may be neuronal and arise from synaptic release from intraspinal serotonergic and noradrenergic neurons onto motoneurons. We performed all investigations in a fast synaptic transmission blocking cocktail (AP5, CNQX, picrotoxin and strychnine, see Methods), which blocked any potential 5-HT and NE release resulting from spinal neuronal circuit activity. However, there was still a good possibility that spontaneous activity of monoaminergic neurons released 5-HT and NE on or near motoneurons. Vesicular release of transmitter, whether spontaneous or induced by action potentials, is mediated by elevated calcium levels in the axon terminal (Angleson and Betz 2001; Katz and Miledi 1969). Nimodipine is not likely to block presynaptic actions, since it does not block EPSPs (Li and Bennett 2003) and does not interfere with the N- and P/Q-type calcium channels that normally mediate vesicular release from synapses. However, cadmium blocks all calcium channels, leading to near complete elimination of calcium-mediated neurotransmitter release (Cooper and Manalis 1984; Forshaw 1977). Thus, if the source of monoamines is from presynaptic terminals, then we should see a reduction of the Na PIC after 45 minutes in cadmium, similar to the delay in reversing the effects of exogenously applied 5-HT (Harvey et al. 2005b) or applying the combination of three monoamine receptor antagonists (as above).

In motoneurons of chronic spinal rats without nimodipine, both persistent sodium and persistent calcium components contribute to the total PIC (Fig. 4-10A, see also Harvey et al. 2005a; Li and Bennett 2003). Cadmium (Cd²⁺) acts quickly (< 5 minutes) to eliminate the

Figure 4-10

Na PICs can be eliminated with long-term cadmium (Cd^{2+}), and restored by exogenous 5-HT. *A*: Motoneuron of chronic spinal rat, recorded without nimodipine (only fast synaptic transmission blocking agents present). Prolonged self-sustained firing (large ΔI) during current ramps (*top*) associated with large PIC in voltage ramp (*bottom*). The total PIC of these cells consists of both Ca and Na-mediated components (see Introduction). *B*: Addition of Cd^{2+} blocked the Ca PIC within 10 minutes, greatly reducing the ΔI (*top*) and PIC amplitude (*bottom*; presumably a Na PIC remaining). *C*: Different motoneuron from same preparation as *A* and *B*, recorded 3 hours after addition of Cd^{2+} . Note complete absence of any persistent inward currents and inability to fire with slow current ramps. *Inset*: Antidromic stimulation (up arrow) induced a spike > 60 mV in height. *D*: Same cell as in *C*, after addition of 5-HT. Note restored ability to fire repetitively with slow current ramps and facilitation of a persistent inward current, presumably a Na PIC as all Ca channels are blocked by Cd^{2+} .

Figure 4-10



persistent calcium component but leaves a large PIC carried by sodium ions (the Na PIC; Fig. 4-10B, see also Li and Bennett 2003). However, motoneurons found after 45 minutes in cadmium did not exhibit any Na PIC (as in Fig. 4-10C), and repetitive firing was difficult to elicit (requiring fast current ramps or steps), consistent with the idea that this long-term exposure to cadmium blocked the presynaptic release of monoamines which were facilitating the Na PIC. Prolonged exposure to cadmium seemed to be somewhat toxic to cells, depolarizing them and making them generally less stable to record from. Thus it was important to demonstrate that a Na PIC could be restored with a return of monoaminergic receptor activation, in order to confirm the idea that cadmium acts to block presynaptic release of transmitters like 5-HT that facilitate the Na PIC. Figure 4-10C is an example of a motoneuron recorded after exposure to cadmium for 3 hours. This cell had no Na PIC and was unable to fire during current ramps despite exhibiting a healthy spike in response to antidromic stimulation (inset of Fig. 4-10C, *top*). The effects of 10 μ M 5-HT on this cell were dramatic; enabling repetitive firing during slow current ramps, and inducing a large Na PIC during voltage ramps (even though cadmium was still present, Fig. 4-10D). Thus, long-term exposure to cadmium results in a loss of the Na PIC, which is not due to direct channel block or toxicity as it can be restored by exogenous application of 5-HT to stimulate 5-HT receptors on the motoneurons, and this is consistent with cadmium causing a presynaptic block of endogenous monoamines that facilitate the Na PIC.

4.4 DISCUSSION

Our results demonstrate that three major monoamine receptors are responsible for the spontaneously occurring Na PICs seen in spinal motoneurons recorded in the *in vitro* whole sacrocaudal spinal cord: 5-HT_{2A}, 5-HT_{2C}, and α 1-NE receptors. These receptors are endogenously activated, likely by endogenous monoamines in the spinal cord, because blocking these three receptors with their respective antagonists (ketanserin, RS 102221 and WB 4101) completely eliminates the Na PIC, and furthermore, blocking presynaptic release of monoamines (and other transmitters) with cadmium likewise eliminates the Na PIC. Concurrent with the loss of the Na PIC in the monoamine receptor blockade, there is also a complete loss of ability to produce steady repetitive firing, consistent with the critical role of the Na PIC in firing (see Introduction, and Harvey et al. 2005a; Lee and Heckman 2001). Thus, the present results lead to the surprising conclusion that monoamines are absolutely essential for normal repetitive firing in motoneurons.

Even in chronic spinal rats, where there are very little endogenous monoamines available in the spinal cord, blockade of the monoamine receptors with the three antagonists eliminated the Na PIC and repetitive firing. This finding, together with the recent finding that the Na PICs are supersensitive to monoamines in chronic spinal rats (Harvey et al. 2005b), confirms the hypothesis that the small amounts of residual monoamines left in chronic spinal rat spinal cords below the lesion act on supersensitive monoamine receptors to produce the large Na PIC seen in motoneurons of chronic spinal rats. Ultimately, it is this supersensitivity to monoamine receptors that explains spastic activity (muscle spasms) in chronic spinal rats, because these spasms have been shown to result from PICs on motoneurons (Bennett et al. 2004; Gorassini et al. 2004; Li et al. 2004a), and this is

elaborated further below.

4.4.1 *Endogenous monoamines are essential for Na PICs.*

The present results from monoamine receptor blockade experiments identify a critical role for endogenous monoamines in enabling such Na PICs. Our previous results (Harvey et al. 2005b) indirectly implicated 5-HT in the regulation of the Na PIC, because 5-HT receptor agonists strongly facilitate the Na PIC in motoneurons. We had not initially expected NE to play such a major role in the Na PIC as it does, with the α 1-NE receptor antagonist WB 4101 being the most effective antagonist in reducing the endogenous Na PIC (Fig. 4-3). In hindsight the importance of NE makes sense, given that the α 1-NE receptor agonist methoxamine is often used to facilitate PICs in decerebrate and spinal animals (Bennett et al. 1998; Hounsgaard et al. 1988; Lee and Heckman 1999), and the PIC-mediated long-lasting ventral root reflexes are strongly enhanced by NE and methoxamine (Li et al. 2004b).

Because receptors can in some cases be activated without the presence of a transmitter (constitutively active receptor, see Egan et al. 1998), it is possible that monoamine receptors are endogenously activated without monoamines present. However, such constitutively active monoamine receptors are unlikely to explain our results, because a block of transmitter release with cadmium has the same effect on the Na PIC (elimination of Na PIC that took about 1 hour) as blocking the monoamine receptors, suggesting that at least some endogenous transmitters must activate the monoamine receptors, and these are most likely NE and 5HT.

The combined block of 5-HT_{2A}, 5-HT_{2C} and α 1-NE receptors is generally required to get a full elimination of the Na PIC and firing, as residual unblocked activity at any one of the three receptors is sufficient for motoneurons to exhibit small Na PICs and generate steady repetitive firing. As a result of all three receptors being coupled to Gq proteins, they likely converge to activate the same intracellular pathway. This convergence of three separate receptors from two different monoamine systems indicates a redundancy in mechanisms by which motoneurons maintain Na PICs and repetitive firing. As such, the systems maintaining the Na PICs in motoneurons can withstand a large degree of tampering or malfunction before Na PICs are lost, thus emphasizing the physiological importance for motoneurons to exhibit Na PICs (see Harvey et al. 2005a).

In a few motoneurons of pentobarbital-anesthetized animals and acute spinal rats there is a spontaneous lack of ability to fire repetitively even though these neurons have healthy action potentials and input resistance (Granit et al. 1956; Harvey et al. 2005a). Interestingly, these motoneurons also lack Na PICs (Harvey et al. 2005a), and thus in light of the present findings, it is possible that these neurons for some reason lack adequate endogenous monoamine receptor activation seen in other motoneurons. Indeed, by adding monoamine receptor antagonists, any motoneuron can be turned into such a motoneuron that selectively lacks Na PICs and repetitive firing. Consistent with the idea that some neurons spontaneously lack monoamine activation, facilitation of the Na PIC with the monoamine

receptor agonist DOI restores the repetitive firing ability of these motoneurons (Harvey et al. 2005b), just as Na PICs and firing can be restored by agonists after deliberately blocking the action of endogenous monoamines (Figs. 4-7, 4-8 and 4-10).

4.4.2 *Critical role of Na PICs in firing.*

When the Na PIC is eliminated by the monoamine receptor blockade there is a loss of repetitive firing ability, confirming previous reports that Na PICs are necessary for sustaining repetitive firing in neurons (Harvey et al. 2005a; Hu and Hvalby 1992; Jahnsen and Llinas 1984; Lee and Heckman 2001; Stafstrom et al. 1982; Taddese and Bean 2002), and further showing that endogenous 5-HT and NE are critical for enabling repetitive firing in motoneurons. This action of the monoamine receptor blockade on the Na PIC and firing behaviour was relatively selective, as it did not affect the input resistance, resting membrane potential or spikes evoked from rest. Thus, the Na PIC appears to be important for steady repetitive firing. As outlined in the Introduction, the Na PIC is a relatively fast-activating current that plays a critical role in triggering spikes, producing the rapid acceleration just prior to each spike, and thus enabling repetitive firing during steady or slowly increasing (ramp) current injections (see Fig. 4-1A, and Harvey et al. 2005a; Lee and Heckman 2001). The slow voltage ramps used to quantify the Na PIC in the present paper do not quantify the speed of activation of the Na PIC, and just quantify the persistent nature of the Na PIC. However, the rapid onset of the Na PIC has previously been demonstrated in these same motoneurons with voltage steps (Li and Bennett 2003).

While most of the Na PIC is very persistent, there is a small portion of the Na PIC that inactivates within 1 second following a voltage step (Li and Bennett 2003). This partial inactivation is not possible to see with the voltage ramps used in the present experiments. This may explain why repetitive firing is still present when there remains only a very small Na PIC evoked by voltage ramps (Fig. 4-5B); the inactivating portion of the Na PIC is probably still present and plays a role in enabling spiking.

When the Na PIC is selectively reduced by monoamine antagonists there is a characteristic increase in the overall firing rate and increase in the minimum firing rate, confirming the critical role of the Na PIC in slow firing (Li et al. 2004a), and consistent with the opposite action of monoamine receptor agonists (Harvey et al. 2005b). Interestingly, monoamine-related changes in the Na PIC are not associated with changes in the F-I slope (Fig. 4-6C), consistent with our previous conclusion that the Na PIC does not regulate the F-I slope (Harvey et al. 2005a). However, this is inconsistent with the results of Lee and Heckman (2001), and we feel that this may have been due to their use of only indirect measurements of the Na PIC (see details in Harvey et al. 2005a).

4.4.3 *Possible mechanisms by which monoamines modulate the Na PIC.*

Associated with the reduction of the Na PIC by the monoamine receptor blockade, we have presented evidence for increased inactivation of the transient sodium channel underlying the

spike during slow ramp depolarizations. That is, during these slow depolarizations, there appears to be greater sodium channel inactivation prior to recruitment than normal, and thus fewer channels are available for the spike. Ultimately this inactivation is seen as smaller and slower-rising spikes evoked from depolarized levels (around -50 mV, Harvey et al. 2005a; Miles et al. 2005; Schlue et al. 1974; Schmidt and Stampfli 1966). In contrast, the spike evoked from rest (about -70 mV) by an antidromic stimulation or current step is not affected by the monoamine antagonists, suggesting that the activation of the transient sodium channels is fairly normal. Therefore, endogenous (see Results) or exogenous (Harvey et al. 2005b) activation of monoaminergic receptors by 5-HT and NE must both increase the non-inactivating sodium current (Na PIC) and reduce the tendency for inactivation of the transient sodium current. Monoamine antagonists reverse these effects of monoamines on sodium channel inactivation.

Considering that the Na PIC is believed to be carried by the same channels as the transient sodium current underlying the spike (Crill 1996), ultimately the mechanism by which monoamine receptor activity modulates both currents may prove to be identical. The voltage-gated sodium channels mediating the transient sodium current normally inactivate rapidly after opening. However, the persistent sodium current appears to flow through a small percentage of these channels which do not inactivate (1 – 3%), potentially by switching to a modal “persistent” state (Alzheimer et al. 1993), or due to allosteric gating kinetics (Taddese and Bean 2002). Any modification of the voltage-gated sodium channel that increases the probability of the channel entering a persistent state (i.e., less likely to inactivate) will ultimately increase the total Na channel availability. This generates larger Na PICs and spikes with less tendency to inactivate following depolarization (i.e., less tendency for spikes evoked from depolarized potentials to be diminished in height and rate-of-rise).

Changes in inactivation properties of the Na channels, and associated changes in persistent sodium currents, can be induced by kinase-mediated phosphorylation (Catterall 1999). Protein kinase C (PKC), a downstream effector activated by Gq-protein-initiated events, directly phosphorylates voltage-gated sodium channels to modulate their activation and inactivation properties (Franceschetti et al. 2000; Numann et al. 1991; Patel et al. 2000). The 5-HT_{2A}, 5-HT_{2C} and α 1-NE receptors are all Gq-coupled and likely lead to activation and translocation to the membrane of PKC (Wang and Friedman 1990), thus describing a plausible intracellular pathway by which monoamine receptors can modulate sodium channel inactivation and ultimately facilitate the Na PIC (see Harvey et al. 2005b). With antagonists blocking Gq-coupled receptors, activity of the intracellular pathway is reduced, Na channel inactivation is increased and the Na PIC disappears.

4.4.4 The general action of 5-HT₂ receptors is very slow to reverse.

The monoamine receptor facilitation of the Na PIC is remarkably slow to reverse, with about 1 hour required to fully reverse the facilitation of the Na PIC following removal of a bath-applied 5-HT receptor agonist (Harvey et al. 2005b), and over 1 hour for the monoamine receptor blockade to eliminate the Na PIC. These results are consistent with the

very long-lasting facilitation of spinal reflexes seen hours after removing 5-HT₂ receptor agonists (Machacek et al. 2001). The slow reversal of action of 5-HT receptors is not simply due to diffusion delays in the relatively large adult *in vitro* sacrocaudal spinal cord, because channel blockers like TTX can diffuse into the cord very rapidly (Harvey et al. 2005a; Li et al. 2004a). Consistent with Machacek et al. (2001), the activation of the 5-HT₂ (and α 1-NE) receptors seems to involve an intracellular switch that is difficult to reverse, and thus leaves the Na PIC available for long periods after removal of 5-HT. In contrast, 5-HT_{1A} effects on spinal reflexes reverse quickly (Machacek et al. 2001), and in as far as 5-HT_{1A} receptors regulate the resting membrane potential (Takahashi and Berger 1990), we have also seen this fast reversal of action of 5-HT_{1A} receptors, because motoneurons depolarize quickly in 5-HT and this is reversed quickly (Harvey et al. 2005b). Further, 5-HT_{1A} receptors appear to rapidly counter many of the effects of the 5-HT₂ receptors, including reducing spinal reflex facilitation (or even producing inhibition of reflexes), reducing 5-HT₂ mediated increases in Ca PICs (see Perrier and Hounsgaard 2003), and rapidly reducing Na PICs and related firing properties (Harvey and Bennett unpublished findings). Thus, while 5-HT₂ receptor activation excites motoneurons for hours with some kind of intracellular switch, the 5-HT_{1A} receptor may be able to quickly reverse this. This is probably of critical functional importance, or else it would be impossible for the brainstem to regulate PICs and normal motoneuron excitability on a minute-by-minute scale, and uncontrolled contractions, like spasms, would be common.

4.4.5 *Other endogenous transmitters could regulate the Na PICs.*

As discussed above, the endogenous monoamines likely play the major role in facilitating the Na PIC, because the Gq-coupled monoamine receptor antagonists completely eliminate the Na PIC. However, there is still a remote possibility that other endogenous transmitters (non-monoamine) also play a significant role in facilitating the Na PIC. That is, the induction of a Na PIC may involve a threshold phenomenon, whereby the underlying changes in the sodium channel inactivation properties (see above) or upstream intracellular signal (e.g., PKC) must exceed a certain threshold before Na PICs are made available to activate. Thus, many endogenous transmitters, including glutamate, acetylcholine (ACh), γ -aminobutyric acid (GABA), 5-HT and NE could regulate the sodium channel and related intracellular signals, and together exceed the threshold for making a Na PIC available. Thus, blocking only the action of two of these transmitters (NE and 5-HT) may be adequate to drop below this hypothetical threshold, and eliminate the possibility of a Na PIC occurring. The finding that the sum of the individual reductions in the Na PIC induced by either 5-HT₂ or α 1-NE receptor antagonists was greater than 100% (non-linear sum), suggests that at least there may be a threshold above which the Na PIC is readily altered by these two monoamines. Application of muscarinic and mGluR1 receptor agonists, which are both Gq-coupled, facilitate Ca PICs in motoneurons (Svirskis and Hounsgaard 1998), though we do not know about their action on Na PICs. Also, application of the GABA_B receptor agonist baclofen facilitates the Na PICs in motoneurons (Li et al. 2005).

Thus, in principle, endogenous glutamate, ACh and GABA may contribute to the spontaneously occurring PICs in spinal motoneurons. However, we do not favor this

interpretation, because the PICs measured in motoneurons are not significantly changed by a complete block of fast synaptic transmission (Harvey et al. 2005a), which should dramatically alter the availability of glutamate and GABA, as it blocks all spontaneous or evoked synaptic events observed on the motoneurons. Further, we have not been able to see changes in PICs induced following intense/prolonged dorsal and ventral root stimulation (unpublished observations), which should increase glutamate and ACh availability. Furthermore, in our hands application of Group I mGluR agonists (ACPD, DHPG) do increase the PICs, but the effects are only transient (habituate, Harvey and Bennett, unpublished findings), and thus steady endogenous glutamate activation should likewise habituate and not usually participate in PICs. Thus, we tentatively conclude that monoamines play the major role in regulating the Na PIC and firing, though antagonists to other transmitters need to be tested to verify this conclusion.

The present experiments were mostly performed in the presence of nimodipine (Ca PIC blocker), and CNQX, AP5, picrotoxin and strychnine (fast synaptic transmission blockade). These drugs may have somehow affected non-monoamine transmitters that normally facilitate the Na PIC, by for example affecting intraspinal neurons that facilitate the Na PIC. However, this did not appear to be an important factor, because the clear elimination of repetitive firing seen in nimodipine with the application of the monoamine receptor antagonists was also seen without nimodipine present (Fig. 4-9). The Na PIC could not be measured directly without nimodipine, but the loss of repetitive firing is strongly suggestive of a loss of the Na PIC. Finally, neither nimodipine nor the drugs involved in the blockade of fast synaptic transmission (CNQX, etc) directly reduce the Na PICs (Bennett et al. 2001a; Harvey et al. 2005a), and thus these drugs do not appear to block transmitter systems that facilitate the Na PIC.

4.4.6 *Monoamines in the acute spinal state likely arise from cut descending terminals.*

Normally, with an intact brainstem and spinal cord, PICs are maintained by innervation from descending monoaminergic axons originating in the raphe and locus coeruleus (reviewed in Heckman et al. 2004). Neurotransmitter (5-HT and NE) release from these terminals onto, or in the vicinity of, spinal motoneurons maintains the necessary level of monoamines (*monoamine tone*) that permits expression of the Na PIC. The level of monoamine tone in the spinal cord is normally modulated by the brainstem to the appropriate level as required by the motor task to be performed (e.g., locomotion, see Gerin et al. 1995; Jacobs et al. 2002). Nevertheless, in the acute spinal rat small Na PICs can remain, and these are eliminated by the antagonists to monoamine receptors. Immediately after spinal cord transection, the terminals of monoaminergic neurons originating in the brainstem remain a major source of 5-HT and NE below the lesion. Although isolated from the cell soma, axon terminals are still able to release, take-up, and re-synthesize neurotransmitter for lengthy periods prior to degeneration (Anden 1977; Karobath 1972; Patrick and Barchas 1974). Monoamines may be released as a bolus at the time of injury, or slowly leak from the terminals. The former is likely to be of minimal importance, as the monoamines released would either be washed-out of the dissection chamber, or cleared by re-uptake mechanisms of the axon terminals and surrounding glia (Blakely et al. 1994; Inazu

et al. 2001), and thus no longer be influencing motoneurons by the time recording started (hours later).

Slow leak of neurotransmitter from the injured monoaminergic terminals throughout the course of the experiment is more likely to be the source of the monoamine tone. The actual mechanism of release is unknown, but it must be independent of spinal circuit activity, as motoneurons continue to exhibit PICs after prolonged periods with fast excitatory and inhibitory transmission blocked (Harvey et al. 2005a). Further, monoamine release is most likely due to a non-spike mediated leak from the injured terminals, because spontaneous activity of the cut descending axon terminals is unlikely. Potentially, an injury-induced depolarization and rise in intracellular calcium concentrations (Schanne et al. 1979) promotes spontaneous release of neurotransmitter from vesicles (Angleson and Betz 2001). Any monoamines released into the synapse in this way undergo the usual re-uptake and re-release by axons or glia, and thus are not depleted over the course of the experiment (hours) in acute spinal rats prior to axonal degeneration. Alternatively, the injury may lead to a reversal of the monoamine re-uptake machinery, and slow Ca^{2+} -independent leak of axoplasmic free transmitter from terminals via carrier-mediated efflux (Levi and Smith 2000). In either case, the response to injury and the amount of leakage would determine the level of monoamine tone in the acute spinal rat spinal cords *in vitro*, and therefore contribute to the wide variability in Na PIC amplitude observed in motoneurons of acute spinal rats (Harvey et al. 2005a).

4.4.7 Endogenous intraspinal monoamines act on supersensitive receptors to induce spasticity with chronic spinal cord injury.

In the spinal cord of chronic spinal rats, the transected descending monoaminergic terminals have long since degenerated (Haggendal and Dahlstrom 1973; Newton et al. 1986) and so can no longer serve as a source of 5-HT and NE. Surprisingly, despite the loss of this major source of monoamines, sacrocaudal motoneurons below the injury have large Na PICs (Li and Bennett 2003), and these large Na PICs contribute to the muscle spasms associated with spasticity (Li et al. 2004a). Our data confirm the hypothesis that the large Na PICs occur because sacrocaudal motoneurons become supersensitive to 5-HT (and likely NE as well), and are strongly facilitated by the residual endogenous monoamines arising from intraspinal sources. Therefore, endogenous monoamines acting on supersensitive receptors cause the large Na PICs that, along with persistent calcium currents, sustain the debilitating muscle spasms characteristic of spinal spasticity. Several investigators have reported a residual level of monoamines (2 - 15%, reviewed in Schmidt and Jordan 2000) remaining below the injury, as measured by immunohistochemistry (Cassam et al. 1997; Newton et al. 1986), fluorometric analysis (Clineschmidt et al. 1971), or high-pressure liquid chromatography-electrochemical detection (Hadjiconstantino et al. 1984). While it is clear that there is a residual source of monoamines independent of brainstem innervation in the chronic spinal sacrocaudal cord, the nature of origin of these monoamines is subject to debate.

A likely source of monoamines after chronic spinal transection is from intrinsic intraspinal monoaminergic neurons. The existence of intraspinal serotonergic neurons, albeit in very

small numbers, have been reported in the low lumbar and sacrocaudal spinal cords of rats (Newton et al. 1986). These cells are associated with the autonomic system and have long spindle shaped cell bodies that can only be readily distinguished in longitudinal sections. However, they are not easily observed in cross-sections of spinal cord, and thus have been missed in other investigations (Holets and Elde 1982; Kojima and Sano 1983; Steinbusch 1981). It may be that these neurons sprout and innervate ventral motoneurons to compensate for the loss of descending serotonergic innervation. Intraspinal noradrenergic neurons are also present below a complete transection, and increase 10-fold in number within two weeks following chronic spinal injury (Cassam et al. 1997). Indirect evidence for a neural supply of NE comes from the effectiveness of amphetamines in facilitating the flexor reflex in chronic spinal rats (Nozaki et al. 1977). The fact that amphetamines, which affect pre-synaptic NE release and re-uptake but have no major post-synaptic effects (Carlsson et al. 1965; Hanson 1967; Randrup and Munkvad 1966), have actions below a chronic spinal transection suggests that there is a neural source of these monoamines below the injury. Our preliminary work also supports the effectiveness of low doses of amphetamines at facilitating spasticity in chronic spinal rat tail muscles *in vivo* (unpublished observations). Thus, motoneurons in chronic spinal rats may receive tonic monoaminergic innervation from intraspinal serotonergic and noradrenergic neurons associated with the autonomic system. Because our experiments were done with fast synaptic transmission blocking agents present, neuromodulator release is not dependent on active spinal circuits, and so arises from either spontaneous activity in these monoaminergic neurons, or else leakage from terminals. Addition of cadmium to block Ca^{2+} entry into the terminals inhibits spike-mediated release from these monoaminergic neurons, and may also over extended periods reduce the amount of calcium available in intracellular stores such that Ca^{2+} -dependent non-spike mediated release of neurotransmitter from spontaneous vesicle exocytosis is eliminated. In this way cadmium inhibits 5-HT and NE release from intraspinal monoaminergic neurons, resulting in the slow disappearance of Na PICs, as we observed, in 45 - 60 minutes, similar to the time required to washout 5-HT or for antagonists to the 5-HT and NE receptors to take effect.

Another potential source of monoamines distal to a spinal transection *in vivo* is the blood stream, which can carry neuromodulators and other chemicals to the motoneurons from remote sources. This cannot be the origin of monoamines *in vitro* however, as these sources are lost once the cord is removed into the recording chamber and blood-borne monoamines are washed out. If this was the case, the PICs would only be expected to last at most 1 - 2 hours *in vitro*, which is the time required for 5-HT₂ receptor agonists to wash-out (Harvey et al. 2005b). In contrast, motoneurons exhibit large PICs for many hours of recording. Blood-borne monoamines may be produced by platelets, which release serotonin when activated to trigger clotting mechanisms. Platelets are likely to remain healthy *in vitro* since the vasculature in the isolated spinal cord still contains blood. However, 5-HT formed in the bloodstream is not able to cross the blood-brain barrier, implying that all 5-HT in the CNS must be synthesized *in situ* from L-tryptophan (Birdsall 1998). Thus platelets are an unlikely source of 5-HT in our preparation.

An alternative possibility is that serotonin- or norepinephrine-containing afferent fibres enter the spinal cord via dorsal roots and sprout to synapse onto motoneurons after chronic spinal

transection. However, Hadjiconstantinou and colleagues (1984), who identified a basal level of 5-HT in the distal spinal cord long after transection, did not find the serotonergic content of the spinal cord to be further reduced when a complete rhizotomy accompanied the chronic transection. Furthermore, Cassam and colleagues (1997) did not observe noradrenergic fibres in the dorsal laminae (that contain primary afferent terminals) weeks after complete transection. Therefore, afferents from dorsal roots are unlikely to be the source of monoaminergic innervation. It is possible that sympathetic fibres, innervating the vasculature of the sacrocaudal spinal cord (McNicholas et al. 1980), sprout to synapse onto motoneurons and supply them with NE following chronic spinal transection, and we can not rule out this possibility.

4.4.8 Summary and implications for management of spasticity.

In summary, endogenous monoamines, acting on 5-HT_{2A}, 5-HT_{2C} and α 1-NE receptors, are necessary for spinal motoneurons to exhibit Na PICs, and therefore are required for initiating and sustaining repetitive firing. After chronic spinal injury, endogenous intraspinal monoamines act on supersensitive monoamine receptors to induce very large Na PICs. Intrinsic intraspinal serotonergic and noradrenergic neurons are a likely source of these endogenous monoamines (Cassam et al. 1997; Newton et al. 1986), and these provide a supply of monoamines unregulated by descending control. As such, motoneurons exhibit large Na PICs most of the time, and could even have further enhanced PICs in response to modulation of these intraspinal monoaminergic neurons, perhaps resulting from their association with the autonomic system (Newton et al. 1986). Large uncontrolled Na PICs and Ca PICs have been shown to underlie uncontrolled contractions (spasms) associated with spasticity (Li et al. 2004a). The present results indicate that intraspinal monoamines may be responsible for these large PICs, ultimately suggesting that spasticity may be a condition resulting from a developed supersensitivity to residual monoamines that persist after injury. Thus, inhibiting PICs using monoamine receptor antagonists may be an effective treatment for spasticity, and indeed the non-selective 5-HT antagonist cyproheptadine has been used clinically to treat spasticity, though not without side effects on appetite and mood (Norman et al. 1998; Wainberg et al. 1990). More selective monoamine receptor antagonists may prove more effective in treating spasticity. However, understanding and preventing the development of the supersensitivity of motoneurons to monoamines in the first place offers a new approach to management of spasticity.

4.5 BIBLIOGRAPHY FOR CHAPTER 4

Alvarez FJ, Pearson JC, Harrington D, Dewey D, Torbeck L, and Fyffe RE. Distribution of 5-hydroxytryptamine-immunoreactive boutons on alpha-motoneurons in the lumbar spinal cord of adult cats. *J Comp Neurol* 393: 69-83, 1998.

Alzheimer C, Schwindt PC, and Crill WE. Modal gating of Na⁺ channels as a mechanism of persistent Na⁺ current in pyramidal neurons from rat and cat sensorimotor cortex. *J Neurosci* 13: 660-673, 1993.

Anden NE. Shortlasting increase in the synthesis and utilization of noradrenaline due to Axotomy-induced irritation. *Acta Physiol Scand* 100: 51-55, 1977.

Angleon JK and Betz WJ. Intraterminal Ca(2+) and spontaneous transmitter release at the frog neuromuscular junction. *J Neurophysiol* 85: 287-294, 2001.

Barbeau H and Bedard P. Denervation supersensitivity to 5-hydroxytryptophan in rats following spinal transection and 5,7-dihydroxytryptamine injection. *Neuropharmacology* 20: 611-616, 1981.

Bennett D, Li Y, and Sanelli L. Role of NMDA in spasticity following sacral spinal cord injury in rats. *Soc Neurosci Abstr* 31: 933.11, 2001a.

Bennett DJ, Gorassini M, Fouad K, Sanelli L, Han Y, and Cheng J. Spasticity in rats with sacral spinal cord injury. *J Neurotrauma* 16: 69-84, 1999.

Bennett DJ, Hultborn H, Fedirchuk B, and Gorassini M. Synaptic activation of plateaus in hindlimb motoneurons of decerebrate cats. *J Neurophysiol* 80: 2023-2037, 1998.

Bennett DJ, Li Y, Harvey PJ, and Gorassini M. Evidence for plateau potentials in tail motoneurons of awake chronic spinal rats with spasticity. *J Neurophysiol* 86: 1972-1982, 2001b.

Bennett DJ, Li Y, and Siu M. Plateau potentials in sacrocaudal motoneurons of chronic spinal rats, recorded in vitro. *J Neurophysiol* 86: 1955-1971, 2001c.

Bennett DJ, Sanelli L, Cooke CL, Harvey PJ, and Gorassini MA. Spastic long-lasting reflexes in the awake rat after sacral spinal cord injury. *J Neurophysiol* 91: 2247-2258, 2004.

Birdsall TC. 5-Hydroxytryptophan: a clinically-effective serotonin precursor. *Altern Med Rev* 3: 271-280, 1998.

Blakely RD, De Felice LJ, and Hartzell HC. Molecular physiology of norepinephrine and serotonin transporters. *J Exp Biol* 196: 263-281, 1994.

Bonhaus DW, Weinhardt KK, Taylor M, DeSouza A, McNeeley PM, Szczepanski K, Fontana DJ, Trinh J, Rocha CL, Dawson MW, Flippin LA, and Eglen RM. RS-102221: a

novel high affinity and selective, 5-HT_{2C} receptor antagonist. *Neuropharmacology* 36: 621-629, 1997.

Carlin KP, Jones KE, Jiang Z, Jordan LM, and Brownstone RM. Dendritic L-type calcium currents in mouse spinal motoneurons: implications for bistability. *Eur J Neurosci* 12: 1635-1646, 2000.

Carlsson A, Lindqvist M, Dahlstrom A, Fuxe K, and Masuoka D. Effects of the amphetamine group on intraneuronal brain amines in vivo and in vitro. *J Pharm Pharmacol* 17: 521-523, 1965.

Cassam AK, Llewellyn-Smith IJ, and Weaver LC. Catecholamine enzymes and neuropeptides are expressed in fibres and somata in the intermediate gray matter in chronic spinal rats. *Neuroscience* 78: 829-841, 1997.

Catterall WA. Molecular properties of brain sodium channels: an important target for anticonvulsant drugs. *Adv Neurol* 79: 441-456, 1999.

Clineschmidt BV, Pierce JE, and Lovenberg L. Tryptophan hydroxylase and serotonin in spinal cord and brain stem before and after chronic transection. *J Neurochem* 18: 1593-1596, 1971.

Conway BA, Hultborn H, Kiehn O, and Mintz I. Plateau potentials in alpha-motoneurons induced by intravenous injection of L-dopa and clonidine in the spinal cat. *J Physiol* 405: 369-384, 1988.

Cooper GP and Manalis RS. Interactions of lead and cadmium on acetylcholine release at the frog neuromuscular junction. *Toxicol Appl Pharmacol* 74: 411-416, 1984.

Crill WE. Persistent sodium current in mammalian central neurons. *Annu Rev Physiol* 58: 349-362, 1996.

Delgado-Lezama R, Perrier JF, Nedergaard S, Svirskis G, and Hounsgaard J. Metabotropic synaptic regulation of intrinsic response properties of turtle spinal motoneurons. *J Physiol* 504 (Pt 1): 97-102, 1997.

Egan C, Herrick-Davis K, and Teitler M. Creation of a constitutively activated state of the 5-HT_{2A} receptor by site-directed mutagenesis: revelation of inverse agonist activity of antagonists. *Ann N Y Acad Sci* 861: 136-139, 1998.

Forshaw PJ. The inhibitory effect of cadmium on neuromuscular transmission in the rat. *Eur J Pharmacol* 42: 371-377, 1977.

Franceschetti S, Taverna S, Sancini G, Panzica F, Lombardi R, and Avanzini G. Protein kinase C-dependent modulation of Na⁺ currents increases the excitability of rat neocortical pyramidal neurons. *J Physiol* 528 Pt 2: 291-304, 2000.

French CR, Sah P, Buckett KJ, and Gage PW. A voltage-dependent persistent sodium current in mammalian hippocampal neurons. *J Gen Physiol* 95: 1139-1157, 1990.

Gerin C, Becquet D, and Privat A. Direct evidence for the link between monoaminergic descending pathways and motor activity. I. A study with microdialysis probes implanted in the ventral funiculus of the spinal cord. *Brain Res* 704: 191-201, 1995.

Gorassini MA, Knash ME, Harvey PJ, Bennett DJ, and Yang JF. Role of motoneurons in the generation of muscle spasms after spinal cord injury. *Brain* 127: 2247-2258, 2004.

Granit R, Henatsch HD, and Steg G. Tonic and phasic ventral horn cells differentiated by post-tetanic potentiation in cat extensors. *Acta Physiol Scand* 37: 114-126, 1956.

Hadjiconstantinou M, Panula P, Lackovic Z, and Neff NF. Spinal cord serotonin: A biochemical and immunohistochemical study following transection. *Brain Res* 322: 245-254, 1984.

Haggendal J and Dahlstrom A. The time course of noradrenaline decrease in rat spinal cord following transection. *Neuropharmacology* 12: 349-354, 1973.

Hanson LC. Evidence that the central action of (+)-amphetamine is mediated via catecholamines. *Psychopharmacologia* 10: 289-297, 1967.

Harvey PJ, Li X, and Bennett DJ. Supersensitivity of motoneuron persistent sodium current to endogenous monoamines leads to spasticity in rats. Program No. 310.8. *2004 Abstract Viewer/Itinerary Planner (Online)*. Washington, DC: Society for Neuroscience, 2004.

Harvey PJ, Li Y, Li X, and Bennett DJ. Chapter 2: Persistent sodium currents and repetitive firing in motoneurons of the sacrocaudal spinal cord of adult rats. *From: The Role of 5-HT in the Development of Motoneuron Persistent Sodium Currents after Chronic Spinal Injury* Ph.D. Dissertation: pp. 25-74, 2005a.

Harvey PJ, Li Y, Li X, and Bennett DJ. Chapter 3: Serotonin facilitates persistent sodium currents in motoneurons, and spinal cord transection leads to a supersensitivity to serotonin. *From: The Role of 5-HT in the Development of Motoneuron Persistent Sodium Currents after Chronic Spinal Injury* Ph.D. Dissertation: pp. 75-120, 2005b.

Heckman CJ, Gorassini MA, and Bennett DJ. Persistent inward currents in motoneuron dendrites: Implications for motor output. *Muscle Nerve* 31: 135-156, 2004.

Hodgkin AL and Huxley AF. A quantitative description of membrane current and its application to conduction and excitation in nerve. *J Physiol* 117: 500-544, 1952.

Holets V and Elde R. The differential distribution and relationship of serotonergic and peptidergic fibers to sympathoadrenal neurons in the intermediolateral cell column of the rat: a combined retrograde axonal transport and immunofluorescence study. *Neuroscience* 7: 1155-1174, 1982.

- Hounsgaard J, Hultborn H, Jespersen B, and Kiehn O. Bistability of alpha-motoneurons in the decerebrate cat and in the acute spinal cat after intravenous 5-hydroxytryptophan. *J Physiol* 405: 345-367, 1988.
- Hounsgaard J and Kiehn O. Ca⁺⁺ dependent bistability induced by serotonin in spinal motoneurons. *Exp Brain Res* 57: 422-425, 1985.
- Hsiao CF, Del Negro CA, Trueblood PR, and Chandler SH. Ionic basis for serotonin-induced bistable membrane properties in guinea pig trigeminal motoneurons. *J Neurophysiol* 79: 2847-2856, 1998.
- Hu GY and Hvalby O. Glutamate-induced action potentials are preceded by regenerative prepotentials in rat hippocampal pyramidal cells in vitro. *Exp Brain Res* 88: 485-494, 1992.
- Inazu M, Takeda H, Ikoshi H, Sugisawa M, Uchida Y, and Matsumiya T. Pharmacological characterization and visualization of the glial serotonin transporter. *Neurochem Int* 39: 39-49, 2001.
- Jacobs BL, Martin-Cora FJ, and Fornal CA. Activity of medullary serotonergic neurons in freely moving animals. *Brain Res Brain Res Rev* 40: 45-52, 2002.
- Jahnsen H and Llinas R. Ionic basis for the electro-responsiveness and oscillatory properties of guinea-pig thalamic neurones in vitro. *J Physiol* 349: 227-247, 1984.
- Karobath M. Serotonin synthesis with rat brain synaptosomes. Effects of serotonin and monoamineoxidase inhibitors. *Biochem Pharmacol* 21: 1253-1263, 1972.
- Katz B and Miledi R. Spontaneous and evoked activity of motor nerve endings in calcium Ringer. *J Physiol* 203: 689-706, 1969.
- Kojima M and Sano Y. The organization of serotonin fibers in the anterior column of the mammalian spinal cord. An immunohistochemical study. *Anat Embryol (Berl)* 167: 1-11, 1983.
- Lee RH and Heckman CJ. Bistability in spinal motoneurons in vivo: systematic variations in persistent inward currents. *J Neurophysiol* 80: 583-593, 1998.
- Lee RH and Heckman CJ. Enhancement of bistability in spinal motoneurons in vivo by the noradrenergic alpha1 agonist methoxamine. *J Neurophysiol* 81: 2164-2174, 1999.
- Lee RH and Heckman CJ. Essential role of a fast persistent inward current in action potential initiation and control of rhythmic firing. *J Neurophysiol* 85: 472-475, 2001.
- Levi R and Smith NC. Histamine H(3)-receptors: a new frontier in myocardial ischemia. *J Pharmacol Exp Ther* 292: 825-830, 2000.
- Li Y and Bennett DJ. Persistent sodium and calcium currents cause plateau potentials in motoneurons of chronic spinal rats. *J Neurophysiol* 90: 857-869, 2003.

- Li Y, Gorassini MA, and Bennett DJ. Role of persistent sodium and calcium currents in motoneuron firing and spasticity in chronic spinal rats. *J Neurophysiol* 91: 767-783, 2004a.
- Li Y, Harvey PJ, Li X, and Bennett DJ. Spastic long-lasting reflexes of the chronic spinal rat studied in vitro. *J Neurophysiol* 91: 2236-2246, 2004b.
- Machacek DW, Garraway SM, Shay BL, and Hochman S. Serotonin 5-HT(2) receptor activation induces a long-lasting amplification of spinal reflex actions in the rat. *J Physiol* 537: 201-207, 2001.
- McNicholas LF, Martin WR, Sloan JW, and Nozaki M. Innervation of the spinal cord by sympathetic fibers. *Exp Neurol* 69: 383-394, 1980.
- Melena J, Chidlow G, and Osborne NN. Blockade of voltage-sensitive Na(+) channels by the 5-HT(1A) receptor agonist 8-OH-DPAT: possible significance for neuroprotection. *Eur J Pharmacol* 406: 319-324, 2000.
- Miles GB, Dai Y, and Brownstone RM. Mechanisms underlying the early phase of spike frequency adaptation in mouse spinal motoneurons. *J Physiol*, 2005.
- Newton BW, Maley BE, and Hamill RW. Immunohistochemical demonstration of serotonin neurons in autonomic regions of the rat spinal cord. *Brain Res* 376: 155-163, 1986.
- Norman KE, Pepin A, and Barbeau H. Effects of drugs on walking after spinal cord injury. *Spinal Cord* 36: 699-715, 1998.
- Nozaki M, Bell JA, Vaupel DB, and Martin WR. Responses of the flexor reflex to LSD, tryptamine, 5-hydroxytryptophan, methoxamine, and d-amphetamine in acute and chronic spinal rats. *Psychopharmacology (Berl)* 55: 13-18, 1977.
- Numann R, Catterall WA, and Scheuer T. Functional modulation of brain sodium channels by protein kinase C phosphorylation. *Science* 254: 115-118, 1991.
- Patel MK, Mistry D, John JE, 3rd, and Mounsey JP. Sodium channel isoform-specific effects of halothane: protein kinase C co-expression and slow inactivation gating. *Br J Pharmacol* 130: 1785-1792, 2000.
- Patrick RL and Barchas JD. Regulation of catecholamine synthesis in rat brain synaptosomes. *J Neurochem* 23: 7-15, 1974.
- Perrier JF and Hounsgaard J. 5-HT2 receptors promote plateau potentials in turtle spinal motoneurons by facilitating an L-type calcium current. *J Neurophysiol* 89: 954-959, 2003.
- Randrup A and Munkvad I. Role of catecholamines in the amphetamine excitatory response. *Nature* 211: 540, 1966.
- Riccioppo Neto F. The local anesthetic effect of cyproheptadine on mammalian nerve fibres. *Eur J Pharmacol* 54: 203-207, 1979.

- Schanne FA, Kane AB, Young EE, and Farber JL. Calcium dependence of toxic cell death: a final common pathway. *Science* 206: 700-702, 1979.
- Schlue WR, Richter DW, Mauritz KH, and Nacimiento AC. Responses of cat spinal motoneuron somata and axons to linearly rising currents. *J Neurophysiol* 37: 303-309, 1974.
- Schmidt BJ and Jordan LM. The role of serotonin in reflex modulation and locomotor rhythm production in the mammalian spinal cord. *Brain Res Bull* 53: 689-710, 2000.
- Schmidt H and Stampfli R. [The effect of tetraethylammonium chloride on single Ranvier's nodes]. *Pflugers Arch Gesamte Physiol Menschen Tiere* 287: 311-325, 1966.
- Stafstrom CE, Schwindt PC, and Crill WE. Negative slope conductance due to a persistent subthreshold sodium current in cat neocortical neurons in vitro. *Brain Res* 236: 221-226, 1982.
- Steinbusch HW. Distribution of serotonin-immunoreactivity in the central nervous system of the rat-cell bodies and terminals. *Neuroscience* 6: 557-618, 1981.
- Svirskis G and Hounsgaard J. Transmitter regulation of plateau properties in turtle motoneurons. *J Neurophysiol* 79: 45-50, 1998.
- Taddese A and Bean BP. Subthreshold sodium current from rapidly inactivating sodium channels drives spontaneous firing of tuberomammillary neurons. *Neuron* 33: 587-600, 2002.
- Takahashi T and Berger AJ. Direct excitation of rat spinal motoneurons by serotonin. *J Physiol* 423: 63-76, 1990.
- Urbani A and Belluzzi O. Riluzole inhibits the persistent sodium current in mammalian CNS neurons. *Eur J Neurosci* 12: 3567-3574, 2000.
- Wainberg M, Barbeau H, and Gauthier S. The effects of cyproheptadine on locomotion and on spasticity in patients with spinal cord injuries. *J Neurol Neurosurg Psychiatry* 53: 754-763, 1990.
- Wang HY and Friedman E. Central 5-hydroxytryptamine receptor-linked protein kinase C translocation: a functional postsynaptic signal transduction system. *Mol Pharmacol* 37: 75-79, 1990.
- Zeng J, Powers RK, Newkirk G, Yonkers M, and Binder MD. Contribution of persistent sodium currents to spike-frequency adaptation in rat hypoglossal motoneurons. *J Neurophysiol* 93: 1035-1041, 2005.

CHAPTER 5: Conclusion

5.1 THE ETIOLOGY OF SPASTICITY FOLLOWING SCI

Our working hypothesis was that an intraspinal source of monoamines remains in the sacrocaudal spinal cord after long-term injury, and the supersensitivity of motoneurons to this endogenous supply of monoamines leads to large PICs, which are essential for a functional level of motoneuron excitability. The results presented in this thesis support this hypothesis. Specifically, it was demonstrated that:

- Motoneurons of chronic spinal rats are inherently more excitable than motoneurons of acute spinal rats, in that they have larger PICs, rest closer to threshold and require less current to trigger repetitive firing.
- Exogenous application of 5-HT has complex actions on spinal motoneurons, all of which act to make motoneurons more excitable (i.e., easier to activate).
- The 5-HT₂ receptor agonist DOI specifically facilitates Na channels and increases Na PIC amplitude.
- Motoneurons of chronic spinal rats are supersensitive to actions of 5-HT and DOI.
- The Na PIC is inhibited by antagonists acting on 5-HT_{2A}, 5-HT_{2C} and α 1-NE receptors in motoneurons of both acute and chronic spinal rats, and is completely eliminated when all three monoamine receptors are blocked pharmacologically.

These results fit a pattern that explains the etiology of spasticity following SCI. Normally, motoneurons require PICs to amplify synaptic inputs and facilitate firing, and these PICs are maintained by descending monoaminergic innervation, which controls the level of monoamine tone in the spinal cord and thus the level of motoneuron excitability. Immediately after complete spinal transection, this source of monoamines is lost, and motoneuron excitability is greatly reduced. As such, motoneurons of acute spinal rats have small PICs and require large currents to activate. This situation likely contributes to the clinical state of spinal shock following traumatic spinal cord injury.

With time, however, motoneurons adjust their sensitivity to the monoamines 5-HT and NE (denervation supersensitivity), thus maintaining an adequate level of excitability. Intrinsic to the sacrocaudal spinal cord are intraspinal serotonergic and noradrenergic neurons which supply a small amount of 5-HT and NE to the motoneurons, but because of the greatly increased sensitivity, this results in very large PICs. Unfortunately, the intrinsic sources of monoamines (and, as a result, the level of monoamine tone) are not regulated in a manner appropriate to voluntary activity, with the consequence that motoneurons exhibit very large PICs tonically, or at entirely inappropriate times. The pathological consequence of this adaptation is large muscle spasms in response to any kind of synaptic input, i.e., spasticity.

5.2 FUTURE DIRECTIONS

The Na PIC represents only half of the total PIC responsible for the muscle spasms, with the Ca PIC representing the other half. As such, it is critical to determine how the large Ca PICs develop after chronic spinal transection. Based on the results from other labs, and preliminary data obtained by X. Li and D. Bennett, the Ca PIC appears to be facilitated by 5-HT acting on 5-HT₂ receptors, and Ca PICs in motoneurons of chronic spinal rats are also facilitated at very low doses of 5-HT and the 5-HT₂ receptor agonist DOI. Thus, because 5-HT₂ receptors are coupled to Gq proteins, the Ca PICs are likely activated through Gq-coupled receptors, as with the Na PIC. However, our results show that the monoamine receptor blockade that eliminates the Na PIC, does not block the Ca PIC, although it may be reduced. This may be because other receptors are being activated by endogenous ligands and facilitating the Ca PIC. Alternatively, the Ca PIC may persist despite receptor block or removal of agonists, and may in fact require activation of the Gi-coupled pathway (such as via 5-HT_{1A} receptors), which can oppose or reverse actions of the Gq-coupled pathways.

Of clinical relevance is the fact that the Na PIC can be eliminated by monoamine antagonists, and as such, serotonergic and noradrenergic antagonists may be effective anti-spastic medications that specifically target the large PICs responsible for the muscle spasms. Therefore, given our understanding of the cellular basis of spinal spasticity that has arisen through the research presented here, a new generation of anti-spastic medications may develop based on monoamine antagonists targeting motoneuron PICs. Furthermore, knowing that spasms arise from motoneuron supersensitivity to endogenous monoamines may lead to the development of medical treatments aimed at preventing spasticity from occurring by blocking the development of supersensitivity to 5-HT and NE.

The value of our results to the study of Na PIC regulatory mechanisms should not be overlooked. Through these experiments, we have identified a means by which the Na PIC can be specifically modulated without blocking the Na channel itself, by pharmacologically modulating activity at 5-HT and NE receptors. While the specific cell-surface receptors may differ in different systems where Na PICs have been observed (e.g., neocortex, cardiac muscle, etc.), we suspect that activation of the Gq-protein intracellular pathway is the central point of convergence for receptors modulating the Na PIC. Further work must be done to better characterize the link between Gq-coupled receptors and the Na channels mediating the Na PIC.

APPENDIX: An investigation into the potential for activity-dependent regeneration of the rubrospinal tract after spinal cord injury.

A.1 BACKGROUND

After peripheral nerve transection and repair with sutures, immediate electrical stimulation of the nerve for as little as one hour accelerates the time course of regrowth and improves the accuracy of reinnervation (Al-Majed et al. 2000b; Nix and Hopf 1983; Pockett and Gavin 1985). The stimulation allows regenerating axons to traverse the site of injury more rapidly, rather than increasing the actual rate of regeneration (Brushart et al. 2002).

In the central nervous system (CNS), the capacity for regeneration is relatively poor, but given a more permissive environment provided by a peripheral nerve grafted onto a CNS injury site, some central neurons will regenerate their cut axons for long distances (David and Aguayo 1981; Ramon y Cajal 1928; Richardson et al. 1980; Tello 1911). In particular, rubrospinal neurons have been shown to regenerate into peripheral nerves grafted at the cervical spinal cord level (Fernandes et al. 1999; Richardson et al. 1984; Tetzlaff et al. 1991). We examined whether the axonal regeneration response of rubrospinal neurons could be enhanced after injury by antidromic electrical stimulation, while providing them with the permissive environment of a peripheral nerve graft in which to extend their cut axons.

Axotomy results in elevated levels of regeneration-associated genes (RAGs) in affected motoneurons at 1 week post-injury. Electrical stimulation of peripheral nerves increases expression of brain-derived neurotrophic factor (BDNF) mRNA and its receptor TrkB (Al-Majed et al. 2000a), as well as of regeneration-associated genes such as growth-associated protein (GAP)-43 (Al-Majed et al. 2004) in femoral motoneurons at much earlier time points (48 hours) after injury and stimulation, but by 7 days, gene expression is the same as in unstimulated injured motoneurons. Thus, electrical stimulation correlates with an earlier cell body response to injury that may lead to improved axonal regeneration. In the CNS, proximal axotomy also leads to a decrease in BDNF, and an increase in GAP-43 mRNA expression by 7 days post-injury, and axonal regeneration of rubrospinal neurons is associated with elevated levels of RAGs such as GAP-43 (Fernandes et al. 1999). Exogenous application of BDNF to cell bodies of rubrospinal neurons enhanced their expression of RAGs, including BDNF mRNA, as well as their regenerative capacity (Kobayashi et al. 1997). Injured rubrospinal neurons may respond in a similar way to electrical stimulation as injured femoral neurons, in which case elevated BDNF and GAP-43 mRNA expression will also be observed at early time points (48 hours). Therefore, in addition to assessing regeneration, we tested whether electrical stimulation of the rubrospinal tract (RST) after injury elevated BDNF and GAP-43 mRNA levels at 48 hours post-injury. To match the stimulation protocol used by Al-Majed *et al.* (2000b), we used 1 hour of supramaximal stimulation of the proximal rubrospinal tract at 20 Hz, immediately after a C5 dorsolateral funiculotomy of the spinal

cord. To minimize damage, we employed flexible microwire electrodes (Mushahwar et al. 2000; Prochazka et al. 1976) that were implanted in the spinal cord near the rubrospinal tract rostral to the lesion. In a series of control experiments, current spread and rubrospinal tract recruitment were quantified by simultaneously recording from the red nucleus during RST stimulation. With these microwires, supramaximal rubrospinal tract stimulation could be achieved with low currents, and no direct damage to the tract was produced by the standard stimulation protocol.

A.2 METHODS

Adult female Sprague-Dawley rats (150 - 300 g) were used in this study. Surgeries were performed under a mixture of sodium pentobarbital (52 mg/kg) and buprenorphine (40 µg/kg) anaesthesia. All experimental procedures were approved by the University of Alberta animal welfare committee in accordance with guidelines for the ethical treatment of animals issued by the Canadian Council on Animal Care.

A.2.1 *Stimulating microwires*

Our major goal was to stimulate the rubrospinal tract (RST) for 1 hour, to examine the stimulation-induced changes in regeneration. However, long-duration supramaximal stimulation of the rubrospinal tract was technically much more difficult to achieve than with the peripheral nerves studied by Al-Majed et al. (2000b). We initially attempted placing a conventional stimulating wire (250 µm silver wire) over the rubrospinal tract on the dorsolateral surface of the cord, and stimulated at 20 Hz at intensities adequate to activate the rubrospinal tract. However, this regime induced very large vibrations in the animal because most of the current spread to nearby roots and produced direct muscle contractions. Thus, movement of the animal relative to the electrode made consistent stimulation impossible and damaged the spinal cord. Even by using a stereotaxic frame, vertebral clamps, and fine tungsten stimulating electrodes, we could not stabilize the animal adequately to avoid damage to the spinal cord during this 20-Hz supramaximal stimulation.

Thus, to stimulate the RST we adopted a flexible fine wire stimulation method that has been proven to work without producing major spinal cord injury. That is, the red nucleus was activated via antidromic stimulation of the cervical rubrospinal tract using flexible microwire electrodes developed by Prochazka and colleagues (1976). These stimulating microwire implants are made from 30-µm diameter PtIr (80% platinum, 20% iridium) wire (California Fine Wire, CA) insulated with 4 µm polyimide. Under a dissecting microscope, the stimulating end of the wire was stripped of insulation up to 300 µm from the end and a tip was cut at a 30° angle. A 90° bend was made 1.0 mm from the stimulating tip so the epidural portion would lie flat on the dura matter and control the depth of penetration. Approximate impedance for these electrodes was 5-20 kΩ. A major disadvantage of using microwires is that their tips are so small that current densities near the tips are very high during stimulation, which can potentially lead to

electrolytic tissue damage. In preliminary trials, we stimulated the rubrospinal tract with monophasic current pulses (0.1 ms, 300 μ A). However, we found that there were lesions in the tissue observed in subsequent histology, even though stimulation was adjusted to a physiological level that would maximally recruit the axons in the rubrospinal tract. Furthermore, when the microwire tip was directly observed in saline under a microscope during prolonged 20-Hz stimulation, the tip clearly oxidized and produced gas bubbles (at 100-700 μ A), as it presumably split water molecules by electrolysis. This process, along with acidosis and oxidation of organic materials, is known to cause lesions (Mortimer 1981). The threshold current for this bubble generation was $416 \pm 121 \mu$ A when using monophasic stimulation for tested electrodes ($n = 5$). This problem was primarily caused by a net negative charge being passed through the electrode, and was solved instead by using balanced biphasic current pulses, so that the net charge passed was near zero (Mortimer 1981). With this method, there were never electrolytic lesions induced during stimulation of rubrospinal axons. The current at which the electrode visibly generated bubbles capable of making electrolytic lesions was 4 mA, well above the current required to maximally activate the rubrospinal tract (see below).

A.2.2 Recording from the red nucleus during rubrospinal tract (RST) stimulation

A series of acute experiments was performed to determine optimum electrode placement and parameters for RST stimulation. Adult female Sprague-Dawley rats (200-300 g) were anaesthetised as described previously. The dorsal aspect of the neck was opened, and the musculature was bluntly dissected and held apart with retractors to allow a dorsal laminectomy at the level of the C4 and C5 vertebrae. The area was kept moist with saline-soaked gelfoam (Pharmacia & Upjohn, MI). Between 1- and 4-PtIr monopolar microwire electrodes were inserted in different locations in the C4 and C5 spinal segments, mostly around the left dorsolateral funiculus, but occasionally on the contralateral side. The current-return wire (Ag~AgCl) was inserted into the right hindlimb. Electromyogram (EMG) electrodes were placed in the left shoulder and triceps in some experiments.

Following wire implantation, the animal was placed in a stereotaxic frame (Narishige), with a spinal clamp gripping the lateral aspects of the cervical vertebral column. The skin and muscle over the skull was opened, and a 3-mm diameter hole was drilled in the skull over the red nucleus, centered at a position 6.0 mm caudal and 2.0 mm right lateral from bregma (contralateral to RST stimulation). The dura was opened, the exposed area being kept moist with mineral oil. Recordings were made with a 12-M Ω tungsten electrode (A-M Systems #575400), which was angled medially at 12° to avoid the central sinus. Field potentials at 1-ms latency to cervical stimulation of the rubrospinal tract were usually found when the electrode tip was positioned at $x = -6.0$, $y = +1.9$ from bregma on the skull surface at a depth of 6.5 to 7.5 mm from the cerebral cortical surface. In two separate experiments, we stimulated the RST and mapped out a large area of field potentials (roughly a sphere of 1-mm diameter) matching the size and position reported for the magnocellular red nucleus in Paxinos & Watson (1986).

Stimulation for RST activation of the red nucleus was done through paired Isoflex stimulators (A.M.P.I., Israel) synchronized using a PulseMaster A300 to produce a biphasic (negative/positive) stimulation current pulse of 100 μ s duration per phase. Between pulses, current was dissipated using a 100-k Ω resistor in parallel to prevent drift in tip potential. Stimulation pulses were monitored with an oscilloscope (Tektronix TDS 3014) to ensure that both positive and negative pulse phases were of equal amplitude and baseline potential was not drifting from zero. Signals from EMG and red nucleus recordings passed through a 3-channel 100 \times pre-amplifier (built by K. Yoshida), were further amplified by 100 times (CyberAmp 380) and sampled at 10 kHz using Axoscope 8.0 software. All animals undergoing this procedure were euthanised at the end of the experiment by sodium pentobarbitol overdose.

Subsequent quantification of red nuclear field potentials was done using custom MATLAB software. Data in a 2-ms window, starting 1 ms after the stimulation, was rectified, filtered and averaged for each sweep. Multiple sweeps were averaged to give a final measure with standard error.

A.2.3 Rubrospinal tract stimulation and regeneration into a peripheral nerve graft

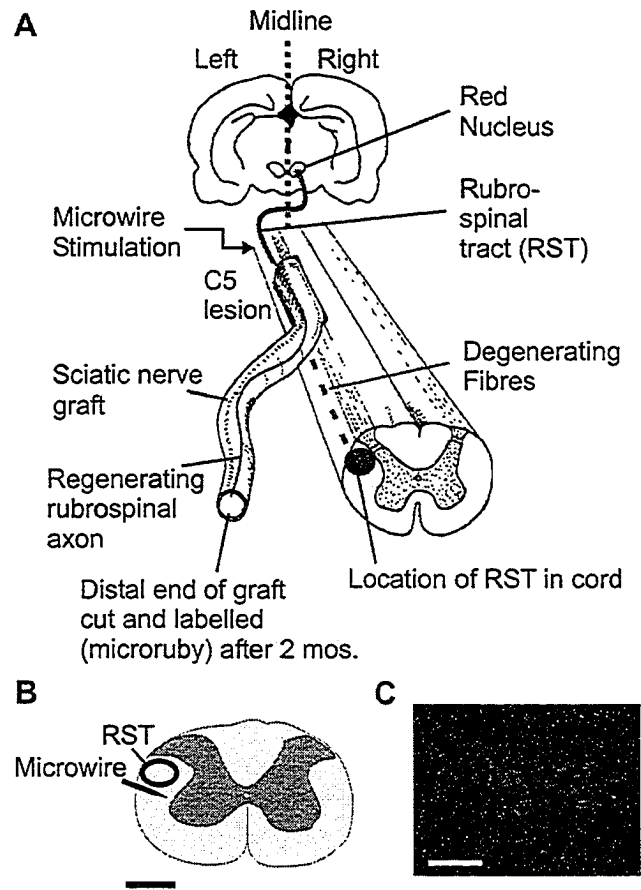
Two groups of female Sprague-Dawley rats (200-300 g) were used for peripheral nerve graft regeneration experiments. The peripheral nerve graft protocol was originally developed by Richardson and colleagues (1984) and has been described previously by Kobayashi *et al.* (1997). Briefly, animals underwent a preliminary surgery under sodium pentobarbitol anaesthesia (52 mg/kg) to cut the right sciatic nerve immediately distal to the exit point from the sciatic notch. After allowing 10 days for recovery and Wallerian degeneration of the nerve, the rats were again anaesthetised (using pentobarbitol and buprenorphine) for a second surgery. A 20- to 30-mm segment of the right sciatic nerve was harvested for grafting. A left hemi-laminectomy was performed at the level of the C4 and C5 vertebral segments, and a segment of the C5 cord, including the left dorsolateral funiculus (the region containing the rubrospinal tract) but sparing the dorsal columns and ventral tracts, was removed by aspiration. The proximal end of the sciatic nerve was placed in the hole abutting the rostral cut face and sutured (10-0 Ethilon, Ethicon, NJ) to the dura as it was closed overtop to anchor it in position (Figure A-1A).

The stimulation apparatus was as described above in the acute experiments. A single PtIr microwire implant was inserted through the dura near the RST (Figure A-1B), 2 mm proximal to the lesion and anchored with superglue (Adhesive Systems RP1500) to the C3 vertebrae. EMG recordings were made from the left acromiotrapezius and triceps brachii. In preliminary acute experiments, we found that we could use stimulus-evoked EMG as an independent indicator of stimulus intensity during RST electrical stimulation. Stimulation of the RST induced a characteristic movement of the shoulder and forearm, which could be detected by EMG wires inserted in the trapezius muscles, even when the rubrospinal tract was lesioned distally. The standard stimulation wire placement

Figure A-1

Protocol for investigating activity-dependent CNS regeneration. *A*: A region of the C5 spinal cord left dorsolateral funiculus was removed by aspiration, and the proximal end of a 10-day pre-degenerated autologous sciatic nerve (30 mm) was placed in the lesion site and anchored to the dura. PtIr microwires (30 μm dia.) were inserted through the dura ventral to the rubrospinal tract (RST) and rostral to the injury site. Threshold for RST activation was estimated using EMG electrodes in the shoulder muscles. Treatment groups received 1 hour of 20-Hz balanced biphasic current pulse stimulation at 200-300 μA . This stimulation recruits the entire red nucleus without axonal damage. Control groups received the microwire implant but no stimulation. Rubrospinal neurons were allowed to regenerate for 8 weeks, at which time the distal portion of the nerve graft was exposed and a retrograde tracer (microruby) applied to the freshly cut stump. After 1 week, all animals were sacrificed, and the midbrain was removed, sliced and mounted on slides to count labelled neurons within the red nucleus. *B*: Transverse sketch of the C4 cervical spinal cord showing the location of the rubrospinal tract (RST) and microwire placement. Scale bar is 1 mm. *C*: Examples of microruby-filled rubrospinal neurons. Scale bar represents 50 microns.

Figure A-1



produced an EMG response with a $78.0 \pm 11.3 \mu\text{A}$ threshold, which was consistently 2 to 3 times the threshold to activate the rubrospinal tract ($30.1 \pm 3.2 \mu\text{A}$).

In the main experiments, 1-Hz test stimulation pulses (0.1 ms biphasic) to the RST of increasing amplitude were applied initially to determine EMG threshold. Then the standard stimulation protocol (20 Hz, 0.1 ms, amplitude roughly 5× EMG threshold but between 200 and 300 μA , see Results) was applied for 1 hour in one group ($n = 16$), and a sham stimulation (leaving the wire in place for 1 hour without stimulation) was given to the second group ($n = 17$). We rationalized the use of 1 hour of stimulation because this duration was just as effective in promoting regeneration of femoral motoneurons as 2 weeks of continuous 20-Hz stimulation via implantable stimulators. By using stimulation durations of 1 hour, we avoided complications that might arise from longer stimulation times that would necessitate prolonged anaesthesia and exposure of the CNS and graft to the environment, or else development of chronic implants that might interfere with regeneration or require special treatments to avoid rejection or infection. During stimulation, the cervical cord and nerve graft were kept moist with saline-soaked gelfoam. After 1 hour, the microwire was removed, the wound closed and the animals were allowed to recover.

After 8 weeks survival, the animals were again anaesthetised and the distal end of the nerve graft was labelled with 30% microruby (Molecular Probes D-7162) in distilled water. Animals were sacrificed 1 week after labelling (to allow for dye uptake into the cell body) by sodium pentobarbital overdose and transcardial perfusion with cold saline followed by 4% paraformaldehyde in phosphate-buffered saline. Regions of the neural axis containing the graft site and the red nucleus were removed, post-fixed overnight and serially cryoprotected before freezing. Midbrains were sliced on a cryostat in 20- μm coronal sections, and the labelled rubrospinal neurons were visualised and counted in the red nucleus by fluorescent microscopy. Only every second slice was counted to avoid double counting of split cells. Cervical spinal segments containing the graft were sliced transversely in 40- μm sections over a 4-mm length spanning the graft junction. The success of the implant surgery was additionally assessed by counting fluorescent local cervical neurons (every second slice) within 1 mm of either side of the graft junction. The ratio of red nucleus counts to cervical counts was calculated to control for surgical variability in the grafting procedure.

A.2.4 Influence of RST stimulation on BDNF and GAP-43 mRNA expression

A separate set of animals ($n = 12$) was tested for changes in gene expression associated with injury and stimulation, but without a peripheral nerve graft. Under the standard anaesthesia, these rats received a lesion to the cervical RST, followed by the stimulation protocol as described above. Stimulation was applied for 1 hour in one group ($n = 8$), and a sham stimulation was given to the second group ($n = 4$). The wire was removed before closing the tissue. In an additional group of animals, we wanted to test longer durations of stimulation. For this we used a mixture of sodium pentobarbital topped-up with isoflurane gas that was carefully regulated to maintain the animals at a surgical level

of anaesthesia. Four animals received 8 hours stimulation, and two animals received a sham stimulation for 8 hours. The animals were sacrificed at 48 hours post-lesion, and the midbrains containing the red nuclei were quickly extracted and frozen at -40°C . Four animals from the 1-hour stimulation group were used for RT-PCR assay of GAP-43 and BDNF mRNA expression. The remaining animals were used for BDNF *in situ* hybridisation (ISH).

A.2.5 RT-PCR

Fresh frozen midbrains from four stimulated rats were used for RT-PCR analysis of BDNF and GAP-43 expression. Right and left red nuclei were visualized and micro-dissected under dark-field illumination from 70- to 80- μm thick serial sections through the caudal pole (400 μm) of the red nucleus containing the magnocellular population. Total RNA for both pooled right (stimulated) and pooled left (control) red nuclei was extracted using Trizol (Life Technologies, Gaithersburg, MD) according to standard protocol provided by the manufacturer, followed by DNase treatment. The procedures for RT-PCR and control experiments were essentially the same as in a previous study (Kobayashi et al. 1996). PCR for rps12 was included as a control, using 5'-GGAAGGC-ATAGCTGCTGG-3' for the forward primer and 5'-CCTCGATGACATCCTTGG-3' for the reverse primer, to ensure that equivalent amounts of cDNA were analysed (data not shown). The primers used for BDNF were 5'-CGGATCCGCTGCAAACATGTCCATG-3' for the left primer and 5'-GCCACTATCTTCCCCTTTTAATGG-3' for the right, according to nucleotide (nt) 437-455 and 825-803 of the rat BDNF sequence respectively, with two mismatches each plus a restriction site (Maisonpierre et al. 1991). The GAP-43 primers used were 5'-ATGCTGTGCTGTATGAGAAGAACC-3' for the forward direction and 5'-GGCAACGTGGAAAGCCGTTTCTTAAAGT-3' for the reverse direction. For BDNF serial dilution PCR, 100, 50, 25 and 12.5 ng of input cDNA were amplified for 40, 50 and 60 cycles (1 min at 94°C , 2 min at 42°C , and 3 min at 72°C). BDNF PCR products were run on a 5% polyacrylamide gel stained with ethidium bromide and photographed under ultraviolet light. GAP-43 serial dilutions of 25, 12.5, 6.75 and 3.3 ng of input cDNA were amplified for 31 cycles, then run on 5% polyacrylamide gel with ethidium bromide and photographed under ultraviolet light. Photographs were digitised and inverted, and a grey-scale analysis was performed on each band using Scion software (Scion Corporation, MD). Band intensity was calculated relative to background in a nearby portion of the gel (immediately above or below protein band).

A.2.6 *In situ hybridisation of red nuclei*

In situ hybridisation was carried out under RNase-free conditions. Synthetic oligonucleotide probes were used for ISH as described by Verge *et al.* (1992). In brief, we used a 50-mer oligonucleotide 5'-AGTTCCAGTGCCTTTTGTGCATGCCCTGCAG-CTTCCTTCGTGTAACCC-3' complementary to bases 694-645 of the rat BDNF sequence (Kobayashi et al. 1996; Maisonpierre et al. 1991), which has been used

previously by Ernfors *et al.* (1990). Oligonucleotides were end-labelled with ^{35}S -ATP (NEN-Dupont, USA) achieving a specific activity of 2.5×10^9 c.p.m./mg (Ausubel *et al.* 1987). For 4 rats from each group, fresh frozen midbrains were cryostat sectioned at 12 μm in the coronal plane, so that each section contained the left and right red nuclei. Alternating sections were collected at 2 sections per slide and were kept at -85°C until use. Fresh cryostat sections were removed from the freezer and hybridised to 10^6 c.p.m. of probe in a 100-ml hybridisation cocktail (for details of the cocktail, hybridisation and washes, see Verge *et al.*, 1992). The sections were dipped in Kodak NTB-2 emulsion, diluted 1:1 in H_2O and exposed for 8 weeks. Diffuse hybridisation signals in the red nuclei from the 1-hour stimulation experimental groups prompted counterstaining of the cell bodies with FluoroNissl (NeuroTrace, Molecular Probes) for the 8-hour stimulation tissue.

A.2.7 Electrical stimulation and regeneration in the peripheral nervous system using the femoral nerve-nerve suture model

Attempts were made to replicate the results of Al-Majed *et al.* (2000b) using the methods described in detail in that paper. Briefly, (under sodium pentobarbital anaesthesia at 52 mg/kg) the left femoral nerve of adult female Sprague-Dawley rats (200-300 g) was transected 20 mm above the bisection into the quadriceps and saphenous nerve branches, and then immediately sutured back together (this repair took 5 – 15 mins). Directly following nerve repair, electrical stimulation was applied via flexible stainless steel Cooner wire loops placed with the cathode proximal to the suture point, and the anode more distally. Charge-balanced current pulses were applied at 20 Hz for 1 hour in the stimulated group of rats ($n = 23$), and the electrodes were left in place for 1 hour without stimulation in a control group of rats ($n = 23$). Stimulation intensity was set at 3 times the threshold to activate the motor axons, which guarantees full activation of all the motor axons (Stein 1980). The motor threshold was determined prior to cutting the femoral nerve by observing the twitch response of the muscle to varying stimulation.

After allowing 3 weeks to recover, the animals were again anaesthetised, and the quadriceps and saphenous branches of the femoral nerve were cut 5 mm distal to the branch point. Fluorogold (4% in cacadylic acid) and microruby (30% in dd H_2O) were applied randomly to either the muscle (quadriceps nerve) or cutaneous (saphenous nerve) branch cut ends. After allowing 1 week for dye uptake, animals were sacrificed, perfused with saline and 4% paraformaldehyde; their lumbar cords were then dissected out, frozen and sliced on a cryostat. Fluorescent motoneurons were counted in the lumbar region, with the counter blind to the treatment group and to which branch had received which dye. Cell counts were corrected using the method of Abercrombie (Abercrombie 1946).

A.2.8 Experimental design and statistical analysis

Because of inherent variability in nerve graft procedures (in RST or femoral nerve experiments), the surgeon performing the graft was not aware of whether the animal

would be stimulated or not after the graft surgery. This avoided a bias of the outcome by inadvertently picking animals with good graft surgeries for the stimulation. Likewise the retrograde labeling and counting of neurons was performed blind to whether the particular animal was stimulated or not.

All data are reported as the mean \pm S.E.M. Comparisons between groups were done using an independent Student's *t*-test with $P < 0.05$ demonstrating significance.

A.3 RESULTS

A.3.1 Microwires used to stimulate the rubrospinal tract

Our primary goal was to test whether one hour of supramaximal stimulation of the rubrospinal tract (RST) could improve axonal regeneration after central axotomy of RST neurons. The premise for this was that Al-Majed and colleagues (2000b) had previously demonstrated that femoral motor axon regeneration across a lesion was accelerated using a similar 1-hour stimulation protocol applied to the injured peripheral nerve. To avoid stimulus-induced electrode movement and damage to the spinal cord, we adopted the fine microwire electrode method of Prochazka and colleagues (Mushahwar et al. 2000; Prochazka et al. 1976), where the microwire essentially floats with the spinal cord, and movement is absorbed by the flexibility of the wire. When these wires were supramaximally stimulated at 20 Hz for 1 hour, there was no detectable damage to the RST, as quantified below using recordings from the red nucleus.

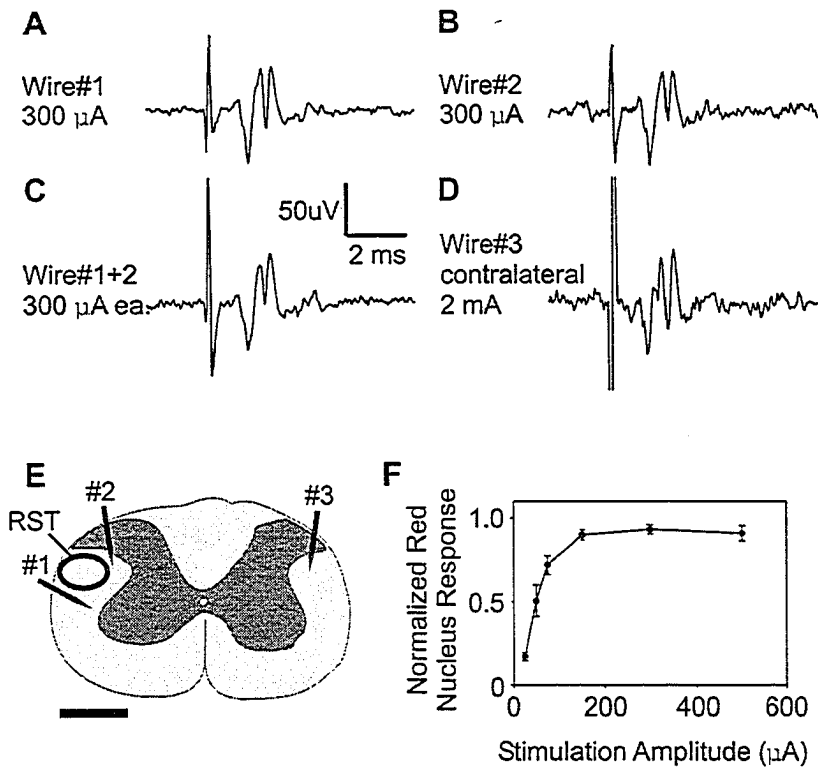
A.3.2 Red nucleus recordings to quantify rubrospinal tract activation with microwires

To determine the stimulus intensities required to supramaximally stimulate the rubrospinal tract with microwires, we recorded from the contralateral red nucleus with tungsten electrodes in acute experimental control animals not treated with a nerve graft ($n = 12$). Figure A-2A demonstrates such a recording, showing supramaximal (300 μ A) stimulation of the cervical rubrospinal tract inducing a field potential in the contralateral red nucleus. In this case, the stimulus threshold to evoke an extracellular field potential in the red nucleus was 42 μ A and maximal stimulation was achieved at 75 μ A (balanced biphasic stimulation). On average, for the standard microwire placement near the rubrospinal tract, the activation threshold was $30.1 \pm 3.2 \mu$ A and a maximal response was evoked at $131.7 \pm 16.6 \mu$ A (Figure A-2F). The maximal response occurred at approximately 4 to 5 \times current threshold, consistent with the current required to antidromically activate the full range of axon diameters in the rubrospinal tract (1.5 - 5 microns: Brown 1974). As the recording electrode was advanced through the 2-mm extent of the red nucleus, the stimulus-evoked field potential changed in shape, but the current required to evoke a maximal response did not change significantly (not shown), indicating that the stimulus likely activated the entire rubrospinal tract.

Figure A-2

Supramaximal stimulation of the rubrospinal tract can be achieved with a single microwire implanted in the dorsolateral cervical spinal cord. Two 30- μm PtIr microwires (#1 and #2) were placed in the left cervical dorsolateral funiculus (as shown in *E*). A third microwire was placed in the right RST. Recordings were made from the right red nucleus with a 12-M Ω tungsten electrode. Because the extracellular field potential appeared the same whether stimulated by wire #1 (*A*), #2 (*B*), or both combined (*C*; at 300 μA each), it appeared that each wire is stimulating the entire RST. When a distant wire, implanted in the right RST (#3), was stimulated at 2 mA, it produced the same response in the right red nucleus as the contralateral microwires (*D*), yet produced no response to 1 mA stimulation (not shown). Scale bar in *E* is 1.0 mm. *F*: Group data for magnitude of field potential measured in the red nucleus (as calculated with Matlab software and normalised to the maximum response for each individual microwire) with increasing stimulation amplitude. The largest field potential amplitude occurred at, on average, 131.7 ± 16.6 μA , such that stimulation at 175 μA or greater produced maximal activation of the tract for microwires placed in the left dorsolateral region of the cervical spinal cord.

Figure A-2



The observed field potentials were verified to be due to antidromic activation because of the lack of jitter and the latency which was too short to account for both conduction and synaptic delays (less than 1 ms for earliest spike). In contrast, stimulation of the interpositus nucleus of the cerebellum, which has strong monosynaptic connections to the contralateral red nucleus, elicited field potentials with delays of over 1 ms and exhibiting jitter (data not shown), despite the considerably shorter conduction distance. With cervical stimulation, components of the field potential had latencies over 1 ms, but because of the consistency and lack of jitter, they were determined to arise from antidromic activation of slower conducting fibres (Eccles et al. 1975 report a wide range of conduction velocities (20-150 m/s) in the rubrospinal tract of cats). Thus, synaptic activation of the red nucleus via cervical stimulation of the dorsolateral funiculus was not observed. Nevertheless, polysynaptic activation of the red nucleus via the interpositus nucleus has been reported with peripheral nerve stimulation (Eccles et al. 1975). As such, synaptic activation may have occurred if our stimulation in the dorsolateral funiculus spread beyond the RST to the dorsal horn afferents (see below); however it was clearly overshadowed by direct antidromic activation.

Considering that these microwires have been previously used to produce focal stimulation of the spinal cord (Mushahwar et al. 2000), a concern was whether the whole 300- to 500- μm diameter rubrospinal tract could be activated with as little as 130 μA . Thus, we directly verified the full rubrospinal tract activation with a paired stimulation wire paradigm, as demonstrated in Figures A-2A to E. That is, pairs of wires were placed in the cervical cord, at deliberately different positions and orientations relative to the rubrospinal tract (Figure A-2E), so that they should generate different field potentials recorded in the red nucleus if they stimulated a different fraction of the rubrospinal tract. However, in all such pairs of wires, the supramaximal stimulation evoked identical field potentials (Figures A-2A and B, not significantly different in amplitude), indicating that each fully activated the red nucleus. Even a wire placed over 2 mm away in the contralateral spinal cord (Figure A-2D) evoked the same supramaximal field potential as the ipsilateral wires, though more current was required. Importantly, when two wires were simultaneously stimulated, no increase in the field potential amplitude was observed (Figure A-2C), and thus each wire must have activated an identical number of axons, that is, all the rubrospinal axons. Thus, we are assured that all RST axons were antidromically activated by the microwires.

The distal transection of the rubrospinal tract used in the main graft experiments did not affect the field potential evoked in the red nucleus ($n = 2$), provided that the wire was placed more than 1 mm rostral to the lesion. A wire placed 0.5 mm from the lesion produced a smaller supramaximal field, presumably due to the lesion. Thus, in the graft experiments, the microwire was placed at >2 mm from the graft at the rostral end of the C4 spinal segment.

A.3.3 *Current spread from the microwires*

To anatomically verify the full recruitment of the rubrospinal tract and determine how much of the rest of the spinal cord was stimulated, we computed the current spread from the microwire stimulation. The current density at a given distance d from the stimulation is inversely proportional to the spherical surface area that the current traverses at that distance ($1/d^2$), and thus the current density decreases with the square of the distance. Therefore, the stimulus current required to reach the threshold current density to activate an axon at a distance d away is approximated by the equation;

$$I_{th} = I_o + B \cdot d^2$$

where I_o is the threshold to activate the nerve from a very close distance [typically 2 μ A for large-diameter axons (Jankowska and Roberts 1972; Stoney et al. 1968)], and B is a fixed proportionality constant (Bagshaw and Evans 1976). Given the measured current thresholds (I_{th}) to evoke a field potential in the red nucleus, and the anatomically estimated distances to the rubrospinal tract d for each of $n = 11$ wires tested, we solved the above relation for the unknowns I_o and B with an optimal least squares method (Norton 1986). This gave $I_o = 31.6 \mu$ A and $B = 240.4 \mu$ A/mm², which is in the range of that computed by others for monopolar electrodes (Asanuma and Sakata 1967; Bagshaw and Evans 1976; Stoney et al. 1968; Wise 1972).

From this relation we estimated the distance over which axons were stimulated for a given stimulus intensity I , using the above formula rearranged as $d = [(I - I_o)/B]^{1/2}$. That is, for the standard $I = 200\text{--}300 \mu$ A stimulation, the current must have spread to activate axons in a 0.84- to 1.06-mm radius. Given the standard location of the electrodes relative to the centre of the rubrospinal tract, about 0.5 mm distant, this calculation indicates that the whole 300- to 500- μ m diameter tract was activated. This stimulation intensity likely also activated afferents in the dorsal root entry zone dorsal to the electrode (potentially allowing for polysynaptic activation of the red nucleus via the interpositus nucleus), and perhaps motoneurons more ventrally and medially, although cell soma activation was unlikely (Nowak and Bullier 1998a, b).

A.3.4 *Lack of rubrospinal tract damage after one hour of supramaximal stimulation*

Our tests showed that balanced biphasic stimulation at a level supramaximal to activate the rubrospinal tract did not lead to hydrolysis at the electrode tip (see methods). However, there was still a concern that 1-hour stimulation might damage the rubrospinal tract, either electrolytically or mechanically, and thus affect the experimental outcome. To directly test this possibility, we applied the standard supramaximal rubrospinal stimulation for 1 hour at 20 Hz using biphasic pulses in acute experimental control animals and then examined how the activation of the red nucleus changed afterwards. We found the rubrospinal tract activation threshold, maximal activation current and maximal evoked field potential amplitude in the red nucleus were not changed significantly after stimulation (data not shown). Thus, the stimulation did not damage the

electrophysiological function of the tract, consistent with the lack of lesions induced by this stimulation. Further, these results demonstrate that any mechanical movement of the animal and electrode (see above) evoked by the stimulation also did not damage the rubrospinal tract.

A.3.5 Rubrospinal tract regeneration into a peripheral nerve graft

To assess the regeneration potential of the rubrospinal axons after injury, a peripheral nerve was grafted to the cut face of the rubrospinal tract, thus providing a permissive environment for regrowth after the injury (Figure A-1A). As expected from previous work, axons grew into the nerve graft (Kobayashi et al. 1997; Richardson et al. 1984), which was assessed 8 weeks after injury by transecting the nerve 10-20 mm from the injury and applying the retrograde dye microruby. This dye labelled on average 42.7 ± 10.2 cells in the red nucleus (Figure A-3; unstimulated control), most of them the large magnocellular neurons in the caudal pole (Figure A-1C), consistent with labelling numbers obtained in previous nerve transplants into the rubrospinal tract (Kobayashi et al. 1997). Given that there are on average roughly 1800-2000 rubrospinal neurons projecting to C5 and below (our unpublished data, see also Richardson et al. 1984), about 2% of the transected large-diameter axons of the rubrospinal tract regenerated into the nerve graft under control conditions, consistent with the expected 1-2% regeneration reported by others (Houle 1991; Richardson et al. 1984; Tetzlaff et al. 1994). Our control animals had a microwire implanted cervically, just ventral to the rubrospinal tract; it was not stimulated, but used to control for potential physical damage caused by the implant. Previous work with identical injury and nerve graft (Kobayashi et al. 1997), but without the microwire implant, gave very similar results (43 ± 9.3 backlabelled neurons), suggesting that the microwire implant itself did not affect the outcome (i.e. did not cause damage).

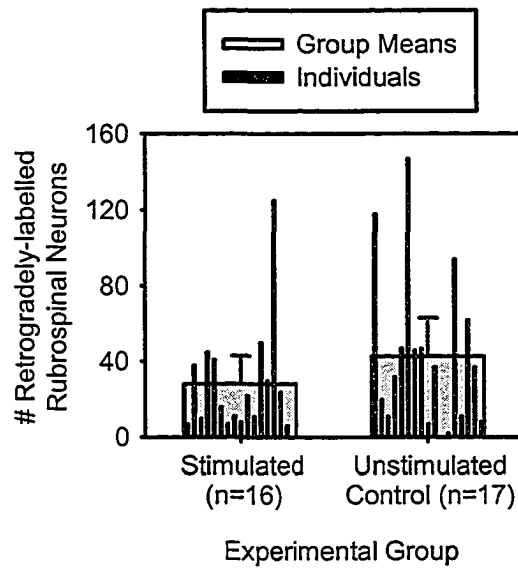
A.3.6 Failure to improve regeneration after one hour of rubrospinal tract stimulation

When the injury and nerve graft was followed immediately by a 1-hour supramaximal rubrospinal tract stimulation (20 Hz, 200–300 μ A, see above), no improvement was observed in the number of rubrospinal axons that regenerated into the nerve (Figure A-3). The microruby labelling of the nerve 8 weeks after injury only revealed on average 28.2 ± 7.4 cells, not significantly different from the number of control cells without stimulation (42.7 ± 10.2 cells). As under control conditions, these cells were mostly large magnocellular neurons of the red nucleus. Though not significant, there was a trend toward less regeneration with stimulation compared to control (there were on average 34% fewer cells labelled in the stimulated animals), opposite to our expectation of stimulation improving regeneration. Considering that the mean number of regenerated axons tended to *decrease* with stimulation, it seems very unlikely that stimulation has any ability to *improve* regeneration. Therefore, to quantify this statistically, we computed the probability that stimulation causes an *increase* in the number of regenerated axons, given

Figure A-3

Regeneration into a cervical peripheral nerve graft, as determined by the number of microtubule-positive neurons in the contralateral red nucleus, was not improved with 1-hour stimulation of the rubrospinal tract compared to sham stimulation in control animals. Shown here are the group means (thick grey bars with standard error) and the individual animals within each group (thin black bars).

Figure A-3



our sample data. To do this, we defined the increase, d (for example, $d = 5, 10, 15$ or 20% increase from the control mean of 42.7 cells), and tested the null hypothesis that stimulation significantly increases the number of regenerated cells by d , using the standard t -test. This yielded probabilities of $P = 0.10, 0.07, 0.05$ and 0.04 that stimulation causes significant increases of $5, 10, 15$ and 20% , respectively. Thus, we can conclude that there was no statistically significant change, but with the level of variability, increases of up to 15% ($P = 0.05$, equivalent to 6 cells) could have been missed.

A.3.7 Counts of regenerating cervical neurons

One reason for the somewhat lower regeneration counts in the stimulated animals might be a difference in the integrity of the graft junction, perhaps by chance, or by stimulus-induced movement. To independently evaluate the graft junction, we counted cervical spinal neurons within 1 mm rostral and caudal to the graft junction that grew an axon into the nerve and were therefore retrogradely labelled ($n = 10$ stimulated, $n = 12$ control). Because these neurons were at least 1 mm from the stimulation, they were not likely to have been directly stimulated (given the calculated current spread); thus their numbers should, in principle, be similar under control and stimulated conditions. As shown in Figure A-4A, these cervical counts were on average 168 ± 29 in control animals and 137 ± 30 in stimulated animals (not significantly different), suggesting that the graft junction and axonal growth into the nerve transplant environment was unchanged in control versus stimulated animals.

There was a trend toward a somewhat lower mean number of cervical cells in the stimulated group compared to control (20% lower, not significant), suggesting again that the integrity of the graft junction in the stimulated group may have been inferior on average. Assuming that these cervical counts indeed provide a rough estimate of the integrity of the graft junction, we normalised the individual rubrospinal counts by the means of the cervical counts in control and stimulated conditions (Figure A-4B). These normalised rubrospinal counts still showed no significant difference with stimulation, but in this case, the normalised means were closer (0.33 ± 0.18 in stimulated versus 0.42 ± 0.14 in control, a 21% difference). Thus, these normalised counts indicate that, when the variability in the integrity of the graft junction is taken into account, the stimulation had no appreciable effect on the rubrospinal regeneration, positive or negative.

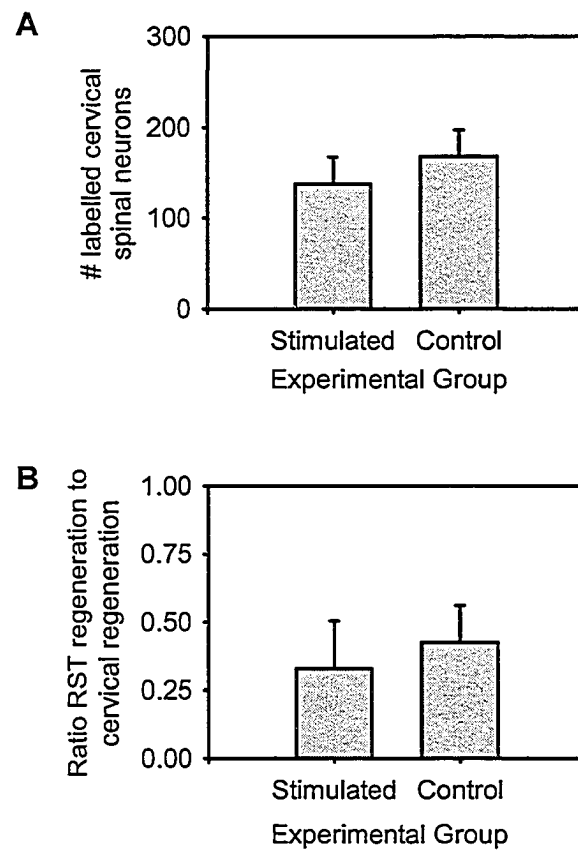
A.3.8 Cell body response to antidromic stimulation as measured by ISH and RT-PCR

To evaluate the influence of electrical stimulation on the red nucleus cell body responses to spinal cord injury, a group of animals underwent a cervical spinal cord injury to transect the left rubrospinal tract at C5, followed by a 1-hour supramaximal 20-Hz stimulation ($n = 4$) or control microwire implant with no stimulation ($n = 4$). After 48 hours survival, the animals were sacrificed and the midbrains removed for *in situ* hybridisation assay of BDNF mRNA expression. In animals that received a lesion but no stimulation to the left RST, the hybridisation signal in both right (injured) and left

Figure A-4

The number of labelled neurons in the red nuclei were normalised to the average number of labelled cervical neurons near the graft junction to control for graft integrity. *A*: The number of microruby-positive cervical spinal neurons within 1 mm rostral and caudal to the graft junction was counted and compared between stimulated and sham stimulated groups as an indicator of local growth into the nerve graft. No significant differences were observed between the groups. *B*: The number of labelled rubrospinal neurons in each animal was taken as a percentage of the mean number of labelled cervical spinal neurons for that condition and the average calculated for each group. The difference in regeneration of rubrospinal neurons between stimulated and sham stimulated animals, as normalised to local growth into the graft, was not significant.

Figure A-4



(control) red nuclei was not distinguishable from background, indicating no detectable levels of BDNF mRNA, and no change in those levels 48 hours after injury. However, the positive control for effective hybridisation did yield a significant positive signal (substantia nigra, as in Figure A-5C).

BDNF mRNA expression in response to axotomy has not been previously described in rubrospinal neurons, but is not detected under normal conditions or after injury (K. Fernandes, personal communication). For comparison, femoral motoneurons upregulate BDNF only after 7 days following axotomy, whereas BDNF is upregulated at 48 hours with electrical stimulation and axotomy (Al-Majed et al, 2000b). In contrast to the results seen with femoral motoneurons, rubrospinal tract-stimulated animals showed no increased density of hybridisation signal in the right (stimulated) red nuclei, as well as no detectable expression of BDNF mRNA above background in the left red nuclei, even though the substantia nigra again exhibited a positive signal. Thus, no BDNF mRNA expression was detected in the red nucleus under control conditions, and expression was not significantly elevated with injury and/or stimulation.

Another group of 4 rats underwent the same procedure, but the right red nuclei (experimental side) were microdissected and analysed for BDNF and GAP-43 mRNA using RT-PCR and compared to the unlesioned and unstimulated left red nuclei (control). Again, no significant differences in expression were observed with lesion and stimulation. Specifically, BDNF mRNA expression was not significantly different from background (Figures A-6A and B), and GAP-43 expression was detected in both sides of the midbrain, but was not elevated in the right (stimulated) nuclei versus the left (control) nuclei (Figures A-6C and D).

A.3.9 Failure of longer duration stimulation to affect BDNF

To test whether longer duration stimulation might improve the outcome, the cord was injured in 4 rats, the RST was stimulated for 8 hours (under a mixture of pentobarbital and isoflurane anaesthesia) and the animals were sacrificed at 48 hrs post-injury to assay BDNF mRNA expression. Two additional animals had a microwire implanted into the RST of the cervical cord for 8 hours with no stimulation. None of the stimulated animals demonstrated any significant difference in mRNA expression for BDNF in the stimulated red nucleus versus the unstimulated contralateral red nucleus as determined by *in situ* hybridisation similar to that detailed above (Figures A-5A and B). A lesion combined with an implanted electrode in the cervical cord for 8 hours, without any stimulation, also did not induce any detectable BDNF mRNA expression. The density of hybridisation probe was not significantly greater than background in any condition, despite positive labelling for BDNF mRNA in the substantia nigra (Figure A-5C).

Figure A-5

BDNF mRNA is not upregulated in the red nuclei 48 hours after axotomy and antidromic stimulation. *In situ* hybridisation for BDNF mRNA in the stimulated (*A*) versus control (*B*) red nuclei of an animal that received 8 hours antidromic stimulation following cervical axotomy of the left RST. Arrows indicate rubrospinal neurons. There was no signal above background observed within identified rubrospinal neurons on either side, whether with 1 hour or 8 hours stimulation. A positive signal was observed in the substantia nigra (*C*) indicating that the probe was successfully labelling for BDNF mRNA. Scale bar represents 50 microns.

Figure A-5

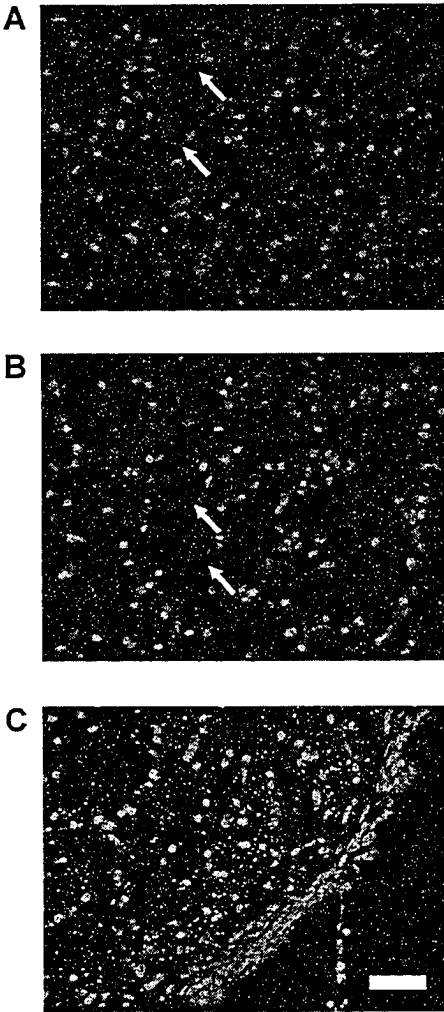
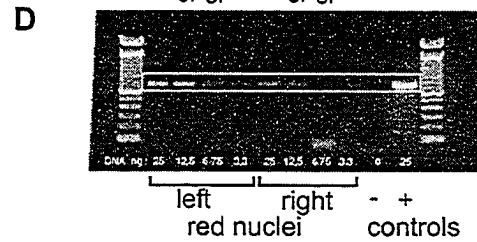
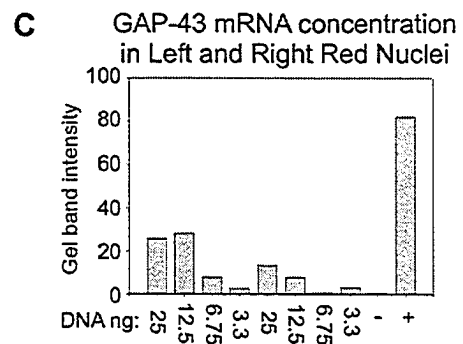
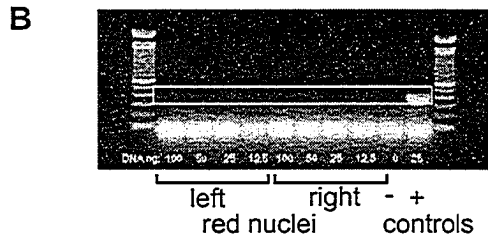
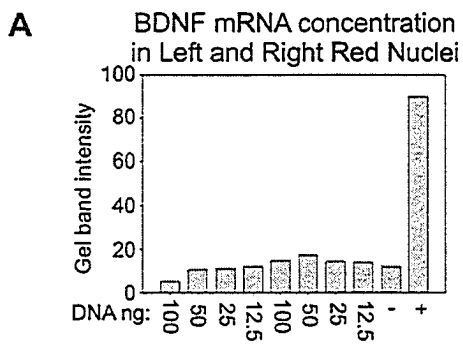


Figure A-6

BDNF was not detected in the red nuclei using RT-PCR, and GAP-43 levels were not elevated with stimulation. *B* and *D*: Gels from RT-PCR assay for BDNF and GAP-43 mRNA from pooled right (stimulated) versus pooled left (control) red nuclei. Cerebral cortex, which expresses moderate amounts of BDNF and GAP-43, was used as a positive control. (*A,B*) Using grey-scale analysis, no BDNF mRNA expression greater than the negative control was detected in either right or left red nuclei at 40, 50 or 60 cycles of amplification (60 cycle data shown here). (*C,D*) GAP-43 mRNA was clearly expressed in both nuclei after 31 cycles, but was not elevated with stimulation compared to control. Samples were pooled, so no standard error is available. White boxes drawn on gels indicate the migration distance for each protein as determined using the positive control at right.

Figure A-6



A.3.10 Failure of one hour of electrical stimulation to improve femoral motoneuron regeneration

Considering that electrical stimulation had no effect on rubrospinal tract regeneration, we attempted to replicate the reported effects of electrical stimulation on peripheral nerves (Al-Majed *et al.*, 2000b) on which our work is based. The femoral nerve was transected and re-sutured, and then immediately stimulated for 1 hour in test rats or not stimulated in control rats, exactly as in Al-Majed *et al.* (2000b; see Methods). Unexpectedly, at 3 weeks post-injury and repair, we did not observe significantly greater numbers of femoral motoneurons regenerating down the muscle branch with one hour of electrical stimulation (104.9 ± 10.4) compared to control sham stimulations (122.6 ± 8.7 ; Figure A-7). Furthermore, the number of motoneurons regenerating down the inappropriate branch (cutaneous) was not significantly different from those regenerating along the appropriate muscle branch in either group. Thus, we did not see the improved regeneration and preferential motor reinnervation observed with electrical stimulation by Al-Majed and co-workers. We attempted to replicate this study many times, with a final total of 46 rats tested (Figure A-7), and with identical equipment and surgeons as in the original Al-Majed study, and yet we found no effect of electrical stimulation on femoral nerve regeneration (see also Harvey and Bennett 2003).

A.4 DISCUSSION

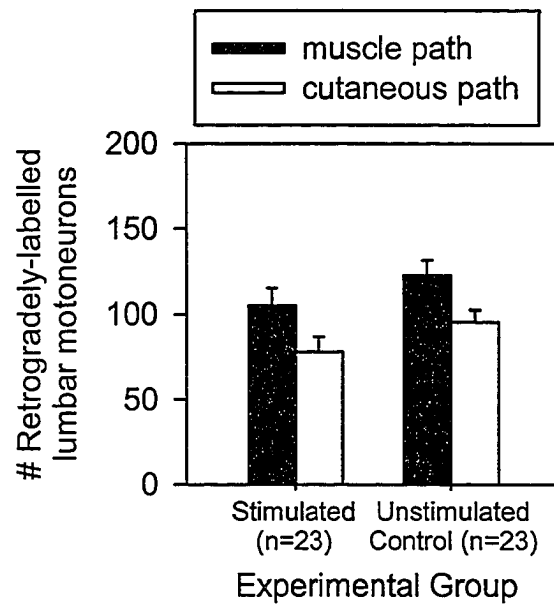
A.4.1 Influence of antidromic stimulation on CNS regeneration

Our results demonstrate that it is possible to reliably stimulate the rubrospinal tract with microwires implanted in the cervical cord using a 1-hour-long supramaximal stimulation paradigm similar to that used to promote peripheral nerve regeneration of femoral motoneurons. Importantly, these microwires do not damage the spinal cord when used with appropriate biphasic stimulation, and have substantial current spread adequate to reliably activate the entire rubrospinal tract. However, despite this we found that regeneration of the RST into a nerve graft was not significantly improved by 1 hour of supramaximal stimulation that antidromically activated axons of the rubrospinal neurons. Given that the mean number of backlabelled neurons in the stimulated group is actually slightly lower than control, it is unlikely that we simply failed to detect, due to variability, a real positive influence of stimulation on CNS regeneration. Further, 1 hour of antidromic electrical stimulation did not increase BDNF or GAP-43 mRNA expression at 48 hours post-injury, in contrast to the effects seen in the periphery (Al-Majed *et al.*, 2000b; 2004). The number of regenerating rubrospinal neurons obtained by Kobayashi and colleagues (1997) are a good comparison for our results. The mean number of regenerating neurons they assessed by retrograde labelling after 10 weeks was 131 ± 19.7 with chronic BDNF infusion near the red nucleus, versus 43 ± 9.3 in controls without BDNF. Similarly, our control group had a mean number of 42.7 ± 10.2 labelled neurons, suggesting that the microwire implant itself did not adversely affect the ability of rubrospinal neurons to regenerate. Further, the lack of BDNF expression in the stimulated animals, while different from that seen by Al-Majed *et al.* (2000a) in femoral

Figure A-7

One hour of electrical stimulation did not increase the number of femoral motoneurons regenerating along the quadriceps branch of the femoral nerve at 3 weeks. Following cut and repair of the femoral nerve, electrical stimulation was applied to one group and sham stimulation applied to the control group. The muscle and cutaneous branches were labelled with different dyes at 3 weeks to identify regenerating motoneurons. Preferential reinnervation of the muscle branch by femoral motoneurons was not observed in the stimulated group at this time point (compare muscle versus cutaneous pathways, not significantly different), nor was there increased regeneration along the muscle branch in stimulated animals compared to unstimulated control animals (compare muscle pathways between stimulated and unstimulated, not significantly different). This is in marked contrast to the results reported by Al-Majed *et al.* (2000) in which the number of femoral motoneurons that had regenerated along the muscle branch by 3 weeks time was doubled with electrical stimulation.

Figure A-7



motoneurons with stimulation, is consistent with no regeneration, if we assume that BDNF or related RAG expression is causally linked to the regeneration seen by Kobayashi and colleagues (1997). The importance of this negative BDNF result must be emphasised, because it is consistent with our conclusion that electrical antidromic stimulation does not facilitate the regenerative capacity of these central neurons.

We attempted to control for variability in graft junction integrity and ability to promote growth by normalising the rubrospinal counts by the mean number of local cervical spinal neurons that grew into the graft. These cervical cells were unstimulated and thus, in principle, should be equally likely to grow into the graft in stimulated and control animals. The normalised number of regenerated rubrospinal neurons was closer in stimulated and unstimulated animals (21% difference), compared to non-normalised counts (34% difference). This suggests that there was a modest difference, albeit insignificant, in integrity of the graft junction, so we tended to underestimate the effect of stimulation on axonal regeneration. When we normalised our data to account for this, there was no obvious difference produced by the stimulation.

It is unlikely that the lower number of regenerated cells in the stimulated animals is due to local electrolytic or mechanical damage caused by the stimulation. This stimulation causes no changes in the threshold or shape of the evoked field potentials in the red nucleus, indicating that it does not damage the tract. Further, the wires were removed immediately after the stimulation, and thus did not do subsequent damage during the ensuing 8-week recovery period. In any case, potential problems with stimulation-induced damage to the cervical RST did not affect the cell body response (i.e. BDNF and GAP-43 mRNA expression) to the stimulation because there was no requirement for axonal growth in this case. Despite this, there was no indication that antidromic stimulation had increased the regenerative capacity of rubrospinal neurons, using RT-PCR and *in situ* hybridisation for GAP-43 and/or BDNF mRNA, either with 1 or 8 hours of stimulation.

A.4.2 Mechanisms of activity-dependent regeneration

The possible intracellular mechanisms responsible for activity-dependent regeneration are of relevance to our results. Although activity can potentially lead to autocrine effects of neurotrophins, this effect is secondary to the Ca^{2+} influx elicited by electrical activation (Hansen et al. 2001). Indeed, evidence is accumulating that depolarisation can alter the response of the neurons to myelin and myelin-associated glycoprotein from repulsion to attraction (Ming et al. 2001) and that this is mediated by elevations of intracellular cyclic AMP (cAMP) levels (Cai et al. 1999; Lohof et al. 1992). *In vivo*, increasing cAMP in dorsal root ganglion neurons can induce regeneration across a central lesion in the dorsal columns (Qiu et al. 2002), similar to the effects seen using peripheral conditioning lesions (Neumann and Woolf 1999). In fact, depolarisation and the accompanying Ca^{2+} influx may be the driving stimuli for a multitude of effects that facilitate survival and regeneration. These effects include increased neurotrophin expression (Abiru et al. 1998; Hughes et al. 1999; Kojima et al. 2001), the driving of neurotrophin receptors to the cell

surface (Meyer-Franke et al. 1998), activation of adenylyl cyclase leading to cAMP elevation, and direct modulation of gene expression via calcium/calmodulin-dependent kinases (Hansen et al. 2001), all of which can be separate and additive pathways. Since the intrinsic calcium buffering capabilities of rubrospinal neurons are greater than spinal motoneurons (Celio 1990; Hontanilla et al. 1995; Lips and Keller 1998; Ren and Ruda 1994; Wang et al. 1996), the antidromically induced Ca^{2+} -mediated signal may be attenuated in our experiments compared to similar stimulation of femoral motoneurons. Higher frequency trains of stimuli may help overcome the intrinsic calcium buffering of rubrospinal neurons; however, Eccles *et al.* (1975) report that rubrospinal tract stimulation at frequencies above 50 Hz leads to a progressively increasing delay of the spike until, eventually, the soma-dendritic component of the spike fails. Thus, there may be an optimal frequency at which rubrospinal neurons respond positively to electrical stimulation.

Alternatively, most protocols demonstrating links between Ca^{2+} influx and regeneration require that the treatment be administered prior to exposure to the inhibitory substrate. This prior treatment may allow the injured neurons time to upregulate certain gene products such that they are ready to cross the lesion site before the glial scar barrier forms. In models of peripheral injury and regeneration, no glial scar barriers form, so electrical stimulation at the time of nerve injury and repair may still be effective. On the other hand, our CNS regeneration experiments may require stimulation several hours or days prior to axotomy to have positive effects. Another factor to be considered is that Pockett and Gavin (1985) reported that delays of 30-60 minutes between crushing the peripheral nerve and applying electrical stimulation resulted in longer periods to recover the reflex, compared with stimulation applied immediately after crush. In our RST regeneration protocol, a delay of about 15 - 30 minutes, from the time of the initial lesion to the time of stimulation, likely occurred because of the time required for surgical implantation of the peripheral nerve graft and the microwire prior to administering stimulation (grafting-delay). However, we found that BDNF mRNA hybridisation did not increase with stimulation, even when this stimulation was applied immediately after the injury (no graft in this case), which would suggest that stimulation with no grafting-delay would also be unsuccessful in improving regeneration. In any case, if delays of as little as 30 minutes following the initial injury can so severely compromise the efficacy of electrical stimulation, then it is not expected to be a very useful clinical procedure.

A.4.3 Relevance of the mode of input in neural response to injury

Antidromic stimulation of rubrospinal neurons, such as we have performed, may be an altogether ineffective means of promoting regeneration. Instead, synaptic activation of the injured neurons may be required. The investigations performed by Al-Majed and colleagues (2000a, b) did not elucidate the pathway by which the stimulation of the femoral nerve was effective in promoting femoral motoneuron regeneration. Stimulation of a mixed nerve like the femoral nerve activates both sensory afferents and motor efferents. Thus, the dramatic effects observed could have been mediated by synaptic stimulation of the motoneurons via dorsal root input. In fact, Verge and coworkers report

that the dorsal root ganglia neurons in stimulated animals (from the same experimental animals used by Al-Majed *et al.*, 2000b) also demonstrated increased regeneration peripherally (Geremia *et al.* 2002), indicating that sensory axons were also stimulated with their protocol.

Evidence suggests that synaptic stimulation has downstream effects on the cell that are different from antidromic activation because the pathway of neural input influences the subsequent intracellular signals and the response to injury (Finkbeiner and Greenberg 1998). For electrical input to a cell, it is the influx of Ca^{2+} that links electrical activity to the various and numerous patterns of gene expression potentially initiated by stimulation (Rosen *et al.* 1995). Greenberg and colleagues (Finkbeiner and Greenberg 1998; Ghosh and Greenberg 1995; West *et al.* 2002) emphasized the importance of cellular localization and mode of Ca^{2+} entry in determining the ultimate cellular response to the stimulus. The type of channel (voltage-sensitive calcium channels versus NMDA channels), the source of calcium ions (extracellular versus intracellular stores), the temporal pattern (prolonged elevation versus transient spikes, see also Spitzer 1995) and particularly the localisation (distal dendrites versus soma) can be differentially activated by antidromic stimulation versus synaptic activation.

Wide-scale synaptic activation of the red nucleus can be achieved easily via stimulation of the contralateral interpositus nucleus of the cerebellum (Eccles *et al.* 1975; Toyoma *et al.* 1970). Our preliminary experiments involving 1-hour stimulation of the interpositus nucleus following cervical RST axotomy demonstrated a small but clear increase in BDNF mRNA expression ($n = 3/3$) compared to the contralateral red nucleus (unpublished experiments). This suggests that synaptic activation may be more effective than antidromic activation, and is a topic of future investigations.

A.4.4 Possible explanations for failure of stimulation to promote regeneration of femoral motoneurons

It is concerning that we were not able to replicate the finding of Al-Majed and colleagues (2000b) that femoral nerve stimulation promotes motor axon regeneration. We made every effort to carefully replicate these experiments, as described in the Results, and thus we are certain that this was not just a methodological error. We replicated the experiments on 23 rats in each group, many more than in the Al-Majed *et al.* (2000b) study (9 rats stimulated and 9 unstimulated). Thus one obvious possibility is that Al-Majed and colleagues found greater regeneration in a few stimulated rats simply by chance, or because of unintentional experimenter bias (see last section of Methods), and in reality stimulation does not promote motoneuron regeneration. Indeed, if we combine the raw data from our results and the Al-Majed *et al.* (2000b) results, there is still no significant effect of stimulation (unpublished observation). However, we feel that there are likely other more fundamental reasons for our results being different from those of Al-Majed *et al.* (2000b). One intriguing explanation might involve the afferent fibres in the femoral nerve. When the femoral nerve is stimulated both the motor axons (efferents) and sensory afferents are activated, as mentioned above. Thus, it is possible that any

putative effect of stimulation might depend on the afferents, rather than efferents, and this possibility has not been ruled out by Al-Majed and colleagues. That is, input of sensory afferents to the motoneurons might promote regeneration (as we also suggest might be the case for the rubrospinal neurons; see above). It is not clear what stimulus intensity Al-Majed et al. (2000b) used, only that they stimulated strongly enough to see gross movements of the leg even after the femoral nerve was cut. We stimulated at a well-defined stimulus intensity, 3× motor threshold, which would have activated group I and II afferents, by not higher threshold afferents such as C-fibres (see Methods). Thus, it is possible that Al-Majed and colleagues stimulated at a higher intensity than we did, and thus activated high threshold afferents, such as C-fibres, that we did not activate. Perhaps these afferents are critical in promoting regeneration. That is, it may be that 1 hour of stimulation of a mixed nerve promotes regeneration only when the high threshold afferents (e.g. C-fibres) are activated by the stimulation. These kind of afferents release neuropeptides such as substance-P that act through G-protein coupled receptors to have complex effects on spinal neurons. Thus it is not improbable that they raise cAMP levels in motoneurons, and this may ultimately promote regeneration. In this regard it is interesting that the same 1-hour femoral nerve stimulation facilitates regeneration of sensory neurons in the dorsal root ganglia (Geremia et al. 2002), so at least we know that the afferents are affected by the stimulation. Further, it has recently been found that cAMP levels in motoneurons are raised by this same stimulation of a peripheral nerve (T. Gordon, in preparation), and numerous studies have implicated elevated cAMP in promoting axon growth (see above). This idea that C-fibre stimulation may promote regeneration is at this point very speculative. What we do know with certainty, from our results, is that full stimulation of the motor axons and low threshold afferents (at 3× motor threshold) does not improve regeneration.

Another possibility that may explain the discrepancy between our results and those of Al-Majed et al. (2000b) might be differences in the time delay between the nerve injury and the start of the stimulation. In both experiments, the stimulation started immediately after the nerve repair, but the nerve-nerve suture took between 5 and 15 minutes to perform. So it is possible that the nerve repairs took longer in our experiments (though not likely). If they did, then stimulation would have been delayed, and this may have had a detrimental effect on stimulation evoked regeneration. Pockett and Gavin (1985) reported that stimulation improved the functional (reflex) recovery after a nerve injury, but a delay in the onset of stimulation of about 30 minutes reduced the beneficial effects of stimulation. Thus, it is not unreasonable to suppose that even a 10-minute delay in our experiments may have had a detrimental effect.

A.4.5 Summary

This study did not support the principle of activity-dependent regeneration in an *in vivo* model. Specifically, we did not observe any beneficial effect of antidromic electrical stimulation of the rubrospinal tract on regeneration of rubrospinal neurons into a peripheral nerve graft, in contrast to the reported improvement of motoneuron regeneration in the peripheral nervous system with 1-hour electrical stimulation. The

stimulation also did not have any effect on BDNF or GAP-43 mRNA expression in the axotomised rubrospinal cell bodies. We suggest that synaptic, as opposed to antidromic, activation of central neurons may be more successful in promoting regeneration, and that this may also be the mechanism by which peripheral nerve stimulation improves motoneuron regeneration following axotomy and repair (as in Al-Majed *et al.*, 2000b, via afferent stimulation). Ultimately, the present results indicate that regeneration of rubrospinal neurons does not respond positively to antidromic electrical stimulation. Whether this holds in the CNS in general or whether synaptic inputs have positive effects on regeneration is currently uncertain.

A.5 LIST OF ABBREVIATIONS

AMP	adenosine monophosphate
BDNF	Brain-derived neurotrophic factor
cAMP	cyclic adenosine monophosphate
cDNA	copy deoxyribonucleic acid
CNS	central nervous system
EMG	electromyogram
GAP-43	Growth-associated protein-43
ISH	<i>In situ</i> hybridisation
mRNA	messenger ribonucleic acid
NMDA	N-methyl-D-aspartate
nt	nucleotide
RAG	regeneration-associated gene
RST	rubrospinal tract
RT-PCR	reverse-transcriptase polymerase chain reaction
TrkB	Tyrosine receptor kinase B

A.6 BIBLIOGRAPHY FOR APPENDIX 1

Abercrombie M. Estimation of nuclear population from microtome sections. *Anat Rec* 94: 239-247, 1946.

Abiru Y, Katoh-Semba R, Nishio C, and Hatanaka H. High potassium enhances secretion of neurotrophic factors from cultured astrocytes. *Brain Res* 809: 115-126, 1998.

Al-Majed AA, Brushart TM, and Gordon T. Electrical stimulation accelerates and increases expression of BDNF and trkB mRNA in regenerating rat femoral motoneurons. *Eur J Neurosci* 12: 4381-4390, 2000a.

Al-Majed AA, Neumann CM, Brushart TM, and Gordon T. Brief electrical stimulation promotes the speed and accuracy of motor axonal regeneration. *J Neurosci* 20: 2602-2608, 2000b.

Al-Majed AA, Tam SL, and Gordon T. Electrical stimulation accelerates and enhances expression of regeneration-associated genes in regenerating rat femoral motoneurons. *Cellular and Molecular Neurobiology* 24: 379-402, 2004.

Asanuma H and Sakata H. Functional organization of a cortical efferent system examined with focal depth stimulation in cats. *J Neurophysiol* 30: 35-54, 1967.

Ausubel FM, Brent R, Kingston RE, Moore DD, Seidman JG, Smith KA, and Struhl K. *Current Protocols in Molecular Biology*. New York: Wiley-Interscience, 1987.

Bagshaw EV and Evans MH. Measurement of current spread from microelectrodes when stimulating within the nervous system. *Exp Brain Res* 25: 391-400, 1976.

Brown LT. Rubrospinal projections in the rat. *J Comp Neurol* 154: 169-187, 1974.

Brushart TM, Hoffman PN, Royall RM, Murinson BB, Witzel C, and Gordon T. Electrical stimulation promotes motoneuron regeneration without increasing its speed or conditioning the neuron. *J Neurosci* 22: 6631-6638, 2002.

Cai D, Shen Y, De Bellard M, Tang S, and Filbin MT. Prior exposure to neurotrophins blocks inhibition of axonal regeneration by MAG and myelin via a cAMP-dependent mechanism. *Neuron* 22: 89-101, 1999.

Celio MR. Calbindin D-28k and parvalbumin in the rat nervous system. *Neuroscience* 35: 375-475, 1990.

David S and Aguayo AJ. Axonal elongation into peripheral nervous system "bridges" after central nervous system injury in adult rats. *Science* 214: 931-933, 1981.

Eccles JC, Scheid P, and Taborikova H. Responses of red nucleus neurons to antidromic and synaptic activation. *J Neurophysiol* 38: 947-964, 1975.

Ernfors P, Wetmore C, Olson L, and Persson H. Identification of cells in rat brain and peripheral tissues expressing mRNA for members of the nerve growth factor family. *Neuron* 5: 511-526, 1990.

Fernandes KJ, Fan DP, Tsui BJ, Cassar SL, and Tetzlaff W. Influence of the axotomy to cell body distance in rat rubrospinal and spinal motoneurons: differential regulation of GAP-43, tubulins, and neurofilament-M. *J Comp Neurol* 414: 495-510, 1999.

Finkbeiner S and Greenberg ME. Ca²⁺ channel-regulated neuronal gene expression. *J Neurobiol* 37: 171-189, 1998.

Geremia NM, Gordon T, Al-Majed AA, Brushart TM, and Verge VMK. Brief electrical stimulation promotes regeneration of sensory fibers into cutaneous & muscle branched of femoral nerve. *Society for Neuroscience Annual General Meeting, Orlando, FL: Abstract #535.514*, 2002.

Ghosh A and Greenberg ME. Calcium signaling in neurons: molecular mechanisms and cellular consequences. *Science* 268: 239-247, 1995.

Hansen MR, Zha XM, Bok J, and Green SH. Multiple distinct signal pathways, including an autocrine neurotrophic mechanism, contribute to the survival-promoting effect of depolarization on spiral ganglion neurons in vitro. *J Neurosci* 21: 2256-2267, 2001.

Harvey PJ and Bennett DJ. One hour of electrical stimulation does not improve regeneration rate of femoral motoneurons. *Peripheral Nerve Society Annual General Meeting, Banff, AB, July 26-29: Abstract #29*, 2003.

Hontanilla B, Parent A, and Gimenez-Amaya JM. Heterogeneous distribution of neurons containing calbindin D-28k and/or parvalbumin in the rat red nucleus. *Brain Res* 696: 121-126, 1995.

Houle JD. Demonstration of the potential for chronically injured neurons to regenerate axons into intraspinal peripheral nerve grafts. *Exp Neurol* 113: 1-9, 1991.

Hughes PE, Alexi T, Walton M, Williams CE, Dragunow M, Clark RG, and Gluckman PD. Activity and injury-dependent expression of inducible transcription factors, growth

factors and apoptosis-related genes within the central nervous system. *Prog Neurobiol* 57: 421-450, 1999.

Jankowska E and Roberts WJ. An electrophysiological demonstration of the axonal projections of single spinal interneurons in the cat. *J Physiol* 222: 597-622, 1972.

Kobayashi NR, Bedard AM, Hincke MT, and Tetzlaff W. Increased expression of BDNF and trkB mRNA in rat facial motoneurons after axotomy. *Eur J Neurosci* 8: 1018-1029, 1996.

Kobayashi NR, Fan DP, Giehl KM, Bedard AM, Wiegand SJ, and Tetzlaff W. BDNF and NT-4/5 prevent atrophy of rat rubrospinal neurons after cervical axotomy, stimulate GAP-43 and α -tubulin mRNA expression, and promote axonal regeneration. *J Neurosci* 17: 9583-9595, 1997.

Kojima M, Takei N, Numakawa T, Ishikawa Y, Suzuki S, Matsumoto T, Katoh-Semba R, Nawa H, and Hatanaka H. Biological characterization and optical imaging of brain-derived neurotrophic factor-green fluorescent protein suggest an activity-dependent local release of brain-derived neurotrophic factor in neurites of cultured hippocampal neurons. *J Neurosci Res* 64: 1-10, 2001.

Lips MB and Keller BU. Endogenous calcium buffering in motoneurons of the nucleus hypoglossus from mouse. *J Physiol* 511 (Pt 1): 105-117, 1998.

Lohof AM, Quillan M, Dan Y, and Poo MM. Asymmetric modulation of cytosolic cAMP activity induces growth cone turning. *J Neurosci* 12: 1253-1261, 1992.

Maisonpierre PC, Le Beau MM, Espinosa Rr, Ip NY, Belluscio L, de la Monte SM, Squinto S, Furth ME, and Yancopoulos GD. Human and rat brain-derived neurotrophic factor and neurotrophin-3: gene structures, distributions, and chromosomal localizations. *Genomics* 10: 558-568, 1991.

Meyer-Franke A, Wilkinson GA, Kruttgen A, Hu M, Munro E, Hanson MGJ, Reichardt LF, and Barres BA. Depolarization and cAMP elevation rapidly recruit TrkB to the plasma membrane of CNS neurons. *Neuron* 21: 681-693, 1998.

Ming G, Henley J, Tessier-Lavigne M, Song H, and Poo M. Electrical activity modulates growth cone guidance by diffusible factors. *Neuron* 29: 441-452, 2001.

Mortimer JT. Motor Prostheses. In: *Handbook of Physiology. Section 1: The Nervous System. Volume II, Parts 1 & 2: Motor Control*. Bethesda, MD: American Physiological Society, 1981, p. 155 - 187.

Mushahwar VK, Collins DF, and Prochazka A. Spinal cord microstimulation generates functional limb movements in chronically implanted cats. *Exp Neurol* 163: 422-429, 2000.

Neumann S and Woolf CJ. Regeneration of dorsal column fibers into and beyond the lesion site following adult spinal cord injury. *Neuron* 23: 83-91, 1999.

Nix WA and Hopf HC. Electrical stimulation of regenerating nerve and its effect on motor recovery. *Brain Res* 272: 21-25, 1983.

Norton JP. *An Introduction to Identification*. Toronto: Academic Press, 1986.

Nowak LG and Bullier J. Axons, but not cell bodies, are activated by electrical stimulation in cortical gray matter. I. Evidence from chronaxie measurements. *Exp Brain Res* 118: 477-488, 1998a.

Nowak LG and Bullier J. Axons, but not cell bodies, are activated by electrical stimulation in cortical gray matter. II. Evidence from selective inactivation of cell bodies and axon initial segments. *Exp Brain Res* 118: 489-500, 1998b.

Paxinos G and Watson C. *The Rat Brain in Stereotaxic Coordinates*. San Diego: Academic Press, Inc., 1986.

Pockett S and Gavin RM. Acceleration of peripheral nerve regeneration after crush injury in rat. *Neurosci Lett* 59: 221-224, 1985.

Prochazka A, Westerman RA, and Ziccone SP. Discharges of single hindlimb afferents in the freely moving cat. *J Neurophysiol* 39: 1090-1104, 1976.

Qiu J, Cai D, Dai H, McAtee M, Hoffman PN, Bregman BS, and Filbin MT. Spinal axon regeneration induced by elevation of cyclic AMP. *Neuron* 34: 895-903, 2002.

Ramon y Cajal S. *Degeneration and regeneration of the central nervous system*. Translated by R.M. May, edited by J. DeFelipe and E.G. Jones. New York: Oxford University Press, 1928.

Ren K and Ruda MA. A comparative study of the calcium-binding proteins calbindin-D28K, calretinin, calmodulin and parvalbumin in the rat spinal cord. *Brain Res Brain Res Rev* 19: 163-179, 1994.

Richardson PM, Issa VM, and Aguayo AJ. Regeneration of long spinal axons in the rat. *J Neurocytol* 13: 165-182, 1984.

Richardson PM, McGuinness UM, and Aguayo AJ. Axons from CNS neurons regenerate into PNS grafts. *Nature* 284: 264-265, 1980.

Rosen LB, Ginty DD, and Greenberg ME. Calcium regulation of gene expression. *Adv Second Messenger Phosphoprotein Res* 30: 225-253, 1995.

Spitzer NC. Spontaneous activity: functions of calcium transients in neuronal differentiation. *Perspect Dev Neurobiol* 2: 379-386, 1995.

Stein RB. *Nerve and Muscle: Membranes, Cells and Systems*. New York: Plenum Pub Corp, 1980.

Stoney SDJ, Thompson WD, and Asanuma H. Excitation of pyramidal tract cells by intracortical microstimulation: effective extent of stimulating current. *J Neurophysiol* 31: 659-669, 1968.

Tello F. La influencia del neurotropismo en las regeneración de los nervios. *Trab Lab Invest Biol* 9: 123-159, 1911.

Tetzlaff W, Alexander SW, Miller FD, and Bisby MA. Response of facial and rubrospinal neurons to axotomy: changes in mRNA expression for cytoskeletal proteins and GAP-43. *J Neurosci* 11: 2528-2544, 1991.

Tetzlaff W, Kobayashi NR, Giehl KM, Tsui BJ, Cassar SL, and Bedard AM. Response of rubrospinal and corticospinal neurons to injury and neurotrophins. *Prog Brain Res* 103: 271-286, 1994.

Toyoma M, Tsukahara N, Kosaka K, and Matsunami K. Synaptic excitation of red nucleus neurons by fibres from interpositus nucleus. *Exp Brain Res* 11: 187-198, 1970.

Verge VM, Merlio JP, Grondin J, Emfors P, Persson H, Riopelle RJ, Hokfelt T, and Richardson PM. Colocalization of NGF binding sites, trk mRNA, and low-affinity NGF receptor mRNA in primary sensory neurons: responses to injury and infusion of NGF. *J Neurosci* 12: 4011-4022, 1992.

Wang YJ, Liu CL, and Tseng GF. Compartmentalization of calbindin and parvalbumin in different parts of rat rubrospinal neurons. *Neuroscience* 74: 427-434, 1996.

West AE, Griffith EC, and Greenberg ME. Regulation of transcription factors by neuronal activity. *Nat Rev Neurosci* 3: 921-931, 2002.

Wise RA. Spread of current from monopolar stimulation of the lateral hypothalamus. *Am J Physiol* 223: 545-548, 1972.